

DEVELOPMENT OF SELF-CURED GEOPOLYMER CEMENT

A thesis submitted for the degree of Doctor of Philosophy

by

Teewara Suwan

Department of Mechanical, Aerospace &
Civil Engineering
Brunel University London

March 2016

ABSTRACT

To support the concept of environmentally friendly materials and sustainable development, the low-carbon cementitious materials have been extensively studied to reduce amount of CO₂ emission to the atmosphere. One of the efforts is to promote alternative cementitious binders by utilizing abundant alumina-silicate wastes from the industrial sectors (e.g. fly ash or furnace slag), among which “Geopolymer (GP) cement” has received most attention as it can perform a wide variety of behaviours, in addition to cost reduction and less environmental impacts.

The most common geopolymer production, fly ash-based, gained some strength with very slow rate at ambient temperature, while the strength is evidently improved when cured in high (above room) temperature, e.g. over 40°C. The major challenge is to step over the limitation of heat curing process and inconvenience in practice. In this study, the testing schemes of (i) GP manufacturing in various processes, (ii) inclusion of ordinary Portland cement (OPC) in GP mixture, called GeoPC and (iii) GeoPC manufactured with dry-mixing method, have been intensively investigated through mechanical testing (Setting time, Compressive strength and Internal heat measurement) and mechanism analysis (XRD, FTIR, SEM and EDXA) in order to develop the geopolymers, achieving reasonable strength without external sources of heat curing.

It is found that the proposed (dry) mixing process could have generated intensive heat liberation which was observed as a comparable factor to heat curing from any other external sources, enhancing the curing regime of the mixture. The additional calcium content in the developed GeoPC system not only resulted in an improvement of an early strength by the extra precipitation of calcium compounds (C,N-A-S-H), but also provided a latent heat from the reaction of its high potential energy compounds (e.g. OPC or alkaline activators). The developments from these approaches could lead to geopolymer production to achieve reasonable strength in ambient curing temperature known as “Self-cured geopolymer cement”, without external heat, and hence provide construction industry viable technologies of applying geopolymers in on-site and off-site construction.

ACKNOWLEDGEMENTS

My PhD programme was completed successfully because of my kind and knowledgeable principal supervisor, Professor Dr Mizi Fan and supervisor Dr Nuhu Braimah. I sincerely appreciate your invaluable advice, guidance and support from day one to completion. You continually inspire me and demonstrate what it means to be a great advisor and researcher. I am honoured to have both of you as my academic advisors.

I would like to thank the rest of my committee members – Professor Asif Usmani, Dr Binsheng (Ben) Zhang and Dr Mujib Rahman. I greatly appreciate the time and energy you gave to being my committee member, as well as your creative suggestions and comments.

I also would like to express my appreciation to Dr Xiangming Zhou for your suggestions on geopolymer cement and my experimental works, as well as Neil Macfadyen, Simon Le Geyt and Paul Szadorski at civil engineering laboratory, for supporting all lab equipment, materials and trainings on my research project – Thank you so much, you are the best!

I will also like to extend special thanks to Brunel ETC's staff, Dr Lorna Anguilano, Ashley Howkins, Dr Jesus Ojeda and Nita Verma for your supports and great techniques on handling all equipment and machines. Thanks to my lovely friends, Jane Paphawasit, Samira Safari, Seyed Ghaffar, Gediminas Kastiukas and Dasong Dai for your help and kindness relating to my research work.

Last but not least, an endless gratitude to my inspiration, my support, my encouragement, my everything – Papa, Mama, Note and Neth, including my beloved aunt, Pa Ni.

TABLE OF CONTENTS

ABSTRACT	i
ACKNOWLEDGEMENTS	ii
TABLE OF CONTENTS	iii
LIST OF TABLES	viii
LIST OF FIGURES	ix
LIST OF ABBREVIATIONS	xiii
LIST OF SYMBOLS	xv
PART 1 INTRODUCTION, LITERATURE REVIEW AND METHODOLOGY	1
CHAPTER 1 INTRODUCTION	2
1.1 Background of Research	2
1.2 Aim of the Research	3
1.3 Research Objectives	4
1.4 Research Scope.....	4
1.5 Research Significance	5
1.6 Organisation of Contents	6
CHAPTER 2 LITERATURE REVIEW	9
2.1 Portland Cement and Fly Ash	9
2.1.1 Ordinary Portland cement.....	9
2.1.2 The use of pozzolanic admixture (fly ash) in Portland cement	15
2.2 Geopolymer Cement.....	17
2.2.1 Fundamentals of geopolymers	17
2.2.2 Geopolymerization reaction and its chemistry	19
2.2.3 Geopolymer binder constituents	21
2.2.4 Design of geopolymer constituents.....	28
2.2.5 Curing procedures of geopolymers.....	30
2.2.6 Properties and application of geopolymer cement.....	34
2.3 Factors Influencing Geopolymer Properties at Ambient Temperature	38
2.3.1 High humidity curing.....	38
2.3.2 Concentration of alkaline activators	39
2.3.3 Fineness and shape of particles.....	39
2.3.4 Mixing procedures	40
2.3.5 Alternative heat curing sources.....	40

2.3.6 Calcium content in mixtures	41
2.4 Remark	42
CHAPTER 3 MATERIALS AND TESTING METHODS	45
3.1 Experimental Programme and Work Packages	45
3.2 Materials and Equipment.....	47
3.2.1 Ordinary Portland cement (OPC)	47
3.2.2 Coal-fired fly ash	47
3.2.3 Alkaline solutions	48
3.2.4 Experimental equipment	49
3.3 Sample Preparation.....	50
3.3.1 Portland cement paste	50
3.3.2 Geopolymer cement paste.....	51
3.3.3 GeoPC pastes	51
3.4 Testing of Physical and Mechanical Properties	52
3.4.1 Particle size distribution analysis.....	52
3.4.2 Setting time	53
3.4.3 Compressive strength test	53
3.4.4 Hydration (internal temperature) test.....	54
3.5 Chemical Group and Microstructure Characterization.....	55
3.5.1 X-Ray diffraction (XRD) analysis	55
3.5.2 Fourier transform Infrared (FTIR) analysis	55
3.5.3 SEM and EDX analysis	56
3.6 Remark	57
PART 2 CURING MECHANISMS AND PROPERTIES OF GEOPOLYMERS.....	58
CHAPTER 4 EFFECT OF MANUFACTURING PROCEDURES ON MECHANISMS AND PROPERTIES OF FLY ASH-BASED GEOPOLYMERS.....	59
4.1 Introduction	59
4.2 Materials and Testing Methods	60
4.2.1 Materials and designation of mixtures.....	60
4.2.2 Manufacturing procedures	61
4.3 Analytical Methods	62
4.4 Results and Discussion	63
4.4.1 Setting time	64
4.4.2 Compressive strength.....	64

4.4.3 Measurement of internal heat accumulated inside the samples	66
4.4.4 Analysis on microstructures and elemental composition	68
4.4.5 Functional group analysis	70
4.4.6 Morphology and crystallinity analysis.....	71
4.4.7 Effect of water-to-solid ratio on pre-dry mixing process (C)	72
4.5 Remark	73
CHAPTER 5 SYNTHESIS AND CHARACTERIZATIONS OF GEOPOLYMER- PORTLAND CEMENT	75
5.1 Introduction	75
5.2 Materials	76
5.3 Experimental Procedures and Methodologies	76
5.3.1 Functionalities of geopolymer constituents	76
5.3.2 Function of OPC in GeoPC system	77
5.3.3 Analytical methods	78
5.4 Results and Discussion	78
5.4.1 Functionality of alkaline activators.....	78
5.4.2 Functionality of OPC in GeoPC system	88
5.4.3 Analysis on elemental compositions and ratios of GeoPC system.....	99
5.5 Remark	103
CHAPTER 6 COMPRESSIVE STRENGTH AND MICRO-MECHANISMS OF GEOPOLYMER-PORTLAND CEMENT AT VARIOUS CURING TEMPERATURES	105
6.1 Introduction	105
6.2 Materials and Testing Methods	106
6.2.1 Materials	106
6.2.2 Designation of Geopolymers, OPC and GeoPC mixtures	106
6.2.3 Sample preparation and curing regimes.....	107
6.3 Analytical Methods	107
6.4 Results and Discussion	108
6.4.1 Functional groups of the mixtures at various curing temperatures.....	108
6.4.2 Microstructures of the mixtures at various curing temperatures	111
6.4.3 Morphology of the mixtures at various curing temperatures.....	112
6.4.4 Compressive strength at various curing temperatures	116
6.4.5 The rule of mixtures for GeoPC composite by mass fraction ratio	120
6.5 Remark	121

PART 3 PRODUCTION OF SELF-CURED GEOPOLYMER CEMENT.....	123
CHAPTER 7 COMBINATION OF PRE-DRY MIXING PROCESS AND GEOPOLYMER-PORTLAND CEMENT FOR THE PRODUCTION OF SELF-CURED GEOPOLYMER CEMENT.....	124
7.1 Introduction	124
7.2 Materials and Methodologies	125
7.2.1 Materials	125
7.2.2 Designation of mixtures and sample preparations.....	125
7.2.3 Analytical techniques.....	126
7.3 Results and Discussion	127
7.3.1 Internal heat liberation of Self-cured geopolymer cement	127
7.3.2 Functional groups of Self-cured geopolymer cement.....	128
7.3.3 Microstructures and morphology of Self-cured geopolymer cement	130
7.3.4 Compressive strength of Self-cured geopolymer cement	132
7.4 Remark	133
CHAPTER 8 EFFECT OF SAMPLE SIZE AND EXTRA INTERNAL HEAT ACCOMULATION ON STRENGTH OF SELF-CURED GEOPOLYMER CEMENT	134
8.1 Introduction	134
8.2 Experimental Procedures.....	135
8.2.1 Materials and mixture designations	135
8.2.2 Sample preparation	136
8.2.3 Analytical techniques.....	136
8.3 Results and Discussion	137
8.3.1 Effect of specimen size on the compressive strength of GP in different manufacturing processes.....	137
8.3.2 Effect of specimen size on the strength of GeoPC and Self-cured geopolymers	140
8.4 Remark	144
PART 4 FINAL APPRAISAL OF THE RESEARCH WORK	145
CHAPTER 9 CONCLUSIONS AND FUTURE RESEARCH	146
9.1 Summary	146
9.2 Conclusions	148
9.3 Future Research and Recommendation	152

BIBLIOGRAPHY	154
APPENDIXES	168
APPENDIX A: ADDITIONAL DATA	169
APPENDIX B: CALCULATIONS OF WATER-TO-SOLID (w/s) RATIOS AND OXIDE MOLAR RATIOS OF THE MIXTURES	173
APPENDIX C: PUBLICATIONS, CONFERENCES AND AWARDS	176
APPENDIX D: PUBLISHED JOURNAL PAPERS	180

LIST OF TABLES

Table 2.1 Typical compositions of Portland cement.....	10
Table 2.2 Typical mineralogical compositions of Portland cement.....	11
Table 2.3 A representation of chemical composition using in geopolymer synthesis by raw prime materials.....	24
Table 2.4 Compressive strength of various alkaline activators in geopolymer synthesis....	27
Table 2.5 Compressive strength for different curing regimes in geopolymer synthesis.....	33
Table 3.1 Chemical compositions of fly ash and commercial OPC	48
Table 3.2 Mixture descriptions	51
Table 4.1 Chemical compositions of fly ash.....	60
Table 4.2 Details of fly ash-based mixtures in different processes.....	61
Table 4.3 Elemental compositions and ratios in the mixtures at 28-day age.....	70
Table 4.4 Mixtures and compressive strengths of GP process C for various w/s ratios	72
Table 5.1 Chemical compositions of fly ash and commercial OPC	76
Table 5.2 Detail of investigation on mixture combinations.....	77
Table 5.3 Images of formation characteristic of individual combinations.....	81
Table 5.4 SEM images of geopolymer constituents at the ages of 3 and 28 days	82
Table 5.5 Compressive strength of GeoPC system.....	90
Table 5.6 FTIR absorption peaks of resulted cement products at the 28-day age	95
Table 5.7 Crystalline phases of resulted cement products at the age of 28 days	97
Table 5.8 SEM images of GeoPC system at the ages of 3 days and 28 days	98
Table 5.9 Elemental compositions and ratios in GeoPC mixtures at the 28-day age	99
Table 5.10 The elemental compositions of ternary diagram of Ca–Na–Al–Si system.....	100
Table 6.1 Chemical compositions of fly ash and commercial OPC	106
Table 6.2 Details of GP, OPC and GeoPC30 mixtures.....	107
Table 6.3 Images of OPC, GP and GeoPC30 at various curing temperatures.....	111
Table 6.4 Percentage of crystallinity and amorphous phases of OPC, GeoPC and GP.....	115
Table 7.1 Chemical compositions of fly ash and commercial OPC	125
Table 7.2 Design of GeoPC mixtures and Self-cured geopolymers	126
Table 7.3 SEM images of GeoPC mixtures in processes B and C at the 28-day age	130
Table 8.1 Testing series of prism and cube specimens	136
Table 9.1 Summary diagram of the advantages of Self-cured geopolymer cement	147

LIST OF FIGURES

Figure 1.1 Research programme of the study of Self-cured geopolymer cement.....	8
Figure 2.1 Portland cement production process	9
Figure 2.2 Rate of heat evolution of OPC hydration at 25°C	13
Figure 2.3 Hydration and structure development in cement paste.....	14
Figure 2.4 Coal-fired power station and fly ash collection.....	16
Figure 2.5 Crystallization temperature against Si/Al ratio of zeolite and geopolymers	18
Figure 2.6 Typical geopolymer synthesis process	19
Figure 2.7 Type of poly-sialates structures	20
Figure 2.8 A reaction pathway involving the poly-condensation	20
Figure 2.9 Model of geopolymerization.....	21
Figure 2.10 Compressive strength vs type of materials	23
Figure 2.11 Theoretical framework of geopolymers cured at ambient temperature.....	42
Figure 2.12 Conceptual framework of the research.....	44
Figure 3.1 Particle size distribution of OPC powder	47
Figure 3.2 Particle size distribution of fly ash particles.....	48
Figure 3.3 SEM images of OPC and fly ash	48
Figure 3.4 Sodium hydroxide and sodium silicate in containers	49
Figure 3.5 Some of main experimental equipment used in laboratory	50
Figure 3.6 Samples wrapping after casting and placing in plastic bags before curing	52
Figure 3.7 Particle size distribution analyzer.....	53
Figure 3.8 Vicat apparatus	53
Figure 3.9 Compressive strength test of prism and cube	53
Figure 3.10 Set-up of the curing measurement in insulated container.....	54
Figure 3.11 Sieved particles in XRD testing discs and XRD machine.....	55
Figure 3.12 FTIR machine and sieve vibration machine	56
Figure 3.13 Samples on pins, samples on SEM disc and SEM machine.....	56
Figure 4.1 Testing diagram of different manufacturing processes (A, B and C).....	62
Figure 4.2 Testing diagram of pre-dry mixing process (C)	62
Figure 4.3 Drying behavior after 1 hour of mixing processes A, B and C	64

Figure 4.4 Compressive strength of geopolymers in different processes	65
Figure 4.5 Heat evolution of alkaline soluble preparation.....	66
Figure 4.6 Average heat evolution of geopolymers during a 24-hour period.....	67
Figure 4.7 SEM images and EDX spectrum of geopolymers at the 28-day age.....	69
Figure 4.8 FTIR spectrum of geopolymers at the 28-day age.....	70
Figure 4.9 X-ray diffraction patterns of geopolymers processes A, B and C at the age of 28 days	72
Figure 4.10 SEM images of geopolymers in pre-dry mixing process (C) for various w/s ratios at the 28-day age	73
Figure 5.1 Setting time of geopolymer constituents	83
Figure 5.2 Heat evolution of geopolymer constituents during alkalinity over a 24-hour period	83
Figure 5.3 Compressive strength of geopolymer constituents at the 28-day age.....	84
Figure 5.4 FTIR spectrums of geopolymer constituents at the 28-day age	84
Figure 5.5 X-ray diffraction patterns of geopolymer constituents at the 28-day age	85
Figure 5.6 Setting time of OPC, geopolymers and GeoPC paste.....	89
Figure 5.7 CaO/SiO ₂ and SiO ₂ /Al ₂ O ₃ ratios vs 28-day strength and setting time	91
Figure 5.8 Heat evolution of GeoPC systems over a 24-hour period	93
Figure 5.9 The maximum temperature against the time for each combination	93
Figure 5.10 FTIR spectrums of GeoPC system at the 28-day age.....	95
Figure 5.11 X-ray diffraction patterns of GeoPC system at the 28-day age	96
Figure 5.12 Projection OPC, GeoPC system and GP onto the ternary Ca–Al–Si system and ternary Na–Al–Si system determined by SEM-EDX analysis.....	101
Figure 5.13 Compressive strength, Ca/Si ratios and Si/Al ratios of mixtures at the age of 28 days	102
Figure 5.14 Coexistence gel in the GeoPC30 at the 28-day age.....	102
Figure 6.1 Images of casting, moisture loss protection, and under curing regimes.....	107
Figure 6.2 FTIR spectrums of OPC and GP cured at 10 to 70°C and 28-day age.....	109
Figure 6.3 FTIR spectrums of GeoPC30 mixture cured at 10 to 70°C and 28-day age	110
Figure 6.4 FTIR spectrums of OPC, GeoPC30 and GP at 20°C and 28-day age	110

Figure 6.5 XRD patterns of OPC and GP cured at 10 to 70°C and 28-day age.....	113
Figure 6.6 XRD patterns of GeoPC30 at various curing temperatures.....	113
Figure 6.7 XRD patterns of OPC, GeoPC30 and GP at 20°C and 28-day age	114
Figure 6.8 Crystallinity and amorphous percentage of OPC, GeoPC30 and GP at various curing temperatures (28-day age).....	116
Figure 6.9 Strength of OPC at various curing temperatures at 3 and 28 days	117
Figure 6.10 Strength of GP at various curing temperatures at 3 and 28 days.....	118
Figure 6.11 Strength of GeoPC30 at various curing temperatures at 3 and 28 days	119
Figure 6.12 Strength development at 3-day age and 28-day age of OPC, GeoPC30 and GP for various curing temperatures	120
Figure 6.13 Linear regression lines of calculated values and tested values of GeoPC30 at the 28-day age	121
Figure 7.1 Testing diagram of GeoPC system as Self-cured geopolymers.....	126
Figure 7.2 Heat accumulated inside various GeoPCs with general mixing process (B)....	127
Figure 7.3 Heat accumulated inside various mixtures with pre-dry mixing process (C)...	128
Figure 7.4 IR spectrums of GeoPC in process B and process C at the 28-day age	129
Figure 7.5 XRD patterns of general GeoPC system (process B) at 28 days.....	131
Figure 7.6 XRD patterns of pre-dry mixing GeoPC system (process C) at 28 days.....	131
Figure 7.7 Compressive strength of GeoPC mixtures synthesized with processes B and C	132
Figure 8.1 Two different sizes and geometries of cube and prism samples	137
Figure 8.2 Compression test of cubic sample and prismatic sample	137
Figure 8.3 Compressive strength of GP in different manufacturing processes.....	138
Figure 8.4 Relationship between mean compressive strength of GP 100 mm cubes and 40mm x 40mm x 160mm prisms in different processes	139
Figure 8.5 Compressive strength of prismatic samples synthesized with general process (B) and Self-cured process (C).....	140
Figure 8.6 Compressive strength of cubic samples synthesized with general process (B) and Self-cured process (C).....	140
Figure 8.7 Compressive strength of GP in different manufacturing processes.....	141

Figure 8.8 Relationship between average 3-day strength of 100 mm cubes and 40mm x 40mm x 160mm prisms for processes B and C.....142

Figure 8.9 Relationship between average 28-day strength of 100 mm cubes and 40mm x 40mm x 160mm prisms for processes B and C143

LIST OF ABBREVIATIONS

A/FA	Alkaline activator-to-fly ash ratio
ACI	American Concrete Institute
AS	Australian Standard
ASR	Aluminosilicate reactivity
ASTM	American Society of Testing Materials
ATR	Attenuated total reflectance
BS EN	British Standard European Norm
C/S	Elemental ratio of calcium-to-silica
CFA	Coarse original fly ash
CKD	Cement kiln dust
EDXA	Energy dispersive X-ray analysis
FA	Fly ash
FFA	Fine fly ash
FTIR	Fourier transform infrared
GBFS	Granulated blast-furnace slag
GeoPC	Geopolymer-Portland cement
GP	Geopolymer cement paste
GW	General wastes and recycles materials
IEA	International Energy Agency
IR	Infrared
IW	Industrial wastes
LCA	Life cycle assessment
MAS	Magic angle spinning
MFA	Medium fineness fly ash
MK	Meta-kaolin
NM	Natural materials
NMR	Nuclear magnetic resonance
OPC	Ordinary Portland cement
PFA	Pulverized fly ash
PPE	Personal protective equipment
RGC	Reinforced geopolymer concrete
RHA	Rice husk ash
RT	Room temperature

S/A	Elemental ratio of silica-to-alumina
SEM	Scanning electron microscope
SH	Sodium hydroxide (NaOH)
SS	Sodium silicate (Na_2SiO_3)
TCLP	Toxicity characteristic leaching procedure
TMW	Tungsten mine waste
UTM	Universal testing machine
w/s	Water-to-solid ratio
WPSA	Waste paper sludge ash
XRD	X-Ray diffraction

LIST OF SYMBOLS

σ_{GeoPC30}	Compressive strength of GeoPC30 mixture at the 28-day age (MPa)
σ_{OPC}	Compressive strength of OPC mixture at the 28-day age (MPa)
σ_{GP}	Compressive strength of geopolymer mixture at the 28-day age (MPa)
σ_{cu}	Compressive strength of 100 mm cube sample (MPa)
σ_{pr}	Compressive strength of 40mm x 40mm x 160mm prismatic sample (MPa)
f_{OPC}	Mass fraction of OPC paste in the composite
f_{GP}	Mass fraction of GP paste in the composite
m_{OPC}	Mass of OPC paste (gram)
m_{GP}	Mass of GP paste (gram)
M	Molarity (concentration of alkaline solution)
M_s	Modulus of sodium silicate ($\text{SiO}_2/\text{Na}_2\text{O}$ molar ratio)
R	Coefficient of correlation
R^2	Coefficient of determination

PART 1
INTRODUCTION, LITERATURE REVIEW AND
METHODOLOGY

CHAPTER 1 INTRODUCTION

1.1 Background of Research

In construction industry nowadays, many attempts have been carried out in the research community to identify low-carbon technologies and products, which support the concept of environmental friendly materials and sustainable development. Ordinary Portland cement (OPC) manufacturing process is known as one of the main participators which consumes intensive energy and releases a large amount of greenhouse gas to atmosphere during its production (Maholtra, 2002). Around seven percent of the worldwide carbon dioxide (CO₂) emission is accounted for this clinker process which seriously contributes to the global climate change (Shi, et al., 2011). The alternative low-carbon cementing binders have been, therefore, extensively studied to reduce that amount of greenhouse gas. One of the efforts is to promote alternative binders by utilizing abundant of alumina-silicate (pozzolanic) wastes from industrial sector, e.g. fly ash (Chindaprasirt, et al., 2007), bottom ash (Hardjito & Fung, 2010), cement kiln dust (Khater, 2012), silica fume (Nuruddin, et al., 2011b) and GBFS (Nath & Sarker, 2012). Alumina-silicate materials, especially fly ash, have been identified as prime materials to produce the eliminated cement based concrete. Partial or total replacement of those pozzolanic by-products has also been investigated in order to decrease the amount of OPC consumption (Komnitsas & Zaharaki, 2007). Many research studies have also revealed that alumina-silicate materials can be used as prime materials to synthesize a cementitious binder by activating with alkaline solutions, which is known as alkaline-activated cement or “Geopolymer cement” (Al Bakri, et al., 2011a).

Apart from that, the term “Geopolymers”, which was established by Joseph Davidovits in 1979, is also used and receives much more attention as an alternative binder for construction material (Alonso, et al., 2011; Davidovits, 1991) It can perform a wide variety of properties and characteristics, including the reduction in cost and less environmental impacts (Duxson, et al., 2007a). The production of geopolymer cement (GP) commonly uses alkaline solutions mixing with raw starting materials to form homogenous slurry. Curing condition is one of the major factors affecting the mechanical properties and micro-structures of geopolymers. Heat curing above ambient temperature is therefore applied, approximately from 40 to 90°C for 6 to 48 hours, to accelerate a geopolymeric reaction and improve its mechanical performances. Afterward, geopolymers is continually cured or left in room temperature for further handlings (Chindaprasirt, et al., 2007). The properties of

geopolymer cement, tested in accordance with the testing standard of OPC, are in the same order as or even better than those made from OPC. Moreover, replacing OPC with alumina-silicate waste brings about the benefits not only for cost saving but also the reduction of environmental impact up to 9% less CO₂ emission when compared with OPC binder (Turner & Collins, 2013). In construction sector, geopolymers is developed and theoretically produced by utilising industrial by-products or wastes. Fly ash, a by-product from coal-fired power station, seems to be the most widely used as a prime material producing geopolymers because of its richness in alumina-silica composition and the considerable un-utilised amount (Nath & Sarker, 2015).

Countless number of research papers has studied the curing conditions affecting geopolymer properties. The basis results clearly proved that fly ash-based geopolymer cement gained some strength with very slow rate in ambient curing conditions (Deevasan & Ranganath, 2010), while the strength development and other mechanical properties are evidently improved when cured in high temperature (above room temperature e.g. in the oven) within the specific durations (Raijiwala & Patil, 2010). The considered challenge is to step over the limitation of heat curing process: precast components, and to be more convenient in practical work or in field applications. The next research perspective has been launched to develop geopolymers which is able to achieve reasonable strength in ambient curing conditions. Those efforts are, for example, using of ground fine or milled prime materials (Chindaprasirt, et al., 2010; Somna, et al., 2011), applying extra heat from environment or other sources, or even increasing extra calcium content to the geopolymer mixtures (Khater, 2011; Suwan & Fan, 2014). The efforts to develop ambient-cured geopolymer cement are not only for initiating commercial viability and on-site operation but also for achieving energy saving and economical aspect.

1.2 Aim of the Research

The main purpose of this research is to introduce an effort in the development of “Self-cured geopolymer” technology. The experimental work of two major approaches, (i) using OPC as an additive and (ii) manufacturing in various processes, have been established and intensively investigated with the typical low calcium fly ash-based geopolymer cement as a controlled-mixture. Beyond the geopolymeric reactions and mechanisms, it is found that extra calcium content from additional OPC on geopolymer cement (Geopolymer-Portland cementitious system, GeoPC) improves curing regime itself for a greater early strength and mechanical properties at ambient curing temperature, while the latent heat generated from

reactions of its high potential energy compounds (e.g. OPC or alkaline activators) was also appreciable. This alternative heat liberation was, therefore, observed as a comparable factor to heat curing from any other external sources. Both of those approaches led to differences in mechanical properties, and the combination of them could also raise a feasibility of geopolymer cement to achieve reasonable strength at ambient curing temperature as “Self-cured geopolymer cement”.

1.3 Research Objectives

As aforementioned, the main purpose of this present research was to study and develop the fly ash-based geopolymer cured in ambient conditions as called “Self-cured geopolymer cement”. Two major approaches, (i) using OPC as an additive and (ii) manufacturing in various processes, have been intensively investigated in terms of mechanical properties and mechanisms. The objectives of this research therefore are:

1. To study the effect of manufacturing procedures on mechanisms and mechanical properties of low calcium fly ash-based geopolymer cement cured at room temperature;
2. To investigate the effect of additional OPC in low calcium fly ash-based geopolymer cement (Geopolymer-Portland cementitious system, GeoPC) on its mechanisms and mechanical properties when cured at room temperature;
3. To identify the influence of curing temperature affecting on the mechanisms and mechanical properties of Geopolymer-Portland cementitious (GeoPC) system;
4. To develop the combination of pre-dry mixing process and GeoPC system for the production of Self-cured geopolymer cement;
5. To examine the contributions of constituents of the established dry-mixture to the curing and microstructure development of Self-cured geopolymers.

1.4 Research Scope

The experimental work of this study focused on engineering properties throughout the investigation on mechanisms and chemical reactions of low calcium fly ash-based geopolymer cement as a construction material. The main materials used in laboratory were fly ash, OPC, sodium hydroxide and sodium silicate, while mixture proportions and manufacturing procedures were systematically varied and shown as work packages in Chapter 3. The physical properties of raw materials and resulted products were tested on particle size distribution analysis, setting time, setting characteristic, compressive strength

and internal temperature measurement. Micro-mechanism observations were analysed by FTIR, XRD, SEM and EDXA. The experimental work consists of:

1. Manufacturing procedures: with three different procedures of General mixing process, Separate mixing process and Pre-dry mixing process;
2. GeoPC system: with the additional OPC in low calcium fly ash-based geopolymer cement from 10 to 90 percent by mass;
3. Curing temperature: with moisture loss protection in curing chambers from 10°C, by increment of 10°C interval, to 70°C;
4. Self-cured geopolymer cement: produced by using pre-dry mixing process with the optimum GeoPC proportion.

1.5 Research Significance

This research presents an inclusive study in developing Self-cured geopolymer cement which is able to achieve superior strength than that of typical geopolymer cement at ambient curing temperature, including ability to work in the field applications. The main prime material in this study was fly ash, which is a low-cost alumina-silicate waste generated worldwide in huge quantities from coal-fired power station. Its significance is to extend the limitation of heat (oven) curing process, e.g. precast components, to be more convenience on-site operation or in-field applications. With of the developed Self-cured geopolymer techniques, there are potentials that could increase the commercial viability of geopolymers as a construction material in construction industry by eliminating heating process and preparation of alkaline liquids. Thus, the significance of this thesis can be summarised as follows:

- Innovations
 - Apply the benefit of liberated heat from pre-dry mixing process for GP curing purpose.
 - Validate the combined GeoPC system and pre-dry mixing process for a Self-cured geopolymer cement to be produced at ambient temperature.
 - Realise the application of Geopolymer cement powder as conventional OPC by just adding water.
- Reuse of wastes
 - Convert alumina-silicate wastes from any industrial or natural sources to prime materials of geopolymer cement production.

- Advantages in construction industry
 - Extend the application from small prefabricated-components to on-site or large-scale applications.
 - Eliminate the difficulties in typical-alkaline solution preparation with a controllable mix proportion, ease of handling and economical saving of pre-dry mixing process.

1.6 Organisation of Contents

All chapters of this thesis are based on systematic experimental work. Major outcomes of Chapters 4, 5, 6, 7 and 8 have been published or submitted to peer-reviews or submitted to academic conferences. Brief details of each Chapter can be summarised as follows (Figure 1.1):

Chapter 2 provides a literature review of Ordinary Portland Cement (OPC), the use of pozzolanic material (Fly ash) in Portland cement and Geopolymer technology. The contents of the review mainly focus on the fundamental of geopolymers, geopolymerization reaction and its chemistry, together with the role of factors affecting the properties and mechanisms of geopolymerization. The literature and summary of efforts developing geopolymer cement cured in ambient conditions are also included.

Chapter 3 provides a general description of materials and methods in the experimental work. Typical materials used in the laboratory are presented with general properties and specific characterizations. Details of testing equipment and general preparation process of samples are described. Testing techniques for the investigation of both mechanical properties and mechanisms are also provided in full details.

Chapter 4 investigates the effect of different manufacturing procedures of low calcium fly ash-based geopolymer cement cured in room (ambient) temperature on the mechanical properties and mechanisms. Compressive strength, internal heat liberation and micro-structure of each manufacturing procedure are the key results to identify an appropriate method to fulfil the development of Self-cured geopolymer cement.

Chapter 5 investigates the effect of OPC inclusion in low calcium fly ash-based geopolymer cement (GeoPC) on the mechanical properties and mechanisms. The typical manufacturing procedure was used to prepare those geopolymers in the test. All samples were prepared, cured and tested at room temperature with the various additional OPC content from 10 to 90% by mass. The sample characterizations and elemental compositions

of each single mixture of geopolymer constituents and GeoPC are also explored and defined. Compressive strength and setting behaviour are the key results to identify the appropriate GeoPC proportion to fulfil the development of Self-cured geopolymer cement.

Chapter 6 investigates the influence of curing temperature on the compressive strength and mechanisms of GeoPC system. The temperatures from 10°C, with an increment of 10°C interval, to 70°C were used for curing purpose of all samples. OPC paste and typical geopolymer paste were prepared for the test series as controlled mixes. GeoPC system in this study was represented by GeoPC30 mixture (70%-geopolymers and 30%-OPC by mass) due to the reasonable terms of strength achieved, economical aspect and environmental concern. The range of curing temperature which provided the reasonable strength is the key to identify an optimum heat curing for GeoPC system.

Chapter 7 presents the study on a combination of pre-dry mixing process and GeoPC system for the production of Self-cured geopolymer cement. The main findings from the pre-dry mixing process (Chapter 4) and optimum GeoPC proportion (Chapter 5) were applied in the experimental work to produce the Self-cured geopolymer cement, which is able to achieve reasonable strength at room curing temperature. The GeoPC system synthesized in typical procedure (general mixing process) was also studied as a compared mixture in term of mechanical properties and mechanisms.

Chapter 8 explores the effect of specimen size on compressive strength of Self-cured geopolymer cement. The crushing tests on the standard cubic samples (100mm x 100mmx100mm) and standard prism samples (40mmx40mmx160mm) were used to analyse the effect of size and geometry of both general mixing GeoPC system and pre-dry mixing GeoPC system (Self-cured geopolymer cement). The advantages in term of additional heat accumulation from pre-dry mixing and larger size (cubic sample) were also addressed.

Chapter 9 contains the final appraisal of the test and future research perspectives. Some advantages and limitations of using this Self-cured technology are also listed together with the economic benefit and life cycle assessment.

CHAPTER 2 LITERATURE REVIEW

2.1 Portland Cement and Fly Ash

2.1.1 Ordinary Portland cement

Portland cement, an active hydraulic binder, is the most widely used construction material for concrete making. To produce Portland cement, raw materials are extracted from quarry and must be crushed, grounded and blended in a raw mill, see Figure 2.1 for material preparation procedure. The main raw materials are natural limestone (CaCO_3), Clay or Shale (SiO_2 , Al_2O_3), Laterite or Iron oxide (Fe_2O_3), Silica sand (SiO_2) and Gypsum (CaSO_4) (Bogue, 1955). Two distinct methods, wet and dry processes, are commonly used to make a raw-feed (meal) for clinker production. However, more energy consumption and fuel costs are notably involved in wet process rather than in dry process. That raw-meal is then sent from silos to a preheater and rotary kiln subsequently. Burning at a temperature around 1250 to 1500°C transforms the raw-meal to become dark-black gravels sizing of 15 to 25 mm. which is called cement clinker. The clinker is afterward finely ground in cement mill with some designated additives of gypsum until the average particle size is approximately 10 to 50 μm . An anhydrous grey powder, known as Portland cement, is kept in cement silos and ready to be packed and dispatched for use (Mehta, 1986; Soroka, 1979) (Figure 2.1).

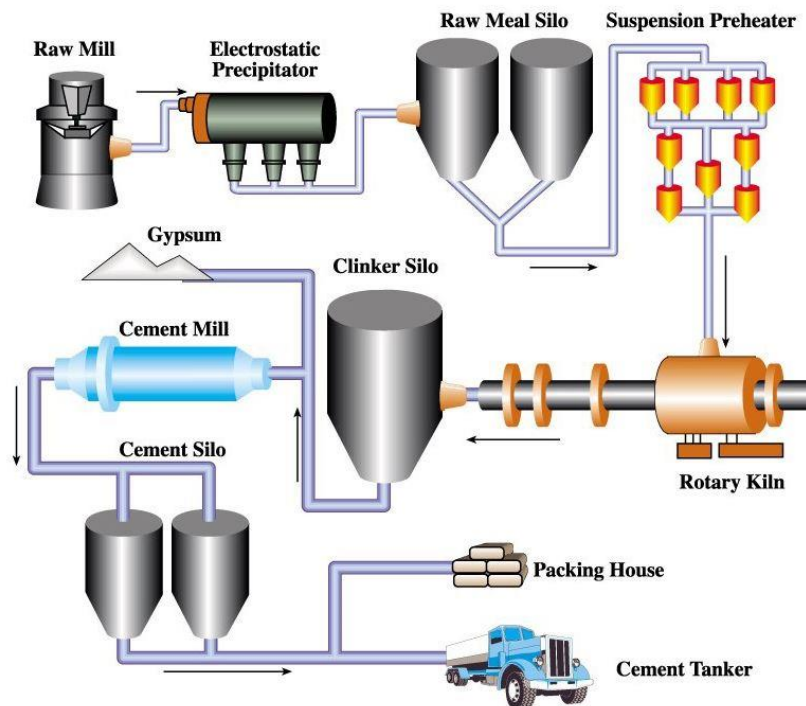


Figure 2.1 Portland cement production process
(ClimateTechWiki, 2016)

Accordingly, raw materials of Portland cement consist mainly of CaCO_3 (limestone) and alumina-silicate minerals (clay or shale), and the combined contents of four major oxides (i.e. CaO , SiO_2 , Al_2O_3 and Fe_2O_3) are therefore approximately 90 percent by cement weight. The minor constituents remaining with around 10 percent probably are MgO , K_2O , Na_2O , SO_3 and gypsum (Soroka, 1979). The typical composition of Portland cement and its special shorthand (symbol) which is used to simplify the chemical formula are given in Table 2.1 (Bye, 1983; Feng, et al., 2012).

Table 2.1 Typical compositions of Portland cement (Bye, 1983)

Oxide	Symbol	Composition (wt. %)
CaO	C	62.0 - 67.0
SiO_2	S	18.0 - 24.0
Al_2O_3	A	4.0 - 8.0
Fe_2O_3	F	1.5 - 4.5
MgO	M	0.5 - 4.0
K_2O	K	0.1 - 1.5
Na_2O	N	0.1 - 1.0
H_2O	H	“nil”
SO_3	-	2.0 - 3.0
Free lime	-	0.5 - 1.5
Loss on ignition, LOI	-	1.0 - 3.0

The compound composition of Portland cement is evidently established by phase diagrams and systems with the aforementioned oxide compositions. With the ternary systems of $\text{CaO-SiO}_2\text{-Al}_2\text{O}_3$, the basis results of equilibrium are attained as formation of various kinds of calcium components i.e. C_3S , C_2S , C_3A and C_4AF . Hence, these four major compounds are intensively studied on the functionalities and properties (Bye, 1983; Soroka, 1979).

Tricalcium silicate (C_3S) is the major constituent of Portland cement with the percentage around 50 to 70. As it is unstable at room temperature, the small amount of other oxides in solid solution is usually used by cement manufacturers to produce impure C_3S as *alite*. The development of mechanical properties of Portland cement is obtained by C_3S , including a quick hydration and fast setting behaviour in a few hours. The moderate heat liberation from hydration is also released by approximately 500 J/g. Dicalcium silicate (C_2S) is presented in Portland cement at around 10 to 30%. There are four distinguished principal forms of C_2S defined as α , α' , β and γ . However, only the impure form of $\beta\text{-C}_2\text{S}$ is considered in commercial clinker as *belite*. It slowly hydrates with water and also releases quite low heat during the hydration of only 250 J/g. Even though the early strength is not that much high, the later age strength is able to reach the same level as C_3S . Tricalcium aluminate (C_3A) content in Portland cement is approximately 3 to 13%. It reacts with water

almost abruptly and releases an intensive heat, i.e. 850 J/g during the hydration. Flash setting is obtained, together with comparative low strength. However, as C₃A is necessary in clinker manufacturing process, gypsum is therefore added in order to retard reaction of C₃A and to achieve normal setting behaviour. Tetracalcium aluminoferrite (C₄AF) appears at only 5 to 10% in Portland cement. Its strength is uncertain but generally quite low, whereas, the hydration is quick with moderate heat liberation of 420 J/g. The main characteristic of C₄AF is said to result in the green-grey tinge of Portland cement.

The proportion of each constituent could affect the properties of hardened cement paste (Barnes, 1983; Soroka, 1993). The relative mineral components or additives therefore categorise the types of cement, for example, American standard ASTM C150:2016 or European standard BS EN 197-1:2011. The summary of calcium compounds is presented in Table 2.2 (McNaught & Wilkinson, 1997). The effects of heat liberated from exothermic reaction of hydration is described in next section *hydration of cement*, and also taken to the study of additive for geopolymers cement afterward.

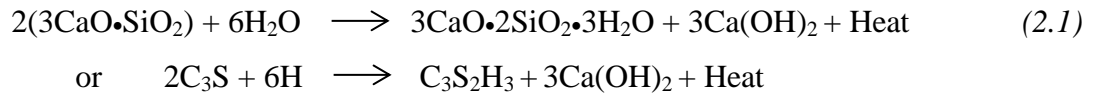
Table 2.2 Typical mineralogical compositions of Portland cement (McNaught, 1997)

Compounds	Tricalcium silicate	Dicalcium silicate	Tricalcium aluminate	Tetracalcium aluminoferrite
<i>Chemical formula</i>	Ca ₃ SiO ₅	Ca ₂ SiO ₄	Ca ₃ Al ₂ O ₆	Ca ₄ Al ₂ Fe ₂ O ₁₀
<i>Oxide formula</i>	(CaO) ₃ SiO ₂	(CaO) ₂ SiO ₂	(CaO) ₃ Al ₂ O ₃	(CaO) ₄ Al ₂ O ₃ Fe ₂ O ₃
<i>Notation</i>	C ₃ S (Alite)	C ₂ S (Belite)	C ₃ A	C ₄ AF (Celite)
<i>Typical percentage</i>	50-70	10-30	3-13	5-10
<i>Rate of hydration</i>	Rapid (hours)	Slow (days)	Instantaneous	Rapid (minutes)
<i>Heat of hydration</i>	Medium ~500 J/g	Low ~250 J/g	Very high ~850 J/g	Medium ~420 J/g
<i>Strength development</i>	Rapid (days)	Slow (weeks)	Very rapid (one day)	Very rapid (one day)
<i>Ultimate strength development</i>	High	Probably high	Low	Low
<i>Mineral function</i>	Characteristic constituent of Portland cement	-	Sensitive with sulphate attack	Impart grey color

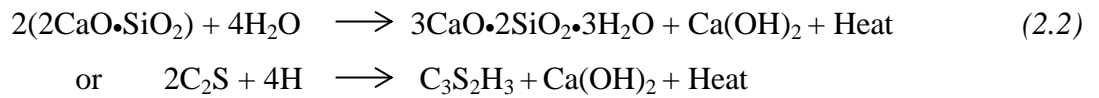
The anhydrous Portland cement acquires the adhesive property when mixed with water to become the cement paste. The chemical reaction between cement and water is commonly called *hydration of cement*. Generally, the hydration of cement may take place either *through-solution* mechanism or *topochemical* mechanism. In the case of *through-solution* mechanism, the cement is dissolved into solution. The resulting products are then precipitated out as hardened cement. The *topochemical* mechanism, sometime called solid-

state reaction, obtains the reactions directly on the surface of cement as a hydrolysis rather than dissolution. However, both mechanisms could be involved in hydration but, due to the less solubility of cement, the solid-state reaction is considered to be more noteworthy (Soroka, 1979). With several compounds in Portland cement, the hydration may complete in different, either or both, periods of time and final properties. The hydration products of individual compound are similar to each other due to the cognate of main constituents i.e. CaO, SiO₂ and Al₂O₃. In Portland cement, the approximate composition of calcium silicate hydrated (C-S-H: C₃S₂H₃) is formed with the assumption of completed hydration process (Mehta & Monteiro, 2006). The hydration of silicate species is presented by the following equations:

for tricalcium silicate (C₃S):

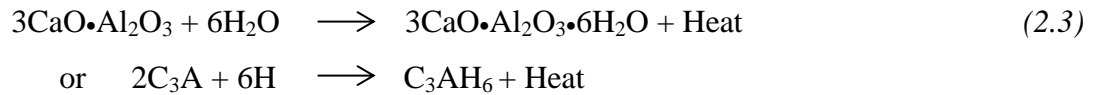


for dicalcium silicate (C₂S):

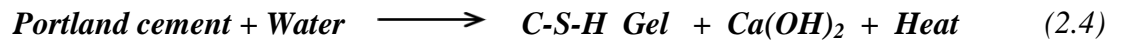


In general, tricalcium aluminate reacts instantaneously with water, forming cubic crystal of C₃AH₆. The presence of gypsum (CaSO₄•2H₂O) retards that immediate reaction and prevents cement paste from flash setting. The delaying effect of gypsum contributes to needle-like crystals formation of ettringite (3CaO•Al₂O₃•3CaSO₄•31H₂O). The hydration of C₃S is temporarily prevented by the layers of those ettringites which transformed to less-sufficient sulphate referred to as monosulphate in later stage. The existence of C₃A, ettringite and monosulphate, significantly influences the setting behavior of cement paste. By this, the hydrations of aluminate species are presented by the following equations:

for tricalcium aluminate (C₃A):



As a result of calcium compound hydration, it can be summarised that calcium silicate hydrated gel (C-S-H), calcium hydroxide or portlandite (Ca(OH)₂) and heat are produced. C-S-H is the most important formation, giving compressive strength with 75 to 80 percent of cement by volume, while Ca(OH)₂ also regenerates with 20 to 25 percent, including heat indicated in paradigm (2.4):



It can be seen that all Portland cement compound hydration emits heat to the environment. This is due to the non-equilibrium products in high-energy state of the cement. When cement acquires stable low-energy state once mixed with water, the exothermic reaction is presented and releases energy in the heat form. Rate of heat liberation depends mainly on the amount of those high potential-energy compounds. For typical Portland cement, it was found that approximately 50 percent of potential heat in Portland cement is liberated in the first three days, and 90 percent within the first three months of hydration (Mehta & Monteiro, 2006). Typically, there are five stages of heat evolution rate of OPC hydration measured by isothermal calorimeter which are: 1) the initial reaction, 2) the induction period, 3) the acceleratory period, 4) the decelerator period and 5) the slow continued reaction (Figure 2.2) (Mostafa & Brown, 2005).

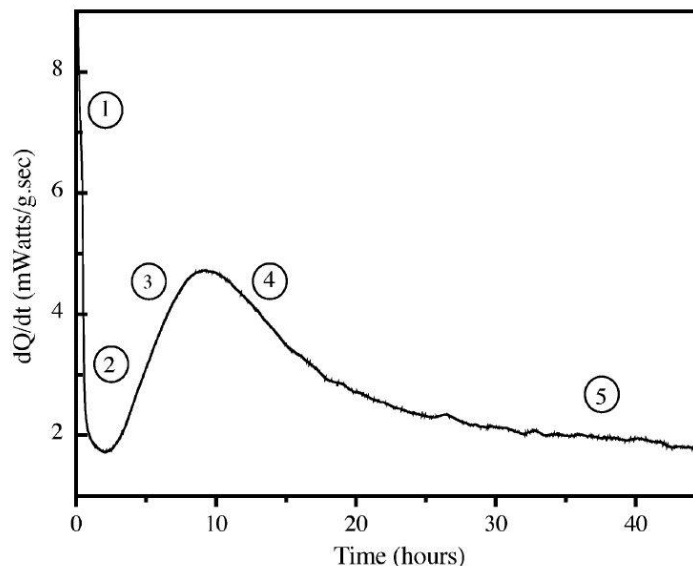


Figure 2.2 Rate of heat evolution of OPC hydration at 25°C (Mostafa & Brown, 2005)

The results of hydrolysis of calcium silicate and other compounds in Portland cement are presented in the paste mixture. During dormant period the main hydration products are Ca(OH)_2 and ettringite. C-S-H gel begins to form in an hour after providing stiffness to the cement while the porosity is decreased. After 1 day, calcium with alumina and iron oxide precipitates as $\text{C}_4(\text{A,F})\text{H}_{13}$, while ettringite starts conversion into monosulphate compound as illustrated in Figure 2.3 (Soroka, 1979). In facts, C-S-H is the most important formation providing mechanical strength to the paste, including 50 to 60 percent of solid volume in completely hydrated cement (Mehta & Monteiro, 2006). In normal case, the standard of strength measurement would be carried out at ages of 1 to 28 days.

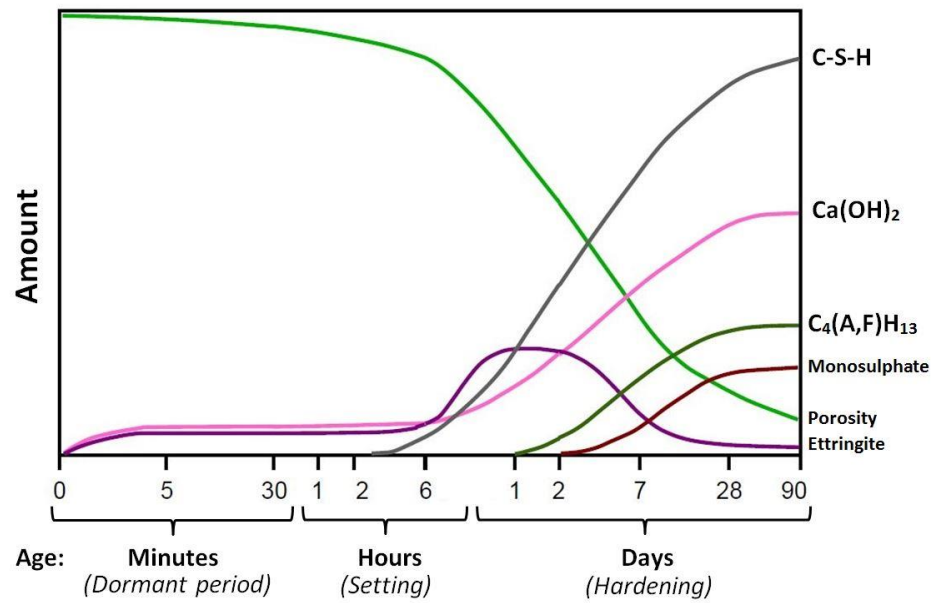


Figure 2.3 Hydration and structure development in cement paste

The demand on cement and concrete consumption is rising up with high economic growth, modern technology and industrial development. Portland cement is annually produced to approximately 1.6 billion tons worldwide and predicted to reach 3.5 billion tons by 2025 (Shi, et al., 2011). Portland cement production is known not only to be responsible for a large amount of greenhouse gas contributor but also to become one of the most energy-intensive manufacturers. Energy consumption for cement production can be theoretically calculated based on the enthalpy of clinker formation which is estimated to consume approximately 1.76 megajoule (MJ) for 1 kg of Portland clinker production (Worrell, et al., 2001) or about 3.2 to 6.3 gigajoule (GJ) per ton, including other manufacturing activities e.g. mining, crushing, gridding, clinker kiln, fuel combustion, etc. (Mehta, 2001; Oss & Padovani, 2003).

In addition, burning process (calcination) of raw materials intensively releases carbon dioxide (CO₂) to atmosphere as shown in following paradigm (2.5). According to the International Energy Agency's (IEA) Greenhouse Gas R&D Programme, it has been reported that one ton of cement production emits approximately 0.8 to 1.0 ton of carbon dioxide to atmosphere, therefore, production of nearly 2 billion tons globally nowadays would account for CO₂ emission around 6 to 7 percent in total (Mehta, 2001). Furthermore, other harmful gases, e.g. nitrogen oxides, sulphur oxides and particulates, are also emitted to the environment (Huntzinger & Eatmon, 2009).



Approximately, CO₂ concentration has dramatically increased from 315 part-per-million (ppm) in 1960 to 400 ppm in 2013, which is already surpassed the safe zone of 350 ppm (Hansen, et al., 2013). At this increasingly rate, those CO₂ concentrations are estimated to increase to over 800 ppm by the end of this century and could significantly cause the rise-up of global temperature and climate (Mehta, 2001). The world is thus led to face the global warming and climate changes faster than had previously been thought (Hoeven, 2014). To reduce those drawbacks of using Portland cement, the alternative materials, e.g. pozzolanic materials from industrial by-products, have therefore been studied to partially or totally replace the consumption of Portland cement.

2.1.2 The use of pozzolanic admixture (fly ash) in Portland cement

The admixtures in cement or concrete are known as ‘a material other than water, aggregates, hydraulic cement and fibre reinforcement used before or during mixing (ASTM C125-15B:2015)’ and ‘materials added during mixing process of concrete to modify the properties of mix in the fresh and/or hardened state (BS 8443:2005)’. The mineral admixtures are mainly classified into three types, which are Low-activity admixtures (e.g. limestone and dolomite), Cementitious admixtures (e.g. natural cement and blast furnace slag) and Pozzolanic admixtures. In contrast, the pozzolan could be subdivided into natural pozzolan (e.g. volcanic clay) and by-products pozzolan (e.g. pulverised fly ash and silica fume) (Soroka, 1993). To address environmental concerns, the main effort of this issue focuses on utilizing pozzolanic industrial by-products, especially for pulverized fly ash (PFA) from the coal-fired power station.

Fly ash is one of by-products from coal combustion, particularly from generating electric power generating process in coal-fired power plants as the process shown in Figure 2.4 (Silo Transport, 2016). When coal is burned off at the furnace, impurity minerals, e.g. clays, quartz and feldspar, are fused together in that high temperature. It is then solidified to glassy spherical particles and flies out with flue gas stream, known as *fly ash*. Most of fly ash particles are solid sphere shapes and could be observed with either or both hollow sphere (cenospheres) or packed with numerous of small spheres (plerospheres). Its particle sizes vary from <1 µm to 100 µm. Fly ash is subsequently collected by electrostatic precipitator and moved to storage area for further handling (Mehta, 1986). Amount of average fly ash production worldwide during 2010 to 2013, was approximately 610 to 650 million tons. Around 60 to 70 percent of total fly ash are produced in China (Tang, et al., 2013), 20 to 30 percent in the US and 10 to 20 percent in EU (ACAA, 2014). With those

large quantities produced annually, the utilizing of fly ash as admixture in cement and concrete is globally carried out.

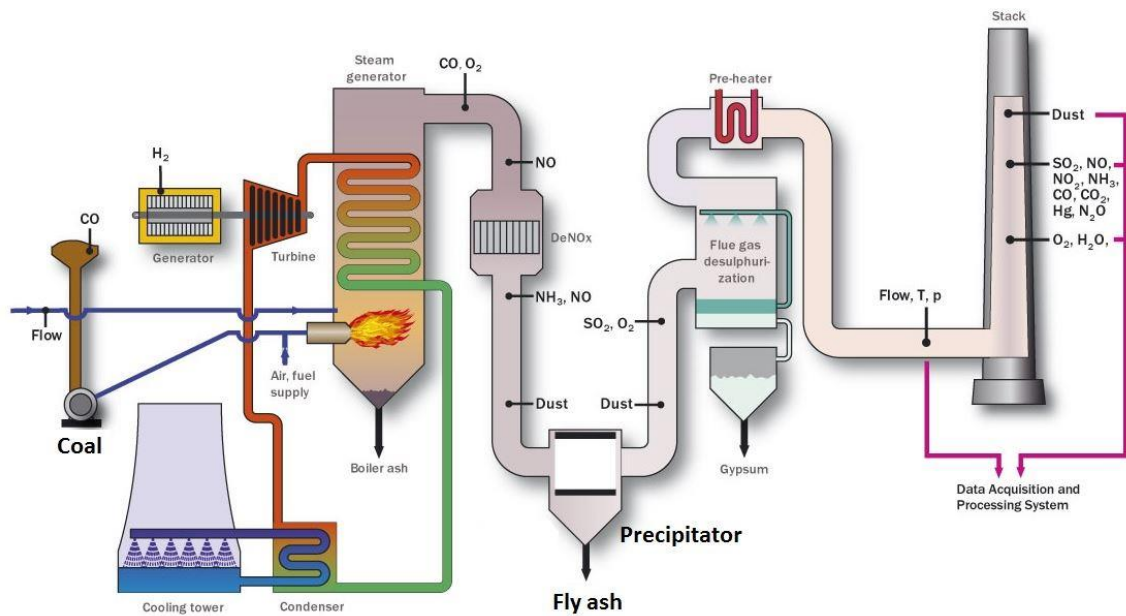
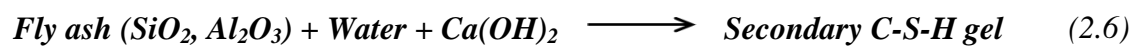


Figure 2.4 Coal-fired power station and fly ash collection (Silo Transport, 2016)

Many advantages of fly ash replacement in Portland cement have been revealed and applied in various applications in order to improve the properties of hardened cement and concrete. Generally speaking, calcium hydroxide ($\text{Ca}(\text{OH})_2$) from Portland hydration process (paradigm (2.4)) is a weak structure on acidic chemical durability and also influences the system into alkaline environment with approximately 12.4 to 13.5 in pH scale. The partial replacement of fly ash in the binder could react with those excess $\text{Ca}(\text{OH})_2$ and afterward, form alternative secondary C-S-H gel, called *Pozzolanic reaction* as presented in paradigm (2.6) (Mehta, 1986).



The secondary C-S-H from pozzolanic reaction is normally formed in later stage than that for normal Portland C-S-H. Thus, the strength development is able to increase at late ages. With high fineness of fly ash particle, pozzolanic C-S-H could provide very fine system which is capable for pore refinement. This filler effect could result in not only strength improvement but also reduce permeability, enhance chemical attack resistance and maintain compact microstructure (Soroka, 1993). Moreover, the heat of pozzolonic reaction is comparatively lower than that of Portland hydration reaction (Hanehara, et al., 2001). Almost half of average heat of Portland hydration could be reduced with the combination of fly ash, mitigating thermal-crack in concrete. With spherical shape and

fineness of fly ash, the workability of concrete is also significantly improved by the reduction of size and volume of voids (Jonathan, et al., 2003).

It can be seen that the disposal of fly ash from coal-fired power stations is one of major issues to utilise industrial by-products for environmental concern and also increase the value-added of wastes to be more sufficient for other aspects in term of economy. In fact, various ranges from 10 to 40 percent of fly ash worldwide are effectively reused in construction sector e.g. replacement in cement and concrete, road construction, underground works, grout mixes as well restoration, dams bases or similar dumps (ACAA, 2014; Cao, et al., 2008). With the scope of construction materials, especially for concrete, the replacement ranges from about 20 percent (low volume) to over 50 percent (high volume) of fly ash in total cement mass can be achieved in the mixes to maintain the strength of hardened concrete (Hanehara, et al., 2001; Lam, et al., 1998).

It has been suggested that the alternative use of fly ash beyond construction industry as a value-added material will expand the effective use, including the reduction in the economic and environmental impacts. The examples of those suggested applications are the production of zeolite or mullite, glass-like composite material, waste adsorbents or stabilizer, material recovery or even soil improvement for agriculture (Iyer & Scott, 2001). Nevertheless, an alternative cementing binder for construction material, which is able to produce from 100 percent fly ash as a prime material and activated with alkaline activators, has been studied and developed under the well-known name of “*Geopolymer cement*” to start up the effective utilization of fly ash (Davidovits, 2005).

2.2 Geopolymer Cement

2.2.1 Fundamentals of geopolymers

Victor Glukhovsky, who firstly assumed the geological process of cementitious systems, described that the formation of volcanic rocks or sedimentary rocks under low temperature and pressure can transform into zeolites. After the zeolitic materials were combined with strong alkaline solutions, the cementitious binder called ‘*Alkaline activated cement*’ was formed with distinguish high pH values. In 1940, the important event of alkaline activated binder was recorded by activating blast furnace slag with sodium hydroxide solution. The results showed that the formation of alumina-silicate hydrated product appeared together with a good load bearing capability (Pacheco-Torgal, et al., 2008a). Later, in 1950, a synthesis of alkaline alumina-silicate minerals was developed in Ukraine as a mixed of C-S-H and alumina-silicate phases and also recorded for tall building use in Russia

(Komnitsas & Zaharaki, 2007). In 1978, Joseph Davidovits firstly established the term of *Geopolymers* to describe a kind of alkaline activated alumina-silicate cementing binder with an amorphous-to-crystalline system, which could form at low temperature in a short time.

The alkaline activated cement is typically represented by zeolitic materials containing alkaline activators, the formation of which requires a relatively high setting temperature in the range of 150 to 180°C. On the other hand, geopolymer cement requires such from ambient temperature to less than 90°C (Figure 2.5).

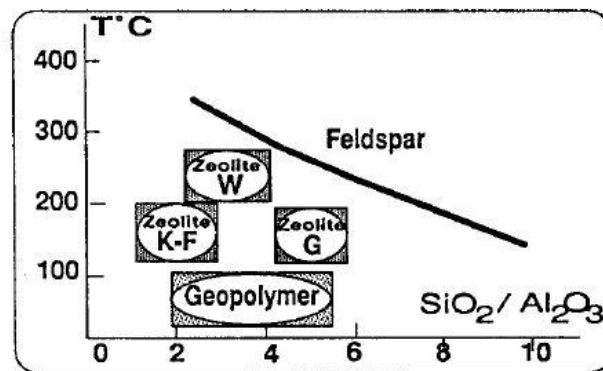


Figure 2.5 Crystallization temperature against Si/Al ratio of zeolite and geopolymers (Davidovits, 1991)

For geopolymer, main components of silicon oxide (SiO_2) and aluminium oxide (Al_2O_3) from any of prime materials (e.g. metakaolin, fly ash and blast furnace slag) are dissolved from their original sources in strong alkaline solutions (e.g. potassium/sodium hydroxide and potassium/sodium silicate) (Duxson, et al., 2007a), forming chain rings polymer of silicon-oxygen-aluminate (Si-O-Al; Sialate chain) (Davidovits, 1991). Even though different terminologies have been stated by many researchers (e.g. alkaline activated cement, hydroceramic, geocement, inorganic polymer concrete, and low-temperature aluminosilicate glass), the term *Geopolymers* is still widely used to represent this cementitious technology (Davidovits, 2011; Petermann, et al., 2010).

To produce alumina-silicate based geopolymer cement, the alkaline hydroxide and/or alkaline silicate solutions are initially mixed with raw prime materials to form the homogenous slurry. As geopolymers is able to poly-condense at the temperature below 90°C, the higher curing temperature is therefore no longer needed like ceramics (Davidovits, 1991). As heat is still a vital factor to accelerate geopolymeric reaction, the geopolymer mixture is hence cured in a temperature-controlled chamber (e.g. oven) at temperature around 40 to 90°C for a period of 6 to 48 hours (Chindaprasirt, et al., 2007;

Komnitsas & Zaharaki, 2007). The pre-cured geopolymer cement will continually be kept at room temperature for further handling or until reach the testing ages (Al Bakri, et al., 2011a). Geopolymer production is generally carried out as process shown in Figure 2.6. At present, geopolymers become a well-known cementitious material due to its terrific properties and applications. It tends to be an alternative choice for the construction industrial sector, although some obstacles have been raised for the development in real use, e.g. some complicated processes as well as not yet being established to the standard (Davidovits, 2002).

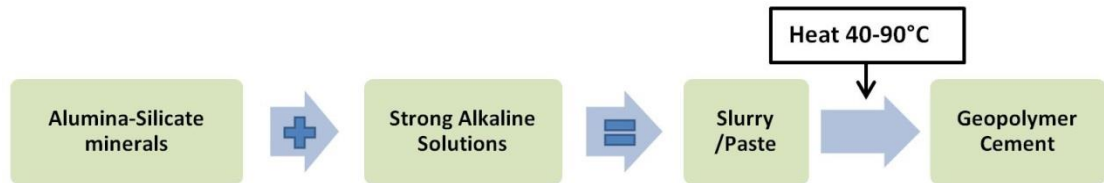


Figure 2.6 Typical geopolymer synthesis process

2.2.2 Geopolymerization reaction and its chemistry

As aforementioned, Portland cement hydration (forming C-S-H) is totally different from *Geopolymerization* of the geopolymer formation process. In geopolymerization, when the silicate and aluminate oxide (Si^{4+} and Al^{3+} in IV-fold coordination) extend their bonding/cross-link to sialate (Si-O-Al) and poly-sialates, the ring chain of polymer silicate (Si) and aluminate (Al) was suggested in the formation of amorphous to semi-crystalline phases. It could be categorised into 3 types, namely (i) Poly-(sialate) type (-Si-O-Al-O-), (ii) Poly-(sialate-siloxo) type (-Si-O-Al-O-Si-O-), and (iii) Poly-(sialate-disiloxo) type (-Si-O-Al-O-Si-O-Si-O-) with a structure model as shown in Figure 2.7 (Davidovits, 2002). The empirical formula of geopolymer resultant product is:



where M is the alkaline element such as potassium (K^+) or sodium (Na^+), n is the degree of polymerisation, z is Si/Al ratio which varies from 1, 2, 3 or higher, and “-” indicates the presence of bonding (Davidovits, 1991). The ratio of Si/Al results in different geopolymer properties, however, the low ratio of $\text{Si/Al} \leq 3$ has been widely used to obtain three-dimensional cross-link networks as cement and ceramics (Duxson, et al., 2007a). Although there are many chemical types of geopolymers (e.g. Phosphate-based, High-molecular phosphate-based, Silicone-based or Humic-acid based geopolymer), the most common name is Alumina-silicate based geopolymers (Davidovits, 2011).

Principally, geopolymer cement consists of two main components: any prime material containing silica and alumina, and alkaline activators (Pacheco-Torgal, et al., 2008b, 2014). Due to the complexity of various factors affecting geopolymerization during synthesis, the definite mechanism is not yet fully understood. However, many researchers agree that its mechanism consists of three-stage model which are dissolution after alkaline hydrolysis (destruction), transportation of cations (re-orientation), and poly-condensation of free silicate and aluminate species (hardening/solidification reactions) as shown in Figure 2.8 (Pacheco-Torgal, et al., 2008a; Rangan, et al., 2005). Somehow, it is also noted that the overlapping can occur during each stage, causing the difficulty to specify every single stage individually (Glukhovsky, 1967).

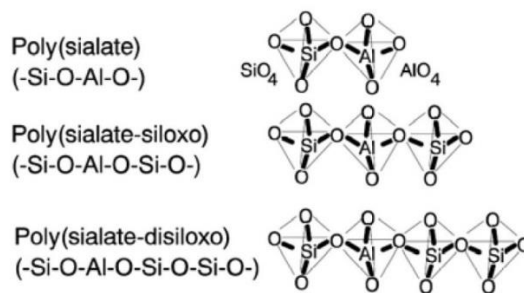


Figure 2.7 Type of poly-sialates structures (Davidovits, 2002)

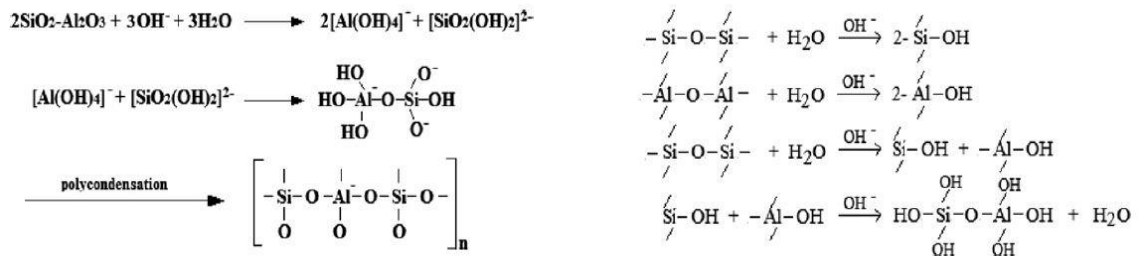


Figure 2.8 A reaction pathway involving the poly-condensation (Pacheco-Torgal, et al., 2008a)

More explanation of geopolymerization was illustrated by Duxson, et al. (2007a) in the schematic formation (Figure 2.9). Dissolution of alumina-silicate sources by alkaline solution produces reactive silica and alumina ion species. A complex mixture of those species is thereby settled to speciation equilibrium. After that, the gelation of oligomers starts forming, while some of H₂O is released in this stage as only nominal water was used in dissolution process. The gelation is then re-arranged and re-oriented to connect together as a gel network of three-dimensional structure under exothermic process (Rangan, et al., 2005). The cross-linked SiO₄ and AlO₄ tetrahedral are formed when the negative charge on Al³⁺ in IV-fold coordination is balanced with positive charge of alkaline ions (Na⁺, K⁺)

(Rovnaník, 2010). At the final setting stage, the polymerization process provides the formation of amorphous to semi-crystalline alumina-silicate network with excellent physical properties (Shi, et al., 2011). The final reaction products of those systems can be C-S-H (Ca + Si), zeolite/polymers (Si + Al) or C,N-A-S-H (Ca,Na + Al + Si) which mainly depend on the characteristics of raw starting materials and alkaline activators (Pacheco-Torgal, et al., 2008a; Pangdaeng, et al., 2014).

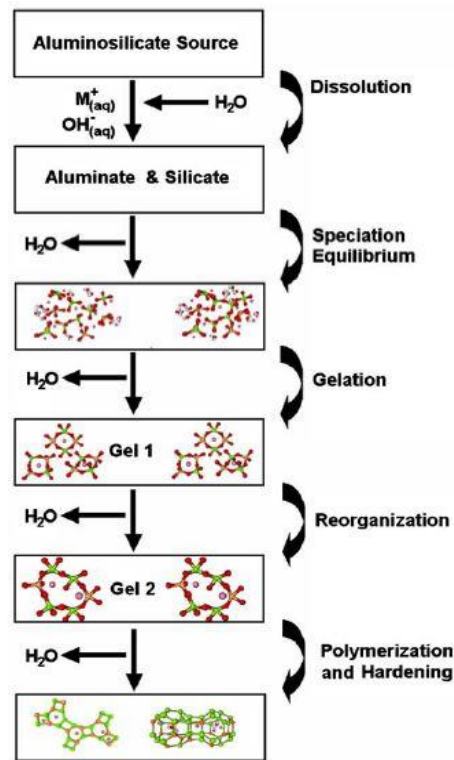


Figure 2.9 Model of geopolymerization (Duxson, et al., 2007a)

2.2.3 Geopolymer binder constituents

2.2.3.1 Main raw materials involved in geopolymer synthesis

Alumina-silicate mineral, a kind of pozzolanic material, could be found everywhere especially as by-products. Therefore, producing geopolymers is not only an alternative choice for recycling a large amount of wastes but could also achieve some specific properties of that ceramic-like cementitious material. The main raw materials for geopolymer synthesis, which have normally been used in research studies, can be classified in three major categories, namely (i) Industrial wastes (IW), (ii) General wastes and recycle materials (GW), and (iii) Natural materials (NM). The specific characters of those raw materials in previous studies are further summarised as follows:

Raw material from industrial wastes: A huge number of industrial wastes are annually produced worldwide from several types of production processes such as coal-combustion ash, metallurgical slag, mine waste or agricultural waste (Sujatha, et al., 2012). Some of these are currently used in Portland cement production or as additives to improve the properties and to utilize the massive amount of those by-products. However, most of these wastes will be disposal-stored or landfilled (Komnitsas, et al., 2004; Nuruddin, et al., 2011b). Some of the industrial wastes, for example, are fly ash, bottom ash, rice husk ash (RHA), granulated blast-furnace slag (GBFS), silica fume, steel slag, mine tailing and cement kiln dust (CKD).

Raw material from general wastes and recycled materials: The general wastes or recycled materials are produced everywhere worldwide. Although these materials sometimes are less in volume than industrial wastes, the value added conversion has utterly attracted much interest in addition to reducing unnecessary waste and pollution. Some of the general wastes, for example, are waste paper sludge ash (WPSA), water sludge and construction wastes.

Raw material from natural materials: Some of raw prime materials for geopolymer synthesis can be obtained or produced from natural sources such as kaolin (kaolinite or china clay), metakaolin (calcined kaolin), silty clay, diatomite (microscopic shells of diatoms), volcanic rock, etc. However, those natural materials are available in some specific geological areas with limited quantities.

Briefly, as geopolymeric formation occurs when alumina-silicate sources react with strong alkaline solution, any material which contains silica and alumina can be used in the synthesis of geopolymers. The overview of raw materials involved in geopolymer synthesis can be categorised into three types, namely industrial waste (IW), general waste (GW) and natural mineral (NM). It was found that the calcium-contained materials could provide similar or better mechanical strength than that of the typical one due to the cross-linkage of calcium silicate hydrate (C-S-H) and geopolymeric gel in the single binder. Figure 2.10 presents the graphical data between mechanical (compressive) strength and type of raw materials in geopolymer cement production. OPC and Cement Repair are also included as references in the synthesis (More details: See Appendix A, Table A.1). It can be seen that the industrial waste (e.g. fly ash, mine tailing and GBFS) achieved the highest strength followed by natural mineral (metakaolin and natural pozzolan), while general waste (construction waste) seems to produce the lowest mechanical strength. However,

other factors, e.g. Si/Al ratio, type of sample, testing age, type of alkaline activator, curing conditions and sample size, also need to be considered on the compressive strength of the final products. Table 2.3 summarises the chemical composition of each raw material (as a representative) such as fly ash, high calcium fly ash, GBFS and so on. The main values presented are the contents of SiO₂, Al₂O₃, CaO and SiO₂-to-Al₂O₃, together with (Si/Al) ratios, which significantly influence the geopolymerization of the cement. Noticeably, the widely used materials, such as fly ash and metakaolin, contain high percentages in SiO₂ and Al₂O₃ (overall amount of SiO₂ and Al₂O₃ is over 70 percent or equal to 1.0 to 3.0 of Si/Al ratio). Other factors of raw materials involved in the properties of geopolymers are presented and described onwards.

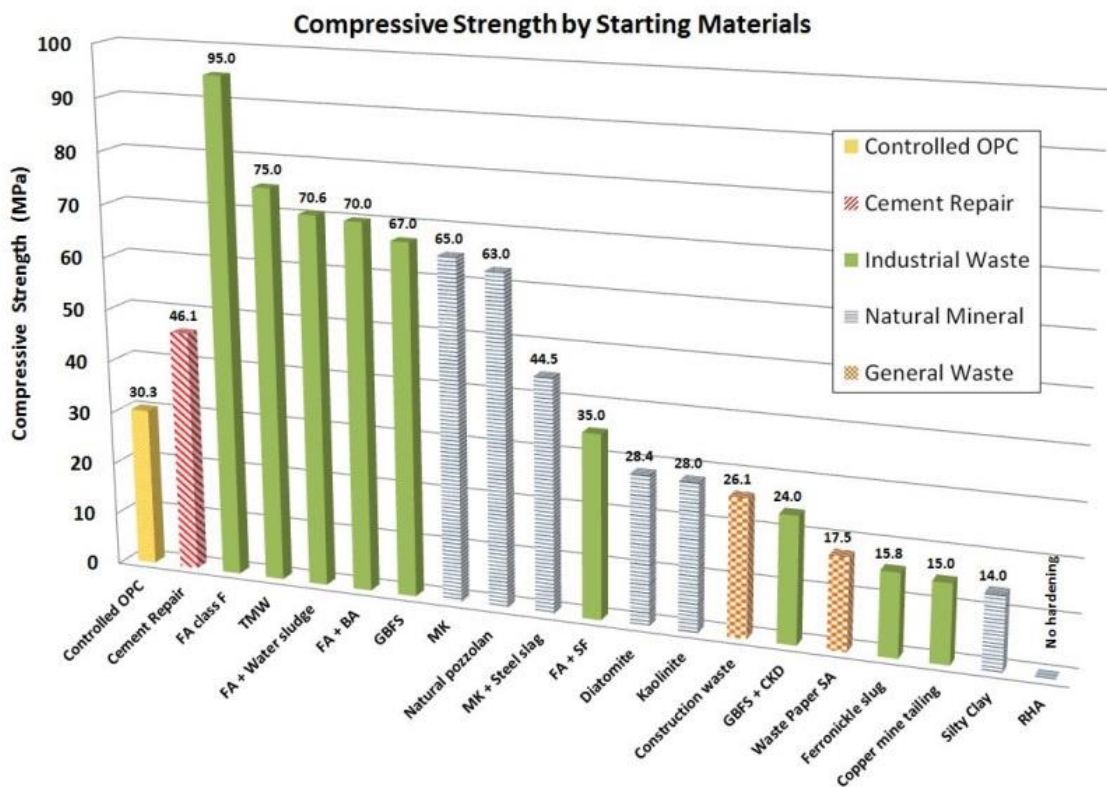


Figure 2.10 Compressive strength vs type of materials

Table 2.3 A representation of chemical composition using in geopolymers synthesis by raw prime materials

Materials	SiO ₂	Al ₂ O ₃	Fe ₂ O ₃	CaO	MgO	Na ₂ O	K ₂ O	SO ₃	FeO	Si/Al	% Si+Al	References
1. Industrial & General waste												
<i>Low calcium Fly ash</i>	50.00	28.25	13.50	1.79	0.89	0.32	0.46	0.38	-	1.77	78.25	(Nath & Sarker, 2012)
<i>High calcium Fly ash</i>	39.70	20.00	14.10	17.30	1.40	1.40	2.70	2.60	-	1.99	59.70	(Rattanasak, et al., 2011)
<i>GBFS</i>	32.46	14.30	0.61	43.10	3.94	0.24	0.33	4.58	-	2.27	46.76	(Nath & Sarker, 2012)
<i>Silica Fume</i>	92.00	0.46	1.60	0.29	0.28	0.51	0.61	0.19	-	200.00	92.46	(Dutta, et al., 2010)
<i>Steel Slag</i>	15.00	6.70	15.40	44.20	10.90	0.20	0.10	0.70	-	2.24	21.70	(Hu, et al., 2008)
<i>Ferronickel Slag</i>	32.74	8.32	0.76	-	2.76	-	-	-	38.80	3.94	41.06	(Komnitsas & Zaharaki, 2007)
<i>Tungsten mine waste</i>	53.48	16.66	12.33	-	1.27	0.62	7.65	-	-	3.21	70.14	(Pacheco-Torgal, et al., 2007)
<i>Cement Kiln Dust</i>	11.00	3.90	2.00	42.00	3.60	-	0.60	-	-	2.82	14.90	(Khater, 2012)
<i>Waste paper sludge ash</i>	26.25	17.50	4.40	23.40	0.90	0.10	0.20	4.63	-	1.50	43.75	(Anuar, et al., 2011)
<i>Water Sludge</i>	70.40	15.40	5.30	1.53	0.96	0.90	3.66	0.31	-	4.57	85.80	(Kongkaew, 2007)
<i>Demolished Wall</i>	76.42	1.88	1.28	9.84	0.26	0.22	0.08	2.09	-	40.65	78.30	(Khater, 2011)
<i>Waste Concrete</i>	71.53	2.14	2.43	12.76	0.39	1.04	1.13	0.33	-	33.43	73.67	(Khater, 2011)
2. Metakaolin	54.78	40.42	0.76	0.10	0.41	0.07	2.72	-	-	1.36	95.20	(Yip, et al., 2005)
3. Kaolin	48.10	36.90	0.26	0.20	0.17	0.20	1.90	-	-	1.30	85.00	(Hounsi, et al., 2013)
4. Rice husk ash (RHA)	86.10	0.17	2.87	1.03	0.84	-	4.65	0.41	-	506.47	86.27	(Nuruddin, et al., 2011b)
5. Silty Clay	20.10	7.55	32.89	26.15	0.47	-	3.17	4.92	-	2.66	27.65	(Sukmak, et al., 2013)
6. Diatomite	59.30	10.00	18.50	1.20	-	-	-	2.74	-	5.93	69.30	(Phoo-ngernkham & Sinsiri, 2011)
7. Volcanic Mud	38.50	14.20	23.76	5.62	-	-	4.31	0.78	-	2.71	52.70	(Al Bakri, et al., 2012)

2.2.3.2 Type of alkaline activators involved in geopolymer synthesis

Geopolymer cement, the alumina-silicate minerals, has major component of SiO_2 (silicon dioxide) and Al_2O_3 (aluminium oxide) which dissolved from their original source in strong alkaline solution, which are, in fact, in the first two columns (group I and II) of the periodic table of the elements, called alkaline metals and alkaline earth metals respectively. The alkaline metals (i.e. Lithium, Sodium, Potassium, Rubidium, Cesium, and Francium) have one electron in their outer shell and are active in bonding with other elements. They are explodable if exposed in the water. The alkaline earth metals (i.e. Beryllium, Magnesium, Calcium, Strontium, Barium, and Radium) have two valence electrons and are one of the reactive elements in nature (Halka & Nordstrom, 2010). The alkaline metals as alkaline activators of geopolymer cement (group I) are more reactive and more often used than the alkaline earth. There are many alkaline activators which were used in geopolymer synthesis e.g. potassium/sodium hydroxide (KOH/NaOH), potassium/sodium silicate ($\text{K}_2\text{SiO}_3/\text{Na}_2\text{SiO}_3$), sodium carbonate (Na_2CO_3), calcium hydroxide (Ca(OH)_2) or the combinations of any alkaline solutions together (Fernández-Jiménez & Palomo, 2005; Panagiotopoulou, et al., 2007). However, the most widely used alkaline activators in geopolymer synthesis can be summarised as follows:

Sodium hydroxide solution (NaOH): NaOH solution is normally used to produce geopolymer cement due to its widely available and cheaper than other alkaline solutions (Hardjito, et al., 2008). Its main role is to provide an alkaline environment of hydroxide ion (OH^-) dissolving alumina-silicate minerals from their origins. It is reported that, in sulphate immersion, the fly ash-based geopolymer synthesized with only sodium hydroxide solution achieved higher strength than those of sodium silicate solution or a combination of sodium and potassium hydroxide solution (Bakharev, 2005a).

Sodium silicate solution (Na_2SiO_3): Na_2SiO_3 solution or water glass is normally used in geopolymer synthesis as an alkaline activator and another source of Silica (Si). It is also cheaper than potassium silicate solution (K_2SiO_3) when produced in large quantity (Dimas, et al., 2009). Similar to other alkaline activators, the strength of geopolymers increases with an increase in concentration. Nevertheless, using sodium silicate solution alone could not achieve the same strength level of those NaOH or KOH solutions. The reason is probably due to the fact that using of Na_2SiO_3 solution achieves less dissolution rate than that of using OH^- compound (Rashad & Zeedan, 2011).

Sodium hydroxide and Sodium silicate solution (NaOH and Na₂SiO₃): A combination of sodium hydroxide and sodium silicate solution is one of the most widely used alkaline activators for geopolymer synthesis. It is known that soluble hydroxide dissolves alumina-silicate minerals from origin sources while soluble silicate improves the poly-condensation of geopolymer cement and also controls the amount of silicate in mixtures as a binder. The optimum proportion of Na₂SiO₃ and NaOH is therefore an important factor in geopolymer synthesis. The fly ash-based geopolymers with Na₂SiO₃ and NaOH has been found performing better than only NaOH or Na₂SiO₃ solution alone (Fernández-Jiménez, et al., 2007; Phoo-ngernkham & Sinsiri, 2011). Theoretically, alkaline metals in periodic table groups I and II can be used as an activator, but the most widely used ones are Sodium (Na) and Potassium (K) due to their strong alkaline properties and global availability. However, with more economical saving aspect, sodium soluble is therefore more extensively used than that of potassium soluble (Hardjito, et al., 2008).

For geopolymerization, it was reported that alkaline cations control almost all reactions in geopolymeric hardening and could provide significant effect on strength development (Van Jaarsveld, 2000). Eventually, most of alkaline activators used in fly ash and metakaolin-based geopolymers are sodium hydroxide (NaOH) and sodium silicate (Na₂SiO₃) solutions due to its roles in dissolving of alumina-silicate minerals, being the additional sources of Si and Na, and providing initiate formation. Heat applying for curing purpose would stimulate and enhance poly-condensation afterwards (Komnitsas & Zaharaki, 2007). The types of alkaline activators used (listed by the compressive strength achievement) are presented in Table 2.4.

Table 2.4 Compressive strength of various alkaline activators in geopolymer synthesis

No	Alkaline		Sample Type	Comp. Strength		Starting Materials (% wt)	Additives (% wt)	Curing Condition		References
	Main (M) ^a	Addition		MPa	Age (d)			C°	Hrs	
1	NaOH (12.5)	Na ₂ SiO ₃	Paste	95.0	28	FA (100) class F ^b	-	85	20	(Fernández-Jiménez, et al., 2007)
2	NaOH (75%) ^c	KOH (25%) ^c	Paste	95.0	28	MK (100)	-	40	20	(Duxson, et al., 2007c)
3	NaOH (15)	Na ₂ SiO ₃	Paste	92.1	7	FA (100) class F	-	75	7 days	(Phoo-ngernkham & Sinsiri, 2011)
4	KOH (7)	Na ₂ SiO ₃	Mortar	72.3	3	FA (100) class F	-	85	24	(Kong & Sanjayan, 2010)
5	KOH (7)	Na ₂ SiO ₃	Paste	71.2	3	FA (100) class F	-	85	24	(Kong & Sanjayan, 2010)
6	NaOH (12)	-	Mortar	70.4	28	FA (100) class F	-	85	20	(Fernández-Jiménez & Palomo, 2005)
7	KOH (-)	Na ₂ SiO ₃	Paste	70.0	28	MK (100)	-	40	20	(Duxson, et al., 2007c)
8	KOH (12)	K ₂ SiO ₃	Paste	70.0	28	FA (90) class F	BA (10)	80	24	(Hardjito & Fung, 2010)
9	NaOH (-)	-	Paste	67.0	28	GBFS (100)	-	38	90 days	(Khater, 2012)
10	Na ₂ SiO ₃ (-)	-	Paste	45.0	28	FA (100) class F	-	60	28 days	(Rashad & Zeedan, 2011)
11	NaOH (-)	Na ₂ CO ₃	Mortar	36.0	-	FA (100) class F	-	85	20	(Fernández-Jiménez & Palomo, 2005)

^a M = Molarity, ^b FA class F = low calcium fly ash, ^c percentage by weight.

2.2.4 Design of Geopolymer constituents

2.2.4.1 Alkaline activators' concentration and ratio

Compressive strength of geopolymer generally increases with the increase in specific concentration of alkaline activators (Hardjito & Fung, 2010; Xu & Van Deventer, 2000). A higher concentration gives rise to a stronger ion-pair formation, provides more complete and faster poly-condensation process of particle interface (Raijiwala & Patil, 2010) and enhances the dissolution of the alumina-silicate materials in the presence of activators (Mishra, et al., 2008). Nevertheless, too high concentration could lead to an increase of coagulated-structure (Alonso & Palomo, 2001), causing less flow ability with fast setting behaviour (Memon, et al., 2013). Although, the dissolution and hydrolysis were accelerated, an incomplete poly-condensation of the system was also found (Phoo-ngernkham & Sinsiri, 2011). The optimum alkaline concentration could also vary by a large number of conditions and factors such as specific properties of prime materials, Alkaline activator-to-Prime material ratio, Na_2SiO_3 -to- NaOH (SS/SH) ratio, curing temperature or even the age of testing. In addition, the NaOH solution concentration between 10 and 15 molars (M), and 30 to 50% w/w of Na_2SiO_3 solution are commonly used in geopolymer synthesis (Anuar, et al., 2011; Chindaprasirt, et al., 2007).

2.2.4.2 Alkaline activator-to-Prime material ratio by mass

Mass ratio of alkaline solution and prime material is widely used in geopolymer synthesis in order to define both alkaline dosage and water content. In most cases, fly ash was used and the ratio would probably be called Alkaline activator-to-Fly ash (A/FA) ratio. Barbosa, et al., (1999) and Hardjito, et al. (2008) have tested the effect of A/FA ratio on the strength development by using 10 M NaOH solution as an alkaline solution with the A/FA ratio of 0.34 to 0.46. It was observed that the compressive strength increased when the A/FA ratio increased until it reached the optimum at around 0.40. Too high A/FA ratio could cause the precipitation at early stage before geopolymerization and this would result in a strength decrease as more sodium carbonate was formed and obstructed the polymerization process (Sukmak, et al., 2013). It must be noted that depending on the type of alumina-silicate materials, the recommended A/FA ratio could be between 0.35 and 0.50 to achieve both compressive strength and workability (Ma, et al., 2012; Xie, et al., 2009).

In addition, as water in the mixture is a vital factor for hardening process, the water-to-solid (w/s) ratio (the total mass of water is the sum of water in sodium hydroxide solution, sodium silicate solution and added water, while the total mass of solid is the sum of fly

ash, sodium hydroxide solid, sodium silicate solid and other added solids such as sand or aggregates) is also considered (Hardjito, et al., 2008). It was found that the w/s ratio should be in the ranges of 0.18 to 0.22 and 0.26 to 0.32 for fly ash-based geopolymer paste and concrete respectively (Chindapasirt, et al., 2010; Panias, et al., 2007). Apart from that, the calculation of additional water required can also be carried out to compensate the evaporation in the mixture (Zhang, et al., 2009).

2.2.4.3 Na_2SiO_3 -to- $NaOH$ solution (SS/SH) ratio by mass

The optimum of SS and SH is an important factor in geopolymer synthesis. It must be noted that the amounts of SS and SH are generally referred to the amount of alkaline solution (by mass) in A/FA ratio as well as the water content and pH level (Chatveera & Makul, 2012). Previous research studies revealed that low calcium fly ash-based geopolymers would achieve the optimum ratio of 1.0, 1.5 or 2.0, depending on the type of prime materials (Nath & Sarker, 2012) while optimum values of the high calcium fly ash based was in the range between 0.67 and 1.00 (Chindapasirt, et al., 2007).

2.2.4.4 Silica-to-Alumina (Si/Al) ratio of prime materials

The amounts of silicon dioxide-to-aluminium oxide and other classification of fly ash are generally classified with the standard of ASTM C618-15:2015 or BS EN 450-1:2012. The ratio of Si/Al is a significant factor, which affects the degree of crystallinity and reaction when mixed with alkaline materials (Xu & Van Deventer, 2003), forming of amorphous to semi-crystalline phases. Both polysialate-siloxo (Si/Al = 2) and polysialate-diloxo (Si/Al = 3) provided good strength to geopolymers, even polysialate-siloxo (Si/Al = 2) seems to be formed faster and has a slight lower compressive strength than polysialate-diloxo (Si/Al = 3). The monomeric group of $[SiO(OH)_3]^-$, $[SiO_2(OH)_2]^{2-}$ and $[Al(OH)_4]^-$ normally form later than Si and Al species as small alumina-silicate oligomers can improve the geopolymeric formation (Weng & Sagoe-Crentsil, 2007). It has been reported that metakaolin-based geopolymers achieves a satisfactory strength with the Si/Al ratio of 1.90 to 3.0, while the appropriate ratio of fly ash-based geopolymers is approximately 2.0 to 4.0 (Andini, et al., 2008; Duxson, et al., 2007c). By this, it can be supposed that the effective Si/Al ratio, for both fly ash-based and metakaolin-based geopolymers, should be around 2.0 to 3.0.

2.2.4.5 Delay time of preparation process

The delay time is the period of time that specimens were left at the room temperature for casting and wrapping, before placing in the oven. Chindaprasirt, et al. (2007) studied the delay time of 0, 1, 3 and 6 hours before putting the high calcium fly ash-based geopolymer samples in the oven at 60°C for a period of 24 hours. The results showed that, like those from Hardjito, et al. (2004), the delay time before oven curing can affect the compressive strength of geopolymers. The optimum delay time of any paste was suggested to be approximately half of its initial setting time. For example, the optimum delay time might be around 1 hour when the initial setting time is 2 hours. In addition, it can be suggested that an optimum delay time depend on starting material's characteristics, adopted from activator system and specific curing conditions (Chindaprasirt, et al., 2010). However, it is noted that geopolymers gained approximately 70 percent of strength within 4 hours after curing in appropriate conditions. This is in contrast with well-known behaviour of OPC in term of gaining strength over time and undergoing with hydration reaction (Khale & Chaudhary, 2007).

2.2.5 Curing procedures of geopolymers

In early 1940s, a combination of zeolitic materials and alkaline solutions was used to produce alkaline-activated cement with specific curing temperature and duration such as a record of mixing blast furnace slag with sodium hydroxide (Roy, 1999). Geopolymer cement was positively reported with terrific mechanical properties, although the high curing temperature above ambient temperature and specific curing duration, including specific mix design, are required to raise probability of durability enhancement (Sofi, et al., 2007). Curing geopolymers is normally carried out in electrical ovens, nevertheless, many alternative methods of geopolymer heating were observed for the best practical handling and resultant. Using microwave for preheating or full curing was found to reduce the duration of oven curing (Chatveera & Makul, 2012; Taebuanhuad, et al., 2012) as well as a preheating of alkaline solution before mixing was also studied to improve final strength of geopolymer concrete (Dutta, et al., 2012). However, oven curing is the most widely used method for geopolymer production nowadays. Curing procedures on various temperatures and durations in geopolymers can be summarised as follows.

2.2.5.1 Effects of curing temperatures on geopolymer properties

Many previous experiments on curing temperature of both geopolymer paste and mortar (between 30 and 90°C) showed that an increase at curing temperature gives an increase of

chemical reaction and this enhances the mechanical strength in early stage of geopolymerization (Van Jaarsveld, et al., 2002). Whist, too high curing temperature (e.g. over 90°C) would lead the samples to experience a substantial loss of moisture with porous structure, causing a negative effect on the final mechanical properties of geopolymeric products (Rovnaník, 2010). The optimum temperature for geopolymers cured in those tests was found to be around 60 to 75°C, which could appropriately improve the geopolymerization process and microstructure development (Chindaprasirt, et al., 2010). Concrete produced by fly ash-based geopolymers has also been studied under different curing conditions. Demie, et al. (2011) and Reddy, et al., (2012) found that a good compressive strength was gained when curing temperature was in the range of 60 to 70°C, while further curing at 80 to 90°C seemed to result in a decrease in concrete strength. However, under Australian Standard (AS 3600:2009) and American Concrete Institute Building Code (ACI 318-11:2011), the minimum structural design standard was achieved by the reinforced-concrete column cured at 60 °C for 24 hours (Sumajouw, et al., 2007).

It can be summarised that curing temperature is one of the important factors affecting the strength of geopolymers. Although, higher temperatures (above room temperature) give a higher strength, too high temperature could cause cracking, resulting in a decrease in its strength. The rapid loss of moisture could also lead to the formation of micro-cavities. The temperature range from 40 to 80°C clearly enhanced mechanical properties, but the optimum range from 40 to 60°C seems to be an appropriate curing condition, which matches all performance, environmental and economical aspects (Hounsi, et al., 2013).

2.2.5.2 Effects of curing duration on geopolymer properties

The curing duration could also affect the mechanical properties of geopolymers. At the most frequently used temperatures of 40 to 60°C, the curing duration was found in range from 4 to 96 hours (4 days), depending on the design of each experimental condition. However, the periods of 6, 12, 24, 48 and 72 hours were often used as controlled-duration for trailing or studying other factors (Komnitsas, et al., 2004). Chatveera and Makul (2012) studied the effect of curing duration of fly ash-based geopolymer cement, reported that at the curing temperature of 85°C, 24 hours gave a higher strength than 48 hours (Chatveera & Makul, 2012), while Chindaprasirt, et al. (2007) studied the curing temperature of 60°C, found that a good strength was obtained at minimum heat curing of 48 hours (2 days) and a higher strength was obtained with 72 hours (3 days). However, both mentioned studies concluded that an increase in the curing time beyond the optimum limit did not enhance

the strength of the geopolymeric specimens. This may be suggested that prolonging curing may result in excessive loss of moisture during curing process, which causes uncompleted formation and generates large pores in the structure (Zhang, et al., 2009). These reasons could cause any failures in microstructures of the final products (Phoo-ngernkham & Sinsiri, 2011). In fact, a curing period of 12 to 24 hours seems to be the suitable duration with satisfied compressive strength and economic approach, although a shorter or longer curing duration than 24 hours might give rise to the different strength developments.

2.2.5.3 Summary of geopolymers curing procedures

For the curing regimes, there is a huge variable range of both curing duration and curing temperature to achieve mechanical properties of geopolymer cement. As aforementioned, the optimum curing conditions mainly depended on prime material's properties, alkaline activators, water content, age of the samples and other ratios (Chindaprasirt, et al., 2007). The curing regimes directly affect not only degree of geopolymerization but also evaporable water in gel structure which firstly fulfils the pores (Duxson, et al., 2007b). When water or moisture is rapidly liberated from either too high temperature or prolonged curing, the remained micro-pores might shrink, deteriorating the geopolymers, e.g. their strength (Bakharev, 2005b). It can be drawn that, beside the aforementioned factors, the suitable curing temperature and period are within the range of 40 to 60°C and 8 to 24 hours respectively. However, in some cases, curing in ambient condition is able to provide an acceptable result with no external heat applied, which is described onwards in Section 2.3. Some of high strength fly ash-based geopolymer pastes (with sodium hydroxide and sodium silicate solution) under different curing conditions are presented in Table 2.5.

Table 2.5 Compressive strength for different curing regimes in geopolymer synthesis

No	Curing Condition		Sample Type	Prime Materials (% wt.)	Comp. Strength		Alkaline Materials		SS/SH	References
	Hrs	C°			MPa	Aged	Alkaline (M) ^a	Others		
1	20	85	Paste	FA (100) class F ^b	95.0	28 d	NaOH (12.5)	Na ₂ SiO ₃	0.18	(Fernández-Jiménez, et al., 2007)
2	168 (7d)	75	Paste	FA (100)	92.1	7 d	NaOH (15)	Na ₂ SiO ₃	2.00	(Phoo-ngernkham & Sinsiri, 2011)
3	24	40	Paste	FA (100) class F	77.0	28 d	NaOH (-)	Na ₂ SiO ₃	-	(Ma, et al., 2012)
4	24	60	Paste	FA (100) class F	67.0	7 d	NaOH (12)	Na ₂ SiO ₃	2.50	(Al Bakri, et al., 2011b)
5	8	75	Paste	FA (100) class C	63.0	28 d	NaOH (-)	Na ₂ SiO ₃	-	(Guo & Shi, 2012)
6	Outdoor/Ambient curing		Paste	FA (100)	48.7	28 d	NaOH (8)	Na ₂ SiO ₃	-	(Nuruddin, et al., 2011b)
7	48	65	Paste	FA (100)	42.0	28 d	NaOH (10)	Na ₂ SiO ₃	-	(Sukmak, et al., 2013)
8	6	65	Paste	FA (100)	34.0	7 d	NaOH (10)	Na ₂ SiO ₃	1.50	(Taebuanhuad, et al., 2012)
9	Indoor/Ambient curing		Paste	FA (100)	19.7	28 d	NaOH (8)	Na ₂ SiO ₃	-	(Nuruddin, et al., 2011b)

^a M = Molarity, ^b FA class F = low calcium fly ash

2.2.6 Properties and application of geopolymer cement

There is a huge amount of literatures on the properties and applications of geopolymer cement, which comply with the standards of testing OPC. Geopolymer cement has been previously proven to have good physical and chemical properties, although depending on experimental conditions. The benefits from being a waste treatment process and a low carbon-dioxide material are also highly concerned together with benefits in cost reduction. Main properties of achieved geopolymer products with suitable manufacturing procedure and heat curing can be summarised as follows.

2.2.6.1 Mechanical properties of geopolymers

Setting time and early strength development are important for any construction work with time restriction such as road or runway repairing. OPC hardening is a chemical timely process known as hydration reaction. It was revealed that less setting time of geopolymers requires higher curing temperature at above room temperature as well as high concentration of alkaline solution, which eventually accelerates the hardening and rate of geopolymerization of geopolymer cement (Hardjito, et al., 2008; Rovnaník, 2010).

Compressive strength is widely used to assess property of geopolymers, due to its representative, simplicity and low cost of testing (Komnitsas & Zaharaki, 2007). The compressive strength of fly ash based-geopolymer cement could achieve up to 95 MPa at the age of 28 days (Fernández-Jiménez, et al., 2007), which is equivalent to ultra-high strength concrete (MacGregor, 1997). In addition, other measurements on strength were also tested and proved to be equal to or even better than those of OPC e.g. flexural strength (Fernández-Jiménez & Palomo, 2005), split tensile strength (Sofi, et al., 2007) and bond strength (Hu, et al., 2008). It can be drawn that the improvement in strength clearly refers to more completion of chemical dissolution and geopolymerization.

Drying shrinkage is the decrease in volume of cement or concrete with time and is independent of the external actions, which leads to cracking or dropping in load-carrying capacity because of a loss in volume. Alternatively, expansion can cause cracks in concrete structure when its parts fail to withstand the force or the repeated cycles of expansion. Previous research studies have indicated that geopolymers had superior shrinkage and expansion resistance (Fernández-Jiménez, et al., 2007; Wallah, 2009), including thermal properties when exposed at elevated temperature (800 to 1,000°C), than those of normal OPC (Gilbert, 2002; Zuhua, et al., 2009).

Geopolymers has low water absorption due to its dense structure (Davidovits, 2002). Pores in structure partially depended on water content and also affect the porosity of geopolymers. It was also found that overheating leads to an increase of early strength with large pores while lower temperature leads to a decrease of early strength with smaller pores. By this, it means that the size of pores is directly related to aging, amount of water used and curing regimes in the processing, which dominate the final density of that geopolymers (Lizcano, et al., 2012).

2.2.6.2 Durability of geopolymers

Concrete or cement can be deteriorated by freeze-thaw actions when its pores are filled with water and become freezing. Low-calcium ferronickel slags geopolymers was tested on freeze-thaw resistance by using cycles of -15°C and $+60^{\circ}\text{C}$ for over a period of 4 months. It was found that the geopolymers was almost unaffected but indicated by slight decrease in compressive strength (Komnitsas, et al., 2004).

There are many testing standards and regulations to assess the behavior of geopolymers in heating and firing. The geopolymers was found to achieve better fire resistance performance than OPC when the temperature is rapidly changed from 200 to $1,000^{\circ}\text{C}$ due to the less amount of portlandite ($\text{Ca}(\text{OH})_2$) in its structure which led to high thermal-shock resistance (Rashad & Zeedan, 2011).

Corrosion is a destructive of attack by chemical or electrochemical reaction with its environment. Chemical attack with physical deterioration would be called corrosion-erosion or corrosive wear (Winston, 2008). The corrosive environment of cement or concrete is commonly found in marine environment and some acidic events. Whilst an abrasion occurs due to rubbing, scraping, skidding or sliding of objects on the surfaces. The experiments have revealed that the properties of geopolymers were better than that of typical OPC due to more homogeneous and well-bonded structure (Reddy, et al., 2012; Pacheco-Torgal, et al., 2007). Ettringite in OPC structure may perform expansive behavior and hence its microstructure was damaged by acid (Khater, 2012; Palomo, et al., 1999). Therefore, less deterioration of geopolymers was also observed in acid solution than OPC when measured with percentage of total loss in weight (Fernández-Jiménez, et al., 2007).

2.2.6.3 Applications of geopolymer cement

Portland cement and concrete have been used for construction for a long time. At the present day, their applications include buildings, infrastructures, dams, bridges and so on.

That is why concrete is used more than any other man-made materials on the earth. Geopolymers is a type of cementitious material which can be used as construction material like OPC. Although geopolymers' characters and behaviours are under studying and understanding, its property has been proved to be similar to or even better than OPC. Some of applications can be summarised as follows:

Precast components: Precast or prefabricated component is one of the applications, which was firstly developed as commercial products (Davidovits, 2014). The production control in plant, such as preparation processes or curing in electrical oven, allows precast-geopolymer cement reach the standard requirements for construction. The heat-cured low-calcium fly ash-based geopolymer concrete was also tested with excellent potential for applications in the precast industry. Its performance is also well in agreement with the value calculated using the design provisions according to the Australian Standard AS 3600:2009 and American Concrete Institute Building Code ACI 318-11:2011 (Sumajouw, et al., 2007).

Geopolymer blocks & bricks: Blocks and bricks are the common construction materials, which were widely studied by using geopolymer cement. The study on bricks made from waste tailing-based geopolymers with Cement Kiln Dust (CKD) showed the improvement in mechanical properties and the durability, when appropriate concentration of alkaline activators were used (Ahmari & Zhang, 2013). Ahmari and Zhang (2012) reported that conventional production of bricks required high energy in burning and released large amount of greenhouse gas. The production of geopolymer bricks with by-product could be considered as an alternative but reduce the energy consumption. Lightweight block from fly ash-based geopolymers was also studied to be efficiently manufactured at 25°C, but a number of factors need to be monitored closely for commercial production (Andini, et al., 2008).

Reinforced geopolymer concretes (RGC): The application of reinforced-geopolymer concrete was studied along with Portland concrete standard, although the heat curing of the geopolymers was still required. Sujatha, et al. (2012) studied the fly ash-based geopolymer reinforcement concrete (slender circular columns of 100 mm dia. and 1800 mm in length with 2.16 percent reinforcement) manufactured with sodium hydroxide and sodium silicate as activators, and cured at 70°C for 24 hours. It was found that the reinforced geopolymer concrete columns had less deformation than controlled OPC concrete for the same percentage of steel. In term of ultimate loads, RGC performed better than both OPC and

calculated value. It is apparent that RGC could be well-produced as reinforced concrete due to its strong and cohesive bonding.

Composite Materials: Geopolymer composites have been developed in many research fields. Construction material is one among those, for example, fiber-reinforced geopolymer cement, geopolymer composite panel and tube. Silica-based geopolymers were also used to produce silica-based geopolymer-carbon reinforced composite to improve the flexibility. The excellent properties such as lightweight, high strength and fire resistance also permit to the development of new composite materials. However, geopolymer composite in construction field is yet to excel especially when the sustainability and environmental aspects are concerned (Tran, et al., 2009).

Geopolymer cement powder: Cement powder is a choice for mixing concrete by just adding aggregates and water. Some researchers studied on the production of geopolymer powder by crushing pieces of completed-formation geopolymers into powder. The geopolymer powder was then added with water and heated in oven at suitable temperature before testing its strength, which sometime called “just adding water geopolymer” (Duxson & Provis, 2008; Feng, et al., 2012; Liew, et al., 2012). In addition, the development of geopolymers with pre-dry mixing process was also studied by Suwan and Fan (2014), and was found that more convenient in practical use can be apparently achieved. Nevertheless, the new route of development in applications has now widely opened, even though the strength was still not able to reach that level of typical geopolymer cement.

Immobilization of hazardous substances: Immobilization of heavy metal pollution causes risks to ecological systems and human health. Industrials waste containing heavy metals such as Pb, Cu, Cr and Ni could contaminate soils or water resources when they went to a landfill. It was reported that heavy metals appear to be immobilized efficiently into the amorphous alumina-silicate matrix (Hu, et al., 2008), tested by leaching tests using the toxicity characteristic leaching procedure (TCLP) and Nuclear Magnetic Resonance (NMR) with transmission electron microscopy using the Magic Angle Spinning (MAS) technique (Van Jaarsveld & Van Deventer, 1999). This may be because (1) metal ions are taken into the geopolymers network; (2) metal ions are bound into the structure for charge balancing roles; and (3) metals ions are partially physically encapsulated and partially chemically bonded in the three-dimensional matrices (Guo & Shi, 2012; Zheng, et al., 2010).

2.2.6.4 Summary of properties and application of geopolymer cement

The properties of geopolymers strongly depend on its major factors, which may include initial raw materials, alkaline activators, curing regimes and others. It is clearly seen that the specific conditions of each synthesis may result in unique characteristics of geopolymers (Khale & Chaudhary, 2007). However, the properties of geopolymers, which were mostly indicated with compressive strength, perform similarly or even better than OPC under the OPC-based standard (Aleem & Arumairaj, 2012; Sofi, et al., 2007). Although geopolymers can be used as OPC in almost all applications, the handling sensitive materials and curing regimes are still being the limitations. Therefore, the near-term applications of geopolymers are precast components, bricks or even composite materials, which are compact enough to place in the curing chamber (Komnitsas & Zaharaki, 2007). Nevertheless, it is believed that not too far from now the potential large scale applications will be established to beneficially obtain a sustainable approach as well as expanded to an on-site operation (Duxson, et al., 2007a).

2.3 Factors Influencing Geopolymer Properties at Ambient Temperature

Recent research studies have revealed that heat curing is required to accelerate and improve the strength development in both early and later stages of fly ash-based geopolymers (Bakharev, 2006; Khater, 2012). The applications applied to geopolymers production nowadays are such as precast concrete members, small-components or bricks due to the limitation of heat curing units (e.g. oven) and heat treatment technology. To widen its applications and being more convenient in practical works with reasonable strength, numerous researchers have attempted to develop fly ash-based geopolymers which suitable for curing at ambient temperature without external sources of heating (Nazari, 2013; Phoo-ngernkham, et al., 2013). In this issue, some studies on significant factors and conditions of geopolymers, which achieve reasonable strength at ambient curing temperature, are contributed as theoretical framework (Figure 2.11) and listed in the following.

2.3.1 High humidity curing

Khale and Chaudhary (2007) have reported the review of geopolymer concrete by investigating the curing process with and without relative humidity control. Even though the curing temperature seems to be more dominant than relative humidity, curing samples in high humidity (in sealed bags) has very small difference in strength compared to those cured without bags. However, the strength of low calcium fly ash geopolymers with OPC

inclusion (10 to 15 percent) tended to be improved when cured with high humidity (vapour-proof membrane: to prevent moisture loss), as well as cured by immersed in water (23°C) (Pangdaeng, et al., 2014).

2.3.2 Concentration of alkaline activators

As aforementioned, the increase in specific concentration of the alkaline activators could possibly produce geopolymers which can achieve reasonable strength at ambient temperature and also give rise in compressive strength (Guo, et al., 2010; Somna, et al., 2011). Higher concentration increases stronger ion-pair formation than the lower one, providing more complete and quicker poly-condensation of particle interfaces (Raijiwala & Patil, 2010; Xu & Van Deventer, 2000). The enchantment in dissolution rate of the alumina-silicate materials could be observed in the rising up of reaction degree, indicating more beneficial for the geopolymerization (Mishra, et al., 2008; Wang, et al., 2005). The optimum concentration may vary due to many factors, e.g. prime material composition or curing environment. Nevertheless, too low concentration could lead to inert binding activity (Nath, et al., 2014), while too high concentration could lead to the forming coagulated structure and hinder the poly-condensation (Alonso & Palomo, 2001; Phoo-ngernkham & Sinsiri, 2011).

2.3.3 Fineness and shape of particles

The particle shape and size (fineness) directly affect mechanical properties of geopolymers after activation. Smaller particles with higher surface area increase the level of both physical and chemical reactions of geopolymerization, such as dissolution rate, ions transportation, forming alumina-silicate species, etc., which thereby control the initial setting time and geopolymeric gel phase (Chindaprasirt, et al., 2010; Petermann, et al., 2010). The compressive strength was also higher due to the change in morphology, allowing more dissolution rate of fly ash particles in the alkaline environment (Kumar & Kumar, 2011; Somna, et al., 2011). Chindaprasirt, et al. (2010) studied the effect of fineness of calcium fly ash-based geopolymer mortar on setting time and strength development by using three different finenesses, namely coarse original fly ash (CFA), medium-fineness fly ash (MFA) and fine fly ash (FFA), the highest strength was achieved for FFA geopolymers, followed by MFA and CFA. The similar results were found in the ground fine fly ash or milled fly ash geopolymers for which the higher compressive strength was obtained by milled-fly ash (6.8 μm) compared to raw-fly ash (14.4 μm), including an ability to be cured at ambient temperature or even at the low temperature (20

to 30°C) (Temuujin, et al., 2009a). In addition, the use of nano-particles (SiO_2 and Al_2O_3) of approximately 1 to 2% in high calcium fly ash geopolymers was also resulted in shorter setting and hardening process due to the formation of additional C-S-H or (C,N)-A-S-H gels, providing ability to achieve strength at room temperature (Phoo-ngernkham, et al., 2014).

2.3.4 Mixing procedures

In general, alumina-silicate prime materials and the combined alkaline solutions (e.g. NaOH and Na_2SiO_3) are incorporated and mixed together to form geopolymer cement (Chatveera & Makul, 2012). It is, however, reported that other sequences of adopting alkaline solution (i.e. NaOH solution is firstly mixed with prime materials, and subsequently Na_2SiO_3 solution is added in) could give shorter setting behaviour and higher strength than typical (general) mixing process due to initial high leaching of Si and Al from hydroxide soluble, followed by more binding activity from later added silicate soluble (Chindapasirt, et al., 2007). Other examples of just adding with water were also studied to simplify working on-site or to achieve some curing criteria at ambient temperature e.g. crushing fully-activated final product into powder (Duxson & Provis, 2008; Feng, et al., 2012; Yang, et al., 2008) or using of pre-dry mixing process (working with solid activators instead of alkaline solutions) (Suwan & Fan, 2014).

2.3.5 Alternative heat curing sources

As high curing temperature is able to improve mechanical strength of geopolymer cement, many studies have attempted to gain benefit from this advantage. Previous studies have revealed that the strength improvement could be obtained by an extra heat curing from both external and internal heat sources. For the examples of external sources, Nuruddin, et al. (2011b) revealed the results of the study on curing at ambient condition (in the shade outside the laboratory) and external exposure condition (covered by a transparent plastic sheet and exposed to direct sunlight) that the strength of exposure condition was definitely better than in shading due to an intensive heat from the sun. The similar results were also obtained from placing geopolymer cement to direct sunlight and covered with water-proof sheets or hot gunnies (Nuruddin, et al., 2011a). In hot surrounding environment (with the maximum temperature of 48°C and the average around 36 to 42°C), the alternative heat could advocate more degree of geopolymerization to the geopolymers. Apart from those sources of surrounding heat, internal heat generation was also investigated by casting geopolymer cement in a cubic yard mould (91cm x 91cm x 91cm) to observe its self-

internal heat from mass pouring (massive volume). The maximum internal temperature was around 42°C in first day and reduced slowly to 35°C in next 10 days (Vaidya, et al., 2011). By this, both external and internal heat could be the possible alternative heat sources for the self-heating geopolymers under ambient curing conditions to achieve a target compressive strength (Nuruddin, et al., 2011b).

2.3.6 Calcium content in mixtures

Theoretically, any alkaline and alkaline earth cation can be used as alkaline element in reaction, however, Sodium (Na^+) and Potassium (K^+) ions were majority of focusing. Although using Calcium (Ca^{2+}) has not been proven to produce similar result as Na^+ and K^+ some researchers reported the resultant of calcium content usage in the same way. Somehow, the early strength development and setting time of geopolymers were improved with some added calcium mineral to the binder (Buchwald, et al., 2005). The main reason leading to a good early strength is due to a rapid reaction between calcium mineral and alkaline solutions in the system, enhancing the strength development under ambient curing conditions. Calcium mineral could lead to the formation of C-S-H gel or (C,N)-A-S-H within a geopolymeric binder and improve the overall properties significantly (Xu & Van Deventer, 2002). The ability to achieve reasonable strength at ambient temperature has been reported by the synthesis with e.g. high calcium fly ash (Temuujin, et al., 2009b), bottom ash (Topçu, et al., 2014) or GBFS (Nath & Sarker, 2014) as prime materials, or even the additional amount of $\text{CaO}/\text{Ca}(\text{OH})_2$ (Yip, et al., 2005; Yu, et al., 1999), cement kiln dust (Ahmari & Zhang, 2013), volcanic ash containing calcium (Tchakoute, et al., 2013) and OPC (Khater, 2011). In contrast, the use of OPC as a calcium source in geopolymers is obviously widespread due to its uniformity complied with any standard and its global availability as a commercial construction material. This hybrid cementitious system is generally classified as an alkali-activated Portland blended cements or alkali-activated Portland fly ash cement (Shi, et al., 2011) or, sometimes, called Geopolymer-Portland cementitious (GeoPC) system (Suwan & Fan, 2014). Incorporating Portland cement to the system leads to significant effects on the setting behaviour and early strength development (Palomo, et al., 2007). The extra heat liberated by an exothermic reaction of OPC-hydration could also provide a positive effect enhancing its mechanical properties and microstructures (Pangdaeng, et al., 2014).

Theoretical framework

1. High humidity curing
2. Concentration of alkaline activators
3. Fineness and shape of particles
4. Mixing procedures
5. Alternative heat curing sources
6. Calcium content in mixtures
7. etc.

Figure 2.11 Theoretical framework of geopolymers cured at ambient temperature

2.4 Remark

This chapter, the literature review, summarised the research findings related to i) conventional OPC and the use of fly ash in OPC, ii) fundamentals of geopolymer cement and iii) factors influencing geopolymer properties at ambient curing temperature.

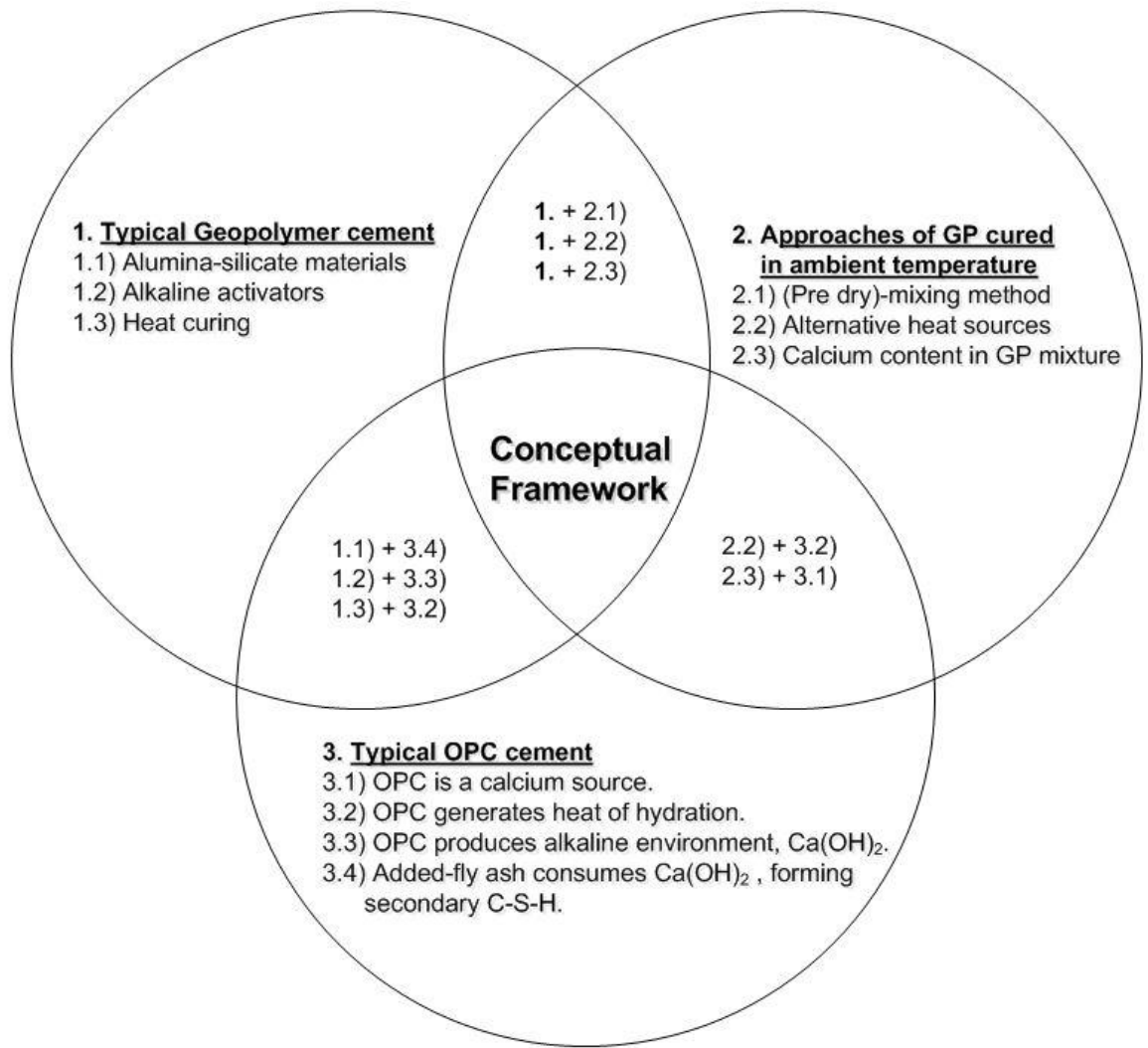
Portland cement is the most widely used construction material for many decades due to its terrific performance and global availability. However, OPC production is known as a large greenhouse gas contributor as well as energy-intensive manufacturer. Although an effort to reduce OPC consumption has been spent with replacement of any of pozzolanic materials (e.g. fly ash, furnace slag), only 10 to 40 percent of replacement was practically applied. The alternative low-carbon cementitious binders have been, therefore, extensively studied to reduce OPC production, and one among those alternative binders is “Geopolymer cement”. OPC is also considered as sources of calcium mineral (CaO) and high potential energy compounds (e.g. C_3S , C_2S , C_3A) and hence used as a catalyst constituent of the GeoPC to be developed in this study.

The fundamentals of geopolymers and geopolymerization have been compiled together with most important factors affecting properties and characteristics of geopolymers, i.e. main binder constituents, alkaline activators and binder concentration, and the curing procedures. Any alumina-silicate material could be used to produce geopolymers. Three main categories of prime materials, Industrial Waste (IW), General Waste (GW) and Natural Mineral (NM), have been classified. The particle size and shape, chemical composition and amount of Silica (Si) and Alumina (Al) contents are the keys of achieving mechanical strength of geopolymers. Coal-fired fly ash seems to be the most studied raw material for the alkaline activated cement due to its physical characteristics (small and spherical shape), chemical characteristics (rich in Si and Al) and eco-friendly origin (by-product). There are a varieties of alkalines used in geopolymer synthesis, but in this study, the sodium hydroxide solution and sodium silicate solution seem to perform the most

appropriate material for geopolymerization. The concentration of silicate soluble (in molarity and percentage), ratio of sodium silicate solution to sodium hydroxide solution by weight (SS/SH ratio), and alkaline solution to fly ash by weight (A/FA) are also the important factors which need to be concerned. Curing regimes, temperature and duration, stimulating the formation of geopolymeric gel, should be optimised. Too high and too long curing lead to rapid loss of moisture content, which has an adverse effect on its mechanical properties. Whereas too low temperature or too short curing period obstructed the geopolymeric formation.

Most of geopolymer properties normally were comparable with OPC standard, even though its formation is totally different. Although the geopolymers has some limitations such as costly alkaline solution, risk associated with the high alkalinity of the activating solution or practical difficulties in curing process, it is still a new choice of construction material for the future with many advantages. Geopolymer cement has been previously proven to have good physical and chemical properties. The benefits from being a waste treatment process and a low carbon-dioxide material are also highly concerned together with benefits in cost reduction. Main properties of the achieved geopolymer products with suitable manufacturing procedure and heat curing are also summarised in this chapter. To widen its applications and make it more convenient in practical work with reasonable strength, the attempt to develop fly ash-based geopolymers which is suitable for curing at ambient temperature without any external heating source should therefore be proposed with the factors influencing its properties under ambient conditions (in Section 2.3) as a Self-cured geopolymers in this study. From the aforementioned reviews, the conceptual frame work of the PhD studies had been deduced with the theoretical structure of the compiled literature reviews (Figure 2.12).

Overall, the future trend of geopolymers research shall focus on the understanding of polymerization mechanisms and this will standardise geopolymers for the commercial production. This might include the route of geopolymer synthesis with designable strength and properties, for example, the material with suitable activators and curing conditions, etc. Long-term assessment in both contamination and durability also need to be investigated before it becomes a new choice of innovative materials. Eventually, ease of use with user-friendly of geopolymer materials like being done with OPC should be further studied.



Conceptual framework

1. Introduction of new mixing procedures (Pre dry-mixing)
2. Inclusion of OPC as a calcium source in GP
3. Inclusion of OPC as an alternative heat source in GP
4. Inclusion of OPC provides alkaline environment

Figure 2.12 Conceptual framework of the research

CHAPTER 3 MATERIALS AND TESTING METHODS

3.1 Experimental Programme and Work Packages

The details of experimental programme are presented and explained in this chapter along with work packages as follows:

Work Package 1 (Chapter 3):

Examine the physical characteristics and chemical compositions of all prime materials i.e. OPC, fly ash, sodium hydroxide and sodium silicate by using SEM, EDXA and particle size distribution analysis techniques.

Work Package 2 (Chapter 2):

Determine the mechanical properties and mechanisms of OPC and typical geopolymer pastes under literature reviewing and then:

- a) Determine the mechanical properties through setting time test, compression test and internal heat measurement at room curing temperature.
- b) Determine the mechanisms using SEM, EDXA, FTIR and XRD at room curing temperature.

Work Package 3 (Chapter 4):

Determine the mechanical properties and mechanisms of geopolymer pastes in different manufacturing procedures at room curing temperature as follows:

- a) Determine the mechanical properties and mechanisms of geopolymer paste manufactured in separate mixing process (A).
- b) Determine the mechanical properties and mechanisms of geopolymer paste manufactured in general mixing process (B) or the typical geopolymer paste.
- c) Determine the mechanical properties and mechanisms of geopolymer paste manufactured in pre-dry mixing process (C).

Work Package 4 (Chapter 5):

Determine the mechanical properties and mechanisms of Geopolymer-Portland cementitious (GeoPC) system at room curing temperature as follows:

- a) OPC (100% OPC)
- b) GeoPC90 (90% OPC : 10% GP by mass)
- c) GeoPC80 (80% OPC : 20% GP by mass)
- d) GeoPC70 (70% OPC : 30% GP by mass)
- e) GeoPC50 (50% OPC : 50% GP by mass)

- f) GeoPC30 (30% OPC : 70% GP by mass)
- g) GeoPC20 (20% OPC : 80% GP by mass)
- h) GeoPC10 (10% OPC : 90% GP by mass)
- i) GeoPC5 (5% OPC : 95% GP by mass)
- j) GP (100% Geopolymers)

Work Package 5 (Chapter 6):

Determine the mechanical properties and mechanisms of OPC, typical geopolymers and Geopolymer-Portland cementitious (GeoPC) systems at various curing temperatures for 24 hours as follows:

- a) Fridge at 10°C
- b) Ambient temperature (Temperature controlled chamber) 20°C
- c) Electrical oven at 30°C
- d) Electrical oven at 40°C
- e) Electrical oven at 50°C
- f) Electrical oven at 60°C
- g) Electrical oven at 70°C

Work Package 6 (Chapter 7):

Determine the mechanical properties and mechanisms of the combined techniques of GeoPC system and pre-dry mixing process (C), which is called “Self-cured geopolymer cement” at room curing temperature as follows:

- a) Examine the optimum proportion of GeoPC to be manufactured in pre-dry mixing process.
- b) Determine the mechanical properties under setting time test, compression test and internal heat measurement at room curing temperature.
- c) Determine the mechanisms using SEM, EDXA, FTIR and XRD at room curing temperature.

Work Package 7 (Chapter 8):

Determine the compressive strength in different specimen sizes of Self-cured geopolymer cement at room curing temperature as follows:

- a) Determine the compressive strength of Self-cured geopolymer paste manufactured in prismatic shape of 40mm x 40mm x 160mm.
- b) Determine the compressive strength of Self-cured geopolymer paste manufactured in cubic shape of 100mm x 100mm x 100mm.

3.2 Materials and Equipment

3.2.1 Ordinary Portland cement (OPC)

Ordinary Portland Cement (OPC) used in this study was a general purpose cement Cemex CEM II/A-L type, which complies with the BS EN 197-1:2011. The particle size distribution (by a particle size distribution analyser) of OPC powder is given in Figure 3.1. The average particle size was 20.26 μm , while the mode was 18.66 μm . 80 percent of OPC powder sizes, in this test, were smaller than 34.25 μm with the specific surface area of 8512 cm^2/cm^3 .

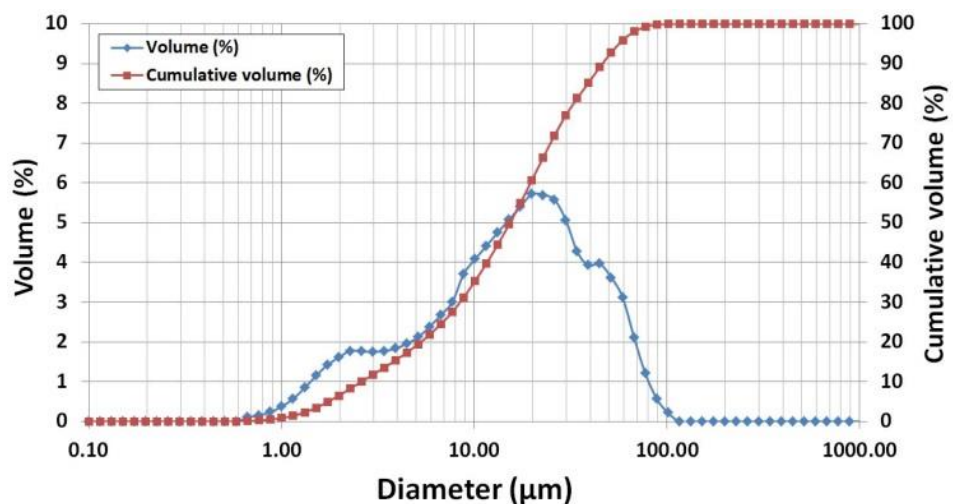


Figure 3.1 Particle size distribution of OPC powder

3.2.2 Coal-fired fly ash

Fly ash (FA) was supplied from the Drax Power Station, North Yorkshire, UK under Cemex brand. Its properties comply with BS EN 450-1:2012 (fineness category S and loss on ignition category B) or equivalent to low calcium class F in ASTM standard C618. The sum of $\text{SiO}_2 + \text{Al}_2\text{O}_3 + \text{FeO}$ is greater than 70 percent of total composition. It is noted that there were two batches of fly ash which were obtained in June 2013 (batch I) and July 2014 (batch II) respectively. As the characteristic of both batches were almost the same, only property of fly ash batch I is presented in this study. The average particle size is 6.72 μm , while the mode was 8.19 μm (Figure 3.2). 80% of fly ash particles were smaller than 8.82 μm with the specific surface area of 11148 cm^2/cm^3 . In addition, microstructure images by SEM and chemical compositions by EDXA of both OPC and fly ash are presented in Figure 3.3 and Table 3.1 respectively.

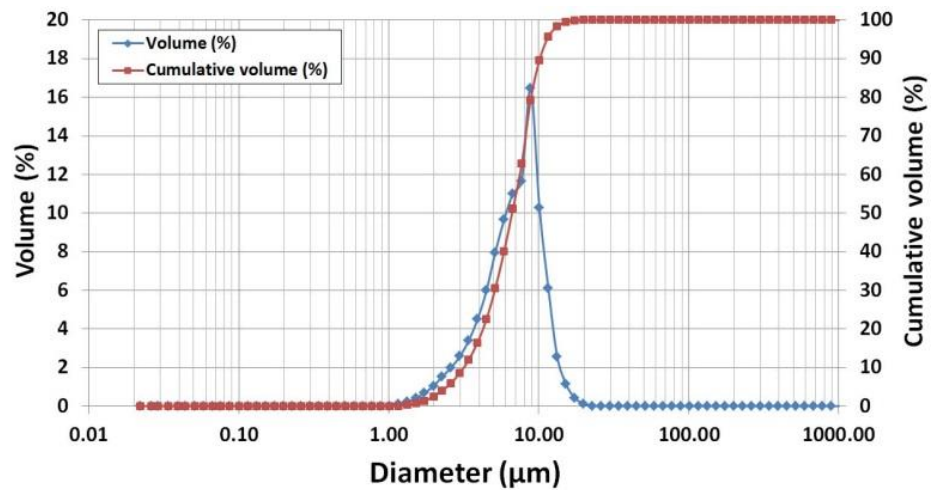


Figure 3.2 Particle size distribution of fly ash particles (batch I)

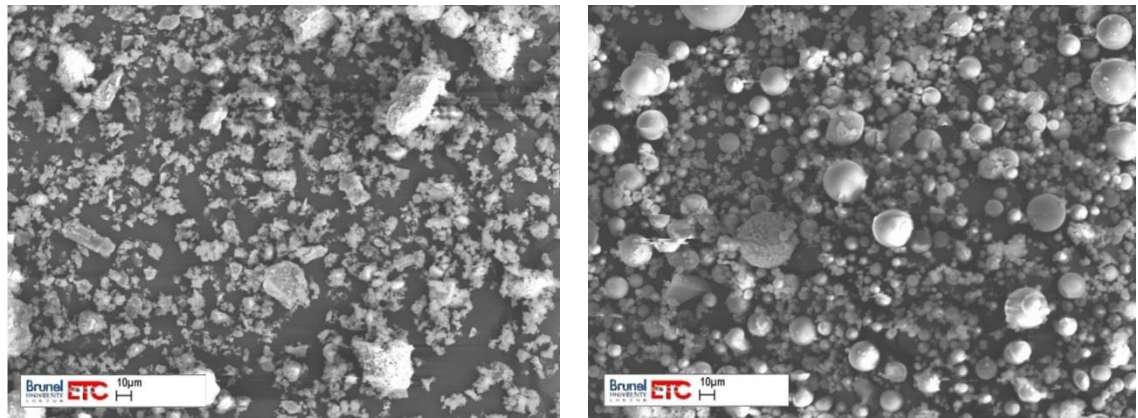


Figure 3.3 SEM images of OPC (left) and fly ash (right)

Table 3.1 Chemical compositions of fly ash and commercial OPC

Materials	SiO ₂	Al ₂ O ₃	FeO	CaO	Na ₂ O	TiO ₂	MgO	K ₂ O	SO ₃
Fly ash (I)*	50.97	27.83	9.21	2.62	1.13	1.15	1.43	3.73	1.93
Fly ash (II)*	45.71	29.40	9.17	1.59	0.90	1.14	0.97	3.16	0.74
OPC	12.22	3.85	2.85	73.82	-	-	0.78	1.17	5.30

*Batch of fly ash

3.2.3 Alkaline solutions

A combination of sodium hydroxide and sodium silicate solutions was used as alkaline activators regarding the previous research literatures. Sodium hydroxide (NaOH, SH) was a general purpose grade in pearl form (2 to 3 mm) with 98% purity, and purchased from the Fisher Scientific, UK. It was prepared as a solution by dissolving the pearl in purified water. The concentration of NaOH solution, in term of molar (M), was 15. For calculation, there was $15 \times 40 = 600$ grams of NaOH solid in 1000 cm^3 of purified water, where 15 and

40 are molar and molecular weight of NaOH respectively. Sodium silicate (Na_2SiO_3 , SS) was a general purpose grade in powder form, and also purchased from the Fisher Scientific, UK with a SiO_2 to Na_2O ratio (M_s , Modulus) of approximately 2.0. It was prepared as a sodium silicate solution with a chemical composition of 48.20% sodium silicate solid and 51.80% purified water by mass ($\text{SiO}_2 = 32.10\%$, $\text{Na}_2\text{O} = 16.10\%$ and water = 51.80%). All alkaline solutions were prepared and left overnight to ensure fully dissolved before using in experimental works (Figure 3.4).



Figure 3.4 Sodium hydroxide (left) and sodium silicate (right) in containers

3.2.4 Experimental equipment

It is noted that all of testing procedures and equipment used were verified under safety control, as well as laboratory and workshop areas. Some of main equipment and tools used in the study are listed as follows (Figure 3.5):

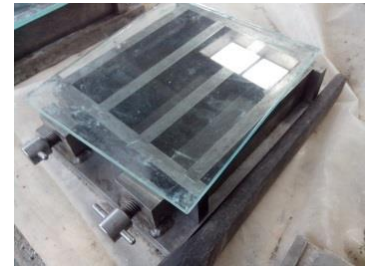
- a) Mortar mixer (ELE international, 5 litre nominal capacity, EN 196-1:2016)
- b) Steel 100mmx100mmx100mm cubic mould (ELE international, EN 12390-1:2012)
- c) Steel 40mmx40mmx160mm prismatic mould (ELE international, EN 196-1:2016)
- d) Plastic 100mm dia. x 200mm cylindrical mould (EN 12390-1:2012)
- e) Temperature-controlled curing chamber (Weiss Voetsch C-340, at 20°C)
- f) Electrical convection oven (ELE, temperature range 20 to 70°C)
- g) Vibration table
- h) Fridge (temperature range $10 \pm 2^\circ\text{C}$)
- i) Digital scales (max. 600 g. and max. 12 kg.)
- j) PPE, Thermometer, containers, spatulas, releasing oil, plastic sheets, etc.



(a) Mortar mixer



(b) Cubic mould



(c) Prismatic mould



(d) Cylindrical mould



(e) Temperature-controlled unit



(f) Electrical oven

Figure 3.5 Some of main experimental equipment used in laboratory

3.3 Sample Preparation

A standard mortar mixer with a speed of 140 ± 5 rpm was used to synthesize each mixture at room temperature of $20 \pm 2^\circ\text{C}$. All mixed pastes were casted in the 40mm x 40mm x 160mm or 100mm x 100mm x 100mm oiled-moulds. The moulds were half-filled and then compacted on vibration table for 30 seconds. The paste was filled up to the full level of the mould and vibrated for another 30 seconds. It is noted that as the high workability-pastes were prepared, the fully-compaction was therefore achieved easily. The mixing procedures of OPC, GP and GeoPC are described as follows.

3.3.1 Portland cement paste

Portland cement paste (OPC) was made of cement powder and the purified water with the water-to-solid (w/s) ratio at its standard consistency of 0.253. OPC was mixed with water for 90 seconds. The mixer was stopped for 30 seconds to remove all the paste adhered to the wall and the bottom to the middle part of the bowl, and was then restarted again for another 90 seconds. After well-mixing, the homogenous paste was used for further testing. The mixture description is shown in Table 3.2.

Table 3.2 Mixture descriptions

Mixture	Fly ash (g)	OPC (g)	Na ₂ SiO ₃ Solution (g)	NaOH Solution (g)	Purified water (g)	w/s ^b ratio
GP	500.0	-	120.0	80.0	-	0.191
GeoPC5	467.6	27.5	112.2	74.8	7.0	0.194
GeoPC10	443.0	55.0	106.3	70.9	13.9	0.197
GeoPC20	393.8	110.0	94.5	63.0	27.8	0.203
GeoPC30 ^a	338.3	162.0	81.2	54.1	69.2	0.259
GeoPC50 ^a	236.3	264.0	56.7	37.8	94.4	0.272
GeoPC70 ^a	138.9	362.0	33.3	22.2	118.6	0.285
GeoPC80 ^a	91.5	409.0	22.0	14.6	130.2	0.292
GeoPC90 ^a	45.2	455.0	10.9	7.2	141.5	0.298
OPC	-	500.0	-	-	126.5	0.253

^a 4% added water, ^b Water-to-solid ratio

3.3.2 Geopolymer cement paste

General fly ash-based geopolymer paste (GP) was composed of fly ash, sodium hydroxide and sodium silicate solutions. The sodium silicate solution to sodium hydroxide solution (SS/SH) ratio by mass was 1.50 and the constant alkaline liquid to fly ash (A/FA) ratio by mass was 0.40. Water-to-solid ratio of GP was 0.191 and calculated by the total mass of water in the mixture (= the mass of water for sodium silicate solution + sodium hydroxide solution) to the total mass of solid in the mixture (= the mass of fly ash + sodium hydroxide solid and sodium silicate solid; mass of Na₂O and SiO₂ in sodium silicate solution). The sodium hydroxide and sodium silicate solutions were prepared and left overnight before uses to ensure a thorough solution achieved. Both of them were mixed together until becoming homogenous. The combined solution was mixed with fly ash for 90 seconds. The mixer was then stopped for 30 seconds to allow removing all the paste adhered to the wall and the bottom and bringing it to the middle part of the bowl. Next, the mixer was restarted again and run for further 90 seconds. After well-mixing, the homogenous paste was ready for further testing. The mixture description is shown in Table 3.2.

3.3.3 GeoPC pastes

A series of Geopolymer-Portland cement paste (GeoPC) was made from the designation mass of GP and OPC paste from GeoPC5 to GeoPC90 (e.g. GeoPC30 is composed of 30% OPC paste and 70% GP paste). The mass of each material used, including alkaline solution and water, was calculated individually from the designed GP and OPC pastes. Water-to-solids ratio of GeoPC pastes was computed by the total mass of water in the mixture (= the

mass of water in the sodium silicate solution + sodium hydroxide solution + OPC paste + added water, if needed) to the total mass of solid in mixture (= the mass of OPC powder + fly ash + sodium hydroxide solid + sodium silicate solid). To mix GeoPC, the designated amounts of OPC powder and fly ash were initially dry-mixed together for 90 seconds in the mixer. A combination of NaOH solution, Na₂SiO₃ solutions and OPC-water was added to into the mixer which was run for 90 seconds. The mixer was then stopped for 30 seconds to allow removing all the paste adhered to the wall and the bottom and bringing it to the middle part of the bowl. Then, the mixer was restarted again and run for further 90 seconds. After well-mixing, the homogenous paste was ready for further testing. It is noted that 4% added-water is applied to some GeoPC mixtures in order to obtain the workability in practical work as shown in Table 3.2 (Calculation details: See Appendix B, Table B.1).

In general testing programme, after casting, the moulds were topped with cover glass and wrapped with plastic sheet to prevent moisture loss and stored at room temperature until the next day for demoulding. After demoulding, the samples were kept in plastic bags and cured in the temperature-controlled chamber at $20 \pm 2^\circ\text{C}$ until reaching the testing age (Figure 3.6).



Figure 3.6 Samples wrapping after casting (Left) and placing in plastic bags before curing (Right)

3.4 Testing of Physical and Mechanical Properties

3.4.1 Particle size distribution analysis

Particle size distribution analysis and specific surface area measurement of OPC powder and fly ash were tested on HORIBA Laser scattering particle size distribution analyzer LA-920 (Figure 3.7), which is able to work with particle sizes from 0.02 to 2000 μm . The

samples of OPC and fly ash were taken from laboratory in dry form and tested in closed-area at room temperature. Ultrasound was used for a period of 60 seconds to maintain sufficient dispersion during analysis.

3.4.2 Setting time

To determine the setting time, a Vicat apparatus was used in accordance with BS EN 196-3:2005+A1:2008 to determine the relation between the distance and time of needle penetrated in the soft cement samples. In general, the quick setting directly relates to early strength development and load bearing capability of the cement paste (Figure 3.8).



Figure 3.7 Particle size distribution analyzer



Figure 3.8 Vicat apparatus

3.4.3 Compressive strength test

Compressive strength of prismatic sample (40mm x 40mm x 160mm) was determined by using the Instron universal testing machine (UTM) in accordance with BS EN 196-1:2016 (Figure 3.9, Left). The samples were placed on the compressive test rig with a loading rate of 144 kN/minute. Fragmented pieces were kept for mechanism test of FTIR, XRD and SEM analysis afterwards. The testing values were automatically recorded and saved by Instron software.



Figure 3.9 Compressive strength test of prism (Left) and cube (Right)

Cubic samples were carried out for compression test with VJ Tech compression machines, EN Automatic Concrete Machine (3000 kN), with BS EN 12390-3:2009. The specimens were placed between platens before loading with a constant rate of 360 kN/minute (Figure 3.9, Right).

3.4.4 Hydration (internal temperature) test

Measurement of internal heat accumulated inside the samples was carried out by recording temperature using thermocouples embedded in three different positions in specimens. Type K thermocouples were placed inside the cylindrical samples (100 mm dia. x 200 mm height) along with the centre of its vertical axis. The probes were aligned vertically with 5 cm spacing from base plate to the top.

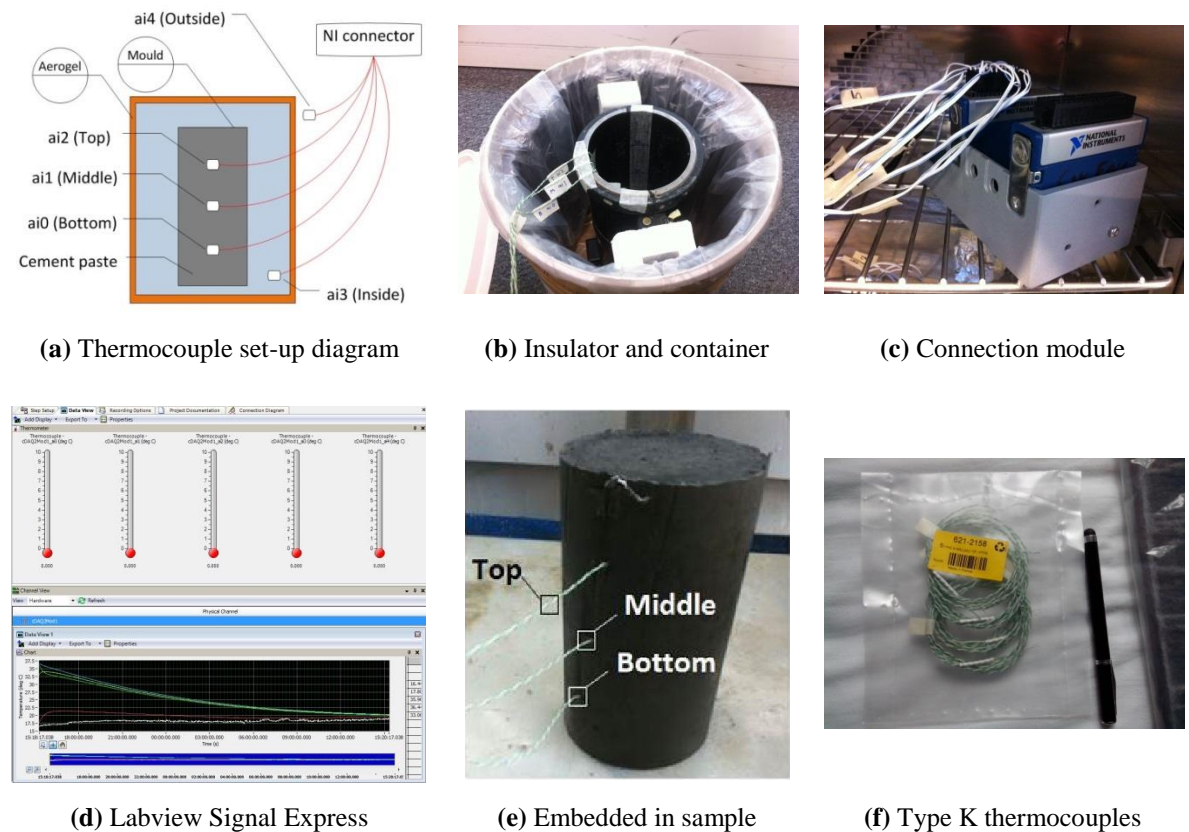


Figure 3.10 Set-up of the curing measurement in insulated container

The heat liberation at the position of bottom (ai0), middle (ai1) and top (ai2) were recorded, together with the temperature inside (ai3) and outside (ai4) the insulated container. An average temperature for ai0, ai1 and ai2 was used to represent the heat liberated from each specimen. The thermocouples were connected to a National Instrument 16-Channel thermocouple input module (NI 9213), which was run concurrently with Labview Signal Express programme. A high performance insulator, 10 mm aerogel, was attached to the bottom, side and top cover of the container in order to prevent the heat loss

during the hydration process (experiment). The physical properties of the aerogel are 0.15 g/cm^3 of density, 0.014 W/mK of thermal conductivity and 1 kJ/kgK of specific heat capacity. The designation of delay time (the period of time from the mixing to recording the data) was 15 minutes to allow placing paste into the mould and setting up the measurement equipment. The data was recorded every 60 seconds for a period of 24 hours to observe the heat generated inside specimens (Figure 3.10 a-f). It is, however, noted that the measurement is intended to report in degree Celsius ($^{\circ}\text{C}$) rather than the rate of energy evolution (J/g) because it can be practically compared with that of typical geopolymers curing at the temperatures of 40 to 90°C in the oven.

3.5 Chemical Group and Microstructure Characterization

3.5.1 X-Ray diffraction (XRD) analysis

XRD was used to characterise phase compositions, including crystallinity, chemical composition, basic crystal dimensions and stacking sequences. XRD patterns were recorded on a Bruker D8 Advance diffractometer fitted with a Lynxeye XE high-resolution energy dispersive 1-D detector. Monochromatic CuK radiation (copper tube $40 \text{ kV}/40 \text{ mA}$) with 0.154 nm wavelength was irradiated to samples for analysis. The samples were determined by using DIFFRAC.SUITE software. The scanning range between 5 and 100° for 2θ at 0.01° intervals with a measurement time of 0.2 second per 2θ intervals was covered over a 35 minute period (Figure 3.11).



Figure 3.11 Sieved particles in XRD testing discs (Left) and XRD machine (Right)

3.5.2 Fourier transform Infrared (FTIR) analysis

Functional groups of materials can be characterised by using infrared spectroscopy. Molecular vibrations, which correspond to the fundamental vibrations of the functional groups, are probed by infrared absorption bands (Lecomte, et al., 2006; Yip & Van

Deventer, 2003). In this study, the Fourier Transform Infrared (FTIR) was used with Attenuated Total Reflectance (ATR) technique on a Perkin Elmer Spectrum One-Fourier transform infrared spectrometer. The spectrums were recorded after running 100 scans in the wavenumber range of 650 to 4,000 cm^{-1} . It is noted that, for both FTIR and XRD analysis, the fragmented pieces of samples (from the previous compression test) were initially dry-ground with mortar and pestle. The smaller particles were finely grounded again before carrying out for sieving through sieve aperture of 250 μm (Figure 3.12).



Figure 3.12 FTIR machine (Left) and sieve vibration machine (Right)

3.5.3 SEM and EDX analysis

The Scanning Electron Microscope (SEM), an ultra-high performance field emission scanning electron microscope Zeiss Supra 35VP 20kV, was used to observe microstructure of small-piece samples under x1,000 and x5,000 magnifications. An Energy Dispersive X-ray Analysis (EDXA), which was equipped with SEM, was used to define the chemical composition of the resulting products and reported in term of weight percentage of each element and oxide compositions (Figure 3.13).



Figure 3.13 Samples on pins (Left), samples on SEM disc (Middle) and SEM machine (Right)

3.6 Remark

The comprehensive experimental work of the Self-cured geopolymer cement have been programmed and set up through each work package. The research methods included both relevant standards and in-house designed methodologies for investigations from sampling, fabrication, characterisation to mechanisms and performance in various circumstances. Raw materials were characterised in both physical appearance (particle size analysis) and chemical composition (EDXA). Mechanical properties of the resulted products were investigated by the testing of setting time, compressive strength and internal heat measurement while their mechanisms were examined by using XRD, FTIR and SEM-EDXA. Specific experimental set-ups or procedures, which may be required in some work packages, are additionally detailed in methodologies part of each chapter.

PART 2
CURING MECHANISMS AND PROPERTIES OF
GEOPOLYMERS

CHAPTER 4 EFFECT OF MANUFACTURING PROCEDURES ON MECHANISMS AND PROPERTIES OF FLY ASH-BASED GEOPOLYMERS

4.1 Introduction

Generally, the production of alumina-silicate based geopolymer cement uses alkaline solutions, mixing with raw starting materials to form the geopolymer cement paste. Other conditions and factors may be considered and set up from experimental designation e.g. material constituents, alkaline activator's concentration, curing regimes, etc. In fact, one of latent factors influencing the properties of geopolymers, which acquires less attention, is a mixing procedure. It is confirmed that the optimum/proper mixing order leads to better results for any of alkaline-activated binders (Pacheco-Torgal, et al., 2008b; Teixeira-Pinto, 2002).

For typical (general) mixing process, alkaline solutions (e.g. NaOH and Na₂SiO₃) are firstly prepared and left overnight to ensure a complete dissolution. Prime materials and those alkaline solutions are incorporated and mixed together at the same time (Ahmari & Zhang, 2013; Nuruddin, et al., 2011b). Apart from that, a separate mixing is also studied. Another sequence of adopting alkaline solution proposed by Chindapasirt, et al. (2010) is that hydroxide soluble (e.g. NaOH solution) is initially mixed with prime materials, and subsequently with later added silicate soluble (e.g. Na₂SiO₃ solution). All constituents are then well-mixed until the homogenous paste/slurry is achieved (Chindapasirt, et al., 2010; Rattanasak & Chindapasirt, 2009). Those two aforementioned procedures, general mixing and separate mixing, provided a satisfactory result as fully dissolved alkaline activators were used. In contrast, the separate mixing process was found to get slightly higher strength than that of general mixing (Chindapasirt, et al., 2007). More details are described and discussed onwards.

Nevertheless, to be more user-friendly like conventional OPC, the attempts to simplify geopolymers mixing process, by crushing fully-activated final product into powder and adding water to re-activate the reaction again as called "one-part geopolymers" or "just adding water geopolymers", were also studied (Duxson & Provis, 2008; Feng, et al., 2012). This technique started from dry-mixing of prime materials (e.g. fly ash, albite and kaolin) with alkaline materials (e.g. NaOH and KOH) and then thermally activated the mix at around 550 to 1,000°C for a period of 1 to 4 hours for calcination purpose. Those calcined materials are finally pulverized and then ready to be synthesized by just adding water to

activate the cementitious formation. The compressive capability at 28-day age was approximately 10 MPa for non-calcium content mixtures (fly ash-based) and up to 44 MPa for the mixtures that contain calcium (albite or kaolin) (Koloušek, et al., 2007; Yang, et al., 2008). Another example was also done by gridding pre-geopolymerized metakaolin-based geopolymers into powder form, which can be synthesized by just adding water under ambient conditions. Although, the compressive strength was not able to reach the same level as typical geopolymers, but the new research direction has been widely opened (Shi, et al., 2011). In addition, another alternative mixing method of Pre-dry mixing process (working with solid activators instead of alkaline solutions) was also intensively studied in this experiment by just adding with water to activate its reaction (Suwan & Fan, 2014).

The main aim of the testing programme in this chapter is to define the effect of manufacturing procedures on mechanisms and mechanical properties of fly ash-based geopolymers at ambient curing temperature, together with the development of the pre-dry mixing process, which is considered as a new alternative method for geopolymer production. The advantages of this approach would primarily focus on its ease of use (in practical work), and then properties.

4.2 Materials and Testing Methods

4.2.1 Materials and designation of mixtures

Coal-fired fly ash used in this test was batch I. Its properties are as stated in Chapter 3. The chemical compositions, examined by using the Energy dispersive X-ray Analysis (EDXA) technique, are summarised in Table 4.1. Alkaline materials used in this study were 15 Molar sodium hydroxide (NaOH) and 48.20% w/w sodium silicate (Na₂SiO₃) solutions.

Table 4.1 Chemical compositions of fly ash

Chemical compounds	SiO ₂	Al ₂ O ₃	FeO	CaO	Na ₂ O	TiO ₂	MgO	K ₂ O	SO ₃
Weight in %	50.97	27.83	9.21	2.62	1.13	1.15	1.43	3.73	1.93

Fly ash-based geopolymer paste was composed of fly ash, sodium hydroxide, sodium silicate and purified water. The sodium silicate solution to sodium hydroxide solution (SS/SH) ratio by mass was 1.50 and the constant alkaline liquid to solid (A/FA) ratio by mass was 0.40 in all manufacturing processes. Water-to-solid (w/s) ratio was calculated by the total mass of water in the mixture (= the mass of water for sodium silicate solution + sodium hydroxide solution) to the total mass of solid (= the mass of fly ash + sodium

hydroxide solid and sodium silicate solid; mass of Na₂O and SiO₂ in sodium silicate solution) in the mixture. The details of mixtures are given in Table 4.2.

Table 4.2 Details of fly ash-based mixtures in different processes

Process	Fly ash (g)	Na ₂ SiO ₃ Solution (g)	NaOH Solution (g)	Na ₂ SiO ₃ Solid (g)	NaOH Solid (g)	Purified water (g)	Overall w/s ratio
A	500.0	120.0	80.0	-	-	-	0.191
B	500.0	120.0	80.0	-	-	-	0.191
C	500.0	-	-	57.8	30.0	112.2	0.191

4.2.2 Manufacturing procedures

Three different manufacturing procedures, i) Separate mixing, ii) General mixing and iii) Pre-dry mixing, were proposed and named as process A, B and C respectively. A standard mortar mixer with speed of 140 ± 5 rpm was used to synthesize each mixture at ambient temperature, $20 \pm 2^\circ\text{C}$.

4.2.2.1 Process A or Separate mixing: (Fly ash + NaOH solution, then Na₂SiO₃ solution)

The sodium hydroxide and sodium silicate solutions were prepared and left overnight before uses to ensure a thorough solution achieved. Fly ash was firstly mixed with sodium hydroxide solution for 90 seconds. The mixer was then stopped for 30 seconds to allow removing all the paste adhered to the wall and the bottom and bringing it to the middle part of the bowl. During this period, sodium silicate solution was added into the mixer and mixed together for another 90 seconds. After well-mixing, the homogenous slurry was carried out for further testing.

4.2.2.2 Process B or General mixing: (Fly ash + NaOH and Na₂SiO₃ solutions)

The sodium hydroxide and sodium silicate solutions were prepared and left overnight before uses to ensure a thorough solution achieved. Both of them were initially mixed together until becoming homogenous. This combined solution was then mixed with fly ash for 90 seconds. The mixer was then stopped for 30 seconds to allow removing all the paste adhered to the wall and the bottom and bringing it to the middle part of the bowl. Then, the mixer was restarted again and run for further 90 seconds. After well-mixing, the homogenous slurry was carried out for further testing.

4.2.2.3 Process C or Pre-dry mixing: (Fly ash + alkaline solids, then add with water)

Fly ash, sodium hydroxide and sodium silicate solids were firstly dry-mixed together for 90 seconds in the mixer. The specific amount of water based on the same ratio of water-to-

solid as those used in the processes A and B was then added into the bowl, and mixed together for 90 seconds. 30 seconds after the stopped time to remove all paste adhered to the middle part of the bowl, the mixer was restarted again and run for further 90 seconds. After well-mixing, the homogenous paste was carried out for further testing. Testing scheme of all manufacturing procedures and testing diagram of pre-dry mixing process (C) are given in Figures 4.1 and 4.2 respectively.

Process A	Process B	Process C
Fly ash (s) + NaOH (l)	Fly ash (s)	Fly ash (s) + NaOH (s) + Sodium silicate (s)
↓ 90 s	↓	↓ 90 s
Sodium silicate (l)	Sodium silicate (l) + NaOH (l)	Water (l)
↓ 90 s	↓ 90 s / 90 s	↓ 90 s / 90 s
Cementitious paste	Cementitious paste	Cementitious paste

Note: s, solid state; l, liquid state

Figure 4.1 Testing diagram of different manufacturing processes (A, B and C)

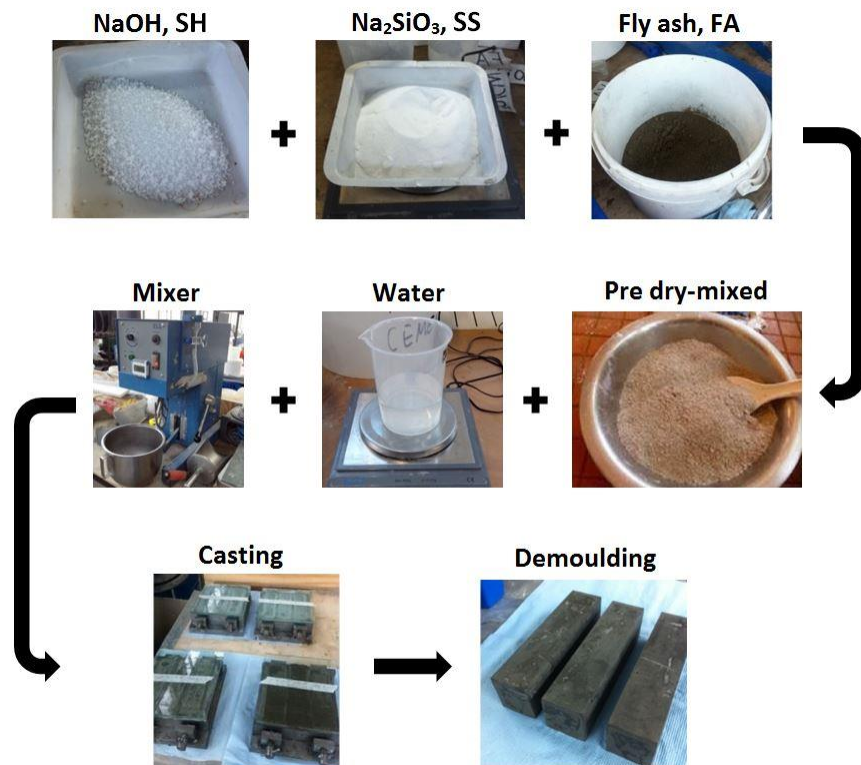


Figure 4.2 Testing diagram of pre-dry mixing process (C)

4.3 Analytical Methods

To determine the setting time of each combination and manufacturing process, a Vicat apparatus was used in accordance with BS EN 196-3:2005+A1:2008 to determine the

relation between the distance and time of the needle penetrating in the soft cement samples. Compressive strength of prismatic samples (40mm x 40mm x 160mm) of all testing was determined by using the Instron universal testing machine (UTM) in accordance with BS EN 196-1:2016. It is noted that the samples used in the compression test of all manufacturing processes (A, B and C) were demoulded after three days as the samples required more setting time at ambient temperature. After demoulding, all samples were kept in plastic bags and cured in the temperature-controlled chamber at 20 ± 2 °C until reaching the testing age. Measurement of internal heat accumulated inside the samples was carried out by recording the temperature using thermocouples embedded in the specimens. All cylindrical samples (100 mm dia. x 200 mm height) were stored in an aerogel-insulated container during the measurement to prevent heat loss. Labview Signal Express software 16-Channel thermocouple input module was used to control the measurement. The data was recorded every 60 seconds for a period of 24 hours to observe the heat generated inside the specimens.

The Fourier Transform Infrared (FTIR) spectrums were obtained by using Attenuated Total Reflectance (ATR) technique on a Perkin Elmer Spectrum One-Fourier transform infrared spectrometer. The spectrums were recorded after running 100 scans in the wavenumber range of 650 to 4,000 cm^{-1} . The X-Ray diffraction (XRD) patterns were recorded on a Bruker D8 Advance diffractometer fitted with a Lynxeye XE high-resolution energy dispersive 1-D detector. The samples were determined by using DIFFRAC.SUITE software. The scanning range between 5 and 100° for 2θ was covered in a 35-minute period. Scanning Electron microscope (SEM) was used to observe the microstructures, and the Energy dispersive X-ray Analysis (SEM-EDXA) technique was used to identify the chemical compositions of the resulted products.

4.4 Results and Discussion

Three different manufacturing processes have been uniquely investigated: Process A was focused on the adding sequence of alkaline activators, while the process B was on the process of raw material with the combined-alkaline soluble. In general, the manufacturing processes A and B are widely used to prepare geopolymers due to the simple use of dissolved alkaline solutions, in which alkaline materials have already disassociated into ion forms. However, both A and B processes require additional heat resources for the curing purpose to achieve higher strength. For a new route of geopolymer synthesis proposed in this chapter, the pre-dry mixing method (Process C) simply pre-mixes all solid materials in

dry, and then the full amount of the required water is added to that dry mix. Process C was designed in order to take advantage of potential energy released from the dissolution of both NaOH and Na₂SiO₃, which could serve as an extra heat for curing purposes. In contrast, process C conducted at ambient temperature without any external heat supply can form its structure under internal heat liberation itself, which could accelerate more geopolymeric gel formation in the matrices. To investigate the effect of those all manufacturing processes, setting time, mechanical strength and internal heat accumulated inside the samples were examined together with their mechanisms.

4.4.1 Setting time

It was found that setting time of all manufacturing processes were not able to be measured in the first 24 hours. However, the process C clearly liberated much more heat and solidified faster than the processes A and B. After one hour of mixing, the Vicat needle was dropped to the paste observing the hardening process. It appeared that the plunged-needle illustrates the wet, viscous and adhesive characteristics of process A and B, while the needle-hole is left on the stiff paste of process C (Figure 4.3). It is noted that process A and B had very similar drying characteristic as alkaline solutions were used in their synthesis. However, it can be clearly seen that high heat generated in process C resulted in an increase of the cementitious reaction which may lead to the fast loss of moisture and fast solidification.

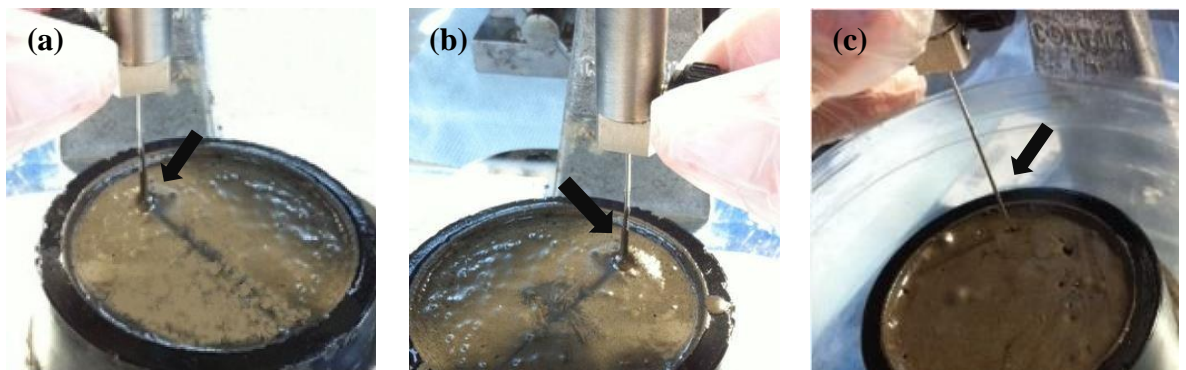


Figure 4.3 Drying behavior after 1 hour of mixing processes (a) A, (b) B and (c) C

4.4.2 Compressive strength

All of geopolymer pastes could not set in the first 3 days, therefore, the first compression test was carried out at 7 days age, followed by 14 and 28 day ages. It has been reported that the different manufacturing procedures or mixing orders of geopolymer paste are able to produce different mechanical properties due to the unique characteristic and sequence of expedient formation (Kobera, et al., 2011; Pacheco-Torgal, et al., 2008). The structural

formation of geopolymer paste was very slow under the ambient curing conditions, therefore, a prolonged period of time was required for the paste solidification (over 3 to 5 days). In this case, uncompleted reaction of geopolymeric gelation can also be observed as it could affect the strength of the geopolymer paste in both early and later ages.

Process A resulted in the highest mechanical strength due to the initial mixing with NaOH solution, which led to the higher rate of leaching of silica, alumina and other ions from prime materials. Whilst more binding activities from later added silicate solution was also obtained and enhanced the degree of geopolymerization (Chindapasirt, et al., 2007). Process B is a widely used method in geopolymer synthesis. The pre-combined alkaline solution used in process B provided a better uniformity, but the structural formation appeared to be inert and led to slightly lower strength than that of process A (Pacheco-Torgal, et al., 2008; Rattanasak & Chindapasirt, 2009). Although, the amount of each single raw material or alkaline solutions are easy to be controlled, too many handling steps are required and take more time to proceed (Hardjito, et al., 2008; Yip, et al., 2005).

Process C solidified much more intensively than those occurred in the process A or B by a strong hydration among prime material, alkaline solids and water in the system. Without moisture loss protection, the heat generated from process C can lead to a rapid loss of moisture on the surface of samples. Micro-cavities, which were left in the structure, could give an adverse effect in mechanical strength. Although the obtained heat provided good curing conditions as similar as happened in mild-to-medium temperature curing (Škvára, et al., 2006; Yip, et al., 2008), incomplete dissolution could lead to a low reaction rate. The compressive strength of process C was, thus, lower than that of process A and B (Figure 4.4).

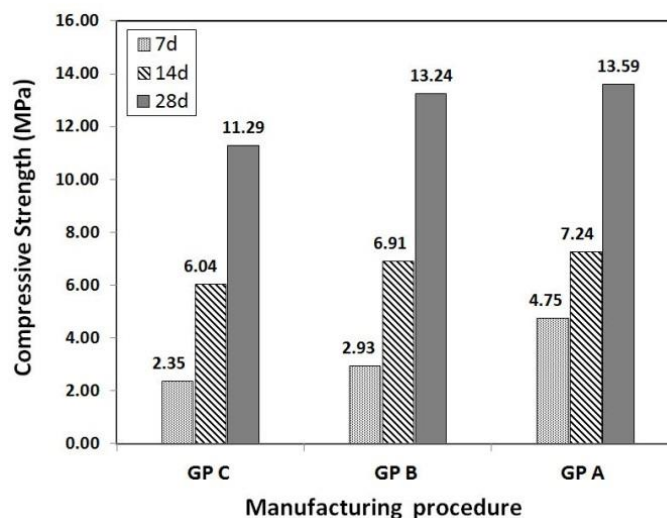


Figure 4.4 Compressive strength of geopolymers in different processes

It should be noted that extra water in the system might be required in order to sufficiently activate all solid materials, therefore, an increase of water-to-solid (w/s) ratio need to be considered as one of the factors affecting its strength. In contrast, it can be drawn that the process C could achieve the quickest setting characters with intensive heat liberation, while the processes A and B took longer time to set. Process A gained the highest compressive strength followed by process B and C respectively in all testing ages (Chindaprasirt, et al., 2010; Sukmak, et al., 2013) (More details: See Appendix A, Table A.2).

4.4.3 Measurement of internal heat accumulated inside the samples

The heat liberation of alkaline activators, sodium hydroxide and sodium silicate, during aqueous alkaline preparation (of 500 g. solution) was previously measured in order to evaluate its effect in the pre-dry mixing process (C). It can be seen that the temperature abruptly increased after adding water to alkaline solids and then steadily decreased to room temperature in approximately 4 hours. NaOH (15M) released the maximum heat of 93°C, followed by NaOH (10M) and sodium silicate at the maxima of 85°C and 46°C respectively. It is apparent that the sodium hydroxide (NaOH) dissolution produced more intensive heat than that of sodium silicate and, in addition, a higher concentration of NaOH generated higher temperature (Figure 4.5). The reason is that the chemical species of alkaline materials were brought to a lower energy state when dissolved with water (H₂O) to be Na⁺ and OH⁻ for sodium hydroxide and 2Na²⁺ + SiO₂((OH)₂)²⁻ for sodium silicate (Sottisoplia & Asavapisit, 2005).

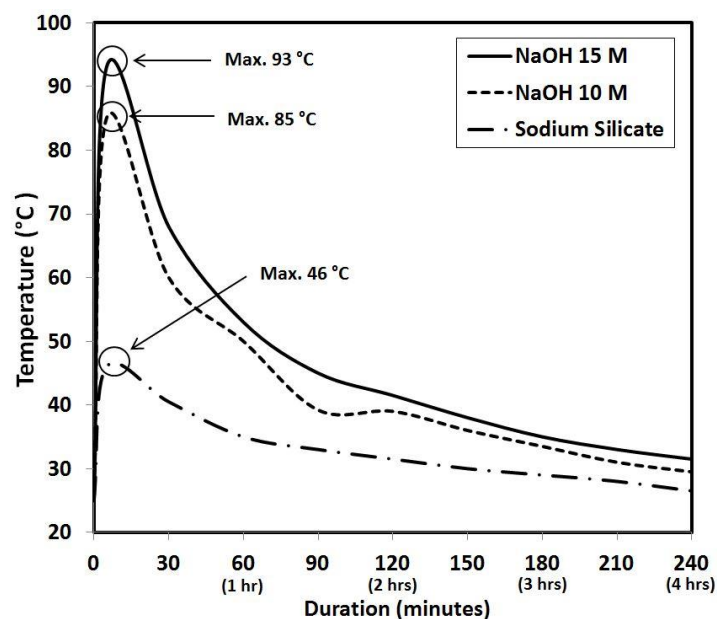


Figure 4.5 Heat evolution of alkaline soluble preparation

As seen in Figure 4.6, the measurement of internal heat accumulated inside the samples were examined as the rise of temperature of geopolymer mixtures with three different processes A, B and C. The average measurement of internal heat accumulated inside the samples from three embedded thermocouples of each process was recorded for a period of 24 hours. It should be noted that the temperature measured from those thermocouples were slightly different: the top position (ai2) had the highest temperature followed by the middle (ai1) and the bottom (ai0) position, e.g. a set of ai2=30.2°C, ai1=29.8°C and ai0=29.5°C. The reason is that the nature of heat moves upward, resulting in higher temperature in upper section of specimens than that in the lower section. The room temperature (RT) recorded during the test was also maintained in temperature range of 18 to 22 °C.

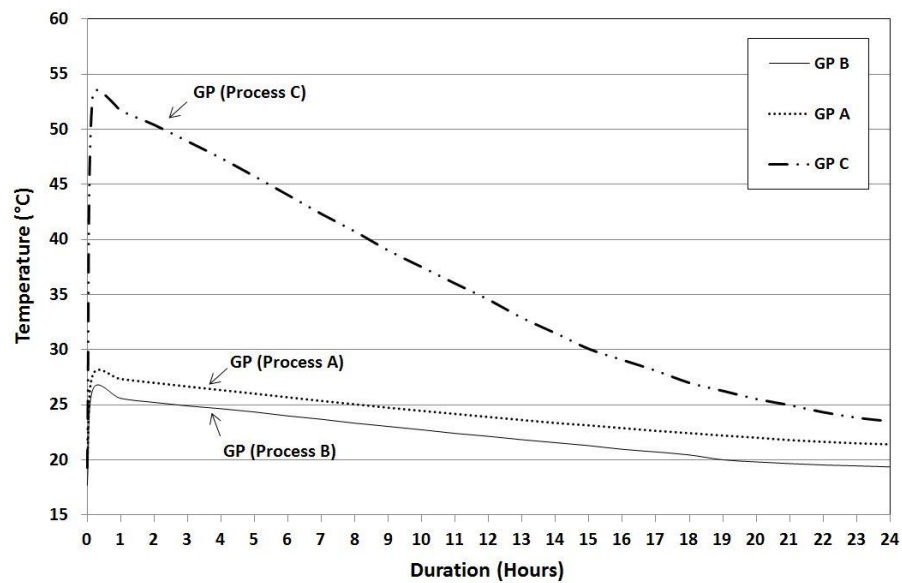


Figure 4.6 Average heat evolution of geopolymers during a 24-hour period

It is apparent that the processes A and B release very limited heat above room temperature at the peaks of approximately 28°C and 27°C in the first 20 minutes of mixing. After that, the temperature reduced steadily to room temperature at 21°C and 19°C within the 24 hours. On the other hand, the process C had much higher temperature than those for A and B after mixing with water. The highest temperature reached around 54°C in the first 20 minutes and maintained above 40°C for over 8 hours. Then, it cooled down slowly to around 24°C at the 24th hour.

The limited heat liberation in the processes A and B was generated by the chemical reactions among various alkaline ions and fly ash inside the paste (i.e. hydration and geopolymerization). The dissolution of fly ash, in initial stage, underwent a slight exothermic reaction which led to less heat emitted. On the contrary, the heat liberation

from the process C was almost two times higher than those from the processes A and B. This means that the pre-dry mixing method (process C) could be able to produce an intensive heat during the hydration of alkaline solid, which could realise the development of a heat based self-cured geopolymer cement.

For general case, the temperature could be kept inside the mixture for longer than 8 hours, if mortar (paste and sand) or concrete (paste, sand and gravels) is manufactured by this process (C), regarding to the extra heat accumulated by those aggregates. It is worth to note that possible alumina-silicate reactivity (ASR) may occur with the added aggregates because some of the selected aggregates, e.g. opaline, cryptocrystalline silica, chalcedony and microcrystalline quartz, could be dissolved in alkaline activating solution (Petermann, et al., 2010). As far as geopolymers are produced in huge volume (massive amount) together with good heat and moisture loss protection, the internal heat could be extendedly maintained and provide positive curing conditions to those geopolymers.

4.4.4 Analysis on microstructures and elemental composition

Scanning electron microscope (SEM) and Energy dispersive X-ray Analysis (EDXA) were used to observe the microstructures and elemental compositions of all manufacturing processes (Figure 4.7). Micrographs of the 28-day age geopolymer samples produced with processes A and B show very similar appearances of porous structure. Some of unreacted fly ash particles are scattered in geopolymeric gel, while and micro-cracks were also observed (Figures 4.7(a) and (b)). The SEM images clearly show that process A achieves the most compact structure, followed by B and C due to an advantage in additional dissolution rate and binding activity from separate mixing of alkaline activators (Chindaprasirt, et al., 2010). Abundant spherical fly ash particles with loose structure are obviously seen in process C images as a dry-mixing requires more water to dissolve all solid materials as well as compensate the moisture loss during its exothermic reaction (Figure 4.7(c)). However, as process C was mixed in a dry-condition, more water (higher w/s ratio) may be required to achieve a better dissolution. Moreover, as process C seemed to be very hot when hydrated, this advantage could also be an alternative self-heating source for curing purpose of the geopolymers enhancing its mechanical properties. More details of w/s ratio in pre-dry mixing process (C) are given in the next sub-section 4.4.7 onwards. As far as appeared in the comparable SEM images, it could noticeably confirm that the microstructures and mechanisms of low calcium fly ash-based geopolymers cured at ambient temperature are obviously influenced by the manufacturing processes.

With the EDXA technique, more emphasis on elemental ratios has been pointed out, especially for Si/Al and Ca/Si ratios, to explain the relationship between those ratios and engineering properties. Although higher compressive strength was obtained by process A and B than process C, there was no significant difference in the elemental compositions as their main minerals (Si, Al, Ca) were very similar to each other.

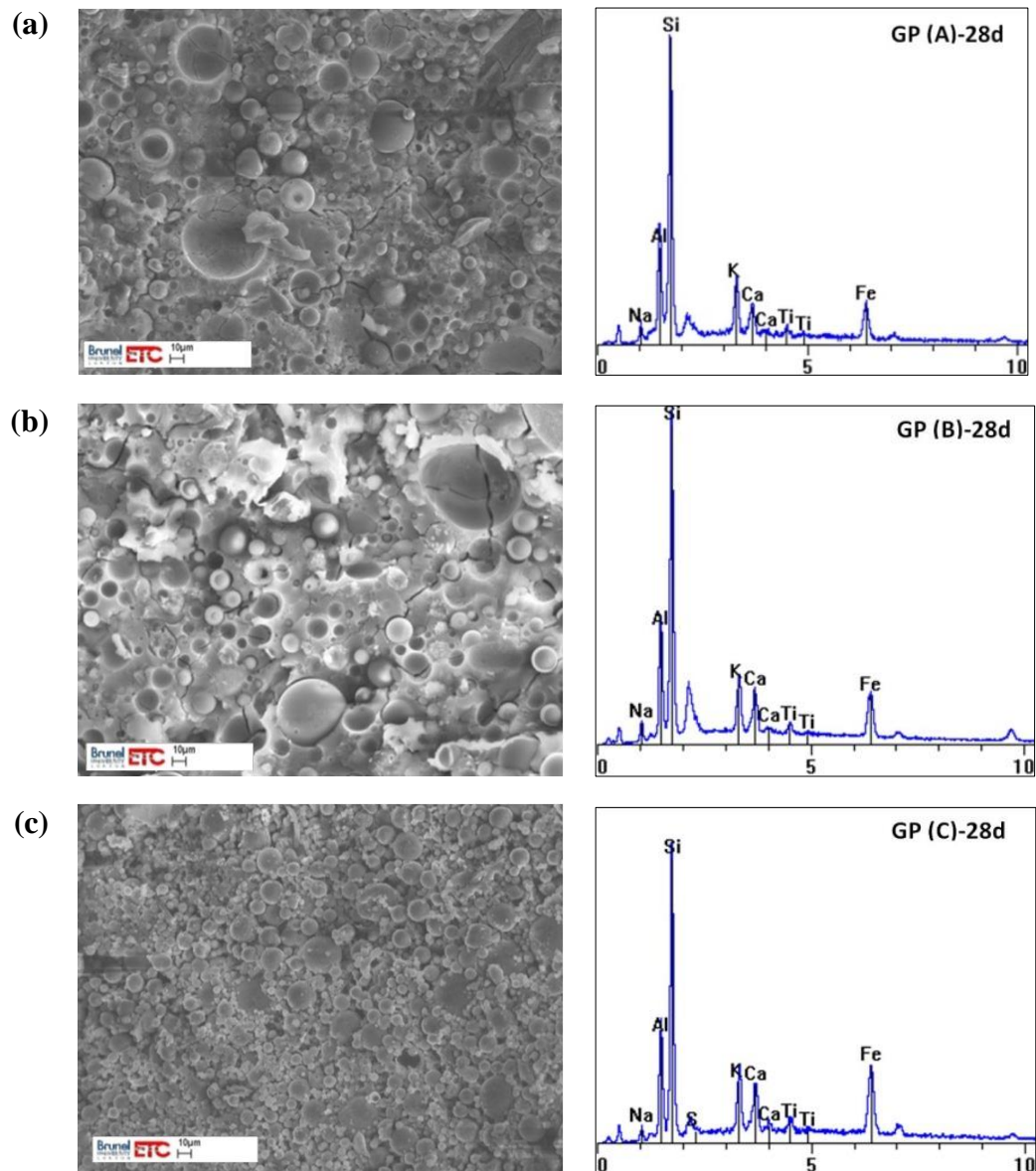


Figure 4.7 SEM images and EDX spectrum of geopolymers at the 28-day age

The Si/Al and Ca/Si ratios for all manufacturing procedures are in the ranges of 2.64 to 3.10 and 0.14 to 0.23 respectively (Table 4.3). The chemical ratios of silica, alumina and calcium in geopolymer were apparently corresponded to related studies, including the formation of geopolymeric gel (C,N-A-S-H, quartz and mullite) (Ahmari, et al., 2012; Nath & Sarker, 2014). With less amount of calcium content, the main geopolymeric gel

was therefore an interfered of (Na)-poly(sialate-disiloxo) or $\text{Na}_n\text{(-Si-O-Al-O-Si-O-Si-O-)}_n$ - (Guo, et al., 2010).

Table 4.3 Elemental compositions and ratios in the mixtures at 28-day age

Mixtures	w/s ^a	Si	Al	Ca	Na	K	Fe	Si/Al	Ca/Si	Si/Na	Na/Al
GP Process A	0.191	45.84	14.78	6.53	3.18	11.73	16.03	3.10	0.14	14.42	0.22
GP Process B	0.191	42.90	15.11	7.75	4.08	9.78	18.08	2.84	0.18	10.52	0.27
GP Process C	0.191	35.98	13.65	8.22	2.51	9.78	25.61	2.64	0.23	14.34	0.18

^a Water-to-solid ratio

4.4.5 Functional group analysis

The functional groups of geopolymers manufactured in different processes (A, B and C) are presented in Figure 4.8. As the main compositions of fly ash were silica (Si), alumina (Al) and oxygen (O), the skeleton of geopolymeric formation was hence observed as Si-O-Al groups. Additional sodium (Na) was generally found by the usage of alkaline solutions (NaOH and Na_2SiO_3).

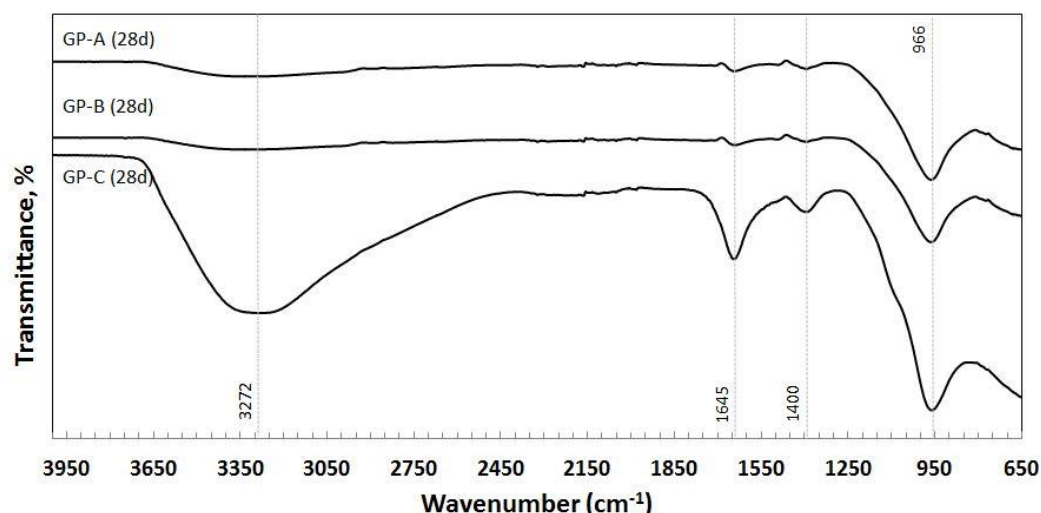


Figure 4.8 FTIR spectrum of geopolymers at the 28-day age

Geopolymer pastes synthesized with alkaline solutions (processes A and B) exhibit a peak at $1,645\text{ cm}^{-1}$, which corresponded to O-H stretching and O-H bending (H_2O or water). Those small peaks found in both spectrums indicate some water was left in the mixtures (Liew, et al., 2012; Yip, et al., 2008). The bondings of Si-O and Al-O asymmetric stretching, which are parts of geopolymeric structure, also formed at band $1,400\text{ cm}^{-1}$ (Ahmari, et al., 2012; Škvára, et al., 2006). The main bonding was exhibited at the band 966 cm^{-1} , indicating the Si-O stretching vibration of SiO_4 and also AlO_4 of geopolymeric and N-A-S-H gel (Puertas & Torres-Carrasco, 2014).

For geopolymer paste synthesized with alkaline solids (process C), a strong wide band centred around $3,272\text{ cm}^{-1}$ and a peak at $1,645\text{ cm}^{-1}$ are also attributed to O-H bonding of water. By this, it can be noticeably seen that much more water, than those in processes A and B, was left in the system. Although, process C obtained intensive heat liberation which is able to accelerate evaporation rate of existing water, an incomplete reaction (confirmed by SEM images) of dry-mixing process led to scattered water kept in the matrices until its later age. This occurrence therefore evidently causes lower strength and loose structure in pre-dry mixing process (C). However, the main change in the IR spectrum of process C became more enlarged and intensive, relating to Si-O and Al-O bonding ($1,400$ and 966 cm^{-1}) of geopolymerization reaction. This transition was previously observed in geopolymer binders cured at high temperature, indicating that higher degree of polymerisation was established (Lecomte, et al., 2006; Nath, et al., 2014).

Beyond the typical production of geopolymer cement with alkaline solutions, the major findings from the functional group analysis can be drawn, i) pre-dry mixing process (C) could gain higher degree of geopolymerization by its internal self-heating and ii) the mechanical properties of this dry-mixing method may be additionally improved by increasing the degree of reaction, together with the reduction of moisture left in the structure. Those enhancements could also be achieved by any other approaches e.g. optimizing water content, improving of mixing procedures, using high fineness materials and maintaining its internal self-heating (Suwan, et al., 2016).

4.4.6 Morphology and crystallinity analysis

The crystallinity of Mullite, Quartz, Nepheline and (C,N)-A-S-H are similarly found in X-ray diffractograms of all manufacturing processes (Figure 4.9). From the qualitative XRD, it is difficult to identify the amount of reaction products or to clearly define the effect of manufacturing processes. However, it was observed that the crystallinity phases of geopolymers manufactured with both alkaline solutions (processes A and B) and alkaline solids (process C) resulted in almost the same patterns. The formation of amorphous structures, which was indicated by broad humps, is slightly different in each process. XRD patterns of processes A and B show broad humps in 10 to 15° and 20 to 35° for 2θ , while only a range of 20 to 35° for 2θ is found in process C.

It can be explained that higher curing temperature (i.e. in process C) is able to achieve additional crystalline phases, indicating in less hump (less amorphousness = more crystallinity) (Suwan & Fan, 2014). Pre-dry mixing process (C) seemed to exhibit superior

characteristics above A and B processes in term of atomic-structure (XRD) but, the weakness in functional groups inter-crosslink (FTIR) could raise adverse effects to the final properties for process C. Therefore, the effects of manufacturing processes may be more visible from the results of the mechanical strength and micro-structural formation as mentioned in SEM-EDXA.

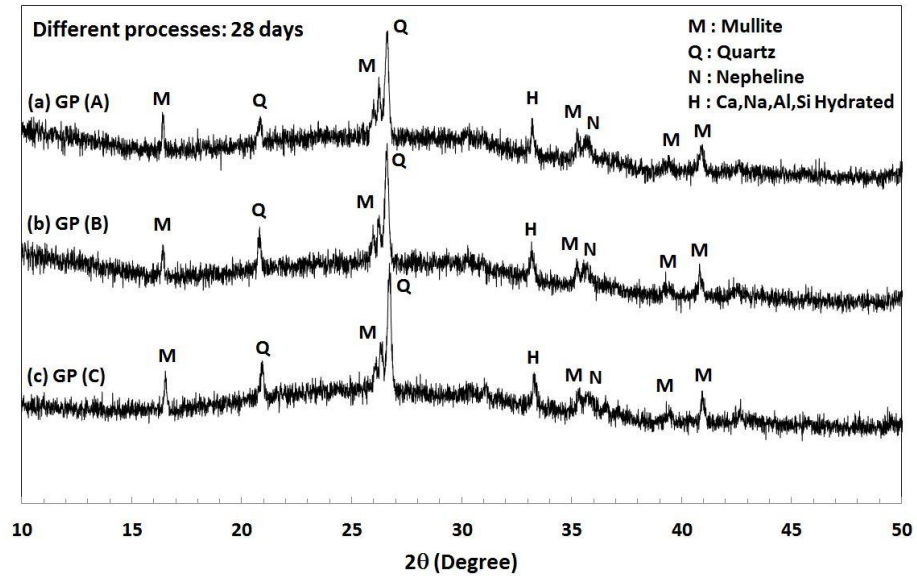


Figure 4.9 X-ray diffraction patterns of geopolymers processes A (a), B (b) and C (c) at the age of 28 days

4.4.7 Effect of water-to-solid ratio on pre-dry mixing process (C)

As pre-dry mixing process seems to provide good conditions for self-curing approach e.g. high heat liberation or even less preparation processes, the further study on its w/s ratio is therefore considered for practical handling. Pre-dry mixing process (C) requires extra water not only for dissolution purpose but also for compensating quick-evaporated water from its self-generated heat. As the typical w/s ratio of geopolymers in this study was 0.191 (A/FA=0.40), the comparable designation of various w/s ratios were, thus, established viz. 0.170 (A/FA=0.35), 0.211 (A/FA=0.45) and 0.230 (A/FA=0.50) as shown in Table 4.4. However, it is noted that process C with w/s ratio of 0.170 (A/FA=0.35), was unable to be carried out for testing because the cement was too dry and stiff.

Table 4.4 Mixtures and compressive strengths of GP process C for various w/s ratios

Mixture	w/s	A/FA	Fly ash (g)	Na ₂ SiO ₃ Solid (g)	NaOH Solid (g)	Purified Water (g)	Comp. 28d (MPa)
GP Process C-0.35	0.170	0.35	500.0	50.61	26.25	98.14	- ^a
GP Process C-0.40	0.191	0.40	500.0	57.80	30.00	112.20	11.29
GP Process C-0.45	0.211	0.45	500.0	65.07	33.75	126.18	11.91
GP Process C-0.50	0.230	0.50	500.0	72.30	37.50	140.20	8.36

^a Too dry to carry out further testing / unable to be tested.

The highest compressive strength was achieved by the mixtures with w/s ratio of 0.211, followed by 0.191 (typical mix) and 0.230 respectively (Table 4.4). No significant differences among those w/s ratios were observed by FTIR, XRD and EDXA. However, it can be obviously explained from SEM micrographs in Figure 4.10(a) that unreacted fly ash particles are scattered in the loose matrix of insufficient water content mixture. More compact and firm geopolymeric matrix is clearly found in Figure 4.10(b) of GP Process C-0.45; w/s = 0.211 with an appropriate amount of water in the mixture. Loose structure with abundant of voids appeared in GP Process C-0.50 (w/s = 0.230) as excess water was left in the system (Figure 4.10(c)).

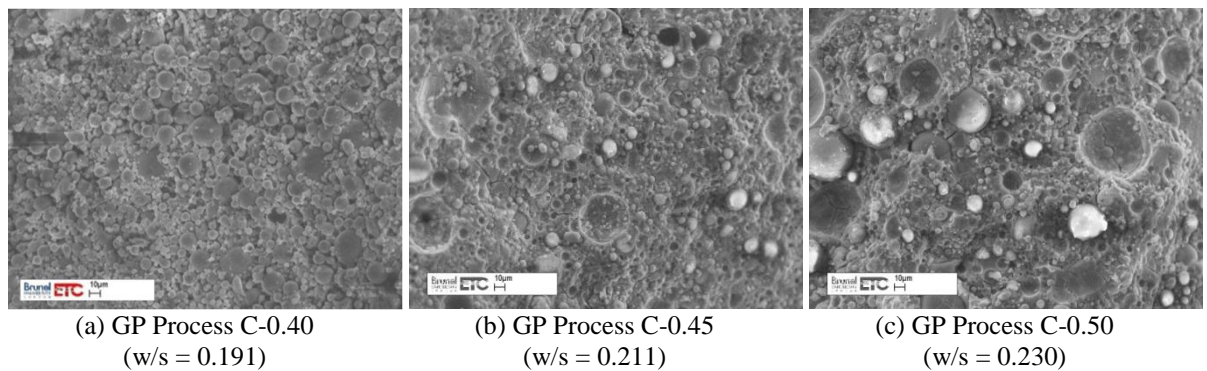


Figure 4.10 SEM images of geopolymers in pre-dry mixing process (C) for various w/s ratios at the 28-day age

It can be summarised that pre-dry mixing process (C) is a potential method to produce Self-cured geopolymer cement at ambient temperature. The amount of water content directly affects the properties and mechanisms of that geopolymers as less water (w/s = 0.170 and 0.191) leads to less dissolution of fly ash, while too much water leads to a weak structure (w/s = 0.230). The optimum w/s ratio of the pre-dry mixing process (C) is therefore slightly higher than that of typical geopolymer mixture of around 0.211 or 0.45 for A/FA ratio.

4.5 Remark

Many previous studies confirmed that the strength of geopolymers can be improved at high curing temperature. At ambient temperature, the degree of geopolymerization underwent a very slow rate and the setting time cannot be measured within the first 3 days. The compressive strength of all pastes at 28-day age was quite low, however, processes A and B led to higher strength than that of dry-mixed process (C) due to the fact that the fully dissolved alkaline activators were used in the synthesis. Nevertheless, process C obviously provided efficient heat liberation during its mixing process which caused more rapid paste setting and offered more beneficial heat curing condition. XRD analysis shows very

similar results in crystallinity and amorphous phases of those three different processes. While the SEM micrographs and FTIR spectrums revealed less compact structure and more moisture left in the process C respectively. In addition, the challenges of manufacturing with process C may be the development as a cement powder to be potentially used on the sites. Over all, the summary of the study, in different manufacturing processes, can be drawn as follows:

- 1) The widely used manufacturing processes of geopolymer cement, A and B, provided higher strength than that of proposed dry-mixing process (C) due to the fact that the fully dissolved alkaline activators were used.
- 2) Pre-dry mixing process (C) provided high potential heat liberation which would be beneficial for curing purpose together with an increase in both commercial scale and economical saving of geopolymer production.
- 3) As pre-dry mixing process requires more water than that of typical process, slightly higher water-to-solid (w/s) ratio was therefore used. The optimum w/s ratio of process C (0.211) could be beneficial for not only its mechanical performances but also its workability.
- 4) With more practicability in field application, by just adding water, this pre-dry mixing process (C) could be developed and applied to work at ambient curing temperature. Other factors, e.g. fineness of fly ash and alkaline solid, inclusion of calcium source and heat loss protection, could also enhance the properties of this process as Self-cured geopolymer cement.

CHAPTER 5 SYNTHESIS AND CHARACTERIZATIONS OF GEOPOLYMER-PORTLAND CEMENT

5.1 Introduction

Fly ash, a by-product from coal-fired power station, is widely used as a prime material producing fly ash-based geopolymer cement (GP). It receives much more attention as an alternative binder due to its high percentage of alumina-silica compositions and its abundant un-utilised amount worldwide (Nath & Sarker, 2015). At ambient temperature ($20 \pm 2^\circ\text{C}$), fly ash-based GP gained some strength at very slow rate. High temperature curing around 40 to 90°C is, therefore, required to accelerate and improve its strength development in both early and later stages (Nath, et al., 2014). To achieve reasonable strength at ambient temperature, a number of researchers have attempted to develop fly ash-based geopolymers without external source of heat curing for being more convenient in practical works and in field applications (Nazari, 2013; Phoo-ngernkham, et al., 2013).

Many efforts were spent to investigate significant factors and conditions for geopolymers cured at ambient temperature as stated earlier in Chapter 2 such as fineness, alkaline concentration and alternative heat sources. However, one of those challenges to develop ambient temperature cured geopolymers is the addition of calcium content. It is agreed by many researchers that the early strength development and setting time of GP were improved with some added calcium mineral to the binder due to an extra precipitation of calcium in alkaline presence (Buchwald, et al., 2005). The ability to cure geopolymers at ambient temperature has also been reported by the synthesis with high calcium fly ash (Rattanasak, et al., 2011), bottom ash (Topçu, et al., 2014) or GBFS (Yip, et al., 2008) as prime materials, or even the additional amount of $\text{CaO}/\text{Ca}(\text{OH})_2$ (Yip, et al., 2005), cement kiln dust (Ahmari & Zhang, 2013) or Portland cement to the geopolymer mixtures (Suwan & Fan, 2014). In fact, the use of OPC as an additive in geopolymeric binder is evidently widespread due to its uniformity complied with any standard as well as its global availability.

In this chapter, OPC was used as a calcium source in geopolymers (Geopolymer-Portland cement, GeoPC) to investigate the curing process of geopolymers at ambient temperature through the analysis of mechanical properties, microstructures, reactions of calcium mineral and alkaline activators, and alternative extra internal heat liberation during OPC hydration in the mixture. Functionality of geopolymer constituents and GeoPC mixtures

were also comparatively studied together with the elemental composition and ratio analysis.

5.2 Materials

Coal-fired fly ash (FA) used in the test was batch I. Ordinary Portland cement (OPC) was a general purpose cement Cemex CEM II/A-L type. The properties of the fly ash and OPC are as stated in Chapter 3. The chemical compositions are given in Table 5.1. Alkaline solutions used were 15 molar (M) sodium hydroxide (NaOH, SH) and 48.20% w/w sodium silicate (Na₂SiO₃, SS). It is noted that the typical geopolymers synthesized in this study has sodium silicate solution to sodium hydroxide solution (SS/SH) ratio by mass of 1.50 and the alkaline solution to fly ash (A/FA) ratio of 0.40.

Table 5.1 Chemical compositions of fly ash and commercial OPC

Materials	SiO ₂	Al ₂ O ₃	FeO	CaO	Na ₂ O	TiO ₂	MgO	K ₂ O	SO ₃
Fly ash	50.97	27.83	9.21	2.62	1.13	1.15	1.43	3.73	1.93
OPC	12.22	3.85	2.85	73.82	-	-	0.78	1.17	5.30

5.3 Experimental Procedures and Methodologies

5.3.1 Functionalities of geopolymer constituents

To investigate the role of each component, various combinations of geopolymer constituents were designed. Experiments were divided into two groups: one for the reactions between the geopolymer constituents (i.e. FA+SH, FA+SS, FA+SH+SS) and the other for the behaviour of individual constituents during the hydration of OPC (i.e. OPC+SH, OPC+SS, OPC+SH+SS). For all mixtures at ambient temperature ($20 \pm 2^\circ\text{C}$), the alkaline solutions (constituents) were prepared and left over night to ensure fully dissolution. The mixed alkaline solutions were then added into a mixing bowl containing prime material and mixed together for 90 seconds at low speed of 140 ± 5 rpm. After 30 second pause to remove all the paste adhered on the equipment, the mixer was restarted and run at low speed again for further 90 seconds. The homogeneous slurry was, then, carried out for setting time measurement and also placed in the prepared mould. After de-moulding, all samples were immediately wrapped with protective film before placing into plastic bags to prevent moisture loss. All samples were then cured in the temperature controlled chamber ($20 \pm 2^\circ\text{C}$) until reaching the testing age. Water-to-solids ratio (w/s) of each paste was computed by the total mass of water to the total mass of solid in the mixture at 0.250 as presented in Table 5.2.

Table 5.2 Detail of investigation on mixture combinations

Mixtures	Description of mixtures	w/s ^b
<i>Functionality of Geopolymer constituents</i>		
OPC	Portland cement and water	0.253
OPC+FA	Portland cement (70%) and fly ash (30%) and water	0.250
OPC+SS	Portland cement and Sodium Silicate solution (SS)	0.250
OPC+SH	Portland cement and Sodium Hydroxide solution (SH)	0.250
OPC+SS+SH	Portland cement and Sodium Silicate (SS) and Sodium Hydroxide (SH) solution	0.250
FA+SS	Fly ash and Sodium Silicate (SS) solution	0.250
FA+SH	Fly ash and Sodium Hydroxide (SH) solution	0.250
FA+SS+SH (GP)	Fly ash and Sodium Silicate (SS) and Sodium Hydroxide (SH) solution (the typical Geopolymers)	0.191
<i>Function of OPC in GeoPC systems</i>		
GeoPC90 ^a	10% GP paste : 90% OPC paste	0.298
GeoPC80 ^a	20% GP paste : 80% OPC paste	0.292
GeoPC70 ^a	30% GP paste : 70% OPC paste	0.285
GeoPC50 ^a	50% GP paste : 50% OPC paste	0.272
GeoPC30 ^a	70% GP paste : 30% OPC paste	0.259
GeoPC20	80% GP paste : 20% OPC paste	0.203
GeoPC10	90% GP paste : 10% OPC paste	0.197

^a 4% added water, ^b Water-to-solid ratio.

5.3.2 Function of OPC in GeoPC system

A series of Geopolymer-Portland cement paste (GeoPC) was made from the designation mass of GP and OPC paste. The mass of each material used, including alkaline solution and water, was calculated individually from the designed GP and OPC pastes (e.g. GeoPC30 is composed of 70% GP paste and 30% OPC paste). Portland cement paste (OPC) was made of cement powder and the purified water with the w/s ratio at its standard consistency of 0.253, while the geopolymer paste (GP) was made of fly ash and alkaline activators with w/s ratio of 0.191. Water-to-solids ratio of GeoPC pastes was computed by the total mass of water in the mixture (= the mass of water in the sodium silicate solution + sodium hydroxide solution + OPC paste + added water, if needed) to the total mass of solid in mixture (= the mass of OPC powder + fly ash + sodium hydroxide solid + sodium silicate solid; mass of Na₂O and SiO₂ in sodium silicate solution). Mixing and curing procedures were followed similarly to the previous sub-section, 5.3.1. It is noted that 4% added-water is applied to some GeoPC mixtures in order to obtain the workability in practical work (Table 5.2).

5.3.3 Analytical methods

The physical appearances (formation characteristic) were observed along with setting time (Vicat apparatus; BS EN 196-3:2005+A1:2008). The internal heat accumulated inside the samples was recorded by using thermocouples embedded in three different positions viz. top, middle, bottom of cylindrical shape samples (100 mm dia. x 200 mm height). Labview Signal Express programme with National Instrument 16-Channel thermocouple input module (NI 9213) was used to track temperature changes. The temperature, in degree Celsius ($^{\circ}\text{C}$), was recorded every 1 minute for 24 hours as it can be practically compared with that of typical geopolymers curing at the temperatures of 40 to 90°C in the oven.

Compressive strength of prismatic sample (40mm x 40mm x 160mm) was determined by using the Instron universal testing machine (UTM) in accordance with the British Standard BS EN 196-1:2016. All samples used for compression tests were placed in plastic bags to prevent moisture loss and then kept in a temperature-controlled chamber ($20 \pm 2^{\circ}\text{C}$) until reaching the testing age of 28 days. The Fourier Transform Infrared (FTIR) spectrums were obtained by using Attenuated Total Reflectance (ATR) technique on a Perkin Elmer Spectrum One-Fourier transform infrared spectrometer. The spectrums were recorded after running 100 scans in the wavenumber range of 650 to $4,000\text{ cm}^{-1}$. The X-Ray diffraction (XRD) patterns were recorded on a Bruker D8 Advance diffractometer fitted with a Lynxeye XE high-resolution energy dispersive 1-D detector. The samples were determined by using DIFFRAC.SUITE software. The scanning range between 5 and $100^{\circ} 2\theta$ was covered over a 35-minute period. The Scanning Electron Microscope (SEM), an ultra-high performance field emission scanning electron microscope Zeiss Supra 35VP, was used to observe the microstructures, and the Energy Dispersive X-ray Analysis (EDXA) was used to define the chemical composition of the resulting products. More details have been stated in Chapter 3.

5.4 Results and Discussion

5.4.1 Functionality of alkaline activators

The strength of typical OPC is mainly obtained from calcium silicate hydrated gel (C-S-H) when the cement reacted with water. Heat is also regenerated by hydration reaction of high potential energy compounds in the OPC (C_3A and C_3S), together with an alkaline presence of $\text{Ca}(\text{OH})_2$ (Deevasan & Ranganath, 2010). As $\text{Ca}(\text{OH})_2$ in Portland cement has an adverse effect on chemical durability to acidic solutions, pozzolanic material (fly ash) is therefore added into the binder to form alternative C-S-H gel in Portland cement, called

pozzolanic reaction (Demie, et al., 2011). The test results of OPC and OPC+FA show that the additional fly ash is able to lengthen the setting time of OPC paste (Figure 5.1) and also reduce the accumulated heat inside the cement (Figure 5.2), which could cause a thermal stress. However, the pozzolanic C-S-H leaves a lot of pores in the matrix and normally forms in latter period, leading to lower strength than that of OPC C-S-H (Figure 5.3). The major phase of OPC and OPC+FA was C-S-H while portlandite ($\text{Ca}(\text{OH})_2$), calcite (CaCO_3) and ettringite also appeared in those hydrated cements confirmed by FTIR and XRD analysis in Figures 5.4 and 5.5 respectively. In addition, less portlandite was detected in OPC+FA mixture from 3 to 28 day age, indicating the formation of additional pozzolanic C-S-H in later stage (Bye, 1983).

Nevertheless, the mechanism of geopolymers is totally different from OPC hydration and obviously influenced by alkaline activators (NaOH and Na_2SiO_3) and composition of prime materials (OPC and FA) (Davidovits, 2011; Glukhovskiy, 1967). To understand the role and functionality of alkaline activators, the resulted reactions between the geopolymer constituents (FA+SH, FA+SS, FA+SH+SS) and individual constituents of OPC (OPC+SH, OPC+SS, OPC+SH+SS) are presented as follows.

5.4.1.1 Role of NaOH played in geopolymerization of fly ash and OPC

NaOH solution is normally used to produce geopolymer cement due to its wide availability and less cost than other alkaline activators (Hardjito, et al., 2008). In the test, two hydroxide mixtures, FA+SH and OPC+SH, were prepared to study the roles in the geopolymer constituents system. The physical appearances (Table 5.3) and setting time measurement of FA+SH mixture showed very viscous and slow rate of reaction (Figure 5.1). No significant change was observed in the internal heat measurement (Figure 5.2) as the temperature was almost the same as room temperature ($20 \pm 2^\circ\text{C}$). Although many studies reported that NaOH solution alone can be used for geopolymer production (e.g. fly ash-based, metakaolin-based or GBFS-based geopolymers), all of those researches were cured at high temperature (40 to 85°C) to achieve the proper strength (Bakharev, 2005a; Panagiotopoulou, et al., 2007). At ambient curing temperature, FA+SH mixture therefore gained quite low strength of 11.29 MPa at the 28-day age (Figure 5.3). FTIR absorption band in the ranges of $3,000\text{-}3,600\text{ cm}^{-1}$ and $1,645\text{ cm}^{-1}$ related to O-H vibration of water (H_2O) remaining in the samples. Large FTIR spectrum bands at $1,400\text{-}1,418\text{ cm}^{-1}$ and $1,114\text{ cm}^{-1}$ corresponded to Si-O and Al-O vibration while the band in a range of $800\text{-}1,200\text{ cm}^{-1}$ was assigned as Si-O-T (T=Si or Al) symmetric stretching of SiO_4 tetrahedral

in geopolymeric gel (Figure 5.4). An XRD diffractogram shows an apparent of quartz, mullite, nepheline and (C,N)-A-S-H as main products. Portlandite and thermonatrite were additionally formed as a direct result of NaOH activation. Broad hump between 15 and 35° 2θ indicates the high percentage of amorphous to semi-crystalline phase of the mixture (Figure 5.5). Noticeably, SEM image shows that fly ash particles seem to be completely dissolved when mixed with strong alkaline solution, NaOH. The micrograph also revealed the formation of new loose structure with scattered cavities in the cement matrix (Table 5.4g).

On the contrary, a flash set was obtained in OPC+SH mixture with approximately 10 minutes of setting time (Figure 5.1). Rapid reaction can be endorsed by accumulated internal heat measurement at the maximum temperature of 38°C in the first 2 hours (Figure 5.2). The 28-day strength of 11.47 MPa could probably be ignored as too fast setting might cause incomplete bonding, leading to a weak matrix (Figure 5.3). FTIR spectrum of portlandite (Ca(OH)₂) can be found in OPC+SH (from OH⁻ in sodium hydroxide presence) at the IR band of 3,640 cm⁻¹. H₂O was also observed in the mixture with the appearance of CO₃ species at the peak 1,487 cm⁻¹ due to the atmospheric reaction. Si-O and Al-O vibrations were defined at the band around 1,418 cm⁻¹ and 1,114 cm⁻¹. The peak at around 948 cm⁻¹ was assigned as Si-O-T (T=Si or Al) symmetric stretching while the peak around 871 cm⁻¹ was attributed to C-S-H formation in the mixture (Figure 5.4). An XRD pattern of OPC+SH is explicitly different from that of FA+SH as the major resulted products were C-S-H and portlandite. The appearance of nepheline, pirssonite, calcite and gismondine can also be found in the system after the 28-day age from participation of Ca and Na (Figure 5.5). SEM micrographs reveal firm and compact structures of OPC+SH mixture in both 3 and 28 day age. The surfaces seemed to be finer than those of normal hydrated OPC and FA+SH (Table 5.4d).

It may be summarised that NaOH solution provides a strong alkalinity to the mixtures. The chemical species of that NaOH solution, Na⁺ and OH⁻, maintained expedient dissolution of prime materials in the mixtures (Sottisoplia & Asavapisit, 2005). In the FA+SH mixture, Silica and Alumina in fly ash were obviously dissolved and reformed to the new main resulted products of mullite (Si-O-Al) and quartz (Si-O). The excess Na⁺ and OH⁻ species could alternatively form nepheline (Na-K-Ca-Al-Si), N-A-S-H and portlandite as additional products. In the OPC+SH mixture, the rapid reaction was obtained by an extra precipitation of calcium in OPC with Na⁺ and OH⁻, forming C,N-A-S-H gel and Ca(OH)₂ respectively.

Table 5.3 Images of formation characteristic of individual combinations

	a) After Mixing	b) After 30 mins.	c) After 1 hr.	d) After 24 hrs.
(A) OPC+SS	(Aa) 	(Ab) 	(Ac) 	(Ad)
(B) OPC+SH	(Ba) 	(Bb) 	(Bc) 	(Bd)
(C) OPC+SS+SH	(Ca) 	(Cb) 	(Cc) 	(Cd)
(D) FA+SS	(Da) 	(Db) 	(Dc) 	(Dd)
(E) FA+SH	(Ea) 	(Eb) 	(Ec) 	(Ed)
(F) FA+SS+SH	(Fa) 	(Fb) 	(Fc) 	(Fd)

Table 5.4 SEM images of geopolymer constituents at the ages of 3 and 28 days

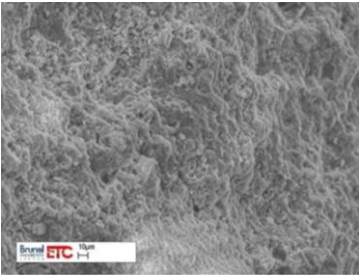
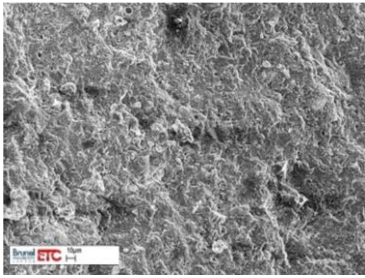
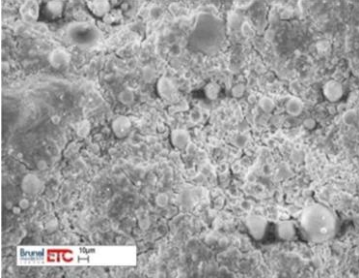
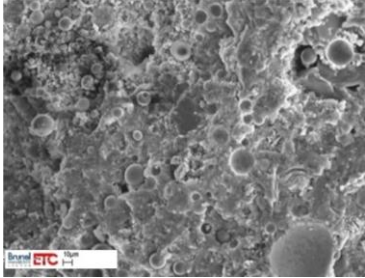
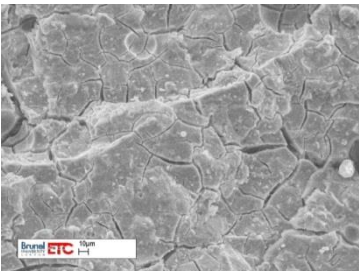
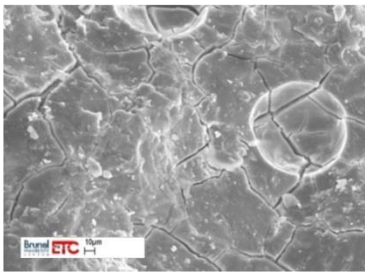
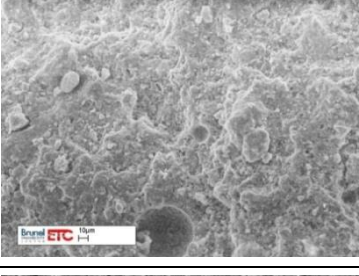
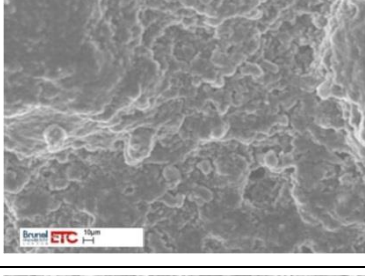
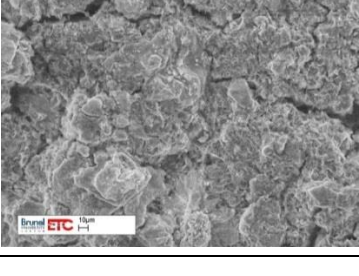
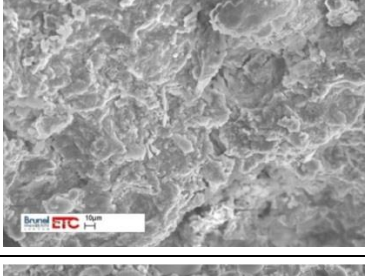
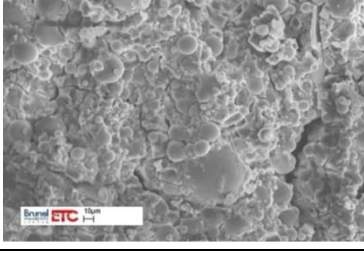
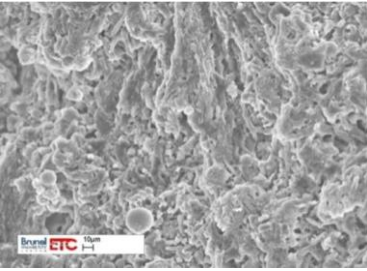
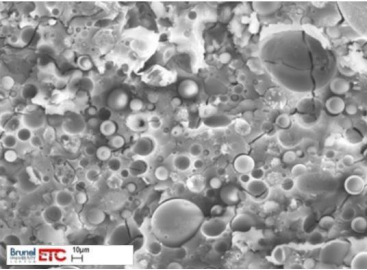
Mixture	3-day age	28-day age	
(a) OPC w/s = 0.250			
(b) OPC+FA w/s = 0.250			
(c) OPC+SS w/s = 0.250			
(d) OPC+SH w/s = 0.250			
(e) OPC+SS+SH w/s = 0.250			
(f) FA+SS w/s = 0.250	<p>“Cannot be tested at 3-day age”</p>		

Table 5.4 (Continued)

Mixture	3-day age	28-day age
(g) FA+SH w/s = 0.250	"Cannot be tested at 3-day age"	
(h) FA+SS+SH or GP w/s = 0.191	"Cannot be tested at 3-day age"	

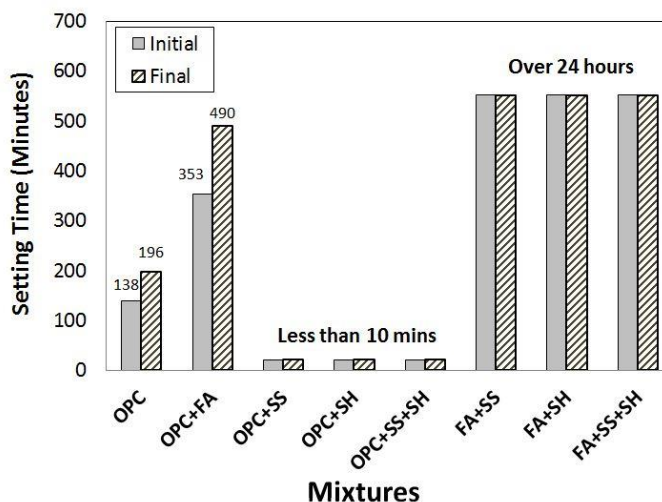


Figure 5.1 Setting time of geopolymer constituents

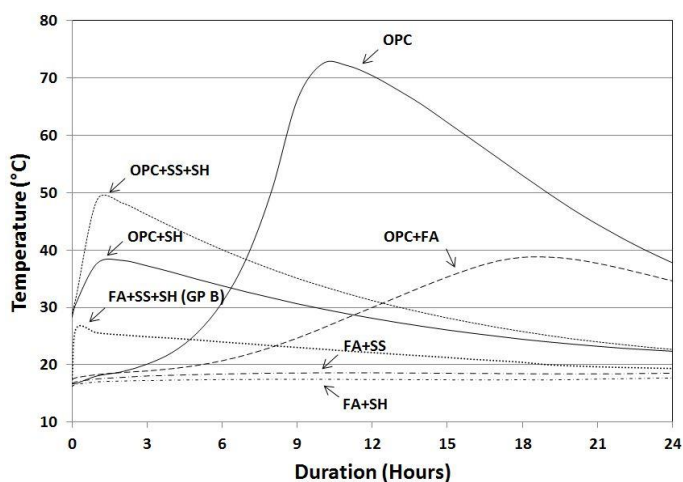


Figure 5.2 Heat evolution of geopolymer constituents during alkalinity over a 24-hour period

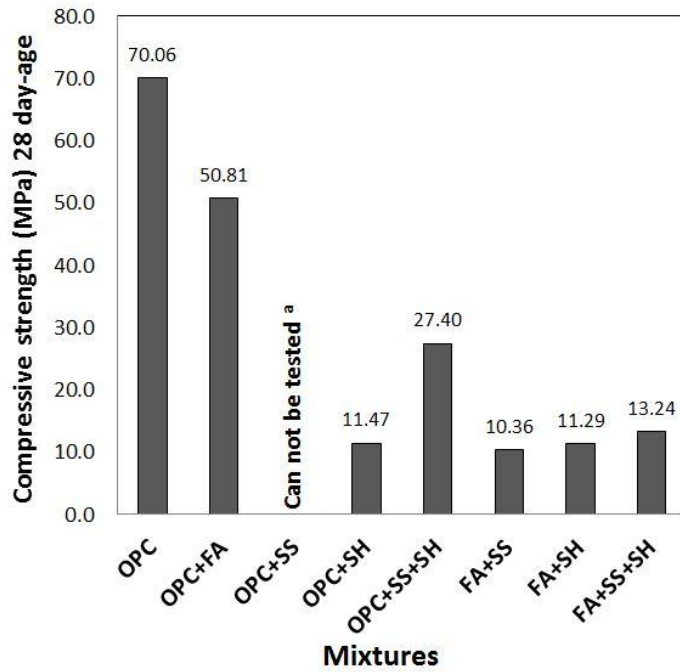


Figure 5.3 Compressive strength of geopolymer constituents at the 28-day age
 (^a Too fast setting to handle in the mould)

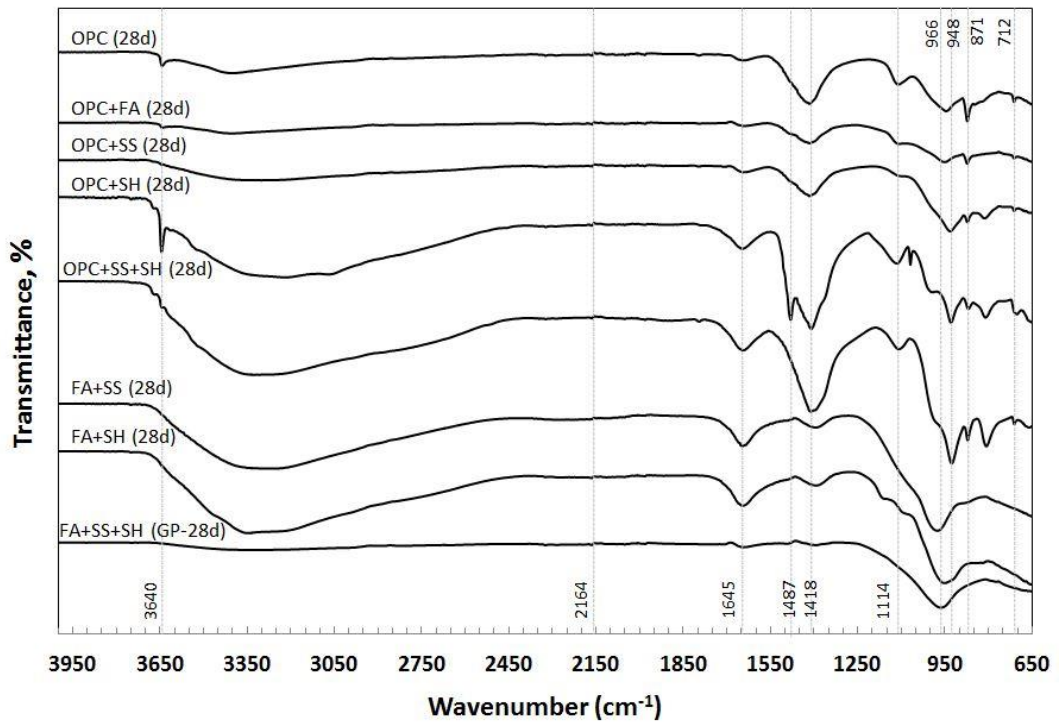


Figure 5.4 FTIR spectrums of geopolymer constituents at the 28-day age

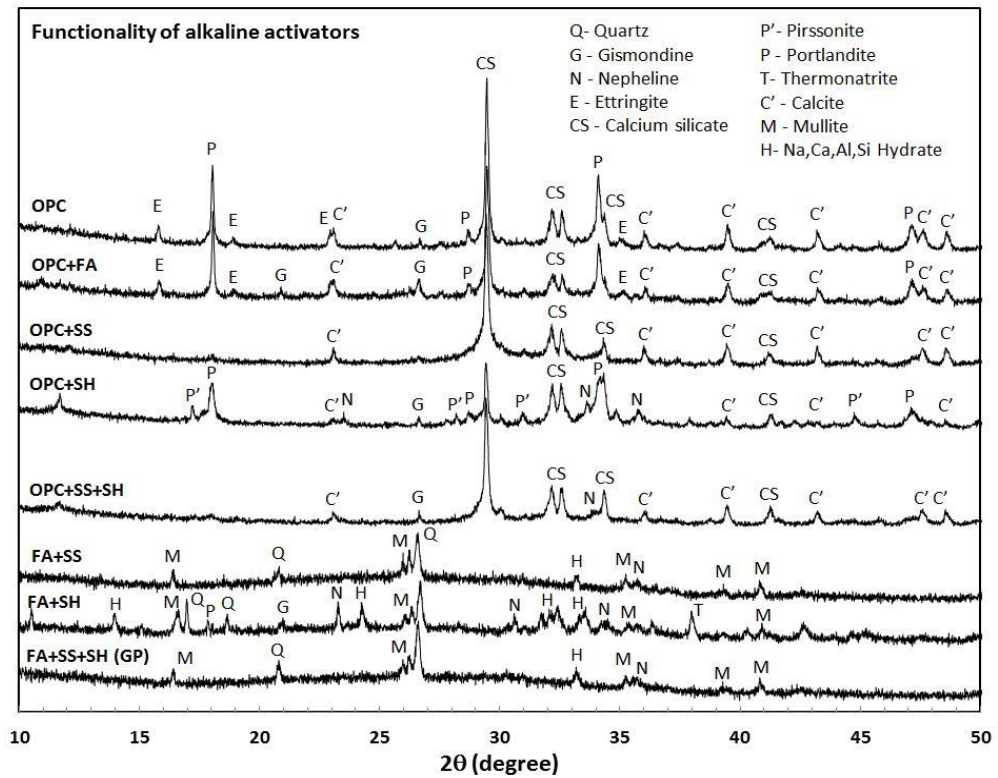


Figure 5.5 X-ray diffraction patterns of geopolymer constituents at the 28-day age

5.4.1.2 Role of Na_2SiO_3 played in geopolymerization of fly ash and OPC

Na_2SiO_3 or water glass is also normally used in geopolymer synthesis as an alkaline activator and another source of silica (Rashad & Zeedan, 2011). It is more economical than potassium silicate solution (K_2SiO_3) when produced in large quantity (Dimas, et al., 2009). In the test, two silicate mixtures, FA+SS and OPC+SS, were prepared to study the roles in the geopolymer constituents system.

The physical appearance (Table 5.3), setting time and internal heat liberation (Figures 5.1 and 5.2) of FA+SS were not different from those of FA+SH mixture. The compressive strength of FA+SS (10.36 MPa) was slightly lower than that of FA+SH (11.29 MPa), which probably due to more dissolution rate achieved in FA+SH than FA+SS (Figure 5.3). The molecular functional group of FA+SS showed very similar spectrums to FA+SH (Figure 5.4). There are only quartz, mullite and N-A-S-H detected by XRD diffractograms with the main formation of amorphous structure which was indicated by broad humps (Figure 5.5). SEM micrograph of FA+SS shows a rough texture with some internal micro-cracks. The fly ash particles in the sample seem to be melted and strongly welded together, while the spherical shape of that fly ash was still scattered visible (Table 5.4(f)).

OPC+SS showed the shortest drying behaviour of less than 5 minutes in setting time (Figure 5.1). With a very fast setting, its compression test and internal heat measurement could not be carried out due to a failure to handle the paste to the mould. Its FTIR spectrum showed Si-O and Al-O and Si-O-T (T=Si or Al) symmetric stretching of SiO₄ at the bands of 1,418 cm⁻¹ and 948 cm⁻¹ respectively. Whilst the band at around 871 cm⁻¹ corresponded to the mix gel of calcium silicate hydrated gel (C-S-H) or calcium alumina-silicate hydrated gel (C-A-S-H) or sodium alumina-silicate hydrated gel (N-A-S-H) (Figure 5.4). The crystalline of C-S-H and calcite were the main phases of OPC+SS reaction, which provided a fast setting behaviour than those of normal hydrated OPC or OPC+FA (Figure 5.5). In addition, an SEM micrograph of OPC+SS obviously exhibits a very fine and smooth texture, but some of micro-cracks are found in the structure which was probably due to a quick setting when OPC reacted with sodium silicate solution (Table 5.4(c)).

Overall, as 2Na²⁺ and SiO₂((OH)₂)²⁻ species were found in sodium silicate solution (Sottisoplia & Asavapisit, 2005), N-A-S-H gel could be formed with incorporation of Na⁺ ion, while SiO₂((OH)₂)²⁻ offers more source of silica in the mixture. The alkaline environment was also emerged, even less level than that of sodium hydroxide Na⁺ and OH⁻. Noticeable characteristic as a binding accelerator was found in FA+SS via SEM image. However, using only sodium silicate solution in geopolymer synthesis could not achieve the same level of strength as NaOH because of less alkalinity and less dissolution of Si and Al (Bakharev, 2005a; Rashad & Zeedan, 2011). Again, calcium mineral in OPC can achieve a rapid reaction in alkaline environment, and the flash setting with scattered micro-cracks were therefore found.

5.4.1.3 Combined effects of NaOH and Na₂SiO₃ in geopolymerization on fly ash and OPC

The mix of sodium hydroxide and sodium silicate solution is one of the most widely used alkaline activators for geopolymer production. From the previous testing, it is known that soluble hydroxide obviously dissolves Si and Al from source of materials while soluble silicate improves the poly-condensation of geopolymer cement and also controls the amount of silicate in mixtures as a binder (Sukmak, et al., 2013).

FA+SH+SS (GP) or typical geopolymers was not able to solidify, even left at ambient temperature for over 24 hours (Figure 5.1 and Table 5.3). However, it seemed to be more viscous and cohesive than those of FA+SS and FA+SH. The combination of sodium silicate and sodium hydroxide solutions with fly ash (GP) offers appropriate conditions for

geopolymerization, leading to a larger increase of geopolymeric gel phase than that of fly ash with either sodium silicate or sodium hydroxide alone. The higher reaction was also shown by a suddenly rising up of internal heat at the maximum of 27°C after mixing above room temperature (Figure 5.2). More dissolved Si and Al (from hydroxide solution) together with additional Si and more condensing activity (from silicate solution) led to the highest compressive strength of 13.24 MPa together with FA+SH (11.29 MPa) and FA+SS (10.36 MPa) (Figure 5.3). The FTIR spectrum clearly depicts Si-O stretching vibration of SiO₄ and AlO₄ of tetrahedral in geopolymeric gel at the band of 966 cm⁻¹. An XRD pattern of FA+SH+SS shows similar phases to FA+SS with main crystallinity of quartz and mullite. Small amount of sodium calcium aluminium silicate hydrate (C,N-A-S-H) was also traced in those two mixtures with the broad humps between 15 and 35° 2θ of amorphous phases. The SEM images of all FA-based mixtures (Tables 5.4(f) to (h)) at the 28-day age are totally different to each other. The mixture of FA+SS+SH (Table 5.4(h)) provided more compact and firm matrix than those of FA+SS and FA+SH. The structure was homogenous and less porous, although some unreacted fly ash particles were also visible. By this, the geopolymers synthesized with FA+SS+SH is the most widely used as it provides better performances than that of only NaOH or Na₂SiO₃ alone.

OPC+SH+SS also performed a rapid set in approximately 5 to 10 minutes of setting time. As SS and SH provided an appropriate condition to be reacted with CaO in OPC, the heat of hydration therefore rose up to the peak of 50°C in the 2nd hour (Figure 5.2). With good dissolution and additional source of Si, the (C,N)-A-S-H could be formed rapidly to achieve higher strength of 27.40 MPa than those of OPC+SH (Figure 5.3). The main functional group of C-S-H was found in the FTIR spectrum and XRD pattern, indicating the mix gel of Na and Ca in the matrix (Figures 5.4 and 5.5). As expected, the OPC+SS+SH micrograph seems to be a mix characteristic structure of OPC+SS and OPC+SH. Small cracks were also discovered around its rough matrix as shown in Table 5.4(e).

The study on functionality of alkaline activators can be summarised as sodium hydroxide solution (NaOH) played a very important role in dissolving prime materials and other compounds in both OPC and FA. The soluble silicate (Na₂SiO₃), which is normally used as another source of silica, improves the binding activity or geopolymerization of geopolymers. Therefore, the resulted products of the mixture synthesis with NaOH and Na₂SiO₃ obviously obtained better performances than those with NaOH or Na₂SiO₃ alone. FA with either single-alkaline or combined of NaOH and Na₂SiO₃ solution exhibits Si-O

and Al-O tetrahedron from geopolymerization. However, with lack of heat curing, the mechanical properties of those FA-based geopolymers were very low. OPC with any alkaline activators provide different reaction from normal hydrated OPC. It was indicated by the appearance of C-A-S-H, N-A-S-H or mix gel rather than normal C-S-H in the mixtures, leading to fast setting characteristic of the pastes. It can, however, be clearly seen that OPC-based mixtures could obtain early strength from rapid reaction, indicated by abruptly released of heat after synthesis. In contrast, more attention is focused on FA+SH+SS as it is a typical GP synthesis. The study on a combination of OPC+FA+SH+SS is presented in the next sub-section 5.4.2 which has been stated as GeoPC mixtures.

5.4.2 Functionality of OPC in GeoPC system

The study of OPC+FA+SH+SS mixture was initially carried out with approximately 30%-OPC paste and 70%-GP paste by mass (GeoPC30). Its properties and mechanisms showed a combined characteristic of typical OPC and GP (except setting time). To extend the understanding of functionality of OPC in GeoPC system, various dosages of OPC in geopolymer system were intensively studied from 5%-additional OPC (GeoPC5) to 95%-additional OPC (GeoPC95). The results from the individual geopolymer constituents (5.4.1) were also used to explain the occurrences through the analysis of mechanical properties, alternative extra internal heat liberation and micro-mechanisms during OPC hydration in the mixture.

5.4.2.1 Effect of OPC dosage on the mechanical properties of GeoPC system

The results of setting time show that the initial and final setting times of OPC were 138 and 196 minutes respectively, while the controlled GP paste did not harden and could not be measured with Vicat needle in the first 24 hours. Geopolymers with the replacement of OPC paste from 10% (GeoPC10) to 80% (GeoPC80) resulted in the fast setting when compared to OPC or GP, while the flash setting occurred with GeoPC30, 50 and 70. The mixtures outside this range required much longer time, that is, the mixtures with OPC replacement less than 10% (e.g. GeoPC5) and greater than 80% (e.g. GeoPC85) as shown in Figure 5.6.

These occurrences could be described by the amount of OPC inclusion and dosage of alkalinity in the system as happening in the individual combinations of OPC+SS or OPC+SH. Rapid solidifying process was observed in all GeoPC pastes as the presence of OPC reduces the setting time and also decreases the workability (Nath & Sarker, 2015;

Phoo-ngernkham, et al., 2013). An increase in the rate of solidification may be influenced by high alkalinity of GP-dominated mixtures (e.g. GeoPC5 to GeoPC30) which offered more dissolved species of prime materials, while additional CaO contained in OPC provided an extra precipitation of calcium compound (C-A-S-H) in the systems (Suwan & Fan, 2014).

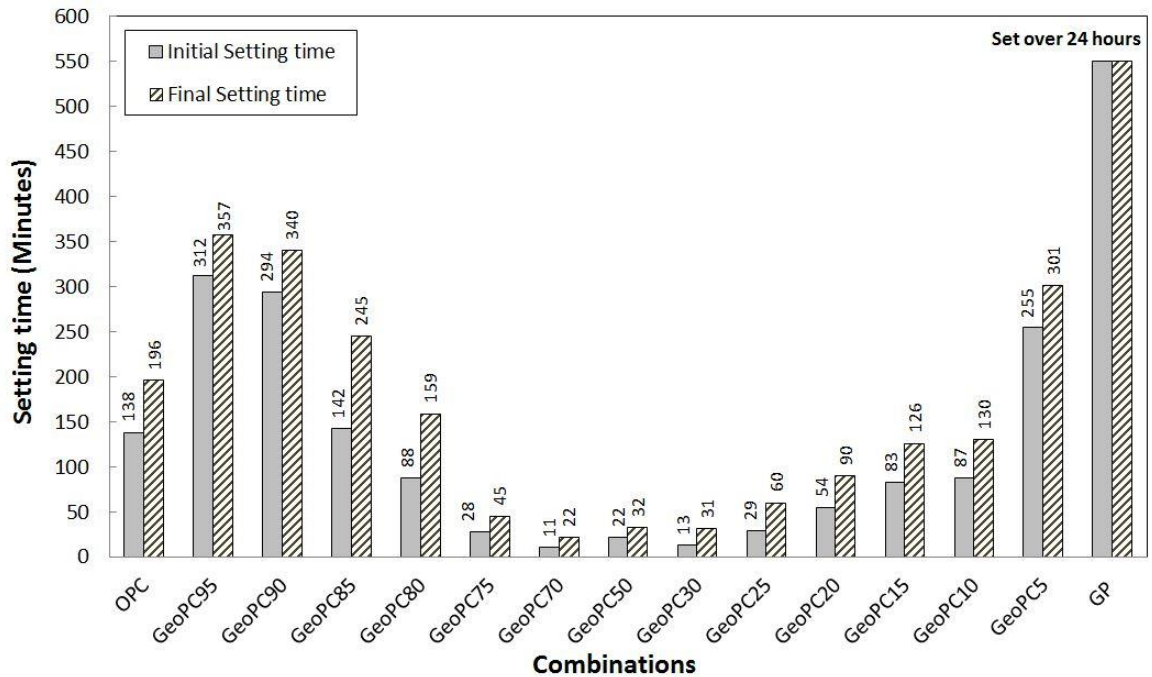


Figure 5.6 Setting time of OPC, geopolymers and GeoPC paste

A similar behaviour has also been reported in the mixtures containing calcium compound such as GBFS, $\text{Ca}(\text{OH})_2$, CaO or high calcium fly ash (Chindaprasirt, et al., 2010; Khater, 2011). Although, a flash setting was observed in the GeoPC30, GeoPC50 and GeoPC70, the setting time was extended again through the GeoPC90 and GeoPC95. As high proportion of OPC paste resulted in reasonable reduction of alkalinity (less proportion of GP), the level of interaction with calcium mineral and other constituents was dropped down. The setting time, thus, became longer together with slower hardening rate. However, it can be seen that the OPC replacement ranging from 5% to 10%, or 80% to 85% of low calcium fly ash-based geopolymers could be able to show similar setting time as typical OPC (Figure 5.6).

The compressive strength of GeoPC system was examined with the testing age of 3, 7, 14 and 28 days (Table 5.5). It can be seen that the strength development of GeoPC system follows that of OPC, i.e. gradually strengthening with the increase of time for the ages from 3 days to 28 days. The strength was increased when the amount of OPC increase, although the strength of the GeoPC cannot reach to the level of that OPC. For example, at

the 28-day age, GeoPC30, GeoPC70 and GeoPC90 achieved the strength of 35.69, 39.11 and 51.32 MPa respectively, while the controlled OPC achieved that of 70.06 MPa. In addition, it is noted that GP could not be tested in the first three days due to the slow hardening under ambient conditions. After 7 days, the GP gained very low compressive strength due to the lack of heat curing process. This occurrence conforms the finding presented by Yang, et al. (2008) that geopolymerization required high temperature to accelerate the hydrothermal reaction. Therefore, the low curing temperature under ambient condition in this study resulted in low strength of GP paste.

From the results of functionality of alkaline activators in 5.4.1, it was found in GeoPC system that soluble hydroxide strongly dissolves the minerals from source of materials, while soluble silicate is used as another source of silica and improves the binding activity or geopolymerization of geopolymers. The strength of GeoPC at ambient curing temperature was obtained by the formation of calcium silicate hydrated, C-S-H (main hydration product of Portland cement) and C-S-H co-existed with N-A-S-H gel, which is responsible for the fast setting and early strength development (Hanjitsuwan, et al., 2014). With a mixed formation of both OPC and GP in GeoPC system, the heat curing is also required to achieve the same level of strength as normal hydrated-OPC (Altan & Erdoğan, 2012; Somna, et al., 2011). However, the internal heat itself, which was generated inside the specimens, would further enhance the formation of geopolymeric gel and improve its mechanical strength (Moon, et al., 2014).

Table 5.5 Compressive strength of GeoPC system

Mixture	w/s ^a	CaO/SiO ₂ ^b	SiO ₂ /Al ₂ O ₃ ^b	Compressive strength in MPa (S.D. ^c)			
				3 days	7 days	14 days	28 days
OPC	0.253	-	-	48.8 (0.99)	59.5 (0.85)	63.1 (0.89)	70.1 (1.31)
GeoPC90	0.298	4.40	4.63	30.2 (0.59)	36.2 (0.84)	44.6 (1.06)	51.3 (1.29)
GeoPC80	0.292	3.14	4.27	18.2 (0.69)	24.6 (1.02)	33.8 (1.15)	39.2 (1.04)
GeoPC70	0.285	2.31	4.06	21.9 (0.71)	23.4 (0.83)	34.1 (0.96)	39.1 (1.09)
GeoPC50	0.272	1.26	3.82	14.1 (0.91)	19.0 (0.72)	33.9 (0.62)	36.5 (0.94)
GeoPC30	0.259	0.63	3.69	13.8 (0.40)	15.4 (0.53)	32.4 (0.60)	35.7 (0.88)
GeoPC20	0.203	0.40	3.64	11.1 (0.72)	14.8 (0.52)	29.4 (0.61)	35.7 (0.64)
GeoPC10	0.197	0.21	3.61	5.6 (0.52)	5.8 (0.45)	18.2 (0.55)	23.5 (0.65)
GP	0.191	0.05	3.58	-	2.9 (0.78)	6.9 (0.51)	13.2 (0.61)

^a Water-to-solid ratio, ^b Oxide molar ratio, ^c Standard Deviation.

CaO-to-SiO₂ (C/S) and SiO₂-to-Al₂O₃ (S/A) oxide molar ratios were plotted against setting time and 28-day compressive strength (Calculation details: See Appendix B, Table B.2). The higher C/S ratio generally provides more C-S-H and (C,N)-A-S-H formation, while

higher S/A ratio offers more available silica and alumina which resulted in an increase in the geopolymeric chain. The setting time had similar characteristic as open-up parabolic curves in C/S and S/A plotting. As aforementioned, the Ca from OPC together with available Si and Al mainly provided an extra precipitation of calcium compounds in alkaline environment (Pangdaeng, et al., 2014), thus, a proper setting time could be achieved with an appropriate combination of those GeoPC mixtures. The optimum combinations (at ambient temperature) with the C/S oxide molar ratio of 0.21 to 0.40 and S/A oxide molar ratio of 3.61 to 3.64 (GeoPC10 to GeoPC20) could be able to achieve up to approximately 23 to 35 MPa at the 28-day age (Figure 5.7).

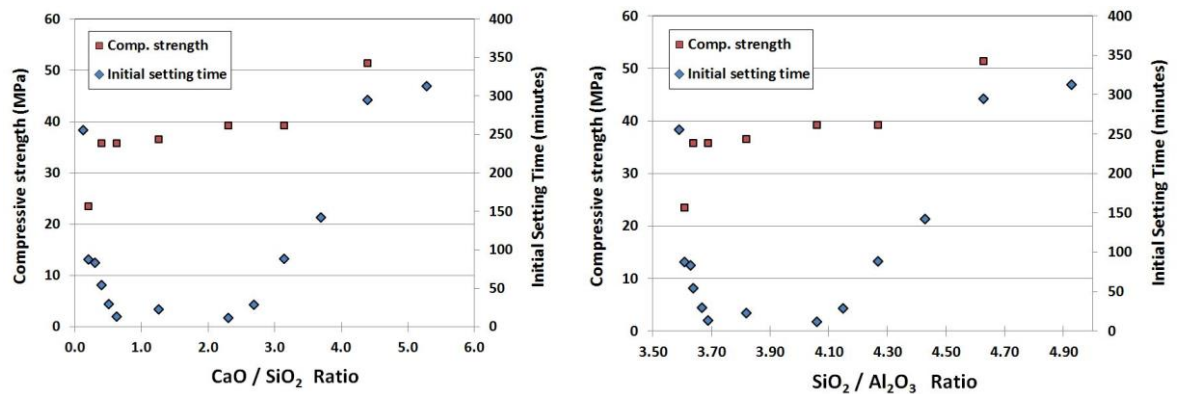


Figure 5.7 CaO/SiO₂ (Left) and SiO₂/Al₂O₃ (Right) of oxide molar ratios vs 28-day strength and setting time

In addition, it is noted that efflorescence can be found on the surface of most samples cured at ambient temperature. This phenomenon commonly occurs when excess alkaline, from insufficient reaction with the alumina-silicate species, migrates to the surface and reacts with the air. With XRD patterns, it was found that the efflorescence crystals are sodium phosphate hydrate ($\text{Na}_3\text{PO}_4 \cdot 12\text{H}_2\text{O}$) or sodium carbonate ($\text{Na}_2\text{CO}_3 \cdot 2\text{H}_2\text{O}$) (Temuujin & Van Riessen, 2009; Temuujin, et al., 2009a). However, the efflorescence could be immobilized at a high-temperature curing geopolymers due to a greater degree of geopolymerization, leading to the complete reaction of geopolymer structures (Kani, et al., 2012). It can be concluded that less efflorescence crystal formation may be achieved for the mixtures with low percentage of GP (low alkaline content), by increasing the amount of OPC or by producing sufficient reaction with alumina-silicate materials under high curing temperature. Consequently, the mixtures with high percentage of OPC replacement and cured at high temperature could hence form less efflorescence formation.

The internal heat accumulated inside the samples was observed for a period of 24 hours. It can be seen that the OPC had the highest heat accumulation of 73°C, while the maximum

temperature of GeoPC90, GeoPC70, GeoPC50 and GeoPC30 were 42°C, 39°C, 35°C and 29°C respectively. GeoPC10 had low internal heat measured with the maximum temperature of 26°C, similar as the controlled GP that liberated heat at the peak of 27°C (Figure 5.8). The internal heat accumulation of GeoPC mixtures may be induced by the hydration reaction of OPC, which consisted of high potential energy compounds, C₃A (Tricalcium aluminate, 866 J/g) and C₃S (Tricalcium silicate, 460 J/g) (Bye, 1983), together with minor heat being promoted by the reaction of OPC and alkaline solution.

It is interesting that increasing OPC not only raised the temperature of the mixtures but also relatively shifted the peak of temperature toward the 10th hour (peak of controlled OPC). The peak of temperature measurement of GeoPC10, GeoPC30, GeoPC50 and GeoPC70 were at the 3rd, 5th, 5th and 9th hour respectively, while GP was in the first 20 minutes of mixing (Figure 5.9). The time of peak temperature was mainly shortened (less than 10th hour of the controlled OPC) by the appropriate proportion with forceful reaction between calcium mineral (Ca) in OPC and alkaline soluble in GP, which led to a rapid formation of the mixed C-S-H and N-A-S-H. For the mixtures with low OPC content (or higher alkaline soluble from GP), e.g. GeoPC10, most of Ca may react with abundant alkaline in the mixtures, and very little amount of Ca was left for OPC-hydration reaction. Less internal heat and shortened-peak time, therefore, were recorded. It can be alternatively concluded that higher GP proportion (i.e. high alkalinity) resulted in the shift of peak time to the left of the graph.

On the other hand, although GeoPC90 achieved higher temperature than other GeoPC combinations (GeoPC70, 50, 30 and 10), the peak of temperature were at the 14th hour or 4 hours longer than normal OPC. It seems that the reaction was retarded with this low-alkalinity combination. This behaviour conforms to the results of setting time (Figure 5.6) that GeoPC90, including GeoPC85 and GeoPC5, exhibited longer setting time than that of OPC. It is apparent that the peak temperature of GeoPC system, which has OPC content less than approximately 85% (GeoPC85), would occur earlier than the normal OPC (10th hours). Therefore, the maximum temperature and time to reach the peak were noticeably influenced by the rate of reaction between prime constituents, and alkaline activators in the systems. In addition, it is worth to know that the internal heat accumulated inside the controlled OPC in this test obtained similar characteristic to that of the general rate of heat evolution of OPC paste tested with isothermal calorimeter (mWatts/g.s or J/g) (Mostafa & Brown, 2005).

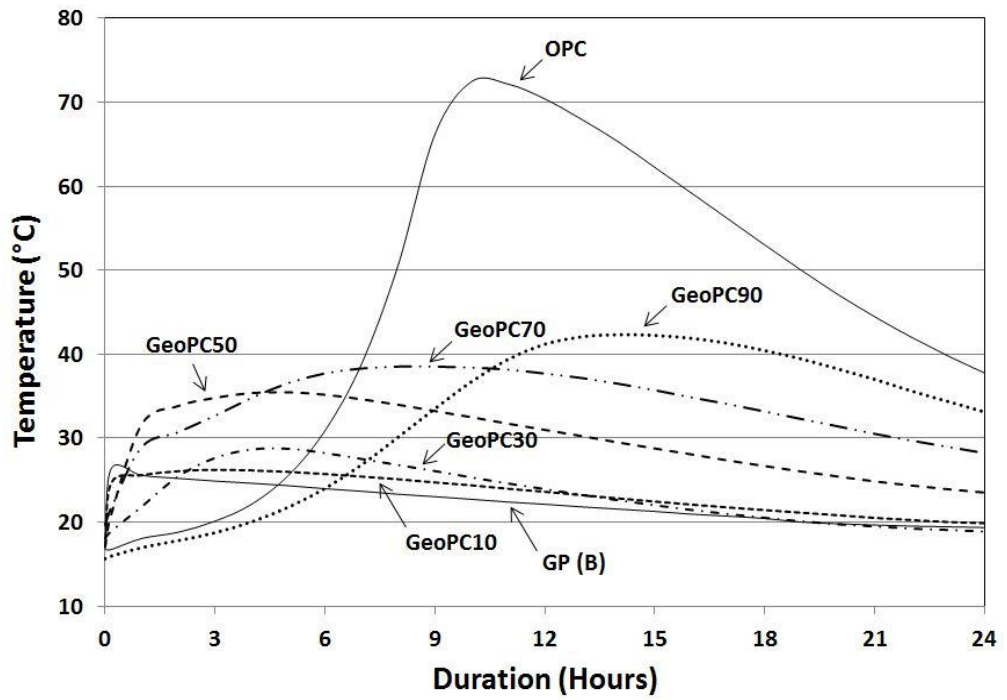


Figure 5.8 Heat evolution of GeoPC systems over a 24-hour period

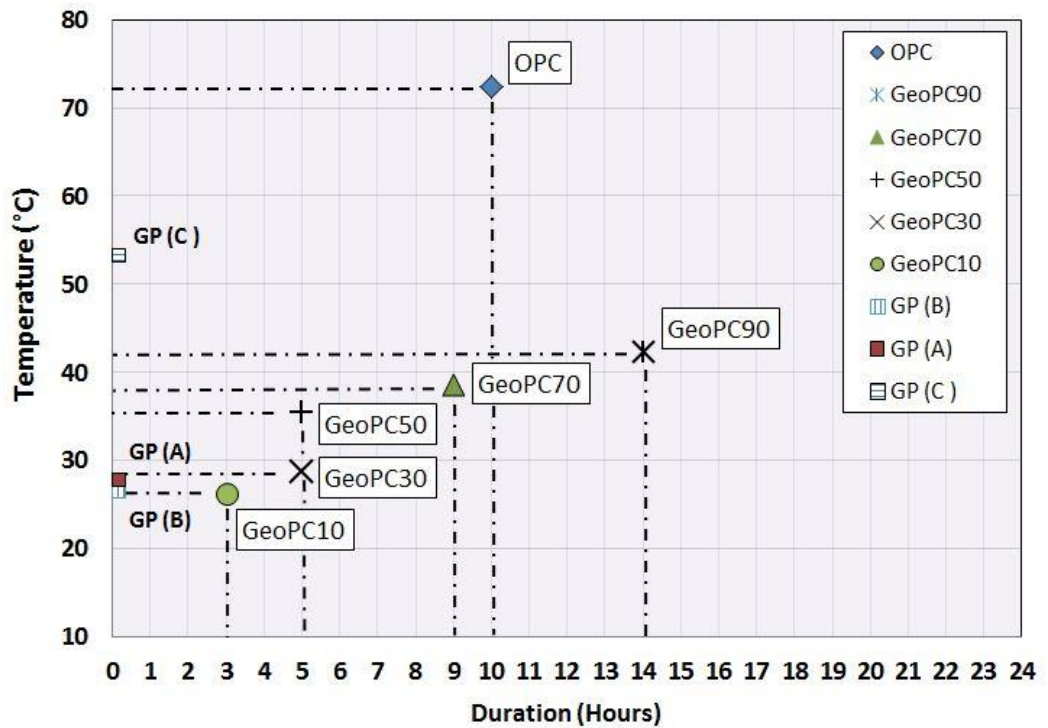


Figure 5.9 The maximum temperature against the time for each combination

5.4.2.2 Functional group analysis on different levels of OPC replacement

The infrared spectrums of hydrated OPC, GP and GeoPC are presented in Figure 5.10. IR spectrum of hydrated OPC shows characteristic peak at 871 cm^{-1} , corresponding to Si-O and Al-O symmetric stretching vibration in C-S-H. Bands 948 cm^{-1} was assigned to Si-O-Si(Al) bonds in SiO_4 and AlO_4 molecules. The other band at $1,114\text{ cm}^{-1}$ was also attributed to Si-O stretching vibrations. Absorption at $1,418\text{ cm}^{-1}$ was assigned to Si-O and Al-O asymmetric stretching vibration. H_2O bending vibration was found at $1,645\text{ cm}^{-1}$ and $3,000\text{-}3,600\text{ cm}^{-1}$ as some water was left from the hydration process. Some portlandite formation was detected in hydrated OPC, GeoPC90, GeoPC70 and GeoPC50 at the band $3,640\text{ cm}^{-1}$ due to the high percentage of OPC content. In contrast, it can be seen that (C,N)-A-S-H mix gel peak at the band $948\text{-}966\text{ cm}^{-1}$ decreased, while C-S-H peak at the band 871 cm^{-1} increased when the amount of OPC replacement is increased e.g. from GeoPC10 to GeoPC90. This meant that the majority of formation was transformed from geopolymeric gel (GP-domination) to different pathways of reaction (C-A-S-H, N-A-S-H or mix gel) or normal C-S-H (OPC-domination). The absorption bands at $1,114\text{ cm}^{-1}$ and $1,418\text{ cm}^{-1}$ appeared, suggesting that T-O (T=Si or Al) asymmetric stretching vibration bonds of geopolymeric formation were slightly changed to OPC-dominated C-S-H with the increase of OPC inclusion. The peak band at 948 cm^{-1} in GeoPC system was shifted to higher frequency at 966 cm^{-1} , indicating more polymerised units of Si-O stretching mode for SiQ^n in geopolymers were established (Lecomte, et al., 2006). However, it is apparent that the mix characteristics between fully-hydrated OPC and GP are clearly seen in the IR spectrum of GeoPC mixtures (GeoPC10 to GeoPC90), confirming a combination in both properties and mechanisms of those major constituents, OPC and GP.

An early age testing at 3 days was additionally done with those at the 28-day age in order to compare the changes. The infrared spectrums between the ages of 3 and 28 days seemed to be consistent as occurred with those individual combination testings. There are no significant differences to be observed, except the reduction of water molecule by the passing age. However, one thing worth to be highlighted is that the shoulders at the band $1,023\text{ cm}^{-1}$ (fly ash powder vitreous alumina-silicate) of GeoPC90 and GeoPC70 decreased by the time. Whist the 871 cm^{-1} peak bands (C-S-H) of GeoPC50 and GeoPC30 almost vanished from the 3rd to 28th day, suggesting the transformation of C-S-H to other forms of geopolymerized products. More details of the FTIR absorption band are as presented in Table 5.6.

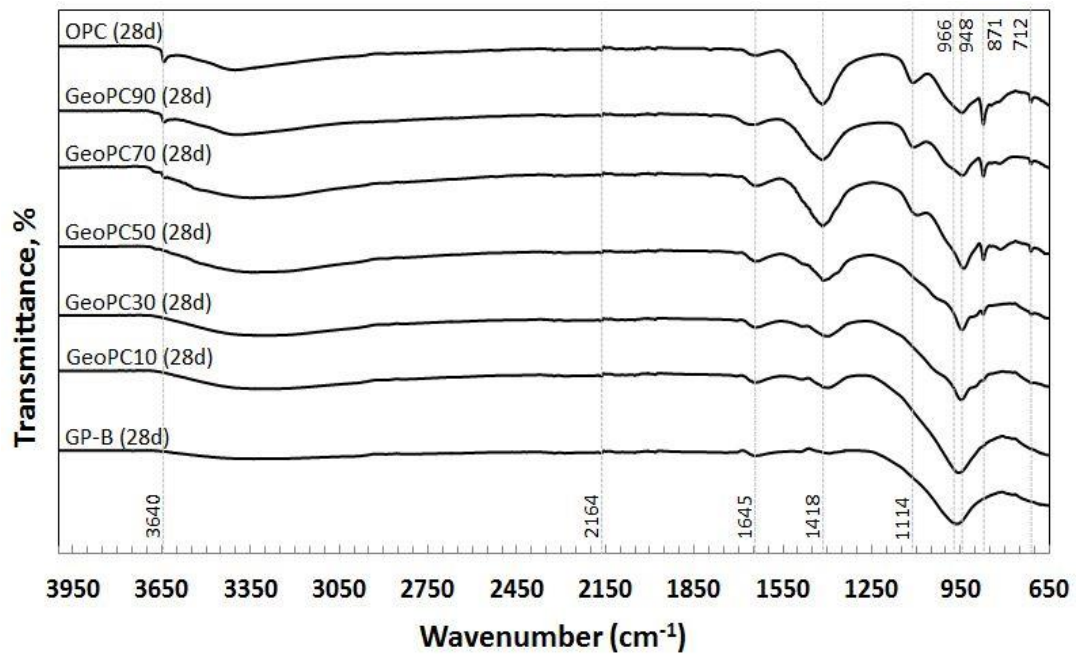


Figure 5.10 FTIR spectrums of GeoPC system at the 28-day age

Table 5.6 FTIR absorption peaks of resulted cement products at the 28-day age

Wavenumber (cm ⁻¹)	Characteristic bands	References*
3,640	O-H stretching vibration of portlandite (Ca(OH) ₂)	[1-3]
3,000-3,600	O-H stretching vibration of water (H ₂ O)	[4-6]
2,164	O-H stretching vibration of hydrogen bonds or CO ₂ absorption	[7,8]
1,645	O-H bending vibration of water (H ₂ O)	[3,9]
1,487	Asymmetric stretching mode of CO ₃ species	[6,10]
1,400-1,418	Si-O and Al-O asymmetric stretching vibration	[2,8]
1,114	Si-O and Al-O symmetric stretching vibration	[2,5]
1,000-1,023	Si-O amorphous or fly ash powder vitreous aluminosilicate, N-A-S-H gel	[11,12]
948-966	Si-O stretching vibration of SiO ₄ and AlO ₄ of Geopolymer, C-S-H, C-A-S-H, N-A-S-H or mix gel	[10,11,13]
871	Si-O and Al-O symmetric stretching in tetrahedron, C-S-H or -CO ₃ vibration in CaCO ₃	[5,10,12]
800-1,200	Si-O-T (T=Si or Al) symmetric stretching of SiO ₄ tetrahedron in Geopolymer	[5,14]
712	Si-O-T (T=Si or Al) symmetric stretching of tetrahedron	[1,4,5]

*[1]= (Liew, et al., 2012), [2]= (Škvára, et al., 2006), [3]= (Ahmari, et al., 2012), [4]= (Yip, et al., 2008), [5]= (Lecomte, et al., 2006), [6]= (Nath, et al., 2014), [7]= (Burciaga-Díaz & Escalante-García, 2012), [8]= (Bakharev, 2005b), [9]= (Andini, et al., 2008), [10]= (Yip & Van Deventer, 2003), [11]= (Shi, et al., 2011), [12]= (Palomo, et al., 2007), [13]= (Puertas & Torres-Carrasco, 2014), [14]= (Kumar & Kumar, 2011)

5.4.2.3 Morphology and crystallinity of GeoPC different levels of OPC replacement

The XRD patterns of OPC, GeoPCs and GP are presented in Figure 5.11. The XRD diffractograms depict the effect of OPC replacement in the GeoPC systems from 0% (GP) to 100% (OPC). At the testing age of 28 days, GP consists mainly of semi-crystalline and amorphous phases which are indicated by the sharp peak (quartz and mullite) and a broad hump in the region of 20 to 35° for 2θ respectively. The peaks corresponding to C-S-H, calcite and nepheline increased when additional OPC increased from 10% (GeoPC10) to 90% (GeoPC90) while the intensity of quartz and mullite continuously decreased. More crystalline phase of portlandite, ettringite and calcite clearly appeared and increased with high percentage of OPC from the GeoPC70 to the fully hydrated OPC. The XRD analysis at the 3 day age was also studied in order to compare its changes in later stage. It, however, exhibited very similar characteristics as 28 days which could lead to good early strength of the final products.

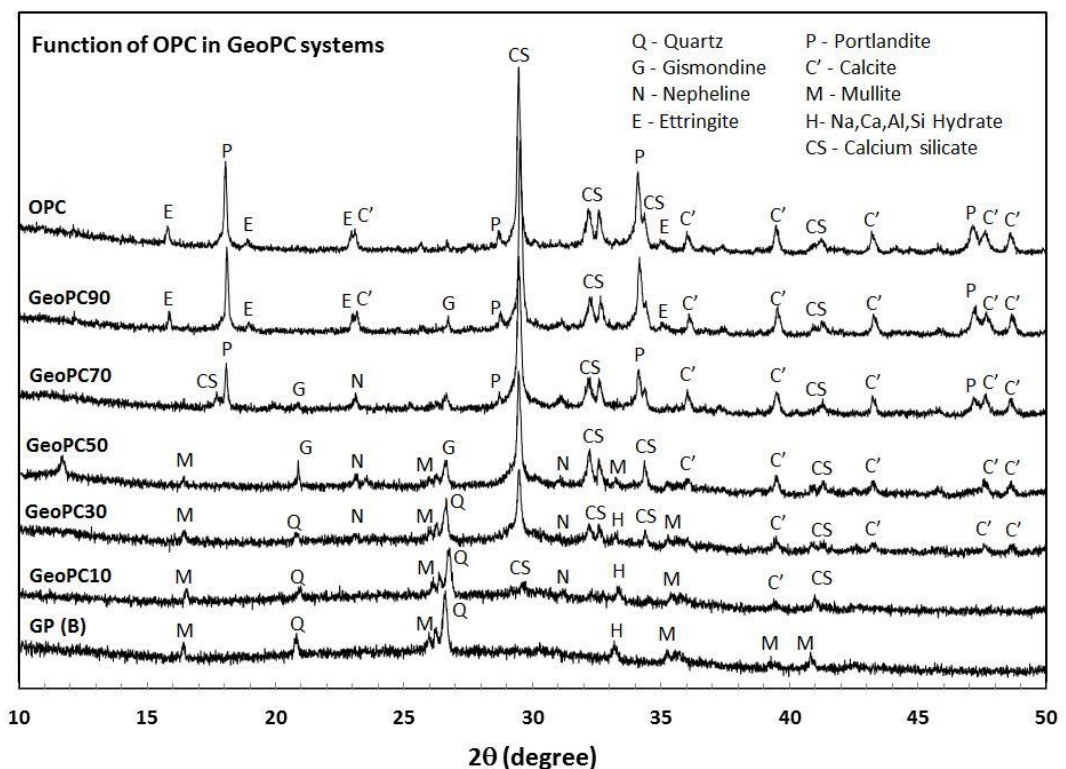


Figure 5.11 X-ray diffraction patterns of GeoPC system at the 28-day age

The appearance of N-A-S-H compound was found according to the high alkalinity of Na-containing solutions. The main composition of fly ash (silica and alumina) could form C-A-S-H phase with the available calcium mineral (Alonso & Palomo, 2001). The findings can be drawn that the GeoPC system has different reaction pathways depending on Na⁺ and OH⁻ concentration and the composition of prime materials, forming the coexistence of

amorphous C-S-H/semi-crystalline phases (XRD peak and hump) or N-A-S-H and C-A-S-H (main reaction product of fly ash activation) interfered in hydration product of GeoPC matrices (Palomo, et al., 2007).

It can be summarised that the hydrated-OPC mixture contains major crystalline phases of C-S-H, ettringite and portlandite while fly ash-based geopolymer cement (GP) is a mixed product of crystalline (quartz and mullite) and amorphous phases. The coexistence formations of both crystalline and amorphous were found in the GeoPC mixtures, illustrating the mix of geopolymeric gel and hydrated OPC product in the single binder. More details of crystallinity phases are presented in Table 5.7.

Table 5.7 Crystalline phases of resulted cement products at the age of 28 days

Abbreviation	Name	Chemical Formula
CS	Calcium Silicate	Ca_3SiO_5
C'	Calcite	CaCO_3
E	Ettringite	$\text{Ca}_6\text{Al}_2(\text{SO}_4)_3(\text{OH})_{12} \cdot 26\text{H}_2\text{O}$
G	Gismondine	$\text{CaAl}_2\text{Si}_2\text{O}_8 \cdot 4\text{H}_2\text{O}$
H	Sodium Calcium Aluminum Silicate	$0.8\text{CaO} \cdot 0.2\text{Na}_2\text{O} \cdot \text{Al}_2\text{O}_3 \cdot 3.0\text{SiO}_2 \cdot 6\text{H}_2\text{O}$
M	Mullite	$\text{Al}_{4.68}\text{Si}_{1.32}\text{O}_{9.66}$
N	Nepheline	$\text{Na}_{2.8}\text{K}_{0.6}\text{Ca}_{0.2}\text{Al}_{3.8}\text{Si}_{4.2}\text{O}_{16}$
P	Portlandite	$\text{Ca}(\text{OH})_2$
P'	Pirssonite	$\text{CaNa}_2(\text{CO}_3)_2(\text{H}_2\text{O})_2$
Q	Quartz	SiO_2
T	Thermonatrite	$\text{Na}_2\text{CO}_3 \cdot \text{H}_2\text{O}$

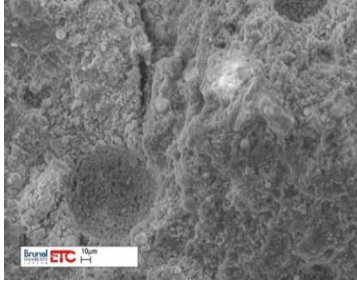
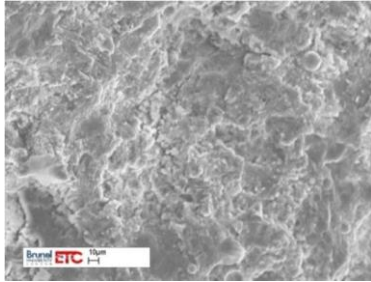
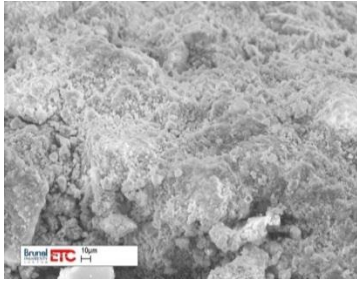
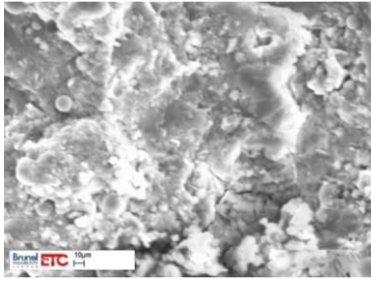
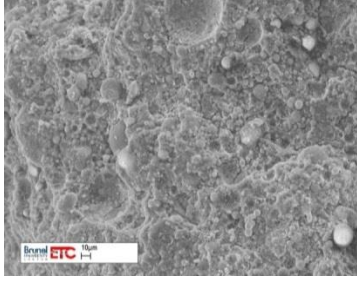
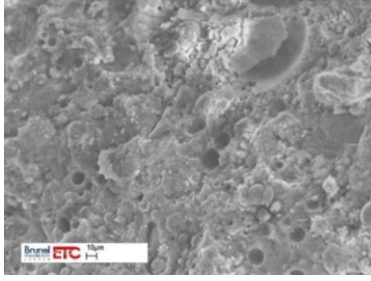
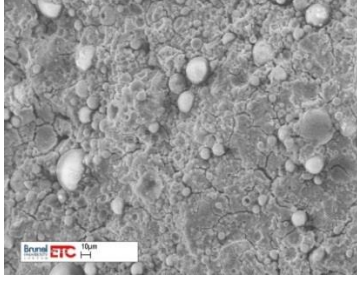
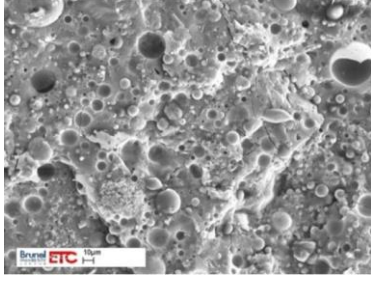
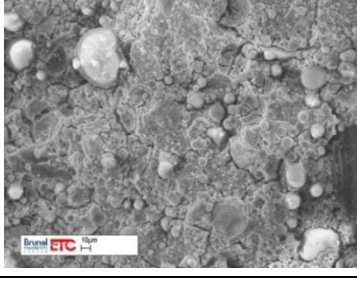
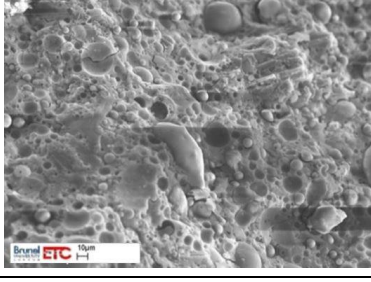
5.4.2.4 Microstructure analysis of GeoPC on different levels of OPC replacement

Table 5.8 reveals the images of OPC, GP and GeoPC mixtures varied from GeoPC90 to GeoPC10 at the ages of 3 and 28 days. Similarly, the micrographs show denser and more compact of 28-day age samples than those of 3 day age samples as the crystalline and structural formation were developed by the time.

The 28-day age microstructures of GeoPC system were used to compare and analyse the differences in the changes of OPC:GP proportions. It is apparent that a micrograph of GeoPC90 is similar to those of controlled OPC. High OPC content resulted in compact and firm structure, leading to an increase in mechanical strength. Microstructures of GeoPC70 and GeoPC50 were less homogeneous than that of GeoPC90. Very few unreacted fly ash particles were found in the matrices as the majority material was OPC and most of remaining fly ash might have reacted within those alkaline environments. Nevertheless, their structures looked denser and more compact than those of the GeoPC30 and GeoPC10. Gel pores of spherical particles and loose matrices can be seen in GeoPC30 and GeoPC10

micrographs. In addition, some of remaining unreacted fly ash particles were also found and could be one of major factors of poor mechanical performances for low-OPC content mixtures (GeoPC30 and GeoPC10) or even GP curing under ambient conditions. It can be seen that the controlled OPC had a dense and compact structure with a majority of C-S-H gel, while controlled GP had totally different structure of less compact structure surrounded with unreacted fly ash particles called “Geopolymeric gel”.

Table 5.8 SEM images of GeoPC system at the ages of 3 days and 28 days

Mixture	3 days age	28 days age
(a) GeoPC90 w/s = 0.298		
(b) GeoPC70 w/s = 0.285		
(c) GeoPC50 w/s = 0.272		
(d) GeoPC30 w/s = 0.259		
(e) GeoPC10 w/s = 0.197		

In summary of function of OPC in GeoPC system, the setting time was shortened by the main contribution of extra precipitation of (C,N)-A-S-H from calcium mineral (in OPC) with alkaline activators. Moreover, the significant increase in compressive strength was also obtained when the amount of OPC replacement increase. The formation of mixed amorphous geopolymeric gel and (C,N)-A-S-H phases were also proved by the FTIR and XRD analysis. As fast reaction had occurred in early stage, the FTIR spectrums and XRD patterns, thus, showed similar characteristics at both 3 and 28 day ages. The final products of this hybrid cement exhibited a combination of OPC and GP characteristics, which depended on the proportion of OPC and GP. The internal heat was also emitted in all mixtures from the reaction of both OPC-hydration and OPC-alkaline activation. By the higher OPC content, higher temperature was obtained, leading to the improvement of curing condition of the systems (Suwan & Fan, 2014). However, it is noted that the reaction of calcium in GeoPC system would give an early strength, while the heat of OPC-reaction would support heat curing in later stage (Tailby & MacKenzie, 2010).

5.4.3 Analysis on elemental compositions and ratios of GeoPC system

Table 5.9 shows significant compositions and ratios of the mixtures at the age of 28 days. The main ratios of Si/Al and Ca/Si are widely considered when EDXA technique is applied. In this issue, more emphasis has been pointed out to the elemental ratios of GeoPC system and geopolymers (GP) to explain the relationship between those ratios and engineering properties.

Table 5.9 Elemental compositions and ratios in GeoPC mixtures at the 28-day age

Mixtures	w/s ^b	Si	Al	Ca	Na	Si/Al	Ca/Si	Si/Na	Na/Al
OPC	0.253	6.85	1.03	83.07	-	6.65	12.13	-	-
GeoPC90 ^a	0.298	7.48	1.44	80.21	0.68	5.19	10.72	11.00	0.47
GeoPC70 ^a	0.285	10.41	3.21	73.75	0.91	3.24	7.08	11.44	0.28
GeoPC50 ^a	0.272	18.37	7.26	52.72	2.22	2.53	2.87	8.28	0.31
GeoPC30 ^a	0.259	21.18	6.46	52.54	2.90	3.28	2.48	7.30	0.45
GeoPC10	0.197	34.22	11.77	22.62	5.26	2.91	0.66	6.51	0.45
FA+SS+SH (GP)	0.191	42.9	15.11	7.75	4.08	2.84	0.18	10.52	0.27

^a 4% added water, ^b Water-to-solid ratio

It is noted that OPC and GP were considered as controlled mixtures. In general, the elemental ratios of OPC are in the ranges of 2.00 to 3.00 for Si/Al (Burciaga-Díaz & Escalante-García, 2012; Lecomte, et al., 2006) and 1.50 to 2.00 for Ca/Si (Yip, et al., 2005) but, in this study, those ratios were distinctly higher than the literatures (Si/Al = 6.65, Ca/Si = 12.13). It might be due to the influence of additional limestone in the cement

clinker of CEM II/A-L type, which affects the calcium content. For the GP, the Si/Al and Ca/Si ratios are 2.84 and 0.18 respectively. The ratios of silica, alumina and calcium in GP were apparently corresponded to related studies, including the formation of geopolymeric gel (C,N-A-S-H, quartz and mullite) (Khater, 2011). As less calcium content, the main geopolymeric gel was therefore an interfered of (Na)-poly(sialate-disiloxo) or $\text{Na}_n\text{-(Si-O-Al-O-Si-O-Si-O)}_n$ - (Guo, et al., 2010).

The chemical species of alkaline materials were brought to a lower energy state when dissolved with water (H_2O) to be Na^+ and OH^- for sodium hydroxide and $2\text{Na}^{2+} + \text{SiO}_2((\text{OH})_2)^{2-}$ for sodium silicate (Sottisoplia & Asavapisit, 2005). The Na^+ ion (from alkaline activators) and Ca^{2+} ion (dissociated from CaO in OPC) were also able to link with central Al⁻ or O⁻ (dissociated from Al_2O_3 in fly ash) forming C-(A)-S-H or N-A-S-H or even the mixed of (C,N)-A-S-H, which provide early strength to the aforementioned GeoPC mixtures. Typically, main product of hydrated Portland cement is an aluminate-substituted calcium silicate hydrated (C-(A)-S-H) gel, whereas the main product of geopolymers is sodium alumina-silicate hydrated (N-A-S-H) gel. With the contribution of calcium source from OPC in GeoPC system, the formation of calcium-sodium alumina-silicate hydrated (C,N)-A-S-H gel was therefore promoted (Garcia-Lodeiro, et al., 2011). The region of those formations can be clearly seen in ternary diagram of Ca-Al-Si and Na-Al-Si as given in Table 5.10 and Figure 5.12.

Table 5.10 The elemental compositions of ternary diagram of Ca–Na–Al–Si system

Mixtures	C-(A)-S-H			N-A-S-H		
	Ca (%)	Al (%)	Si (%)	Na (%)	Al (%)	Si (%)
OPC	91.34	1.13	7.53	0.00	13.07	86.93
GeoPC90	89.99	1.62	8.39	7.08	15.00	77.92
GeoPC70	84.41	3.67	11.92	6.26	22.09	71.65
GeoPC50	67.29	9.27	23.44	7.97	26.07	65.96
GeoPC30	65.53	8.06	26.41	9.50	21.15	69.53
GeoPC10	32.97	17.15	49.88	10.26	22.97	66.77
GP	11.79	22.98	65.23	6.57	24.34	69.09

In addition of the GeoPC system, it was found that low percentage of OPC replacement (e.g. GeoPC10) showed the notable ratio of Si/Al at around 3.00 and Ca/Si at around 0.70, which conformed to the related literatures of calcium-added geopolymer cement (Nath & Sarker, 2014; Shi, et al., 2011). The coexistence C-S-H and geopolymeric gel was formed as C-(A)-S-H or N-A-S-H from the entering of Ca^{2+} and Na^+ to Si-O-Al-O skeleton to compensate loading of Al atoms (Khater, 2011; Topçu, et al., 2014). In addition, high

percentage of additional calcium source (OPC) was further experimented in this study viz. GeoPC30, GeoPC50, GeoPC70 and GeoPC90. With more percentages of Ca-containing over GeoPC10 mixture, it can be observed that the Si/Al and Ca/Si ratios dramatically rise up, approaching the value of fully hydrated OPC by over 3.00 (Si/Al) and over 2.00 (Ca/Si) (Figure 5.13).

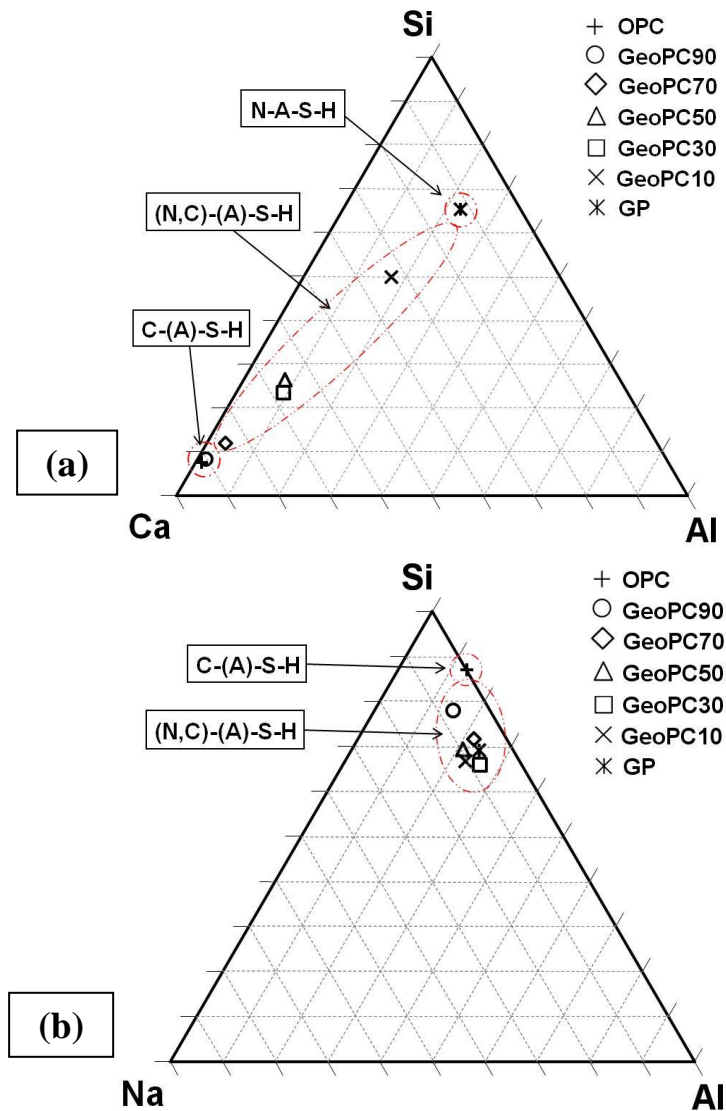


Figure 5.12 Projection OPC, GeoPC system and GP onto (a) ternary Ca–Al–Si system and (b) ternary Na–Al–Si system determined by SEM-EDX analysis

To confirm the coexistence formation of OPC and GP in GeoPC system, the point analysis by SEM-EDXA of GeoPC30 cured under ambient condition was investigated. Figure 5.14 shows an image and spectrums of the coexistence of C-(A)-S-H (OPC-dominated) and (N,C)-A-S-H (GP-dominated) interfered in the same binder. It can be said that the GeoPC mixture has a different formation beyond normal OPC C-S-H and geopolymeric gel of GP. Alternatively, the occurrence could also happen in mixture containing other sources of calcium e.g. high calcium fly ash, GBFS, additional CaO/Ca(OH)₂ or even OPC.

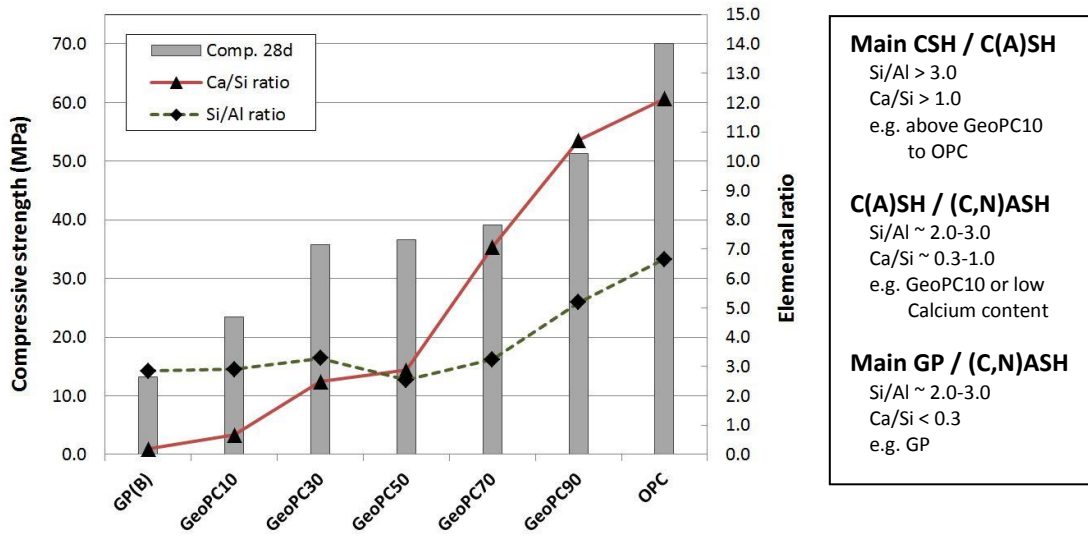


Figure 5.13 Compressive strength, Ca/Si ratios and Si/Al ratios of mixtures at the age of 28 days

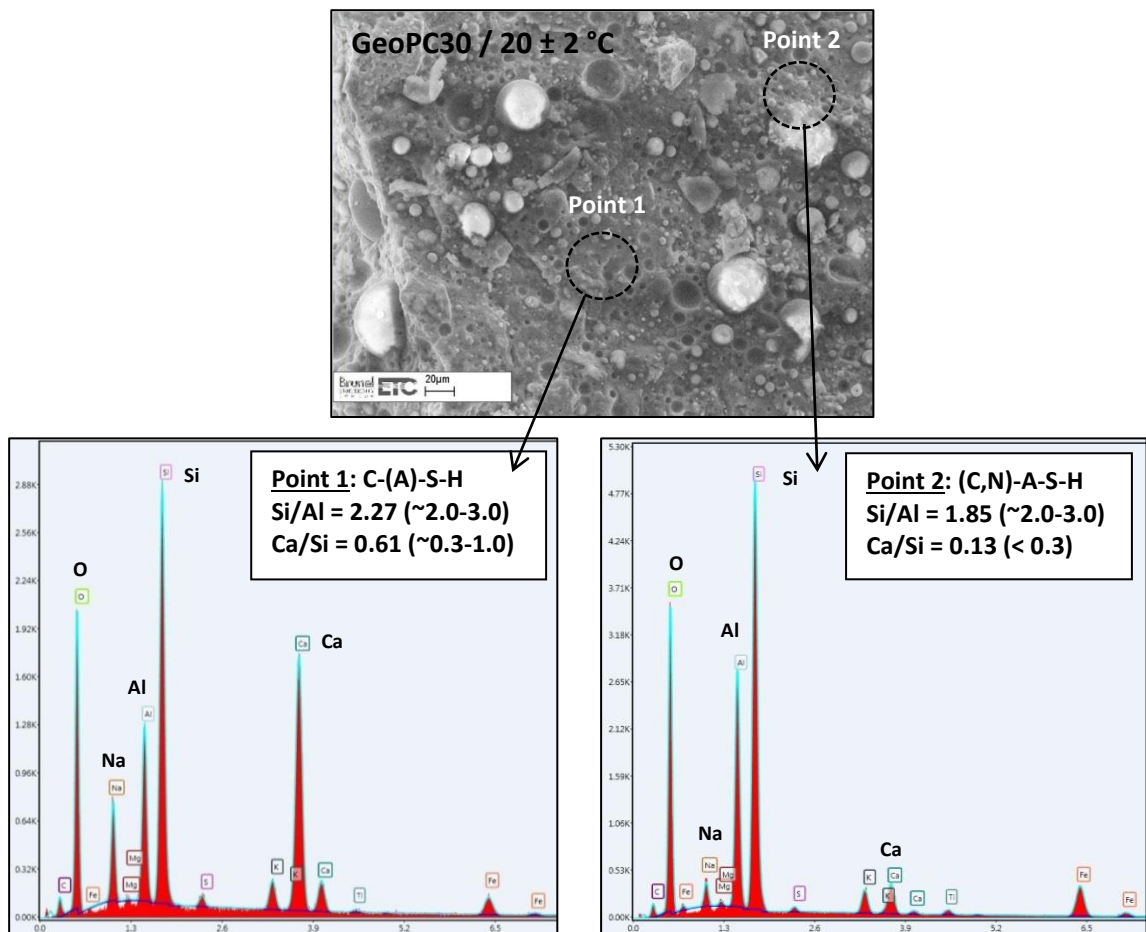


Figure 5.14 Coexistence gel in the GeoPC30 at the 28-day age (70%GP + 30%OPC) Cured under room conditions by point analysis

5.5 Remark

The aim of this chapter is to study the ability of Self-cured geopolymers curing under ambient conditions by using OPC as additive called “GeoPC system”. Micro-mechanisms and mechanical properties were intensively investigated to explain its behaviours and performances as a construction material. In this chapter, the formation and occurrence of each constituent affecting the binding systems was uniquely investigated by the study of the individual combinations. Whist GeoPC system was mainly focused on the influence of OPC inclusion (from 10% to 90%) on the properties and mechanisms of final products. The overall conclusions and major outcomes can be drawn as follows:

1) Reaction of fly ash-based geopolymer constituents (FA+SS, FA+SH and FA+SS+SH) underwent very slow rate at room temperature, leading to low mechanical performances of the final products. Whereas, the reaction of OPC-based constituents (OPC+SS, OPC+SH, OPC+SS+SH) underwent very quick rate at room temperature due to an extra precipitation of calcium compounds (C,N-A-S-H) in high alkalinity environment. The main findings of the study on functionalities of geopolymer constituents are that the sodium hydroxide solution (NaOH) influences the dissolution of the mixtures by its strong alkalinity OH^- , while sodium silicate solution (Na_2SiO_3) is a source of extra Si and also influences both solidification and binding behaviour of the mixtures, which was proved by FTIR, XRD and SEM analysis. The unique characteristics of those sodium silicate and sodium hydroxide soluble could thus lead to an enhancement in geopolymers manufactured with FA+SS+SH (or typical GP) in this study.

2) Calcium source in OPC mainly quickly reacted with alkaline solutions and formed the additional compounds of C-(A)-S-H and N-A-S-H, providing good early strength development to the systems. The setting time of GeoPC system was therefore shortened by this extra precipitation of Ca and alkaline reaction. These can be confirmed by the results of rapid setting, heat liberation in the early stage of mixing and the XRD analysis. In GeoPC system, more compact structure and higher compressive strength were achieved with the increase in the amount of OPC replacement by the additional coexistence formation of those C-(A)-S-H and N-A-S-H gels in the single binder, confirmed by the elemental ratios and SEM-EDX point analysis.

3) Internal heat liberation inside the samples was induced by the amount of OPC addition in the mixtures. The heat emitted in this study may be different from the heat of normal OPC-hydration as the alkaline solutions were used, indicated by the time of the maximum

measured temperature e.g. within 2 hours for OPC with alkaline (OPC+SH, OPC+SS and OPC+SH+SS) and over 9 hours for normal hydrated OPC. This extra heat liberation was obtained by either of or both OPC-hydration and the reaction of OPC and alkaline activators. The geopolymerization of those mixtures cured at ambient temperature could be promoted, enhancing the mechanisms and mechanical properties.

4) The enhancement in mechanical properties of suitable GeoPC mixtures, together with alternative heat supplies from pre-dry mixing process C (Chapter 4) and OPC-hydration in GeoPC combinations (Chapter 5) could provide sufficient heat for the curing regime of GP. Furthermore, GeoPC system also offered the advantages in setting behaviour and early strength development, indicating the potential development of Self-cured geopolymers for on-site applications. It is found that the optimum amount of OPC addition to GeoPC mixtures in this study would be in range of GeoPC5 to GeoPC30, which could achieve in both reasonable strength and economical saving. More studies on heat curing and Self-cured geopolymers technique are carried out and presented in the following Chapters 6 and 7 respectively.

CHAPTER 6 COMPRESSIVE STRENGTH AND MICRO-MECHANISMS OF GEOPOLYMER-PORTLAND CEMENT AT VARIOUS CURING TEMPERATURES

6.1 Introduction

Geopolymer cement (GP) is a kind of amorphous cement binder which is mainly established by a cross-link chain of silica, oxygen and alumina (Si-O-Al). Those silica (Si) and alumina (Al) minerals are dissolved from their original sources in strong alkaline solutions, such as sodium hydroxide (NaOH) and sodium silicate (Na_2SiO_3). Heat is normally applied to the geopolymer paste to accelerate geopolymeric reactions and improve its mechanical performance (Chindaprasirt, et al., 2007). Numerous of research papers have been published on geopolymer properties, demonstrating that the mechanical properties are evidently improved when GP is cured at high temperature around 40 to 90°C with curing duration between 6 to 48 hours (Deevasan & Ranganath, 2010). Nevertheless, the adverse effects may occur when too high curing temperature or too long curing duration is applied, causing the excessive loss of moisture and thermal stress in the structure (Hardjito, et al., 2004; Raijiwala & Patil, 2010). However, as the heat is usually provided by oven or heating unit, the applications of geopolymers nowadays is therefore limited to e.g. pre-cast components and small-scale parts.

Recently, many efforts have been taken to develop geopolymers to achieve reasonable strength under ambient curing conditions, such as (i) using of grounded fine or milled prime materials (Kumar & Kumar, 2011), (ii) applying extra heat from environment or other sources e.g. exposing to direct sunlight (Nuruddin, et al., 2011b), covering with hot gunnies (Nuruddin, et al., 2011a), internal heat accumulation in massive volume (Vaidya, et al., 2011), adding high potential energy compounds (C_3S or C_3A) (Tailby & MacKenzie, 2010) and manufacturing with pre-dry mixing method (Suwan & Fan, 2014) or (iii) increasing extra calcium content to geopolymer mixtures, e.g. high calcium fly ash (Chindaprasirt, et al., 2010), GBFS (Nath & Sarker, 2012) as prime materials, or additional $\text{Ca}(\text{OH})_2$ (Yip, et al., 2005), cement kiln dust (Ahmari & Zhang, 2013) or OPC (Palomo, et al., 2007).

The use of OPC as an additive material, which was previously studied (Chapter 5), is typically classified as an alkali-activated Portland blended cements or fly ash cements (Shi, et al., 2011) or, sometimes, called Geopolymer-Portland cementitious system (GeoPC) (Suwan & Fan, 2014). It is found that calcium mineral in OPC can react with alkaline

activators in the system, providing an extra precipitation of (C,N)-A-S-H formation, giving rise to good early strength and reduction in the setting time of the paste at ambient curing temperature (Garcia-Lodeiro, et al., 2011; Nath & Sarker, 2015). Moreover, an additional heat from its internal reaction would be able to provide a positive effect on heat curing condition to those GeoPC mixtures. To investigate the behaviours and characteristics of GeoPC system at high curing temperature, the micro-mechanisms and hence compressive strength of the Geopolymer-Portland (GeoPC) cementitious system subjected to various curing temperatures from 10 to 70°C were therefore intensively studied in this chapter. It is noted that, from the range of optimum proportion found in Chapter 5, GeoPC system in this study is thus represented by GeoPC30 mixture (70%-geopolymers and 30%-OPC by mass) in order to achieve all of the properties, environment concern and economical saving. The outcomes of the study also allowed the definition of a suitable curing temperature for using in real applications.

6.2 Materials and Testing Methods

6.2.1 Materials

Coal-fired fly ash (FA) used in the test was batch II. Ordinary Portland Cement (OPC) was a general purpose cement Cemex CEM II/A-L type. The chemical compositions of OPC and fly ash are given in Table 6.1. Sodium hydroxide (NaOH, SH) and sodium silicate (Na_2SiO_3 , SS) were purchased from Fisher Scientific Ltd., UK with concentration of 15 molar (M) and 48.20 % w/w respectively.

Table 6.1 Chemical compositions of fly ash and commercial OPC

Materials	SiO ₂	Al ₂ O ₃	FeO	CaO	Na ₂ O	TiO ₂	MgO	K ₂ O	SO ₃
Fly ash	45.71	29.40	9.17	1.59	0.90	1.14	0.97	3.16	0.74
OPC	15.88	2.77	2.49	75.87	-	-	0.20	0.79	2.00

6.2.2 Designation of Geopolymers, OPC and GeoPC mixtures

Geopolymer paste (GP) was made of fly ash and alkaline activators (NaOH and Na_2SiO_3 solutions) with water-to-solid (w/s) ratio of 0.191. The alkaline solutions were prepared with sodium silicate to sodium hydroxide solution (SS/SH) ratio of 1.50. The ratio of alkaline solution to fly ash (A/FA) was 0.40 by mass. OPC paste was made of cement powder and the purified water with w/s ratio at its standard consistency of 0.253. A 70%-geopolymer paste with 30%-Portland cement paste by mass (GeoPC30) was made from the designation mass of GP and OPC paste with w/s ratio of 0.259. Water-to-solids ratio of

GeoPC paste was computed by total mass of water in the mixture (= the mass of water in both SH and SS solutions + OPC paste + added water) to total mass of solid in mixture (= the mass of OPC powder + fly ash + SH solid + SS solid) as the details given in Table 6.2.

Table 6.2 Details of GP, OPC and GeoPC30 mixtures

Mixture	OPC (g)	Fly ash (g)	Na ₂ SiO ₃ Sol. (g)	NaOH Sol. (g)	Purified water (g)	Sum water (g)	Sum solid (g)	Overall w/s ratio
GP	-	500.0	120.0	80.0	-	112.2	587.8	0.191
OPC	500.0	-	-	-	126.5	126.5	500.0	0.253
GeoPC30	161.9	338.1	81.1	54.1	69.2	145.0	559.4	0.259

6.2.3 Sample preparation and curing regimes

For GeoPC mixtures, the same procedures as carried out in Chapter 5 were used in this study. Apart from that, the liquid constituents (mixed alkaline solutions and OPC-water) were added into a mixing bowl containing prime material(s) and then mixed together for 90 seconds at a low speed of 140 ± 5 rpm. The mixer was then stopped for 30 seconds to allow removing all the paste adhered to the wall and the bottom and bringing it to the middle part of the bowl. Then, the mixer was restarted again and run for further 90 seconds. The homogeneous paste was then casted in the prepared mould wrapped with plastic sheet to prevent moisture loss, and grouped in the designated heating regimes of a fridge (10°C), temperature-controlled chamber (20°C) and temperature-controlled electrical oven of 30°C, 40°C, 50°C, 60°C and 70°C for a period of 24 hours (Figure 6.1). After removing from curing units, all samples were demoulded, kept in plastic bags and stored in temperature-controlled chamber ($20 \pm 2^\circ\text{C}$) until reaching the testing age.



Figure 6.1 (a) Casting, (b) Moisture loss protection, and (c) Under curing regimes

6.3 Analytical Methods

Compressive strength of prismatic samples (40mm x 40mm x 160mm) was determined by using the Instron universal testing machine (UTM) in accordance with BS EN 196-1:2016 at the ages of 3 and 28 days. Fourier Transform Infrared (FTIR) spectra were obtained by

using Attenuated Total Reflectance (ATR) technique on a Perkin Elmer Spectrum One-Fourier Transform Infrared (FTIR) spectrometer with a 100 scans per sample in the wavenumber range of 650 to 4,000 cm^{-1} . The X-Ray diffraction (XRD) patterns were recorded on a Bruker D8 Advance diffractometer fitted with a Lynxeye XE high-resolution energy dispersive 1-D detector. The samples were determined by using DIFFRAC.SUITE software acquired at room temperature over the 2θ range of 5 to 100° over a 35-minute period. The Scanning Electron microscope (SEM), an ultra-high performance field emission scanning electron microscope Zeiss Supra 35VP, was used to observe the microstructures at x1,000 magnification, and the Energy dispersive X-ray Analysis (SEM-EDXA) technique was used to define chemical compositions of the raw prime materials and resulting products. More details have been stated in Chapter 3.

6.4 Results and Discussion

6.4.1 Functional groups of the mixtures at various curing temperatures

IR spectrums of OPC (Figure 6.2(a)) presents an absorption band at $1,650 \text{ cm}^{-1}$ related to O-H vibration of water (H_2O) remaining in the samples. The large bands at $1,420 \text{ cm}^{-1}$ and $1,114 \text{ cm}^{-1}$ were corresponded to Si-O and Al-O asymmetric and symmetric stretching vibrations respectively. The band and peak in a range of 825 to $1,000 \text{ cm}^{-1}$ was assigned as major bonding of calcium silicate hydrated gel (C-S-H) and CaCO_3 . The infrared spectra patterns of the samples cured at 10 to 70°C seemed to be consistent, but some small differences can be observed by the hump appearing at $1,650 \text{ cm}^{-1}$ when the curing temperature rose up from 10 to 70°C , indicating less moisture (H_2O) left in the samples. Less Si-O symmetric stretching groups were also detected at high curing temperature for band $1,114 \text{ cm}^{-1}$ which was directly affected by heat curing.

FTIR spectrums of geopolymers under various curing temperatures (Figure 6.2(b)) show small peak at $1,650 \text{ cm}^{-1}$ corresponded to O-H stretching and bending (H_2O). The bondings of Si-O and Al-O asymmetric stretching were also formed at band $1,400 \text{ cm}^{-1}$. The main bondings of geopolymers were exhibited at the band 955 to 973 cm^{-1} , indicating the Si-O stretching vibrations of SiO_4 and AlO_4 of Geopolymers and mixed (C,N)-A-S-H gel (Liew, et al., 2012). It can be noted that higher curing temperature leads to a reduction of moisture content ($1,650 \text{ cm}^{-1}$) and Si-O and Al-O asymmetric stretching bonding ($1,400 \text{ cm}^{-1}$) in the mixtures. In addition, the peak band at 955 cm^{-1} in the lower curing temperature mixture was shifted to a higher frequency at 973 cm^{-1} , indicating more polymerised units of Si-O

stretching mode for SiQ^n in geopolymers were established and provided more strength to the mixtures (Lecomte, et al., 2006).

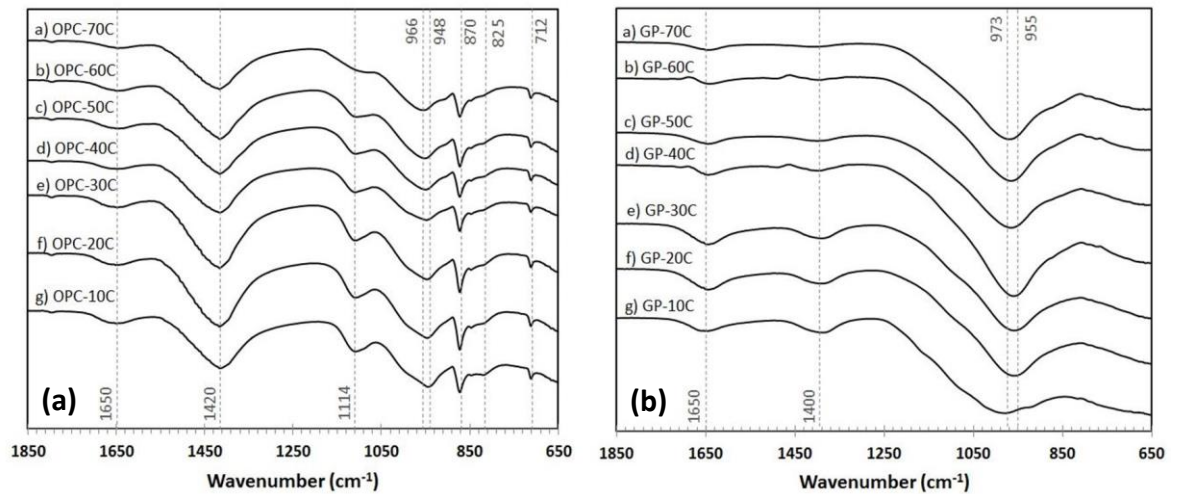


Figure 6.2 FTIR spectrums of (a) OPC and (b) GP cured at 10 to 70°C and 28-day age

It can be seen that the infrared spectrums of GeoPC at various curing temperatures (Figure 6.3) illustrate the absorption bands of $1,650\text{ cm}^{-1}$ and $1,420\text{ cm}^{-1}$, corresponding to O-H (water) and T-O (T=Si or Al) asymmetric stretching vibrations respectively, which also appeared in both OPC and GP mixtures (Figures 6.2(a) and (b)). However, a scrutiny of Figures 6.2 and 6.3 indicates that the band of $1,650\text{ cm}^{-1}$ is more significant for GeoPC than for either OPC or GP, which means internal reactions of OPC and GP may take place. The decrease in the intensity of the peaks with the increase of curing temperature (i.e. from 10 to 70°C) indicates an increase of the reaction. The band of $1,420\text{ cm}^{-1}$ of GeoPC is the combined contributions of GP and OPC. It can be seen that a decrease of asymmetric T-O bonding ($1,420\text{ cm}^{-1}$), moderate to high curing temperature (50 to 70°C), seemed to be transformed to SiO_4 and AlO_4 formation ($948\text{--}966\text{ cm}^{-1}$) in geopolymeric gel and shifted to higher frequency. It is also apparent that the intensity of both peaks decreased with the increase of curing temperature (Figure 6.3), indicating more intensive reactions may occur when the temperature increased. The Si-O symmetric stretching group, corresponding to the band of $1,114\text{ cm}^{-1}$, was detected in OPC and its intensity decreased when the curing temperature increased, however, this was not observed in GP and disappeared in GeoPC, reflecting the influence of heat on the curing/reaction of mixes.

The intensity of the peak ranging from $948\text{ to }966\text{ cm}^{-1}$ was also clearly presented when the curing temperature increased, indicating more Si-O and Al-O stretching vibrations of SiO_4 and AlO_4 of geopolymeric gel and mixed (C,N)-A-S-H gel of geopolymer cement. Si-O and Al-O symmetric stretching vibrations in C-S-H appeared at the peak of 870 cm^{-1} which

was influenced by OPC constituents, presenting the formation of C-(A)-S-H for all curing regimes of GeoPC mixture. The spectrums of GeoPC clearly exhibit the combined characteristics of OPC and GP. The compared spectrums of OPC, GeoPC30 and GP at 20°C at the age of 28 days are also given in Figure 6.4. The combined characteristics of OPC and GP appeared in the GeoPC mixture. With higher proportion of GP (70%) than OPC (30%), the IR pattern therefore tends to be more cognate with GP, including strength development behaviour under high curing temperature.

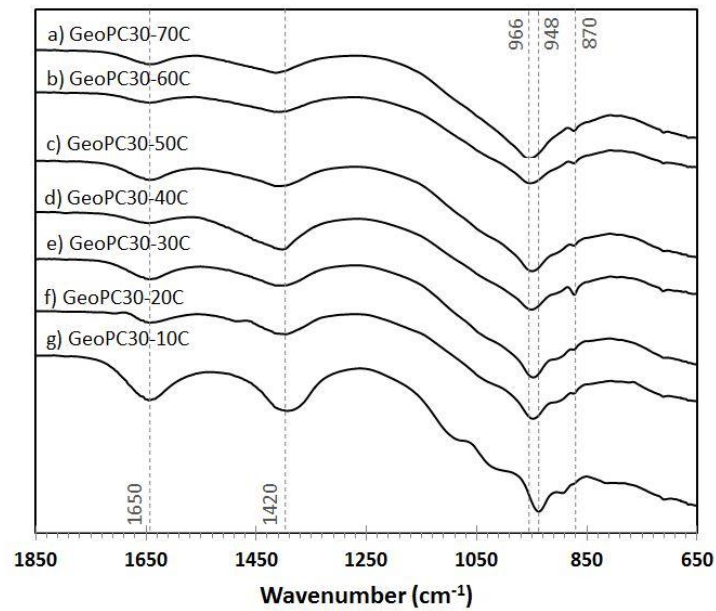


Figure 6.3 FTIR spectrums of GeoPC30 mixture cured at 10 to 70°C and 28-day age

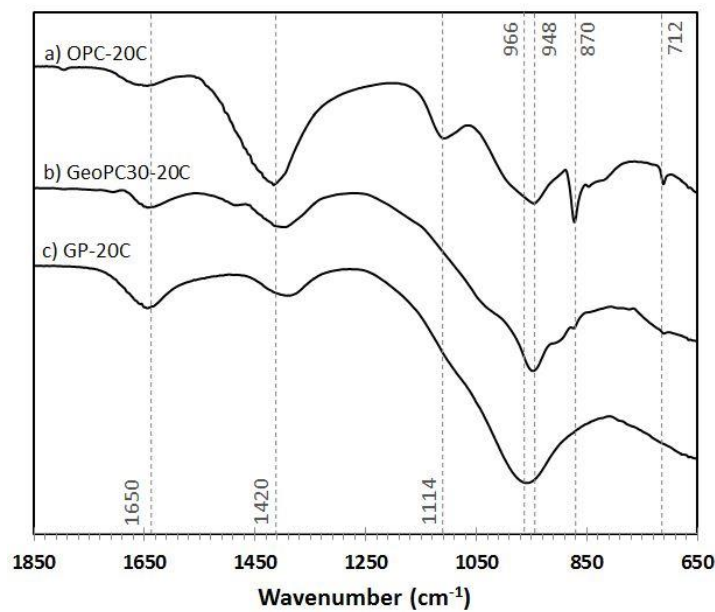
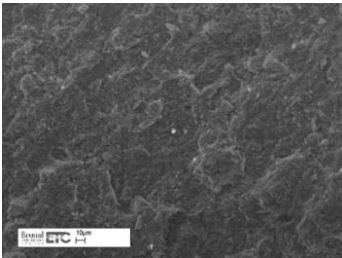
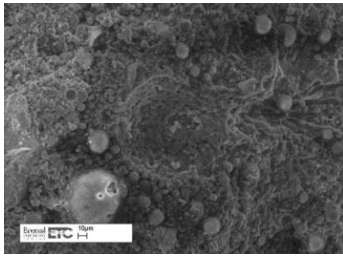
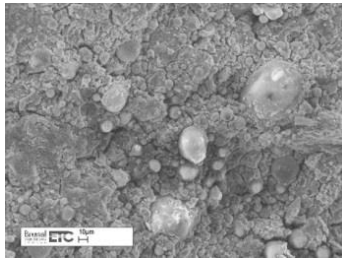
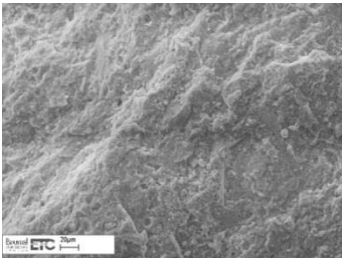
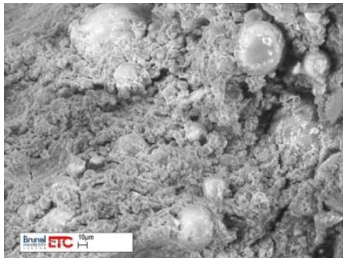
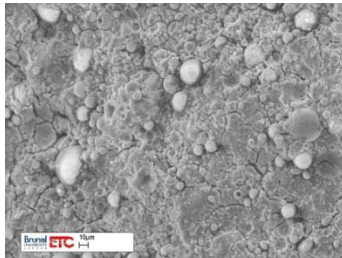
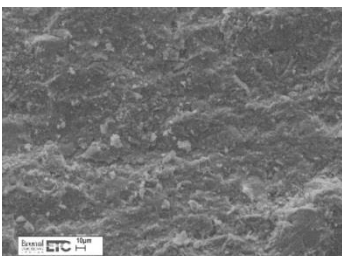
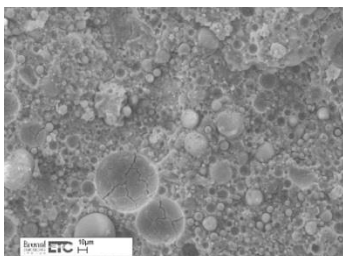
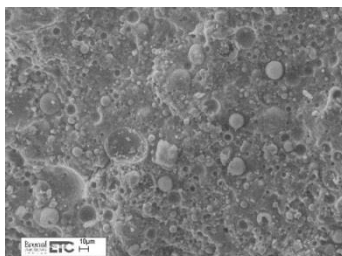
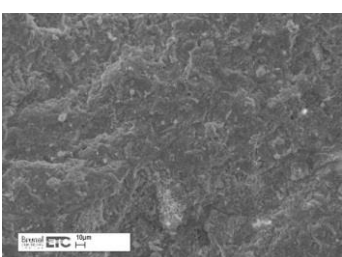
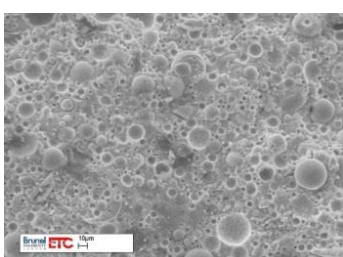
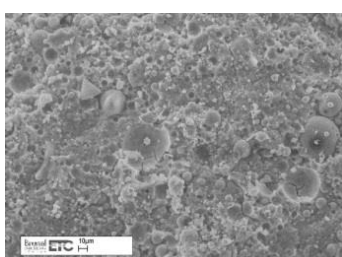
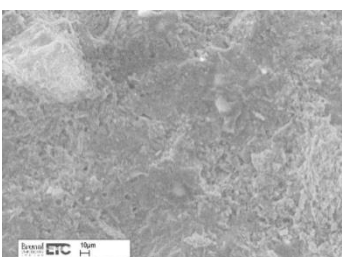
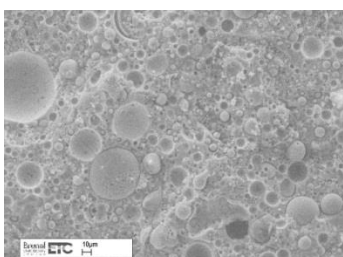
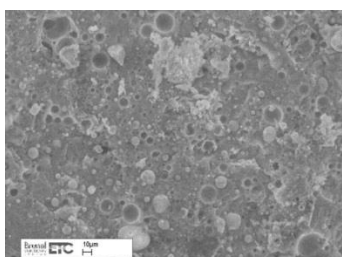


Figure 6.4 FTIR spectrums of OPC, GeoPC30 and GP at 20°C and 28-day age

6.4.2 Microstructures of the mixtures at various curing temperatures

Taking some of the selected SEM micrographs of OPC, GP and GeoPC under various curing conditions as an example at 28 days age (Table 6.3), it is apparent that the microstructures of fully-hydrated OPC samples were denser and more compact than those of GP and GeoPC samples.

Table 6.3 Images of OPC, GP and GeoPC30 at various curing temperatures

Temp	<i>OPC</i>	<i>GP</i>	<i>GeoPC30</i>
10°C			
20°C			
40°C			
60°C			
70°C			

The microstructures of GP at low curing temperature (e.g. 10 to 40°C) show the appearance of porous and loose amorphous structure, and abundant unreacted fly ash particles were found and surrounded by scattered geopolymeric gel with visible micro-cavities (middle column of Table 6.3). However, in high curing environment (e.g. 70°C), very few unreacted fly ash particles can be observed in the matrices and the structures looked denser and more compact. The 28-day age microstructure of GeoPC seems to be a mixed characteristic of OPC and GP. At the low curing temperatures (e.g. 10 and 20°C), the microstructures of those GeoPC were less compact and homogeneous than that of hydrated OPC, but it seems to achieve denser matrix than typical GP. Less unreacted fly ash particles were observed in the matrices when the heat curing rose up to 40°C together with gel formation. Firm and dense structures were found at the high curing temperature of 70°C with some spherical-shape marks on the surfaces (Table 6.3). In addition, there are no significant differences in elemental ratio (by EDXA) found in the test (More details see: Appendix A, Table A.3).

6.4.3 Morphology of the mixtures at various curing temperatures

The 28-day X-ray diffractograms of OPC at various curing temperatures show major crystalline phases of C-S-H (Ca_3SiO_5), portlandite ($\text{Ca}(\text{OH})_2$), calcite (CaCO_3) and ettringite ($\text{Ca}_6\text{Al}_2(\text{SO}_4)_3(\text{OH})_{12}\cdot 26\text{H}_2\text{O}$). Gismondine ($\text{CaAl}_2\text{Si}_2\text{O}_8\cdot 4\text{H}_2\text{O}$) may sometimes be found because calcium, aluminium and silicon are the constituents of OPC powder (Figure 6.5(a)). In the effective region of 20 to 40° for 2θ, the crystallinity of all samples was over 90%. The highest crystallinity was obtained by OPC cured at room (20°C) temperature as 94.30% while the lowest was obtained by OPC cured at 70°C as 90.40% (Table 6.4). It can be drawn that the strength of hydrated OPC mixture was mainly obtained by the formation of C-S-H and its crystallinity. Different curing temperatures slightly affected the crystallization of those OPC pastes as shown in Table 6.4.

The XRD results of geopolymer samples are given in Figure 6.5(b). The major phase of the samples at all curing temperature was an amorphous as indicated by broad hump in the 18 to 38° for 2θ region. The crystalline phases contained in all pastes were mullite ($\text{Al}_{4.68}\text{Si}_{1.32}\text{O}_{9.66}$), quartz (SiO_2), nepheline ($\text{Na}_{2.8}\text{K}_{0.6}\text{Ca}_{0.2}\text{Al}_{3.8}\text{Si}_{4.2}\text{O}_{16}$), gismondine and (C,N)-A-S-H. The formation of crystallinity was collected in the XRD region of 18 to 38° for 2θ at around 50% (Table 6.4). It can be clearly seen that the percent crystallinity slightly increased from 44.90 to 54.30 when the curing temperature increased from 10°C to 70°C (Table 6.4). The strength development of GP was obviously affected by heat curing

and its major structures providing load capability were the mixed amorphous and crystalline phases.

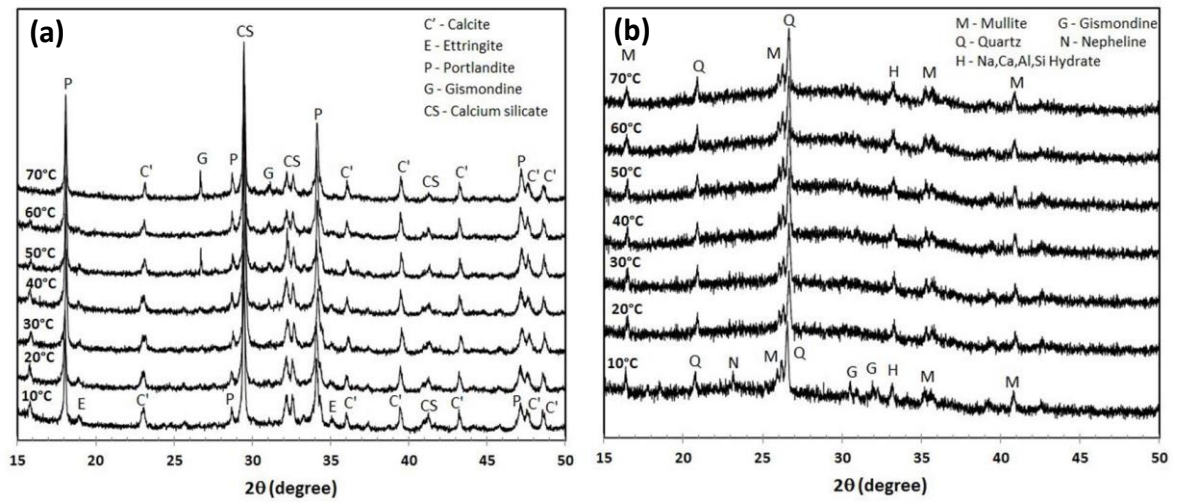


Figure 6.5 XRD patterns of (a) OPC and (b) GP cured at 10 to 70°C and 28-day age

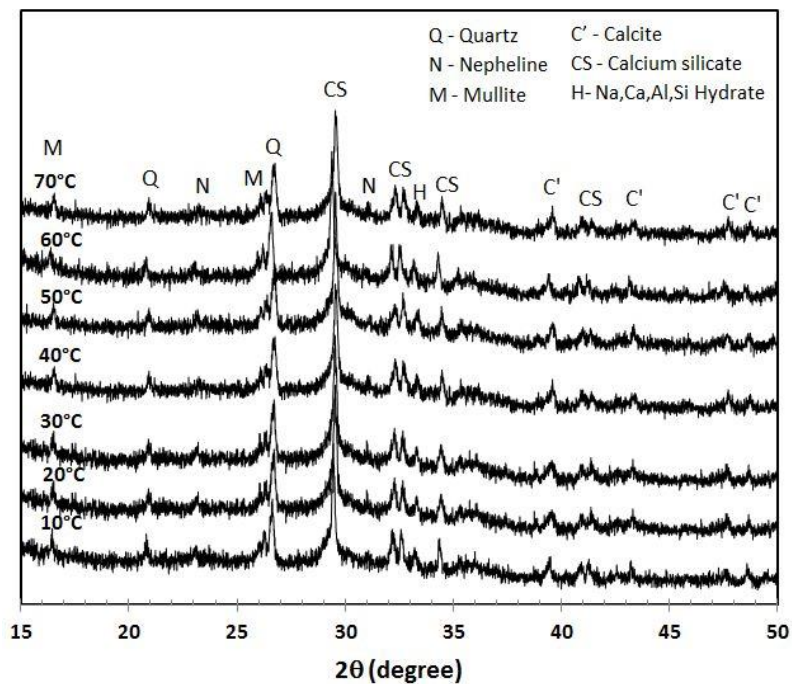


Figure 6.6 XRD patterns of GeoPC30 at various curing temperatures and 28-day age

The XRD patterns of GeoPC at various curing temperatures confirm the mixed characteristics of OPC and GP (Figure 6.5(a) and (b)) which were indicated by the crystalline phases of quartz, mullite, C-S-H, and calcite. Small peaks of nepheline and (C,N)-A-S-H were also detected in all samples according to the Na-containing alkaline solutions. The main composition of fly ash (silica and alumina) could form C-A-S-H phase with the available calcium mineral in the mixtures. The major amorphous phase of the GP also appeared in GeoPC mixtures as indicated by broad hump in the 18 to 38° region for

2θ. It can be drawn that the GeoPC system has different reaction pathways to both typical GP and OPC, depending on OH⁻ concentration and composition of prime materials to form coexistence of amorphous C-S-H/semi-crystalline phase (XRD peaks and humps) or N-A-S-H and C-A-S-H (main reaction product of fly ash activation) interfered in hydration product of GeoPC matrices. However, no visibly significant change appeared in XRD patterns of GeoPC at elevated curing temperatures (Figure 6.6). The mixed characteristics of OPC and GP were indicated by the sharp peaks of quartz, mullite, C-S-H and calcite which are clearly seen in Figure 6.7. However, the percentage of crystallinity of GeoPC30, in the region of 20 to 38° for 2θ, was around 60 to 72, increased from 60.80% to 72.90% when the heat curing increased from 30°C to 70°C (Table 6.4).

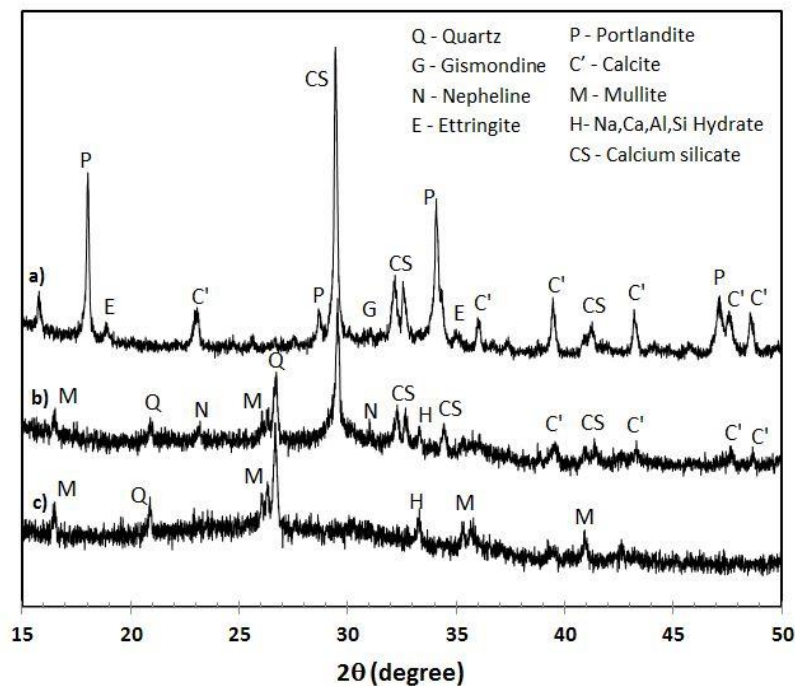


Figure 6.7 XRD patterns of (a) OPC, (b) GeoPC30 and (c) GP at 20°C and 28-day age

A computing of crystallinity and amorphousness of XRD patterns was carried out by using Bruker DIFFRAC.SUITE software. The formulas used to compute those percentages are as follows:

$$\% \text{Amorphous} = \frac{\text{Global area} - \text{Reduced area}}{\text{Global area}} \times 100 \quad (6.1)$$

$$\% \text{Crystallinity} = 100 - \% \text{Amorphous} \quad (6.2)$$

where, *Global area* is the sum of areas under XRD spectrum's hump and sharp peak in the specific region (in 2θ degree); *Reduced area* is the sum of only the areas under sharp peaks in the specific region (in 2θ degree). The summarised results of computing the crystallinity

and amorphousness are presented in Table 6.4. It can be seen that the crystallinity of GeoPC appeared to be a mix of OPC and GP characteristics. The percentage of its crystallinity, in the region of 20 to 38° for 2θ, increased from 60.8 to 72.9% when the curing temperature increased, by comparison with 90.4 to 92.3% for OPC and 44.9 to 54.3% for GP. It must be noted that as expected heating OPC does not result in an increase in crystallinity (Table 6.4).

Table 6.4 Percentage of crystallinity and amorphous phases of OPC, GeoPC30 and GP

Mixtures	Range: from/to (2θ degree)	Global area	Reduced area	% Crystallinity	% Amorphous
<i>Portland cement (OPC)</i>					
1. 10 °C	20 - 40	38.46	35.49	92.30	7.70
2. 20 °C	20 - 40	36.09	34.02	94.30	5.70
3. 30 °C	20 - 40	37.08	33.96	91.60	8.40
4. 40 °C	20 - 40	37.76	34.69	91.90	8.10
5. 50 °C	20 - 40	36.39	33.60	92.30	7.70
6. 60 °C	20 - 40	37.28	35.10	94.20	5.80
7. 70 °C	20 - 40	36.55	33.02	90.40	9.60
<i>Geo-Portland cement (GeoPC30)</i>					
1. 10 °C	20 - 38	38.46	23.65	61.50	38.50
2. 20 °C	20 - 38	45.42	29.36	64.60	35.40
3. 30 °C	20 - 38	38.61	23.49	60.80	39.20
4. 40 °C	20 - 38	36.41	21.48	61.90	38.10
5. 50 °C	20 - 38	35.80	23.39	65.30	34.70
6. 60 °C	20 - 38	34.76	24.11	69.30	30.70
7. 70 °C	20 - 38	34.37	25.06	72.90	27.10
<i>Geopolymer cement (GP)</i>					
1. 10 °C	18 - 38	51.22	23.00	44.90	55.10
2. 20 °C	18 - 38	52.53	23.69	45.10	54.90
3. 30 °C	18 - 38	53.06	32.81	47.80	52.20
4. 40 °C	18 - 38	50.42	23.68	48.10	51.90
5. 50 °C	18 - 38	56.81	27.96	49.20	50.80
6. 60 °C	18 - 38	48.39	24.46	50.60	49.40
7. 70 °C	18 - 38	37.81	22.06	54.30	45.70

Overall, by the analysis of SEM images and XRD, it can be summarised in terms of microstructure and morphology that the hydrated OPC contains major crystalline phases of C-S-H, ettringite and portlandite, forming firm and compact matrices. An increase in curing temperature slightly reduces its crystallinity but the average percentage of crystallinity is still over 90%. Whist fly ash-based geopolymer cement (GP) is a mixture of crystalline (quartz and mullite) and amorphous phases. The proportion of crystalline and

amorphous is therefore around 50:50 percent. Heat curing over room temperature strongly provides positive effect on its mechanical properties indicated by denser matrices at high curing temperature. The coexistence formations of both crystalline and amorphous were also found in the GeoPC mixtures, illustrating the mix of geopolymeric gel and hydrated OPC product in the single binder with approximately 65%-crystalline and 35%-amorphous. As the major proportion of those GeoPC sample was GP, the same expedient behaviour and micrographs under high heat curing were therefore achieved (Figure 6.8).

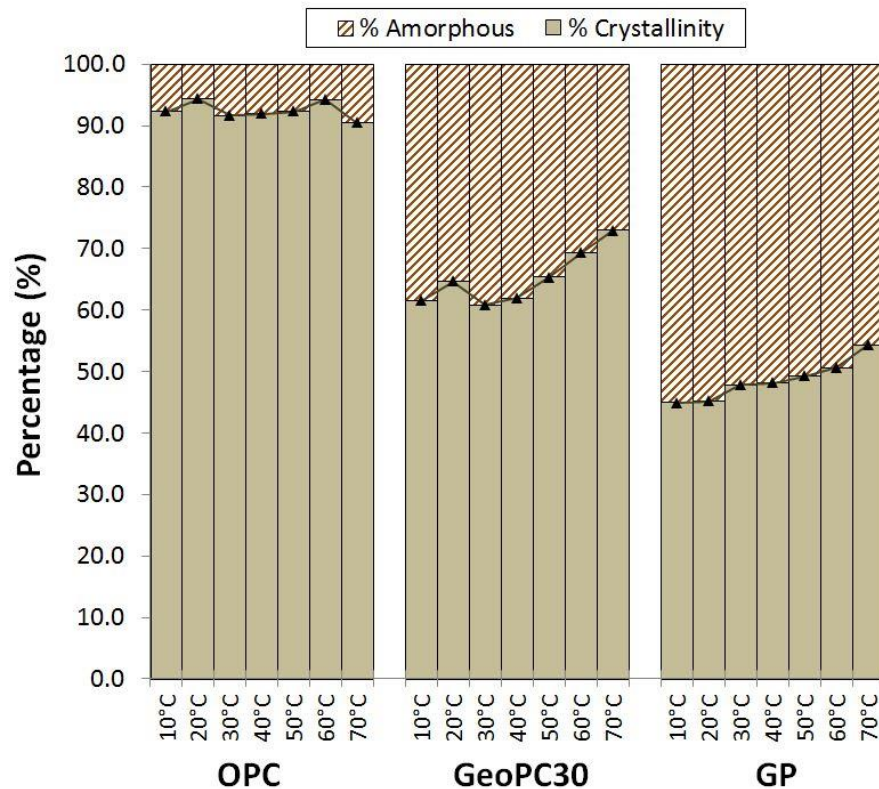


Figure 6.8 Crystallinity and amorphous percentage of OPC, GeoPC30 and GP at various curing temperatures (28-day age)

6.4.4 Compressive strength at various curing temperatures

Compressive strength of OPC pastes was examined on the samples at 3 and 28 day age as shown in Figure 6.9. At the 3 day age, the lowest strength was obtained by curing at 10°C as 31.36 MPa. Its strength was dramatically increased to 50.79 MPa when cured at room temperature (20°C). The compression capability was slightly dropped to 47.32, 47.65 and 47.75 MPa when the curing temperatures rose up to 30, 40 and 50°C respectively. The maximum strength of those 3 day age OPC sample was recorded with the samples cured in 60°C of 54.50 MPa, and followed by 70°C of 53.46 MPa. The 28-day strength of OPC developed by the time, however, the minimum strength was observed with curing temperature at 10°C (58.76 MPa). The highest compressive strength belonged to the

samples cured at room temperature (20°C) of 65.08 MPa. Its strength was slightly decreased to around 60.78 to 63.44 MPa when the curing temperature was between 30 and 70°C. It can be seen that good early strength (3-day age) was achieved when the curing temperature increased. On the other hand, the strength in later stage seemed to be decreased when heat curing was increased to over ambient temperature. The experiments showed that the strength of OPC was developed by the time from lower at 3 days to higher at 28 days age. The strength of OPC is mainly obtained by the formation of calcium silicate hydrated (C-S-H) confirmed by the FTIR and XRD analysis. High curing temperature improves its early strength due to an accelerated OPC-hydration reaction (Al-Amoudi, et al., 1995). However, the excessive moisture evaporation significantly reduced the hydration in later age indicated by the reduction of H₂O bonding in FTIR spectrum when temperature rose up. Non-uniform resulted structure was also produced and dispersed in the matrices (Chithra & Dhinakaran, 2014; Ezziane, et al., 2007) when porosity and pore size may also be increased together with micro-cracking from thermal stress in the sample (Alamri, 1988; Bushlaibi & Alshamsi, 2002) which was possibly seen in SEM images and a dropping of crystallinity percentage at 70°C curing. As an adverse effect could probably be addressed in hot environment e.g. throughout summer time or in tropical climate areas, the proper curing should therefore be seriously considered for achieving its strength and durability by providing a continuous hydration and less porosity (Al-Amoudi, et al., 1995; Soroka, 1993).

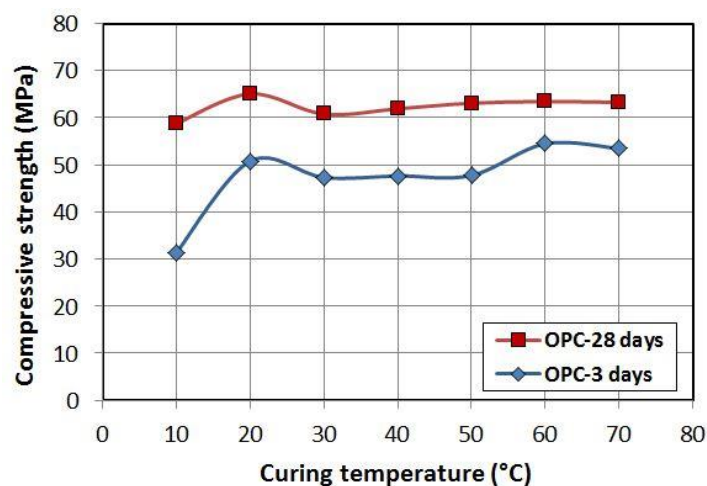


Figure 6.9 Strength of OPC at various curing temperatures at 3 and 28 days

Figure 6.10 presents the results of strength measurement of GP at various curing temperatures for 3 and 28 day ages. Three-day age strength cannot be tested with the curing at 10, 20 and 30°C, while a very low strength of 3.21 MPa was obtained on the samples cured at 40°C. Remarkable results were observed with the curing temperatures of

50, 60 and 70°C as the strength distinctly increased to 23.99, 46.76 and 60.03 MPa respectively. Strength development of GP at 28 days was increased by the time at 8.90, 13.24, 14.43 and 20.65 MPa with curing at 10, 20, 30 and 40°C. The strength was also obviously found to rise up to 45.46, 57.29 and 64.93 MPa with curing temperatures at 50, 60 and 70°C respectively. It can be clearly seen that both early and late compressive strengths of this fly ash-based geopolymer paste could be distinctly improved with high curing temperatures from over 40°C to 70°C. In agreement with previous researches with low curing temperature (10°C to 30°C), the compressive strength could not be measured in the first 3 days while very low strength was obtained at the 28-day age. An increase in curing temperature (40°C to 70°C) gives an increase of chemical reaction, accelerating more geopolymeric gel formation in the matrices (Hardjito & Fung, 2010) and enhancing the mechanical strength in early stage of geopolymerization (Rovnaník, 2010). However, many researchers have revealed that too high temperature curing (e.g. over 70°C) or too long curing duration (e.g. over 24 hours) seemed to result in a decrease in strength (Demie, et al., 2011; Reddy, et al., 2012). The FTIR analysis indicated more polymerised unit of Si-O stretching mode for SiQⁿ in geopolymers when the curing temperature increased, while XRD analysis shows that the structures were the mixed amorphous and crystalline phases of quartz and mullite. The SEM images also confirm denser and more compact structure with very few unreacted fly ash particles in high curing environment over 50°C increased degree of reaction. By those strong bonding of geopolymers at high curing temperature, the compressive strength at 28 days therefore was higher than that of the typical fully-hydrated OPC.

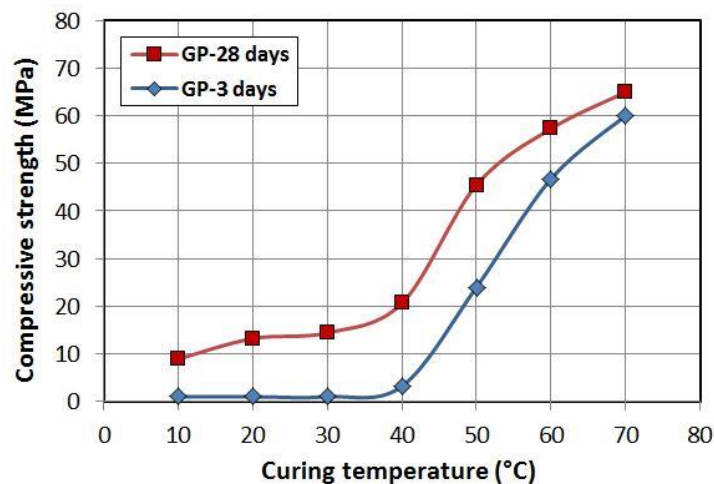


Figure 6.10 Strength of GP at various curing temperatures at 3 and 28 days

For GeoPC system, in generally, pozzolanic materials such as fly ash, slag and silica fume help improve the mechanical properties of OPC on exposure to higher temperature, which

is mainly due to a modification of the kinetic of hydration, reduction of the heat evolution and producing additional secondary C-S-H. The same trend was observed in GeoPC system when its strength developed by the time and increased when the curing temperature increased (Figure 6.11). The conjunction effects of temperature could be that (i) an elevated curing temperature accelerates OPC-hydration in the system, which then provides available Ca(OH)_2 for pozzolanic reaction, and (ii) the pozzolanic reaction then creates a secondary C-S-H, providing more strength to the system (Al-Amoudi, et al., 1995; Ezziane, et al., 2007). In a high alkaline environment, the early strength of GeoPC was enhanced by the contribution of rapid reaction between calcium mineral (in OPC) and alkaline activators in the system. The formation of mixed amorphous geopolymeric gel and (C,N)-A-S-H phases were also proved by the FTIR as the band shifted to higher frequency, indicating more polymerised unit geopolymers while percent of crystallinity (by XRD) rose up when the curing temperature increased. More homogeneous and compact structures than that of GP were obtained when cured at low temperature (i.e. 10 to 40°C) and appeared denser when curing at 50 to 70°C. The internal heat was also emitted from the reaction of both OPC-hydration and OPC-alkaline activation, leading to the possible improvement of curing condition of the systems. However, it is noted that the reaction of calcium in GeoPC system may give an early strength, while the heat of OPC-reaction would support heat curing in later stage. As GP was a main proportion, 70% in the mixture, the compressive strength therefore tended to increase at high curing temperature by GP-domination controlling.

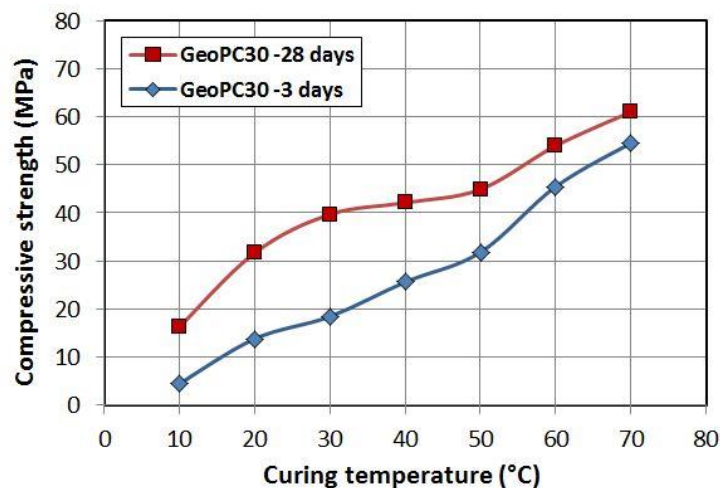


Figure 6.11 Strength of GeoPC30 at various curing temperatures at 3 and 28 days

The comparative strengths of OPC, GP and GeoPC system are presented in Figure 6.12. Beyond the advantage of GeoPC in good early strength, acceptable 28-day age strength of 31.69 MPa was achieved at room curing temperature. In addition, the optimum curing

temperature was found to be around 30°C to 40°C (mild temperature), which achieved the strength of 39.69 MPa and 42.11 MPa respectively, while typical GP gained only 14.43 MPa at 30°C and 20.65 MPa at 40°C (Figure 6.12). This finding could benefit the use in hot climate area or even throughout the summer, including any applying of alternative heat sources.

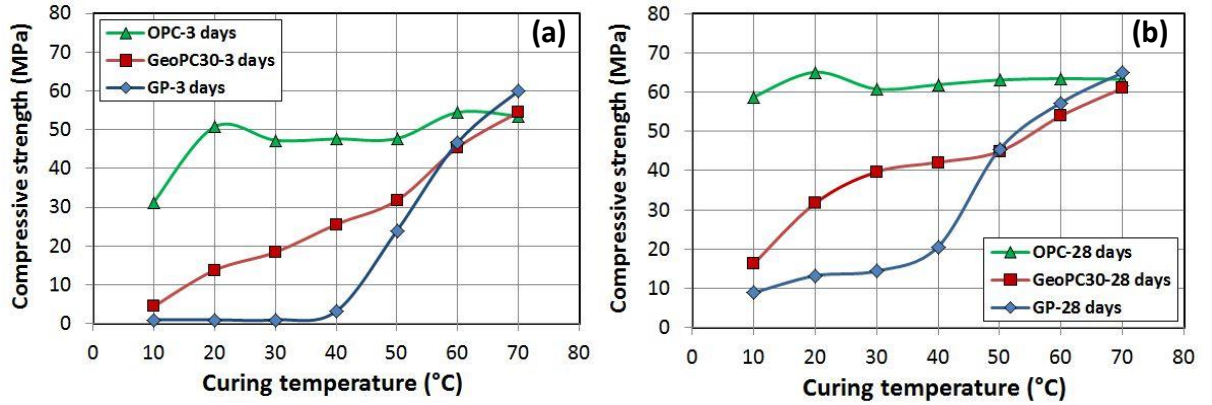


Figure 6.12 Strength development at (a) 3-day age and (b) 28-day age of OPC, GeoPC30 and GP for various curing temperatures

6.4.5 The rule of mixtures for GeoPC composite by mass fraction ratio

The rule of mixtures was used to predict the results of Geopolymer-Portland (GeoPC) cementitious system as one of the composites materials. In general, two types of constituents which were applied to the system would represent a group of three quantities: mass fraction, volume fraction and mole fraction (McNaught & Wilkinson, 1997). In this case, mass fraction (mass of a constituent divided by the total mass of all constituents in the mixture) was used for GeoPC mixture. The GeoPC30 mixture, which was assumed as a composite material, was composed of 70%-GP and 30%-OPC by mass. It is used for the determination of compressive strength of mixed OPC and GP parts at various curing temperatures. As controlled-OPC and controlled GP mixtures were also tested, the strength by using the rule of mixtures of mass fraction ratio was estimated using equation (6.3):

$$\sigma_{\text{GeoPC30}} = f_{\text{OPC}} \sigma_{\text{OPC}} + (1 - f_{\text{OPC}}) \sigma_{\text{GP}} \quad (6.3)$$

$$f_{\text{OPC}} = \frac{m_{\text{OPC}}}{m_{\text{OPC}} + m_{\text{GP}}} \quad (6.4)$$

where, σ_{GeoPC30} is the strength of GeoPC30 mixture (in MPa); σ_{OPC} is the strength of controlled OPC paste (in MPa); σ_{GP} is the strength of controlled GP paste (in MPa); f_{OPC} is the mass fraction of the OPC paste in the composite and $(1 - f_{\text{OPC}})$ is the mass fraction of

the GP paste (f_{GP}) in the composite. The mass fraction of OPC paste can be defined by equation (6.4), where m_{OPC} is the mass of OPC paste (in gram) and m_{GP} is the mass of GP paste (in gram) in the mixture (McNaught, 2014). The linear regression (best-fit) line of the calculated results of GeoPC30 at various curing temperatures from equation (6.3) are plotted as a dash-trend line with $R^2 = 0.91$ (R^2 - coefficient of determination), while the tested results are shown as a solid best-fit line with $R^2 = 0.94$ (Figure 6.13).

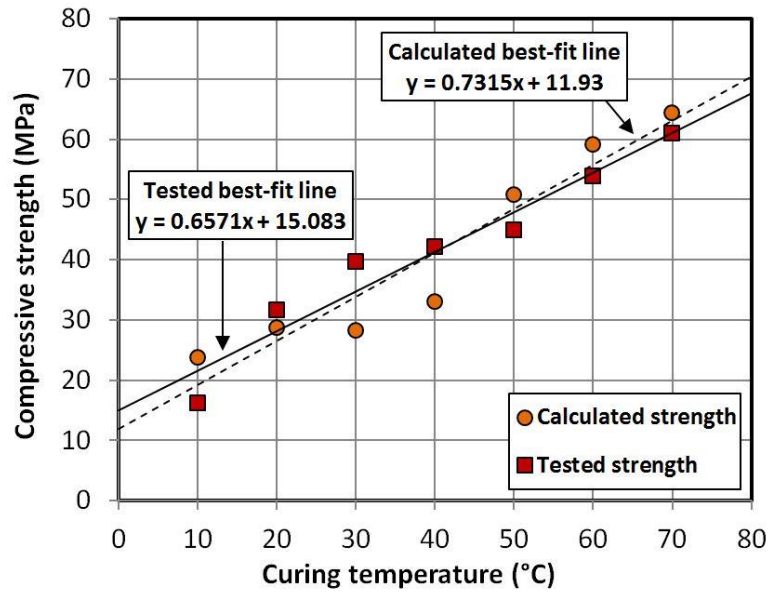


Figure 6.13 Linear regression lines of calculated values (dash line) and tested values (solid line) of GeoPC30 at 28-day age

It is noted that the consistency between those calculated and tested results achieved approximately $R = 0.89$ (or 89%); R = coefficient of correlation. Noticeable remark is that the experimented values had huge gap over calculated values at 30°C and 40°C curing temperatures, indicating more effective strength development in mild curing temperature of GeoPC system.

6.5 Remark

The main aim of this chapter is to study the micro-mechanisms and mechanical properties of Geopolymer-Portland cementitious (GeoPC) system at various curing temperatures. GeoPC30 mixture was used to represent the GeoPC system due to its reasonable combinations in mechanical performances, economical saving, as well as being more environmental friendly. The major outcomes of the test in this chapter can be drawn as follows:

1) From the testing of typical OPC at various curing temperatures, it was found that high curing (above room) temperature improved the early strength due to the acceleration in OPC-hydration. However, in the later age, the strength significantly decreased as an adverse effect of excessive moisture evaporation was obtained, causing larger porosity and uncompleted-formation in the structures as well as the appearance of micro-cracking caused by the thermal stress. Apart from that, for typical (general mixing) GP, its mechanical performances at various curing temperatures were obviously improved in both early and later ages as high curing temperature gave a rise and accelerated the geopolymerization in the GP matrices.

2) GeoPC system achieved a better strength than that of typical GP at ambient curing temperature due to the presence of OPC, forming mixed amorphous geopolymeric gel and (C,N)-A-S-H phases. As GP is the main constituent in GeoPC mixture, the strength therefore increased when the curing temperature increased by the stronger and longer chain of Si-O-Al bonding. The microstructures and mechanisms of GeoPC were also improved for high temperature curing. The optimum curing temperature of GeoPC mixture was observed to be in the range of mild curing (30 to 40°C), which can be achieved in hot environment throughout summer time or even in tropical climate areas.

3) At ambient curing temperature, an alternative extra heat emitted from OPC-hydration (which depends on the concentration of OPC inclusion) may support the curing regimes and could be sufficient for the proper curing conditions of GeoPC system. Somehow, there was no significant heat liberation to be observed in typical (general mixing) GP as its reaction underwent very slow rate under room conditions. However, another alternative heat source could be obtained from the mixing method of exothermic reaction of pre-dry mixing process (C), referring to Chapter 4. Consequently, a study on the advantages of GeoPC system and pre-dry mixing method has therefore been established as “Self-cured geopolymer cement” which will be mentioned in Chapter 7.

PART 3
PRODUCTION OF SELF-CURED GEOPOLYMER CEMENT

CHAPTER 7 COMBINATION OF PRE-DRY MIXING PROCESS AND GEOPOLYMER-PORTLAND CEMENT FOR THE PRODUCTION OF SELF-CURED GEOPOLYMER CEMENT

7.1 Introduction

The study of GP manufacturing procedures (Chapter 4) has proved that the optimum mixing techniques (order) could lead to better mechanical properties. Although the separate mixing process (A) and general mixing process (B) obtained higher strength than the dry-mixing process (C) because the fully dissolved alkaline activators were used in the synthesis, the process C obviously provided efficient heat liberation during its mixing process, which provided more rapid paste setting and created more favourable heat curing conditions for in-field applications. For another approach, the inclusion of OPC in geopolymers (Chapter 5) mainly reacted with alkaline solutions and formed the additional compounds of C-(A)-S-H and N-A-S-H gel which could also shorten the setting time and develop good early strength to the systems. Moreover, some heat liberation induced by the amount of OPC addition/hydration could promote extra geopolymerization reaction and enhance the mechanical properties of GeoPC system cured at ambient temperature. In addition, more information has also been received from the study of GeoPC mixtures at various curing temperatures (Chapter 6). It is revealed that the mechanical strength of the GeoPC mixture increased (by additional formation of mixed amorphous geopolymeric gel and (C,N)-A-S-H phases) when the curing temperature increased as the reaction was accelerated by heat. The potential optimum curing temperature can be in the range of mild curing temperatures, 30 to 40°C.

The above conclusions from the previous chapters lead to the possible development of Self-cured geopolymers at ambient temperature, taking advantages of those beneficial findings, i.e. heat from exothermic reaction and convenience in field operation (Pre-dry mixing), early strength development and ability to gain reasonable strength at ambient temperature, as well as in mild curing condition (GeoPC system). The technique of the combination of pre-dry mixing and GeoPC could provide sufficient heat for the curing regime of GP and offer the potential production of Self-cured geopolymers for on-site engineering applications. Therefore, this Chapter is to develop the optimum processing technologies and hence production of *Self-cured geopolymer cement*.

7.2 Materials and Methodologies

7.2.1 Materials

Coal-fired fly ash (batch II) and general purpose OPC were the same type and grade as used in the previous experiment (Chapters 4, 5 and 6). Their chemical compositions are given in Table 7.1. A 15 molar sodium hydroxide solution and 48.20 % w/w sodium silicate solution were prepared as alkaline activators. Sodium silicate solution to sodium hydroxide solution (SS/SH) ratio by mass was 1.50, while the alkaline solution to fly ash (A/FA) ratio was 0.40.

Table 7.1 Chemical compositions of fly ash and commercial OPC

Materials	SiO ₂	Al ₂ O ₃	FeO	CaO	Na ₂ O	TiO ₂	MgO	K ₂ O	SO ₃
Fly ash	45.71	29.40	9.17	1.59	0.90	1.14	0.97	3.16	0.74
OPC	12.22	3.85	2.85	73.82	-	-	0.78	1.17	5.30

7.2.2 Designation of mixtures and sample preparations

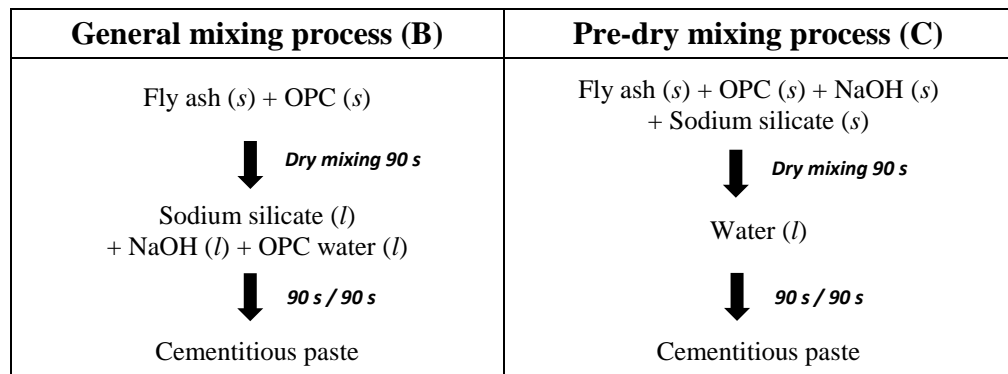
The mixtures of GeoPC5, 10, 15 and 20 were manufactured with a pre-dry mixing process (C) for the study of its mechanisms and mechanical properties. GeoCP mixtures synthesized in general mixing process (B) were also prepared with the same designation of pre-dry mixing process as a controlled-mix. The combinations of GeoPC mixtures in this test were complied with the designated proportions in Chapters 4 and 5 accordingly. As aforementioned in Chapter 4, the pre-dry mixing method requires more water in the system than those normal mixtures. With an increase of A/FA ratio in GP part (in GeoPC system) from 0.40 to 0.45, the resulted water-to-solid (w/s) ratio of the pre-dry mixing process (C) was therefore slightly higher than that of process B. The details of GeoPC mixtures in both processes are given in Table 7.2.

For general mixing process (B), sodium hydroxide solution, sodium silicate solutions and OPC-water were mixed together until becoming homogenous before uses. This combined solution was then added into the pre-dry mixing powder of OPC and fly ash. After running the mixer at low speed of 140 ± 5 rpm for 90 seconds. The mixer was then stopped for 30 seconds to allow removing all the paste adhered to the wall and the bottom and bringing it to the middle part of the bowl. Then, the mixer was restarted again and run for further 90 seconds. After well-mixing, the homogenous slurry was carried out from the bowl for further testing. For pre-dry mixing process (C), fly ash + OPC + sodium hydroxide solid + sodium silicate solid were initially dry-mixed together for 90 seconds in the mixer.

Table 7.2 Design of GeoPC mixtures and Self-cured geopolymers

Mixture	Fly ash (g)	OPC (g)	Na ₂ SiO ₃ Sol ^m (g)	NaOH Sol ⁿ (g)	Na ₂ SiO ₃ Solid (g)	NaOH Solid (g)	Purified water (g)	Overall w/s ratio
GP (B)	500.0	-	120.0	80.0	-	-	-	0.191
GeoPC5(B)	467.6	27.5	112.2	74.8	-	-	7.0	0.194
GeoPC10(B)	443.0	55.0	106.3	70.9	-	-	13.9	0.197
GeoPC15(B)	418.4	82.5	100.4	67.0	-	-	20.9	0.200
GeoPC20(B)	393.8	110.0	94.5	63.0	-	-	27.8	0.203
GP (C)	500.0	-	-	-	65.1	33.8	126.2	0.211
GeoPC5(C)	451.5	27.5	-	-	58.8	30.5	120.9	0.213
GeoPC10(C)	427.8	55.0	-	-	55.7	28.9	121.9	0.215
GeoPC15(C)	404.0	82.5	-	-	52.6	27.3	122.8	0.217
GeoPC20(C)	380.2	110.0	-	-	49.5	25.7	123.8	0.219

The specific amount of water (as shown in Table 7.2) was then added into the mixtures. The mixer was restarted again and were repeated the mixing procedures as those for process B. Testing diagram of controlled (general) mixing process (B) and pre-dry mixing process (C) is as shown in Figure 7.1.



Note: s, solid state; l, liquid state

Figure 7.1 Testing diagram of GeoPC system as Self-cured geopolymers

7.2.3 Analytical techniques

Measurement of internal heat accumulated inside the samples was carried out by recording temperatures using thermocouples and Labview Signal Express software every 1 minute for a period of 24 hours. The Fourier Transform Infrared (FTIR) spectrums were recorded after running 100 scans in the wavenumber range of 650 to 4,000 cm⁻¹. Scanning Electron microscope (SEM) was used to observe the microstructures, and the Energy dispersive X-ray Analysis (EDXA) technique was used to identify the chemical composition of raw materials. The X-Ray diffraction (XRD) patterns were recorded on a Bruker D8 Advance diffractometer fitted with a Lynxeye XE high-resolution energy dispersive 1-D detector.

The samples were determined by using DIFFRAC.SUITE software. Compressive strength of prismatic samples (40mm x 40mm x 160mm) of all combinations was determined by using the Instron universal testing machine (BS EN 196-1:2016). More other details are as stated in Chapter 3.

7.3 Results and Discussion

7.3.1 Internal heat liberation of Self-cured geopolymer cement

The inclusion of OPC directly induces internal heat liberation of GeoPC mixtures by the high potential energy constituents (e.g. C_3A , C_3S), together with minor heat being promoted by the reaction of fly ash, OPC and alkaline solutions. The maximum heat emitted from general mixing process (B) was therefore increased with higher amount of OPC inclusion viz. around 27.4, 28.6, 29.0, 30.0, 30.4 and 31.8°C of GP (B), GeoPC5 (B), GeoPC10 (B), GeoPC15 (B), GeoPC20 (B) and GeoPC30 (B) respectively (Figure 7.2). The peaks were shifted forward to be longer with higher percentage of OPC addition as OPC may require extra time to be hydrated in high alkalinity solutions.

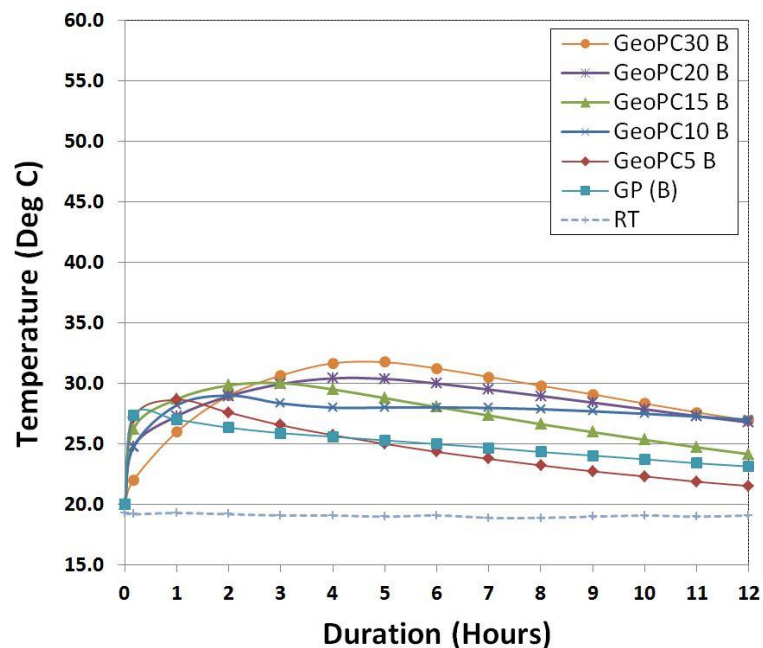


Figure 7.2 Heat accumulated inside various GeoPCs with general mixing process (B)

However, the production of Self-cured geopolymers (GeoPC with Pre-dry mixing process C) released much more heat than those with process B, not only from the hydration of OPC but also an abrupt reaction of alkaline solids in water, more detailed explanation can be found in Chapter 4. It can be seen that the major heat emission in a low-amount of OPC inclusion (i.e. GeoPC5 to GeoPC30) was mainly dominated by the proportion of solid alkaline. The maximum temperatures of 53.2, 53.7, 44.5, 39.2, 37.7 and 39.7°C from an

intensive exothermic reaction were therefore achieved by GP (C), GeoPC5 (C), GeoPC10 (C), GeoPC15 (C), GeoPC20 (C) and GeoPC30 (C) respectively (Figure 7.3). As additional degree of geopolymerization is generally promoted at high curing temperature, the positive effect from additional heat liberation would therefore be achieved with the combination of GeoPC and pre-dry mixing approaches.

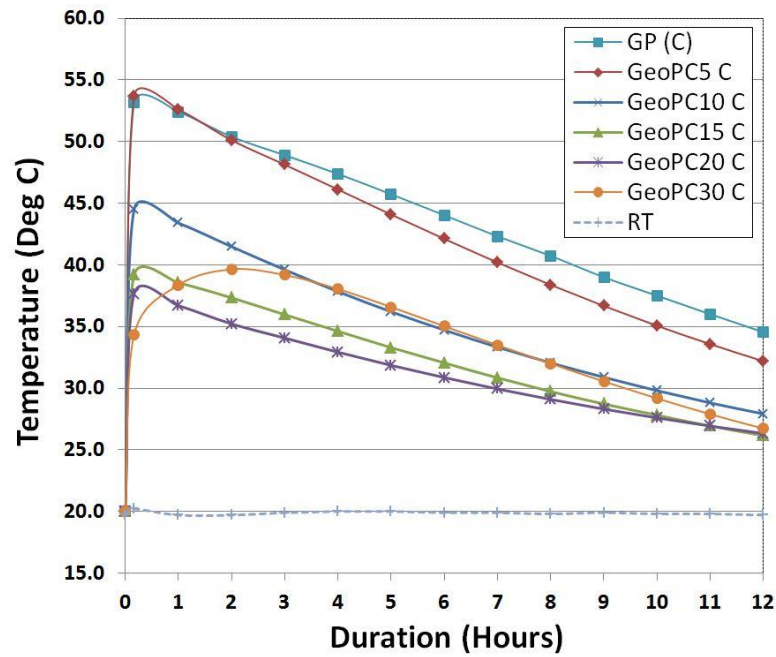


Figure 7.3 Heat accumulated inside various mixtures with pre-dry mixing process (C)

7.3.2 Functional groups of Self-cured geopolymer cement

The IR spectrums of GeoPC mixtures manufactured with general process B (Figure 7.4(a)) and Pre-dry mixing process C (Figure 7.4(b)) showed very similar characteristics at band 871 cm^{-1} and peaks at band $948\text{-}966\text{ cm}^{-1}$, corresponding to Si-O and Al-O symmetric stretching vibrations of (C,N)-A-S-H of OPC and Si-O-Si(Al) bonds in SiO_4 and AlO_4 molecules of GP respectively (Palomo, et al., 2007). Small shoulder at $1,094\text{ cm}^{-1}$ appeared in the Self-cured geopolymers (GeoPC process C), indicating that more Si-O and Al-O symmetric stretching vibrations were also formed (Škvára, et al., 2006). The absorption band at $1,418\text{ cm}^{-1}$ of Si-O and Al-O asymmetric stretching vibrations was observed in both processes and increased with the inclusion of OPC (from 0% to 20%), indicating additional formation of Si-O-Al chain of C-(A)-S-H (Bakharev, 2005b). Nevertheless, more intensity was obtained in dry-mixing method probably due to an advance in heat liberation. In addition, small peaks at $1,487\text{ cm}^{-1}$ of CO_3 species were found in general GeoPC process (B) mixtures, suggesting that CaCO_3 might be formed under incomplete reaction of that hybrid system (Yip & Van Deventer, 2003). O-H bending vibration of

water at the band $1,645\text{ cm}^{-1}$ was also detected much more intensive in dry-mixing process than the general one. In fact, it is noted that GP process C in this testing ($w/s = 0.211$; $A/FA = 0.45$) achieved less moisture left in the system, even though its w/s ratio was slightly higher than the previous GP process C testing in Chapter 4 ($w/s = 0.191$; $A/FA = 0.40$). More dissolution rate (from appropriate water content) could be a key factor for additional degree of reaction. Due to an increase in a small amount of OPC (i.e. from GeoPC5 to GeoPC20), the overall functional groups found in the processes B and C were almost the same. However, by contrast, some differences in the process C bonding would be accounted for extra heat supplied by dry-mixing method and for some of water left in the system, which directly affected its mechanisms and performance.

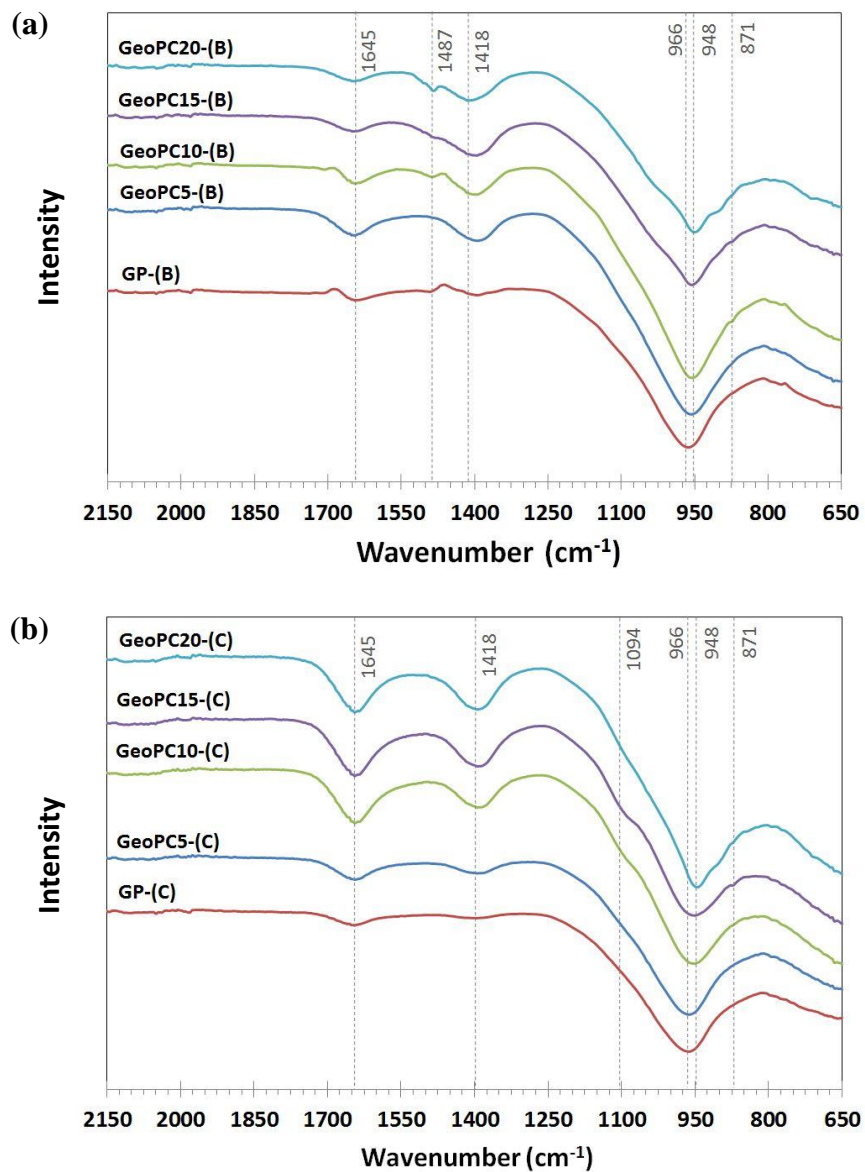
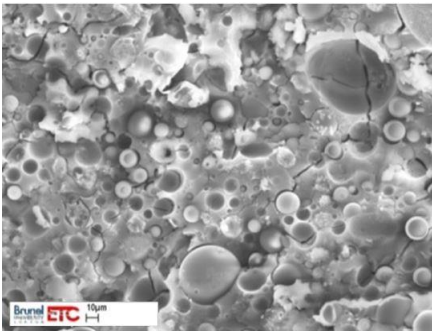
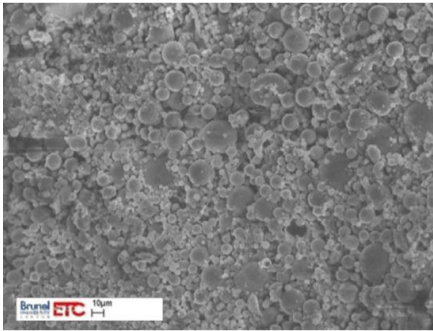
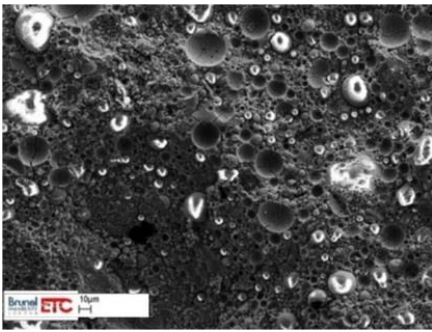
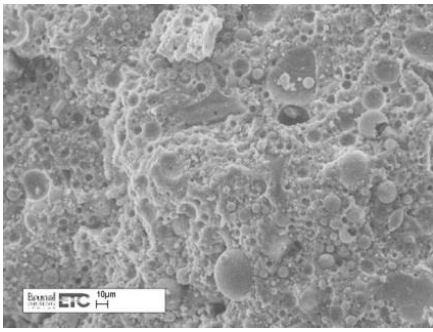
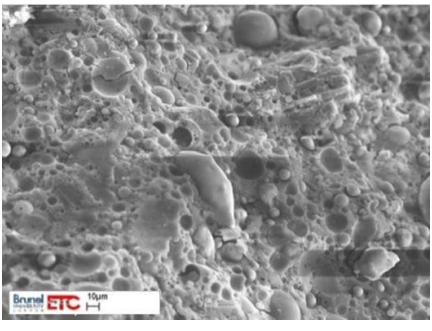
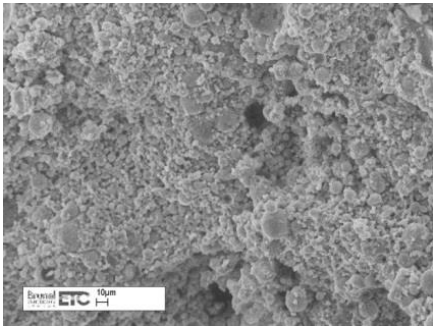
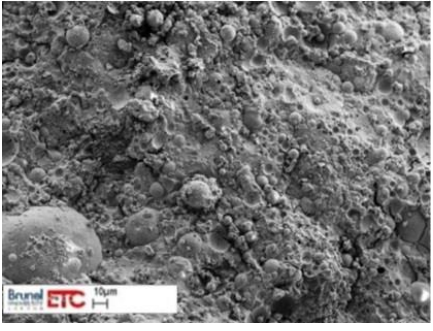
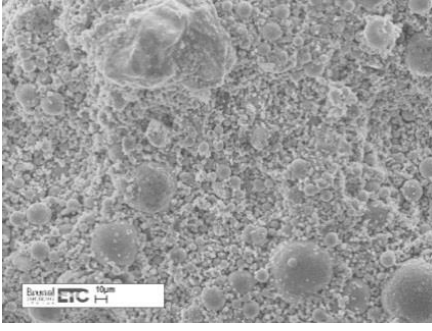


Figure 7.4 IR spectrums of GeoPC in (a) process B and (b) process C at the 28-day age

7.3.3 Microstructures and morphology of Self-cured geopolymer cement

The GeoPC mixtures manufactured with general mixing process B show more uniformity and compact structure than the Self-cured mixtures in all cases, as fully dissolved alkaline solution were used. However, in both processes, the microstructures were distinguishably improved and seemed to be denser when the little amount of OPC was added to the system i.e. GeoPC5 to GeoPC20. Remarkable enhancement can be comparatively seen in SEM images of GP with process B and GeoPC with process C (Tables 7.3(a) to (d)).

Table 7.3 SEM images of GeoPC mixtures in processes B and C at the 28-day age

Mixture	<i>General process B</i>	<i>Pre-dry mixing process C</i>
(a) GP		
(b) GeoPC5		
(c) GeoPC10		
(d) GeoPC20		

From X-ray diffraction patterns, an amorphous phase was represented by the broad hump in approximately 20 to 40° region for 2θ. The crystallinity of mullite (M), quartz (Q), nepheline (N) and (C,N)-A-S-H were detected in all samples. In addition, an extra formation of calcium (aluminato) silicate hydrated (C-(A)-S-H, CS) and calcite (C') were only found in high calcium content mixtures (i.e. GeoPC10, 15 and 20) (Figure 7.5).

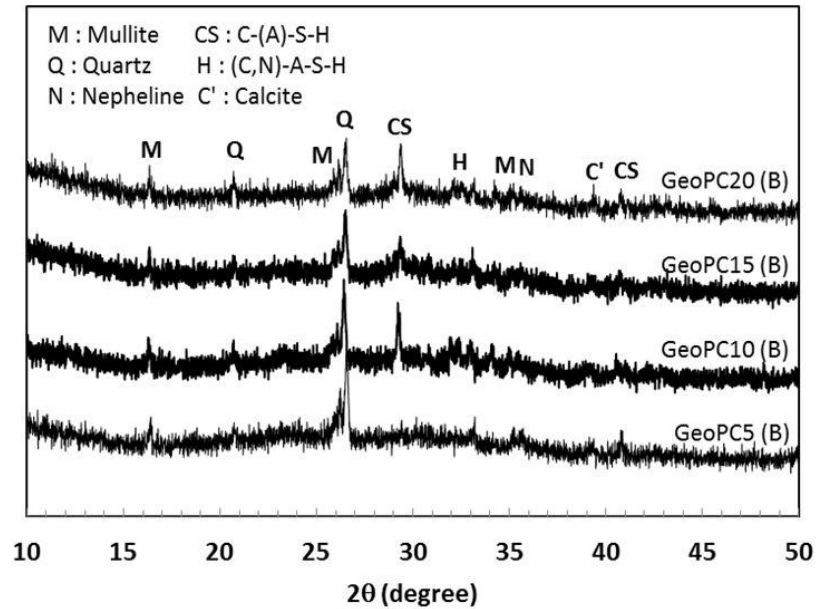


Figure 7.5 XRD patterns of general GeoPC system (process B) at 28 days

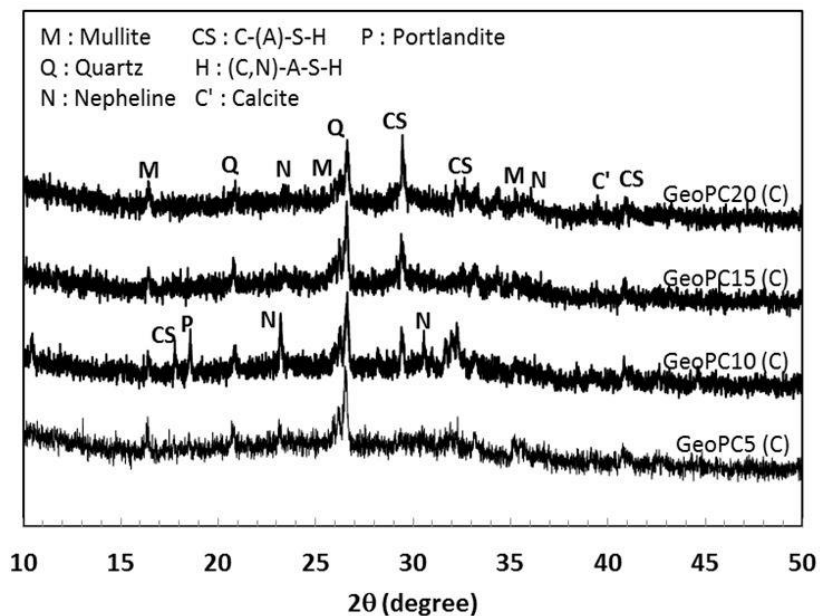


Figure 7.6 XRD patterns of pre-dry mixing GeoPC system (process C) at 28 days

Although the combination of amorphous and crystallinity phases were similarly observed in two mixing methods (B and C), the presence of C-(A)-S-H in pre-dry mixing process C was slightly greater than that of general process B. It might be due to the fact that the

additional OPC gain more opportunity to react with added-water, forming more C-(A)-S-H rather than occurred in alkaline activated solution (Figure 7.6).

7.3.4 Compressive strength of Self-cured geopolymer cement

The compressive strength of GeoPC system in both manufacturing processes B and C was examined on the samples at 3, 7, 14 and 28 days. It is noted that GP could not be carried out for testing in the first three days as it gained a very slow hardening rate at ambient temperature. From the previous findings, it was already found that GP cured at room temperature resulted in lower strength than that cured at high temperatures (Figure 7.7).

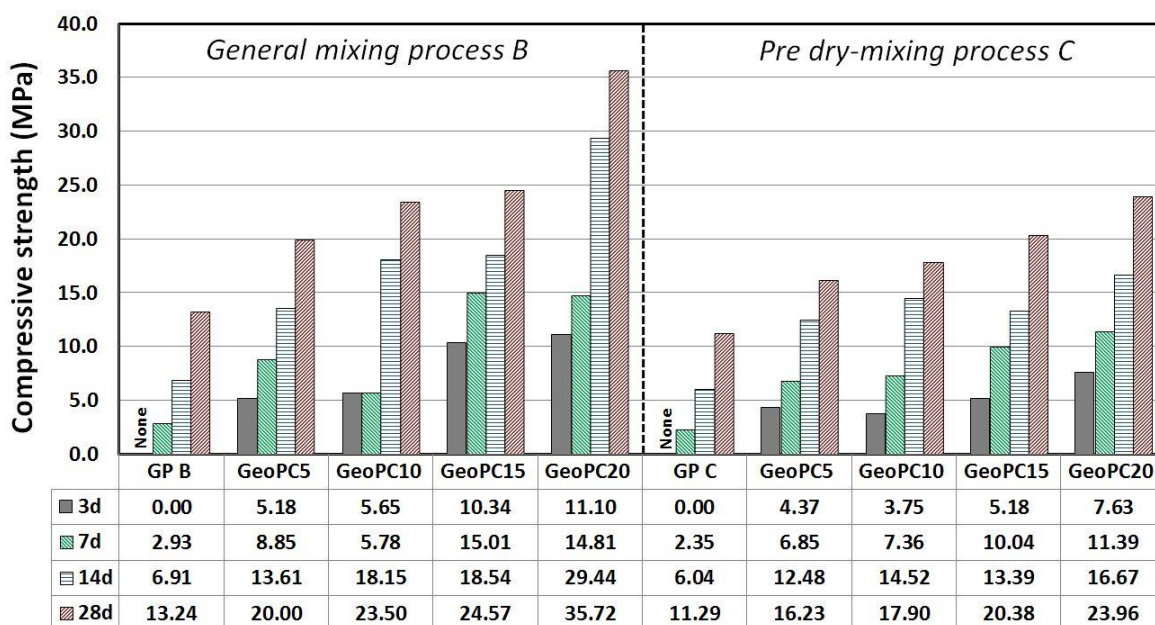


Figure 7.7 Compressive strength of GeoPC mixtures synthesized with processes B and C

The strength also increased when the amount of OPC inclusion increased, indicating the formation of (C,N)-A-S-H gel. Furthermore, low percentage of OPC inclusion (GeoPC5 to 20) in general process (B) and pre-dry mixing process (C) illustrated quite similar characteristics to the recent GeoPC testing. Although mostly identical results were obtained in the functional groups (FTIR) and crystallinity phase analysis (XRD), some disparate bonding performance could lead to different strengths. It can be seen that the compressive strengths of GP and GeoPC5 are not much different from those two processes of only 2 to 4 MPa at 28-day age. By contrast, the greater gaps of strength of around 5 to 11 MPa at 28-day age were observed for GeoPC10 to GeoPC20. It can be explained by the existing of water (O-H bonding, FTIR) and incomplete reaction in GeoPC10 to GeoPC20 of dry-mixing process C (Figure 7.4), leading to the scattered voids and loose structures as presented in SEM images (Table 7.3).

It is apparent that the inclusion of OPC in this test involved in early strength development much more significant than the heat emitted during OPC-hydration. The improvement in strength of dry-mixing GeoPC system (or Self-cured GP) should be further focused on how to increase the reaction rate e.g. using high fineness materials or enhancing the quality of mixing procedures, which is beyond the scope of this study. Apart from that, the benefit from latent heat of exothermic reaction (dry-mixing) may be lightly obtained due to the lack of heat loss protection to the specimens as well as the rapid heat loss in the small size specimens (prisms; 40mm x 40mm x 160mm).

7.4 Remark

The advantages of pre-dry mixing process C (Chapter 4) and GeoPC system (Chapter 5) have been taken and combined as a new scenario, called Self-cured geopolymer cement. The Self-cured geopolymers were set up together with the GeoPC mixtures manufactured in general process (B) for comparison. The results of both procedures by FTIR and XRD revealed very slightly different mechanisms. Nevertheless, more moisture content than that of typical (general) process B was left in the mixture of Self-cured geopolymer process, which was probably due to an incomplete reaction with solid particles of the main constituents. In addition, in general process (B), more compact and denser microstructures were clearly observed by SEM, which led to the slight higher in strength when compared with Self-cured process. Although high strength was achieved by general process (B) as fully dissolved alkaline solutions were used, the strength of Self-cured geopolymer cement could be improved by the use of finer solid particles and prolong curing period. Moreover, the internal heat liberation of Self-cured geopolymer cement was obviously higher than that of general process (B) and could give higher degree of geopolymerization.

The success of the synthesis of Self-cured geopolymers could facilitate its application in practical work as conventional OPC by eliminating the difficulties of highly viscous and corrosive alkaline solutions. The internal heat itself, with appropriate heat loss protection, increases the ability to work at ambient temperature as well as to obtain the early strength development by OPC content. Furthermore, an increase in commercial availability and economical saving could also be achieved by using solid activators when compared to the use of highly cost alkaline solutions.

CHAPTER 8 EFFECT OF SAMPLE SIZE AND EXTRA INTERNAL HEAT ACCOMULATION ON STRENGTH OF SELF-CURED GEOPOLYMER CEMENT

8.1 Introduction

The study of geopolymers and GeoPC system cured at various temperatures (Chapter 6) showed that the mechanical properties of GeoPC increased at both early and later ages when the curing temperature is over 40°C. Heat curing is one of significant factors to accelerate the formation of geopolymeric gel (for GP) and (C,N)-A-S-H gel (for GeoPC), improving the mechanical strength. The alternative heat sources, from exothermic reaction of pre-dry mixing process and OPC hydration reaction of GeoPC system, were also found to provide beneficial conditions for curing purpose under ambient-cured conditions. Some of other non-electrical heat sources were previously reported in literatures and proved to enhance GP properties, for example, exposing GP to direct sunlight or even operating in hot environment or hot climate areas (Nuruddin, et al., 2011b). More heat could be generated by merging internal heat and external hot environment to generate higher degree of reaction (Nuruddin, et al., 2011a).

Another example for non-electrical heating is the internal heat accumulation obtaining from mass-pouring (Vaidya, et al., 2011). For example, a large volume of OPC-concrete casting (e.g. casting of dam or huge foundation) can produce very high internal temperature, up to 80°C (Soroka, 1979; Taylor, 1992). The same behaviour could also occur with a massive volume of geopolymer cement casting at room temperature, which has been reported by the heat measurement of a cubic yard sample (91cm x 91cm x 91cm) of geopolymer cement which achieved internal heat up to 40°C compared with standard cylindrical sample at just 25°C (Nath & Sarker, 2012). As far as geopolymer cement was produced with the huge volume (massive amount) together with good protection in heat and moisture loss, it could also maintain internal heat and provide positive curing conditions itself. Furthermore, the temperature could be kept inside the mixture a bit longer if geopolymer mortar (paste and sand) or concrete (paste and aggregates) are manufactured due to the total heat accumulated by those mixtures in relation with its thermal mass and specific heat capacity (Dodoo, et al., 2012; Kim, et al., 2003). However, it is noted that the bigger specimen size with greater strength does not mean only an enhancement by extra heat from massive-volume, but an effect of specimen size and geometry should also be considered for the properties of final products. As the compressive strength is unable to be

compared with the different specimen sizes and shapes (e.g. prism and cube), the relationship of the strength between any specimen types in this study is therefore plotted on equality chart for comparison and further analysis.

The dry-mixing process (in GeoPC mixture) is supposed to provide an improvement in strength capability, but unexpected results were obtained in the previous testing, see Chapter 7. The combination of GeoPC system in pre-dry mixing process C (with prismatic samples) achieved lower strength than that of GeoPC in general mixing process B. The possible reasons may be assumed to be that an extra heat, which was obtained from dry-mixing process (C), rapidly escaped from un-insulated and small (prism) specimen sizes. It is considered that the massive volume (large specimen) of geopolymer cement may be able to maintain the temperature inside the samples, therefore, the main aim of this chapter is to study sample size, sample geometry and extra heat accumulation inside the sample which may affect compressive strength of Self-cured geopolymer cement.

The experimental work in this chapter was extended from the study of previous work. Apart from other suggested factors (e.g. fineness of materials, mixing quality or usage of specimens' insulation), the 40mm x 40mm x 160mm prismatic specimens were used as small size of specimens for laboratory testing, while 100mm x 100mm x 100mm cubic specimens as large specimen sizes referring to general precast components or huge volume of cement uses. The comparative results of GeoPC mixtures manufactured with typical process B and with pre-dry mixing process C (Self-cured GP) were presented, along with the expression in the compressive strengths of those two types of specimens. It is noted that the materials used and mixtures designed were similar to the previous experiment in Chapter 7.

8.2 Experimental Procedures

8.2.1 Materials and mixture designations

Fly ash, OPC and alkaline activators were the same type and grade as those used in Chapter 7. For the manufacturing of geopolymer pastes, three different manufacturing procedures, i) separate mixing process (A), ii) general mixing process (B) and iii) pre-dry mixing process (C), were carried out with the same mixtures design mentioned in the previous experiment. The same mixture designs of GeoPC system, i.e. GeoPC5, 10, 15 and 20 were also used to prepare samples for both mixes, general mixing process (B) and pre-dry mixing process C (Self-cured GP). The mixing procedures were repeatedly carried out

with the standard mixer at ambient temperature ($20 \pm 2^\circ\text{C}$). The testing series are presented in Table 8.1.

Table 8.1 Testing series of prism and cube specimens

Mixture	Prism 40mmx40mmx160 mm	Cube 100mmx100mmx100mm	Testing age (days)
<i>Geopolymers</i>			
Process A	√	√	7, 14 and 28
Process B	√	√	7, 14 and 28
Process C	√	√	7, 14 and 28
<i>GeoPC in general mixing process B</i>			
GeoPC5 (B)	√	√	3, 7, 14 and 28
GeoPC10 (B)	√	√	3, 7, 14 and 28
GeoPC15 (B)	√	√	3, 7, 14 and 28
GeoPC20 (B)	√	√	3, 7, 14 and 28
<i>GeoPC in pre-dry mixing process C (Self-cured GP)</i>			
GeoPC5 (C)	√	√	3, 7, 14 and 28
GeoPC10 (C)	√	√	3, 7, 14 and 28
GeoPC15 (C)	√	√	3, 7, 14 and 28
GeoPC20 (C)	√	√	3, 7, 14 and 28

8.2.2 Sample preparation

The 40mm x 40mm x 160mm prismatic specimen (volume = 256cm^3) was represented as small volume of paste casting, while the 100 mm cubic specimen (volume = $1,000\text{cm}^3$) was cast as large volume (Figure 8.1). After demoulding, both types of specimens were neatly sealed with plastic films and then covered with plastic sheets to protect moisture loss. All of samples were stored in the curing chamber under ambient conditions of $20 \pm 2^\circ\text{C}$ until reaching the testing age.

8.2.3 Analytical techniques

The compressive strength of prismatic samples was determined by using an Instron universal testing machine and complied with BS EN196-1. It is noted that the compressive surface area of prism samples under Instron machine is 16 cm^2 ($1,600\text{ mm}^2$) by the standard crushing-head size of 40mm x 40mm. Cubic samples were carried out for compression tests with VJ Tech compression machines, EN Automatic Concrete Machine (3000 kN) to BS EN 12390-3:2009. A compressive cross-section of area of all cubes is 100 cm^2 or $10,000\text{ mm}^2$ (Figure 8.2). All GPs in different manufacturing processes were produced for compression tests on their 7, 14 and 28 day ages, while all GeoPC mixtures were tested at 3, 7, 14 and 28 day ages on both prism and cube specimens. The strength value was calculated by using the average value of three identical samples. The compressive strengths of prismatic and cubic samples were plotted on equality chart. The

linear regression analysis was used to analyse the relationship between those results in different testing series (Mansur & Islam, 2002; Yi, et al., 2006).

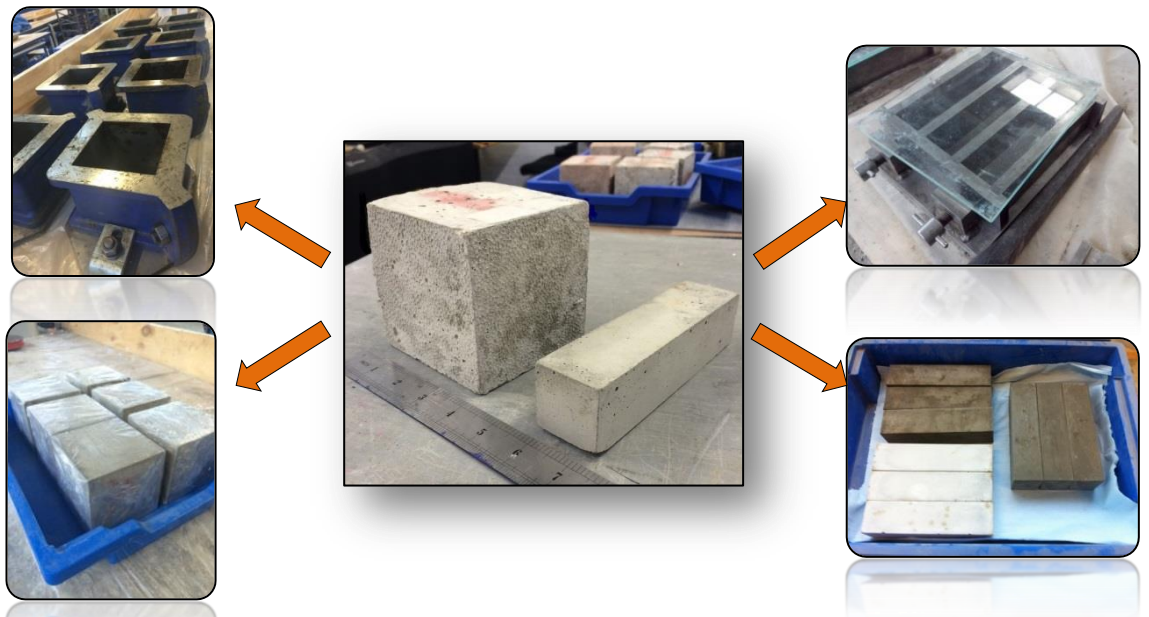


Figure 8.1 Two different sizes and geometries of cube and prism samples



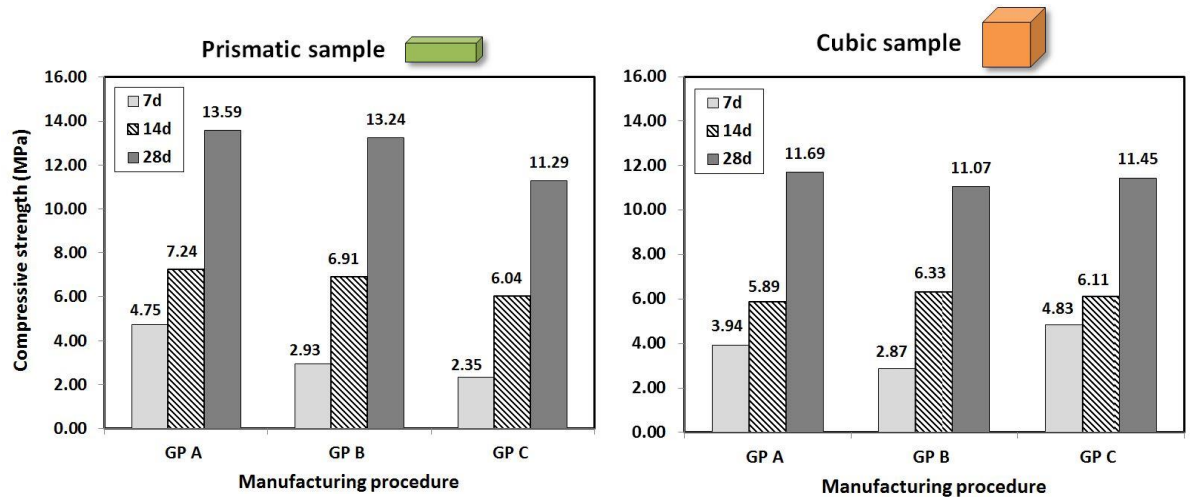
Figure 8.2 Compression test of cubic sample (Left) and prismatic sample (Right)

8.3 Results and Discussion

8.3.1 Effect of specimen size on the compressive strength of GP in different manufacturing processes

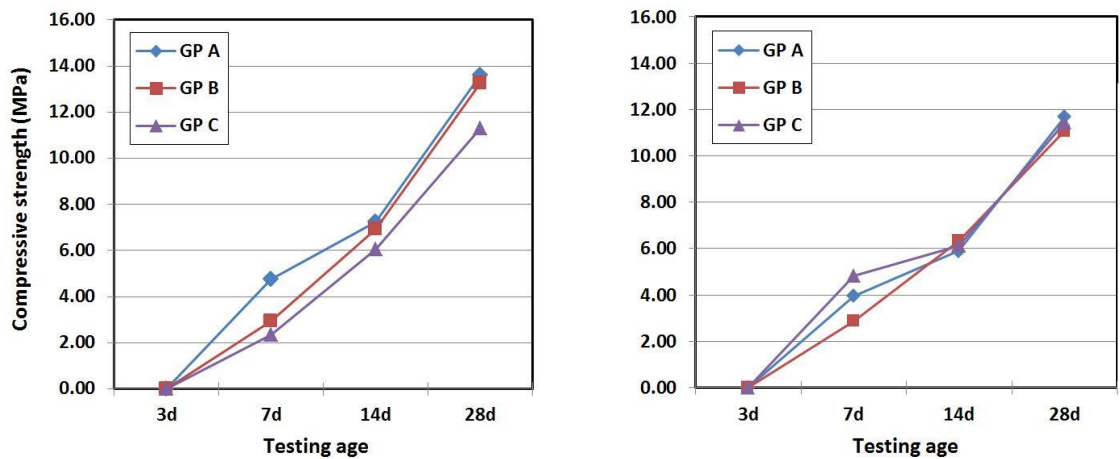
The compression tests were carried out at 7, 14 and 28 days age as all GP pastes could not set in the first 3 days. For the compressive strength of prism samples (the results are as reported in Chapter 4), the separate mixing (process A) achieves higher strength than that of the general mixing (process B), and followed by the pre-dry mixing (process C)

respectively (Figure 8.3). This may be due to the fact that the fully-dissolved alkaline solutions could provide higher degree of geopolymerization, leading to more intensive matrix bonding of processes A and B. Even though, the pre-dry mixing process (C) obtained an intensive heat from the alkaline exothermic reaction, insufficient alkaline dissolution together with lack of heat loss protection could significantly result in low mechanical strength.



(a) Prismatic samples (Bar chart)

(b) Cubic samples (Bar chart)



(c) Prismatic samples (Line chart)

(d) Cubic samples (Line chart)

Figure 8.3 Compressive strength of GP in different manufacturing processes

It can be drawn that process A gained the highest compressive strength, followed by processes B and C in all testing ages (Figure 8.3(a)). By contrast, the strength value of 100 mm cubic samples was slightly different from those of the prisms (Figure 8.3(b)). The compressive strength of dry-mixing process (C) seemed to be improved when compared with processes A and B. In addition, it can be clearly seen from the results of prismatic samples (Figure 8.3(c)) and cubic samples (Figure 8.3(d)) that the strength developments

were slightly different, changing from the process $A > B > C$ in all testing ages of prisms to $C > A > B$ (7-day age) and $A > C > B$ (28-day age) on cubes. It is noted that the difference in strength seemed to be obtained mainly due to the effect of specimen size. Even though the compressive strengths of prismatic and cubic specimens cannot be compared due to the differences in size and shape geometry (Del Viso, et al., 2008; Yi, et al., 2006), it can be apparently analysed by plotting the relationships between cubic and prismatic strength values.

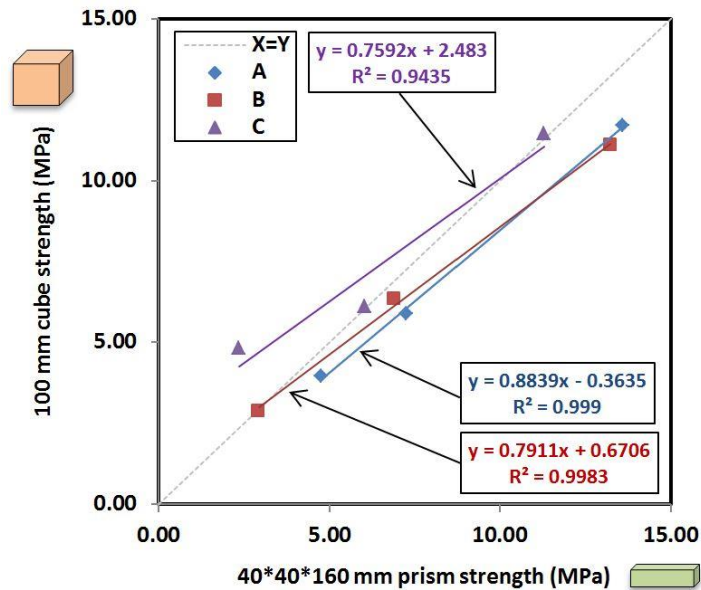


Figure 8.4 Relationship between mean compressive strength of GP 100 mm cubes and 40mm x 40mm x 160mm prisms in different processes

The strength of 100mm x 100mm x 100mm cubes was plotted against that of the 40mm x 40mm x 160mm prisms to examine the relationship of specimen sizes (Figure 8.4). Solid lines indicate the best-fit lines (from linear regression analysis) of each GP strength data, while a dash-line indicates the line of equality $y = x$. It can be seen that the best-fit lines of GP process A and B are almost aligned each other and both of them are drawn below the line of equality, indicating that the prism strength is higher than that of the cube strength. By contrast, it may be seen that a best-fit line of GP process C is consistently above those corresponding best-fit lines for A and B over the entire range of testing ages, and is almost located above the equality line, demonstrating higher strength of the cubic samples over the prisms. The reason may be due to an extra heat accumulation (exothermic reaction; solid alkaline activators and water) which could be kept inside larger specimens (100 mm cubes), enhancing its geopolymerization through chemical bonding.

8.3.2 Effect of specimen size on the strength of GeoPC and Self-cured geopolymers

The compressive strength of GeoPC system in the general mixing and Self-cured GP process C was examined on the samples at 3, 7, 14 and 28 days. Figure 8.5 shows the results of the prismatic samples with the general mixing process B (left) and Self-cured GP process C (right) which were presented in Chapter 7.

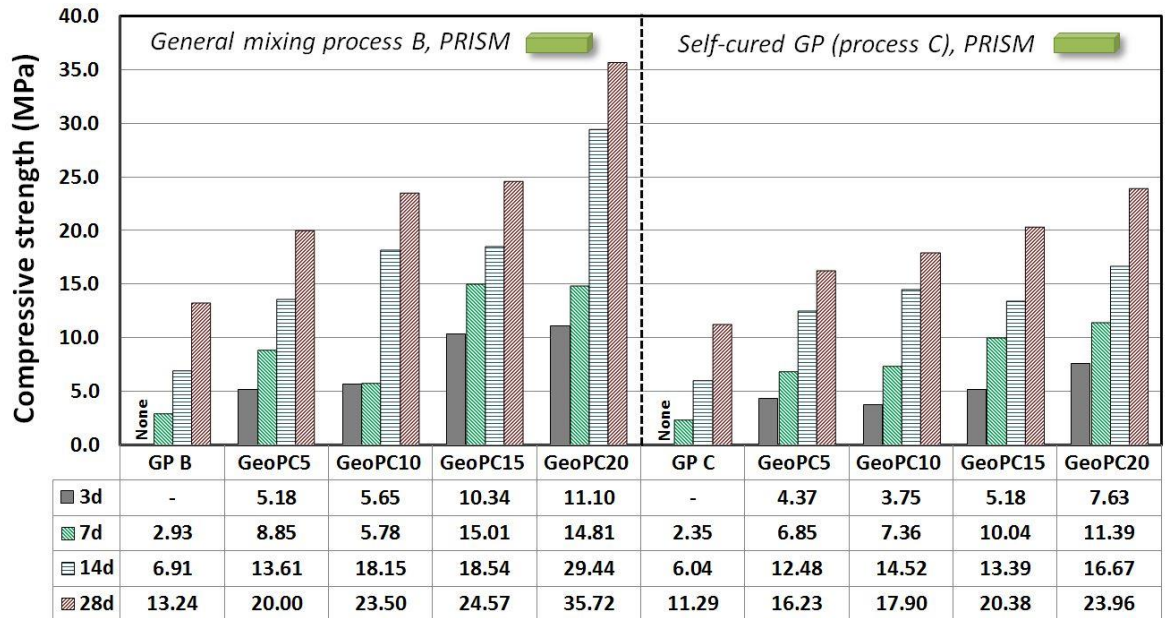


Figure 8.5 Compressive strength of prismatic samples synthesized with general process (B) and Self-cured process (C)

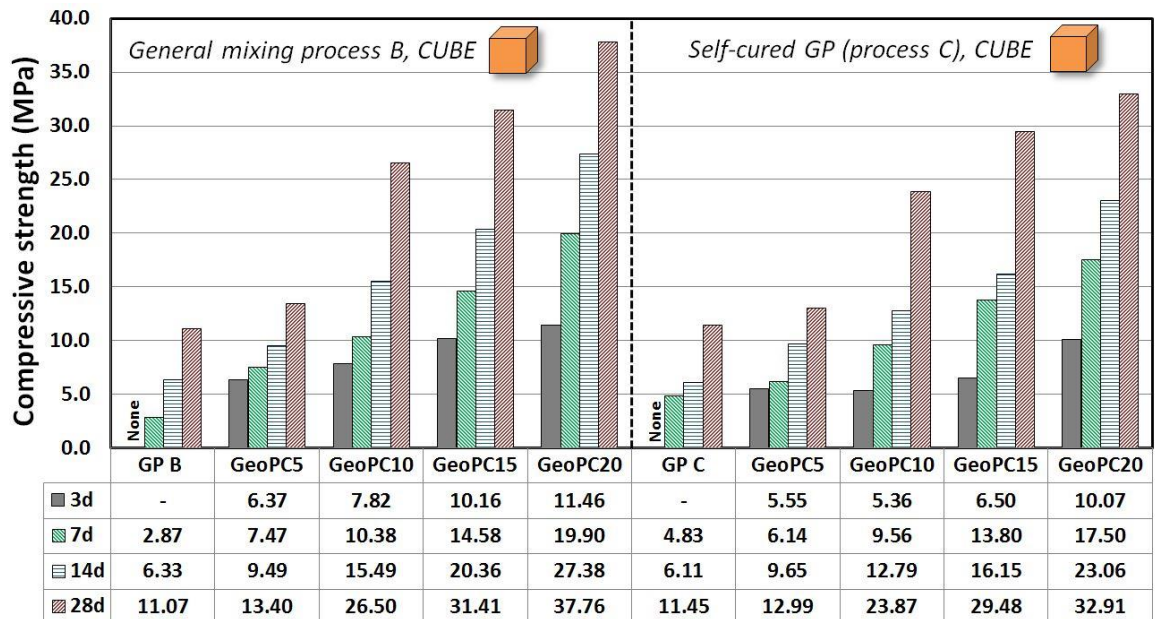


Figure 8.6 Compressive strength of cubic samples synthesized with general process (B) and Self-cured process (C)

It can be seen that the overall strength values of the GeoPC (B) mixtures were comparatively higher than that of the GeoPC (C) mixtures when the amount of OPC increased (from GeoPC5 to GeoPC20). This may be not only due to the effects from incomplete reaction and excess water left in the mixture that cause weakness in GeoPC (C), but also the rapid loss of alternative self-generated heat by solid alkaline-exothermic reaction which could scarcely be kept inside small size specimens, prisms.

The strength of cubic samples shown in Figure 8.6 is for general mixing process B (left) and Self-cured GP process C (right). Even though the larger size of cubic specimens may be able to maintain heat accumulated longer inside the samples and provide some advantages for curing regime than the smaller prisms, GeoPC (C) mixtures still gained lower strength than that of GeoPC (B) mixtures in all cases.

However, a distinctive point can be comparatively observed when the compressive strength was plotted in line charts of prism and cube (Figure 8.7). The gap of strength lines between process B and C of the cubic samples (Figure 8.7(b)) became narrower at both 3-day and 28-day ages when compared with the prismatic samples (Figure 8.7(a)). The same behaviour in GP (Figure 8.3(d)) was also observed as large size specimens (cubes) may achieve a greater heat curing environment than the small size specimens (prisms). In addition, as alternative extra heat was obtained from dry-mixing process (C), the strength improvement at both early and later ages was therefore remarkably achieved.

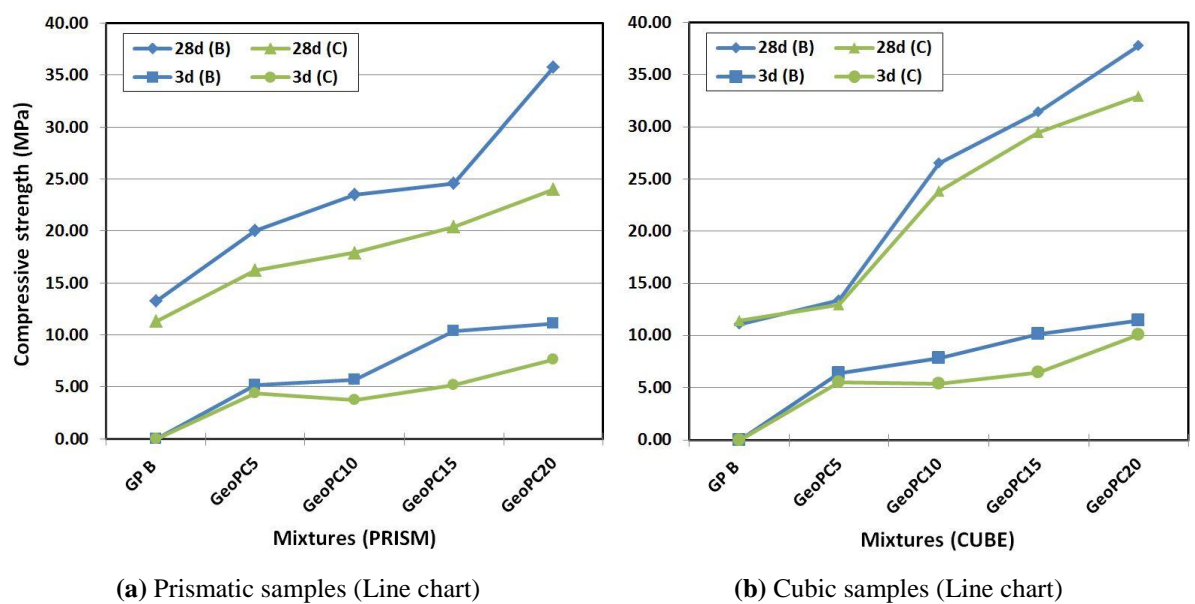


Figure 8.7 Compressive strength of GP in different manufacturing processes

The strength of the prismatic and cubic samples, which were manufactured with general mixing process (B) and Self-cured process (C), was plotted at the testing ages of 3 days

and 28 days. The best-fit lines of strength at 3-day age of process B and C (Figure 8.8) are drawn above equality line, meaning the cube strength is higher than prism strength in both cases. It can be seen that the best-fit line of process C is not only laid over process B, but also obtains greater slope of 1.48 against 0.90 (of process B). By this relationship, it can be interpreted, for the cubic specimens, that Self-cured process (C) achieved higher strength than general process (B). Moreover, the trend shows greater differences in the compressive values when GeoPC of higher strength grade (more OPC inclusion in the GeoPC system) is tested.

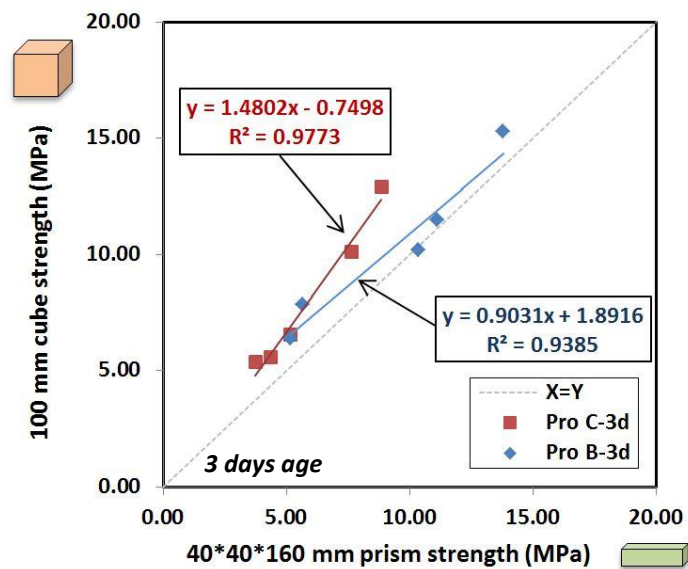


Figure 8.8 Relationship between average 3-day strength of 100 mm cubes and 40mm x 40mm x 160mm prisms for processes B and C

For the GeoPC at the 28-day age (Figure 8.9), the best-fit lines of processes B and C indicate that prism strength is slightly higher than that of corresponding low cube strengths of approximately 20 MPa (process B) and 10 MPa (process C) respectively. At the values about 23 MPa (process B) and 13 MPa (process C), the strengths of prisms and cubes become identical. Thereafter, the cubic specimens exhibit higher compressive strength than the prismatic specimens. In addition, like the results at 3 days, the best-fit line of process C is stacked over process B and obtains greater slope of 1.78 against 1.24 (of process B). An extra heat released from dry-mixing process could provide more appropriate curing regime together with longer heat maintaining inside larger specimens size, *cubes*.

Based on the relationship determined by linear regression analysis at the 28-day age (Figure 8.9), the empirical formula for cube strength of GeoPC system in both processes can be obtained as follows:

- For General mixing process (B):

$$(\sigma_{cu})_{100\text{mm}} = 1.2468(\sigma_{pr})_{40*40*160\text{mm}} - 5.3472 \quad (8.1)$$

- For Pre-dry mixing process (C):

$$(\sigma_{cu})_{100\text{mm}} = 1.7872(\sigma_{pr})_{40*40*160\text{mm}} - 10.216 \quad (8.2)$$

where σ_{cu} and σ_{pr} are the cube and prism strengths in MPa respectively. The coefficient of correlation (R-values) for those best-fit lines is close to each other, equal to approximately 0.88.

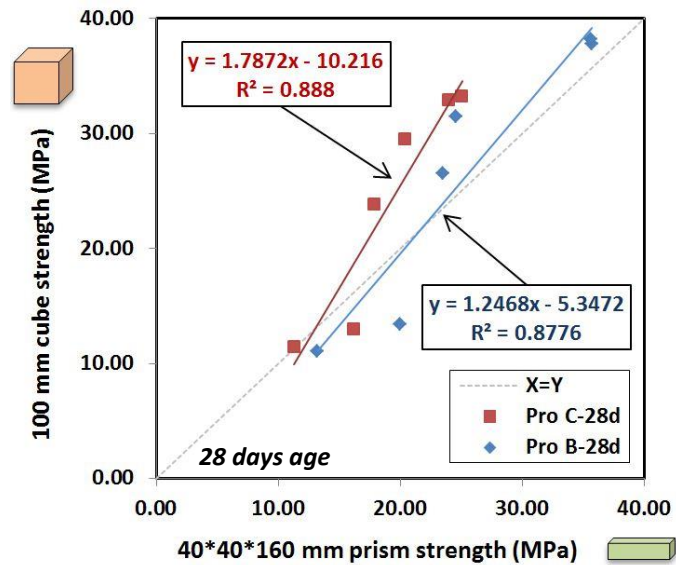


Figure 8.9 Relationship between average 28-day strength of 100 mm cubes and 40mm x 40mm x 160mm prisms for processes B and C

According to all relationships between the cube and prism strengths throughout the scenarios considered in this study, it can be seen that GP in pre-dry mixing process (C) produced with large size 100 mm cubes could clearly provide better compressive strength than small prisms. It may be due to an extra heat accumulation which can be kept longer inside the larger sample (Nath & Sarker, 2012; Vaidya, et al., 2011). The similar results were also observed in GeoPC mixture as not only extra heat is obtained from dry-mixing and larger specimen size which enhance its curing environment, but also some alternative heat liberation came from the hydration of the included OPC. The final results are closely related to the study of using dry-mixing method (Suwan & Fan, 2014) and producing large volume of concrete casting (Taylor, 1992). With most of cementitious materials could serve as effective thermal mass (*Thermal mass* - heat storage capacity of a material, the ability to provide inertia against temperature variations) (Dodoo, et al., 2012), this advantage could therefore promote curing regime for those of GP and Self-cured GP. Beyond the strength obtained by chemical reaction, the heat is a vital factor positively

affecting the strength. The internal heat generated from process C and massive volume of paste with good protection in thermal loss and moisture loss could enhance the rate of structural formation and strengthen the binder matrices.

8.4 Remark

1) For the geopolymer cement, the strength of prisms manufactured in general mixing process (B) was greater than that of cubes (prism > cube), while on the contrary, the strength of cubes was greater than prisms (cube > prism) in pre-dry mixing process (C). By contrast, for GeoPC mixtures, most of the cube strengths trend to be greater than those of prisms strengths (cube > prism) in both general mixing process (B) and Self-cured geopolymers (process C).

2) The improvement in mechanical strength for (i) Geopolymer cement and (ii) GeoPC system could be achieved. The alternative extra heat (from dry mixing process (C) and/or OPC hydration) which was kept in larger specimen (100 mm cubes) could provide more suitable conditions for curing purpose. Whist in Self-cured geopolymer cement (Pre-dry mixing of GeoPC system), the strength increased not only due to extra internal heat itself but also the rapid formation of (C,N)-A-S-H, providing an early strength development of the samples.

3) Overall, it could be concluded that larger specimen size of geopolymers and GeoPC mixtures would obtain higher internal heat accumulation, leading to greater strength. More enhancements could be also achieved by optimizing the water content, increasing fineness of materials as well as providing heat loss and moisture loss protections.

PART 4
FINAL APPRAISAL OF THE RESEARCH WORK

CHAPTER 9 CONCLUSIONS AND FUTURE RESEARCH

9.1 Summary

This thesis comprises of four parts: The first part “Introduction, Literature Review and Methodology” consists of introduction (Chapter 1), literatures review (Chapter 2), and materials and test methods (Chapter 3). The second part “Curing Processes and Properties of Geopolymers” is committed to examine the curing mechanisms and properties of geopolymers through the designated experimental works of various manufacturing procedures (Chapter 4), inclusion of OPC to GP (known as GeoPC system, Chapter 5), and curing at various temperatures (Chapter 6). The significant contributions of those two parts lead to Part 3 “Production of Self-cured Geopolymer Cement”, including Chapter 7 and Chapter 8. The final part “Final Appraisal of the Research Work” in Chapter 9 provides exclusive conclusions of this study, including future research and recommendations.

The fundamentals of geopolymers and geopolymerization, in the first part, have been intensively discussed together with important factors, which could affect the curing, structure and characteristics of geopolymers. It was found that coal-fired fly ash seems to be the most appropriate raw prime material due to its physical characteristics (small and spherical shape), its chemical characteristics (rich in Si and Al) and its eco-friendly origin (by-product). Sodium hydroxide solution, SH (15M), and sodium silicate solution, SS (48.20 %w/w), were identified as activators for this research work with SS/SH ratio and A/FA ratio of 1.50 and 0.40 respectively. Curing regimes stimulate the formation of geopolymeric gel, however, the appropriate temperature and duration (40 to 90°C, 6 to 48 hours) could lead to the improved results for geopolymer synthesis. To widen its applications and being more convenient in practical works with reasonable performance, many attempts have been carried out on the fly ash-based geopolymers to develop suitable curing process at ambient temperature. In this study, three distinct approaches, namely pre-dry mixing method and alternative heat source and calcium content in GP mixture have been complied to develop the conceptual framework of the Self-cured geopolymers.

For the investigation on curing mechanisms and their relationship with the properties of geopolymers, it was found that manufacturing procedures significantly affected the properties of geopolymers cured at room temperature. The widely used manufacturing processes of geopolymer cement (Separate mixing process (A) and General mixing process (B)) gave rise to higher strength than the purposed dry mixing process (C) because the fully dissolved alkaline activators were used. However, the pre-dry mixing process (C)

provided high potential heat liberation, which would be beneficial and facilitate the production of Self-cured geopolymers. The inclusion of OPC in GP mixture (GeoPC system) mainly quickly reacted with alkaline solutions and formed the additional compounds of C-(A)-S-H and N-A-S-H, resulting in good early strength to the systems. Alternative extra heat liberation from OPC-hydration was also observed in the mixtures depending on the dosage of OPC replacement. GeoPC system therefore had a better strength than that of typical GP at ambient curing temperature due to the presence of OPC. Moreover, at various curing temperatures, the strength of GeoPC system (represented by GeoPC30 in this study) increased when the curing temperature increased due probably to stronger and longer chain of Si-O-Al bonding, even though the GP was the main constituent of the mixture. The optimum curing condition would only be in the range of mild curing temperatures 30 to 40°C.

The above developments were therefore applied for the production of Self-cured geopolymers by merging advantages of pre-dry mixing process with the inclusion of OPC in the mixture as a new scenario, Self-cured geopolymers. The self-cured geopolymers could provide more convenience in practical work as conventional OPC by eliminating the difficulties of highly viscous and corrosive alkaline solutions. The internal heat itself increased the ability to work at ambient temperature as well as the early strength development by OPC content. The advantages of Self-cured geopolymers resulted from pre-dry mixing process and GeoPC system are summarised in Table 9.1.

Table 9.1 Summary diagram of the advantages of Self-cured geopolymer cement

Pre-dry mixing process	GeoPC system	Self-cured GP
1. Intensive heat liberation	1. Alternative heat liberation from OPC hydration	➡ Extra heat for curing purpose
2. Ability in practical work	2. -	➡ In-field applications
3. Economical saving from using solid activators	3. -	➡ Economical saving
4. -	4. Early strength improvement by (C,N)-A-S-H formation	➡ Gain strength in room temperature
5. -	5. Energy saving from oven-free	➡ Energy saving

In addition, with the production of larger specimens or components, the Self-cured geopolymers could obtain both higher and longer internal heat accumulation, leading to an improvement in curing mechanisms and mechanical strength. Its advantages lie in not only an increase in commercial viability and practical work but also an expanding to other

applications e.g. infrastructural applications, bio-based composite geopolymers, light weight cement or aggregate, etc. However, it must be noted that the limitation may be addressed regarding the standards and handling.

9.2 Conclusions

1) Portland cement is known as a large greenhouse gas contributor as well as energy-intensive manufacturer. The alternative low-carbon cementitious binders have been, therefore, extensively studied to reduce OPC production, and one among those alternative binders is “Geopolymer cement”. The fundamentals of geopolymer cement have been compiled together with most important factors affecting its properties and characteristics, i.e. main binder constituents, alkaline activators and binder concentration, and the curing procedures. From the literature review, coal-fired fly ash seems to be the most studied raw material due to its physical characteristics (small and spherical shape), chemical characteristics (rich in Si and Al) and eco-friendly origin, while the widely used alkaline activators in geopolymer synthesis are the sodium hydroxide solution and sodium silicate solution.

To widen the applications of geopolymer cement and make it more convenient in practical work with good engineering properties, the comprehensive experimental work of the Self-cured geopolymer cement has been programmed and set up through each work package. The research methods included both relevant standards and in-house designed methodologies for investigations from sampling, fabrication, characterisation to mechanisms and performance in various circumstances. Raw materials were characterised in both physical appearance (particle size analysis) and chemical composition (EDXA). Mechanical properties of the resulted products were investigated by the testing of setting time, compressive strength and internal heat measurement while their mechanisms were examined by using XRD, FTIR and SEM-EDXA.

2) Many previous studies confirmed that the strength of geopolymers can be improved at high curing temperature. At ambient temperature, the degree of geopolymerization underwent a very slow rate and the setting time cannot be measured within the first 3 days. The compressive strength of all pastes at 28-day age was quite low, however, processes A and B led to higher strength than that of dry-mixing process (C) due to the fact that the fully dissolved alkaline activators were used in the synthesis. Nevertheless, pre-dry mixing process obviously provided efficient heat liberation during its mixing process, which caused more rapid paste setting and offered more beneficial heat curing condition. As pre-

dry mixing process requires more water than that of typical processes, slightly higher water-to-solid (w/s) ratio was therefore used to benefit not only its mechanical performances but also its workability. With more practicability in field application, by just adding water, this pre-dry mixing process (C) would facilitate the self-curing processes of geopolymer production at ambient curing temperature.

3) The ability of Self-cured geopolymer cement curing under ambient conditions by using OPC as additive called “GeoPC system” was intensively investigated to explain its behaviours and performances as a construction material. The GeoPC system was mainly focused on the influence of OPC inclusion (from 10% to 90%) on the properties and mechanisms of final products. It was found that the reaction of fly ash-based geopolymer constituents (FA+SS, FA+SH and FA+SS+SH) underwent a very slow rate at room temperature, leading to low mechanical performances of the final products. Whereas, the reaction of OPC-based constituents (OPC+SS, OPC+SH, OPC+SS+SH) underwent a very quick rate at room temperature due to an extra precipitation of calcium compounds in high alkalinity environment. The main findings of the study on functionalities of geopolymer constituents are that the sodium hydroxide solution (NaOH) influences the dissolution of the mixtures by its strong alkalinity OH^- , while sodium silicate solution (Na_2SiO_3) is a source of extra Si and also influences both solidification and binding behaviour of the mixtures.

Calcium source in OPC mainly quickly reacted with alkaline solutions and formed the additional compounds of C-(A)-S-H and N-A-S-H, providing good early strength development to the systems. The setting time of GeoPC system was therefore shortened by this extra precipitation of Ca and alkaline reaction. In GeoPC system, more compact structure and higher compressive strength were achieved with the increase in the amount of OPC replacement by the additional coexistence formation of those C-(A)-S-H and N-A-S-H gels in the single binder. Internal heat liberation inside the samples was induced by the amount of OPC addition in the mixtures. The heat emitted in this study may be different from the heat of normal OPC-hydration as the alkaline solutions were used, indicated by the time of the maximum measured temperature e.g. within 2 hours for OPC with alkaline (OPC+SH, OPC+SS and OPC+SH+SS) and over 9 hours for normal hydrated OPC. This extra heat liberation was obtained by either of or both OPC-hydration and the reaction of OPC and alkaline activators. The geopolymerization of those mixtures cured at ambient temperature could be promoted, enhancing the mechanisms and mechanical properties. The enhancement in mechanical properties of suitable GeoPC mixtures, together with

alternative heat supplies from pre-dry mixing process (C) and OPC-hydration in GeoPC combinations could provide sufficient heat for the curing regime of GP. Furthermore, GeoPC system also offered the advantages in setting behaviour and early strength development, indicating the potential development of Self-cured geopolymers for on-site applications. It is found that the optimum amount of OPC addition to GeoPC mixtures in this study would be in range of GeoPC5 to GeoPC30, which could achieve in both reasonable strength and economical saving.

4) The micro-mechanisms and mechanical properties of Geopolymer-Portland cementitious (GeoPC) system were studied at various curing temperatures. GeoPC30 mixture was used to represent the GeoPC system due to its reasonable combinations in mechanical performances, economical saving, as well as being more environmental friendly. It was found that high curing (above room) temperature improved the early strength of OPC due to the acceleration in OPC-hydration. However, in the later age, the strength significantly decreased as an adverse effect of excessive moisture evaporation was obtained, causing larger porosity and uncompleted-formation in the structures as well as the appearance of micro-cracking caused by the thermal stress. Apart from that, the strength of low calcium fly ash-based geopolymers was found to be very low at ambient curing temperature, but dramatically increased at higher curing temperature (e.g. over 40°C) for both early and later ages as high curing temperature gave a rise and accelerated the geopolymerization in the matrices.

The GeoPC system achieved a better strength than that of typical geopolymers at ambient curing temperature due to the presence of OPC, forming mixed amorphous geopolymeric gel and (C,N)-A-S-H phases. As geopolymers is the main constituent in GeoPC mixture, the strength therefore increased when the curing temperature increased by the stronger and longer chain of (Ca)-Al-O-Si bonding. The microstructures and mechanisms of GeoPC were also improved for high temperature curing. The optimum curing temperature of GeoPC mixture was observed to be in the range of mild curing (30 to 40°C), which would probably be achieved by an alternative extra heat emitted from OPC-hydration or from hot environment throughout summer time or even in tropical climate areas. At ambient curing temperature, an alternative extra heat emitted from OPC-hydration (which depends on the concentration of OPC inclusion) may support the curing regimes and could be sufficient for the proper curing conditions of GeoPC system.

5) The advantages of pre-dry mixing method and GeoPC system have been taken and combined as a new scenario, called *Self-cured geopolymer cement*. The Self-cured geopolymers were set up together with the GeoPC mixtures manufactured in typical (general) process B for comparison. More moisture content than that of general process (B) was left in the mixture of Self-cured geopolymer process, which was probably due to an incomplete reaction with solid particles of the main constituents. In addition, in general process (B), more compact and denser microstructures were clearly observed by SEM, which led to the slight higher in strength when compared with Self-cured process. Although high strength was achieved by general process (B) as fully dissolved alkaline solutions were used, the strength of Self-cured geopolymer cement could be improved by the use of finer solid particles and prolong curing period. Moreover, the internal heat liberation of Self-cured geopolymer cement was obviously higher than that of general process (B) and could give higher degree of geopolymerization at mild to high curing temperature.

The success of the synthesis of Self-cured geopolymers could facilitate its application in practical work as conventional OPC by eliminating the difficulties of highly viscous and corrosive alkaline solutions. The internal heat itself, with appropriate heat loss protection, increases the ability to work at ambient temperature as well as to obtain the early strength development by OPC content. Furthermore, an increase in commercial availability and economical saving could also be achieved by using solid activators when compared to the use of highly cost alkaline solutions.

6) The study on the effect of specimen size was extendedly explored by the comparison of small specimens (40mm x 40mm x 160mm prisms) to large specimens (100 mm cubes). The improvement in mechanical strength for (i) Geopolymer cement and (ii) GeoPC system could be achieved by the alternative extra heat (from dry mixing process (C) and/or OPC hydration) which was kept in larger specimen (100 mm cubes), providing more suitable conditions for curing purpose. Whist in Self-cured geopolymer cement (Pre-dry mixing of GeoPC system), the strength increased not only due to extra internal heat itself but also the rapid formation of (C,N)-A-S-H, providing an early strength development of the samples. It could be concluded that larger specimen size of geopolymers and GeoPC mixtures would obtain higher internal heat accumulation, leading to greater strength. More enhancements could be also achieved by optimizing the water content, increasing fineness of materials as well as providing heat loss and moisture loss protections. The development of Self-cured geopolymer cement could provide convenience to on-site practice as

conventional OPC by eliminating the difficulties of highly viscous and corrosive alkaline solutions. The internal heat itself increases the ability to work at ambient temperature as well as the early strength. Furthermore, an increase in commercial availability and economical saving could also be achieved by using solid activators when compared to the use of highly costly alkaline solutions.

9.3 Future Research and Recommendation

The findings of this research provide an alternative approach for producing Self-cured geopolymer cement. Beyond the designated experimental programme, some further developments may be carried out, and they are:

- 1) Water-to-solid ratio: Self-cured geopolymers requires extra water not only for dissolution purpose but also to compensate quick-evaporated water from its self-generated heat. To achieve maximum strength, the optimum water-to-solid ratio could be extendedly studied for other cases of the Self-cured geopolymers.
- 2) Concentration of alkaline activators: The dosage of alkaline activators used in this study was based on recent geopolymer literatures. With different scenarios of GeoPC system as well as Self-cured geopolymers, optimum alkaline concentration might be investigated as Self-cured geopolymers improves different reactions to normal OPC and GP.
- 3) Fineness of raw materials: Smaller particle and higher surface area increase the level of both physical and chemical reactions of geopolymerization, such as dissolution rate, ions transportation, forming alumina-silicate species, etc. The synthesis of Self-cured geopolymers with high fineness materials could enhance the setting time, geopolymeric gel phase and ability to achieve strength at room temperature. This should also be further investigated.
- 4) Heat and moisture loss protection: The protection of moisture loss is strongly recommended to the Self-cured geopolymers. Maintaining moisture could significantly maintain and improve curing regimes for the mixtures to achieve the designation properties of construction materials and applications.
- 5) Life Cycle Assessment (LCA): LCA of Self-cured geopolymers could be considered and studied in order to demonstrate its environmental benefits as sustainable alternative binding materials. In commercial practice, partially or fully replacement of OPC clinker

with geopolymer cement could be addressed to reduce the amount of OPC consumption which is more costly and causes high CO₂ emission.

BIBLIOGRAPHY

- ACAA, T. A. C. A. A., 2014. *Coal Combustion Products Production & Use Statistics*. [Online]
Available at: <https://www.acaa-usa.org/Publications/Production-Use-Reports>
[Accessed 23 August 2015].
- Ahmari, S., Ren, X., Toufigh, V. & Zhang, L., 2012. Production of geopolymeric binder from blended waste concrete powder and fly ash. *Construction and Building Materials*, 35, 718-729.
- Ahmari, S. & Zhang, L., 2012. Production of eco-friendly bricks from copper mine tailings through geopolymerization. *Construction and Building Materials*, 29, 323-331.
- Ahmari, S. & Zhang, L., 2013. Utilization of cement kiln dust (CKD) to enhance mine tailings-based geopolymer bricks. *Construction and Building Materials*, 40, 1002-1011.
- Al Bakri, A., Mohammed, H., Kamarudin, H., Niza, I.K. & Zarina, Y., 2011a. Review on fly ash-based geopolymer concrete without Portland Cement. *Journal of Engineering and Technology Research*, 3(1), 1-4.
- Al Bakri, A., Kamarudin, H., Binhussain, M., Niza, I.K., Zarina, Y. & Rafiza, A.R., 2011b. The effect of curing temperature on physical and chemical properties of geopolymers. *Physics Procedia*, 22, 286-291.
- Al Bakri, A., Rafiza, A.R., Hardjito, D., Kamarudin, H. & Niza, I.K., 2012. Characterization of LUSI mud volcano as geopolymer raw material. *Advanced Materials Research*, 548, 82-86.
- Al-Amoudi, O., Almusallam, A., Khan, M. & Maslehuddin, M., 1995. Effect of hot weather on compressive strength of plain and blended cement mortars. *Proceedings of the 4th Saudi Engineering Conference, King Abdulaziz University Jeddah, 1995*. Jeddah, Saudi Arabia, King Abdulaziz University, 193-199.
- Alamri, A., 1988. *Influence of Curing on the Properties of Concretes and Mortars in Hot Climates*. Leeds: University of Leeds.
- Aleem, M. & Arumairaj, P., 2012. Geopolymer concrete-A review. *International Journal of Engineering Sciences & Emerging Technologies*, 1(2), 118-122.
- Allahverdi, A., Mehrpour, K. & Kani, E., 2008. Taftan pozzolan-based geopolymer cement. *IUST International Journal of Engineering Science*, 19(3), 1-5.
- Alonso, S. & Palomo, A., 2001. Alkaline activation of metakaolin and calcium hydroxide mixtures: influence of temperature, activator concentration and solids ratio. *Materials Letters*, 47(1), 55-62.
- Alonso, S. Palomo, A., Bakharev, T., Sanjayan, J.G., Cheng, Y.B., Brooke, N., Megget, L., Ingham, J. & Davidovits, J., 2011. *Geopolymer Chemistry and Applications*. 3rd ed. Saint-Quentin, France: Institut Géopolymère.

Altan, E. & Erdoğan, S., 2012. Alkali activation of a slag at ambient and elevated temperatures. *Cement and Concrete Composites*, 34(2), 131-139.

American Concrete Institute. ACI 318-11: 2011. Building code requirements for structural concrete and commentary. 2011. ACI standards Online.

Andini, S., Cioffi, R., Colangelo, F., Grieco, T., Montagnaro, F. & Santoro, L., 2008. Coal fly ash as raw material for the manufacture of geopolymer-based products. *Waste Management*, 28(2), 416-423.

Anuar, K., Ridzuan, A. & Ismail, S., 2011. Strength characteristics of geopolymer concrete containing recycled concrete aggregate. *International Journal of Civil and Environmental Engineering*, 11(1), 59-62.

ASTM International. ASTM C125-15B: 2015. Standard terminology relating to concrete and concrete aggregates. 2015. ASTM Standards Online.

ASTM International. ASTM C150/C150M-16: 2016. Standard specification for Portland cement. 2016. ASTM Standards Online.

ASTM International. ASTM C618-15: 2015. Standard specification for coal fly ash and raw or calcined natural pozzolan for use in concrete. 2015. ASTM Standards Online.

Australia Standard. AS 3600-2009: 2009. Concrete structures. 2009. Australia Standards Online.

Bakharev, T., 2005a. Durability of geopolymer materials in sodium and magnesium sulfate solutions. *Cement and Concrete Research*, 35(6), 1233-1246.

Bakharev, T., 2005b. Geopolymeric materials prepared using class F fly ash and elevated temperature curing. *Cement and Concrete Research*, 35(6), 1224-1232.

Bakharev, T., 2006. Thermal behaviour of geopolymers prepared using class F fly ash and elevated temperature curing. *Cement and Concrete Research*, 36(6), 1134-1147.

Barbosa, V., Mackenzie, K. & Thaumaturgo, C., 1999. Synthesis and characterisation of sodium polysialate inorganic polymer based on alumina and silica. *Geopolymer '99 International Conference, 30 June to 2 July 1999*. Saint-Quentin, Geopolymer Institute.

Barnes, P., 1983. *Structure and Performance of Cements*. Great Yarmouth, GB: Applied Science Publishers Ltd.

Bogue, R., 1955. The chemistry of Portland cement. *Soil Science*, 79(4), 322.

British Standard Institution (BSI). BS 8443:2005. Specification for establishing the suitability of special purpose concrete admixtures. 2005. British Standards Online.

British Standard Institution (BSI). BS EN 196-1:2016. Methods of testing cement Part 1: Determination of strength. 2016. British Standards Online.

British Standard Institution (BSI). BS EN 196-3:2005+A1:2008. Methods of testing cement. Determination of setting times and soundness. 2005. British Standards Online.

British Standard Institution (BSI). BS EN 197-1:2011. Cement, composition, specifications and conformity criteria for common cements. 2011. British Standards Online.

British Standard Institution (BSI). BS EN 450-1:2012. Fly ash for concrete. Definition, specifications and conformity criteria. 2012. British Standards Online.

British Standard Institution (BSI). BS EN 12390-1:2012. Testing hardened concrete. Shape, dimensions and other requirements for specimens and moulds. 2012. British Standards Online.

British Standard Institution (BSI). BS EN 12390-3:2009. Testing hardened concrete. Compressive strength of test specimens. British Standards Online.

Buchwald, A., Dombrowski, K. & Weil, M., 2005. The influence of calcium content on the performance of geopolymetric binder especially the resistance against acids. *Proceedings of the World Geopolymer*, 35-39.

Burciaga-Díaz, O. & Escalante-García, J., 2012. Strength and durability in acid media of alkali silicate-activated metakaolin geopolymers. *Journal of the American Ceramic Society*, 95(7), 2307-2313.

Bushlaibi, A. & Alshamsi, A., 2002. Efficiency of curing on partially exposed high-strength concrete in hot climate. *Cement and Concrete Research*, 32(6), 949-953.

Bye, G., 1983. *Portland Cement Composition, Production and Properties*. Stoke on Trent (UK): Institute of Ceramics.

Cao, D., Selic, E. & Herbell, J., 2008. Utilization of fly ash from coal-fired power plants in China. *Journal of Zhejiang University Science A*, 9(5), 681-687.

Chatveera, B. & Makul, N., 2012. Properties of geopolymer mortar produced from fly ash and rice husk ash: Influences of fly ash-rice husk ash ratio and Na_2SiO_3 -NaOH ratio under curing by microwave energy. *KMUTT Research & Development Journal*, 35(3), 299-309.

Chindaprasirt, P., Chareerat, T., Hatanaka, S. & Cao, T., 2010. High-strength geopolymer using fine high-calcium fly ash. *Journal of Materials in Civil Engineering*, 23(3), 264-270.

Chindaprasirt, P., Chareerat, T. & Sirivivatnanon, V., 2007. Workability and strength of coarse high calcium fly ash geopolymer. *Cement and Concrete Composites*, 29(3), 224-229.

- Chithra, S. & Dhinakaran, G., 2014. Effect of hot water curing and hot air oven curing on admixed concrete. *International Journal of ChemTech Research CODEN (USA): IJCRGG*, 1516-1523.
- ClimateTechWiki, 2016. *Energy Efficiency and Saving in the Cement Industry*. [Online] Available at: <http://www.climatetechwiki.org/technology/energy-saving-cement> [Accessed 5 February 2016].
- Davidovits, J., 1991. Geopolymers: inorganic polymeric new materials. *Journal of Thermal Analysis*, 37(8), 1633-1656.
- Davidovits, J., 2002. 30 years of successes and failures in geopolymer applications: Market trends and potential breakthroughs. *Geopolymer 2002 3rd International Conference, Melbourne Australia, 28 to 29 October 2002*. Melbourne, Australia, Geopolymer Institute .
- Davidovits, J., 2005. *Geopolymer, Green Chemistry and Sustainable Development Solutions*. Saint-Quentin, France: Geopolymer Institute.
- Davidovits, J., 2011. *Geopolymer Chemistry and Applications*. 3rd ed. Saint-Quentin, France: Institut Géopolymère.
- Davidovits, J., 2014. 'World first' production run: 2,500 tonnes of geopolymer. [Online] Available at: <http://www.geopolymer.org/news/world-first-production-run-2500-tonnes-of-geopolymer/> [Accessed 9 February 2016].
- Deevasan, K. & Ranganath, R., 2010. Geopolymer concrete using industrial byproducts. *Proceedings of the Institution of Civil Engineers-Construction Materials*, 164(1), 43-50.
- Del Viso, J., Carmona, J. & Ruiz, G., 2008. Shape and size effects on the compressive strength of high-strength concrete. *Cement and Concrete Research*, 38(3), 386-395.
- Demie, S., Nuruddin, M., Ahmed, M. & Shafiq, N., 2011. Effects of curing temperature and superplasticizer on workability and compressive strength of self-compacting geopolymer concrete. *National Postgraduate Conference (NPC), 19 to 20 September 2011*. Tronoh Perak, Malaysia, IEEE, 1-5.
- Dimas, D., Giannopoulou, I. & Panias, D., 2009. Polymerization in sodium silicate solutions: a fundamental process in geopolymerization technology. *Journal of Materials Science*, 44(14), 3719-3730.
- Dodoo, A., Gustavsson, L. & Sathre, R., 2012. Effect of thermal mass on life cycle primary energy balances of a concrete-and a wood-frame building. *Applied Energy*, 92, 462-472.
- Dutta, D., Chakrabarty, S., Bose, C. & Ghosh, S., 2012. Evaluation of geopolymer properties with temperature imposed on activator prior mixing with fly ash. *International Journal of Civil and Structural Engineering*, 3(1), 205-213.
- Dutta, D., Thokchom, S., Ghosh, P. & Ghosh, S., 2010. Effect of silica fume additions on porosity of fly ash geopolymers. *Journal of Engineering and Applied Sciences*, 5(10), 74-79.

- Duxson, P., Fernández-Jiménez, A., Provis, J.L., Lukey, G.C., Palomo, A. & Van Deventer. J.S.J., 2007a. Geopolymer technology: The current state of the art. *Journal of Materials Science*, 42(9), 2917-2933.
- Duxson, P., Lukey, G. & Van Deventer, J., 2007b. Physical evolution of Na-geopolymer derived from metakaolin up to 1000 C. *Journal of Materials Science*, 42(9), 3044-3054.
- Duxson, P., Mallicoat, S.W., Lukey, G.C., Kriven, W.M. & Van Deventer. J.S.J., 2007c. The effect of alkali and Si/Al ratio on the development of mechanical properties of metakaolin-based geopolymers. *Colloids and Surfaces A: Physicochemical and Engineering Aspects*, 292(1), 8-20.
- Duxson, P. & Provis, J., 2008. Designing precursors for geopolymer cements. *Journal of the American Ceramic Society*, 91(12), 3864-3869.
- Ezziane, K. et al., 2007. Compressive strength of mortar containing natural pozzolan under various curing temperature. *Cement and Concrete Composites*, 29(8), 587-593.
- Feng, D., Provis, J. & Deventer, J., 2012. Thermal activation of albite for the synthesis of One-part mix geopolymers. *Journal of the American Ceramic Society*, 95(2), 565-572.
- Fernández-Jiménez, A., Garcia-Lodeiro, I. & Palomo, A., 2007. Durability of alkali-activated fly ash cementitious materials. *Journal of Materials Science*, 42(9), 3055-3065.
- Fernández-Jiménez, A. & Palomo, A., 2005. Composition and microstructure of alkali activated fly ash binder: effect of the activator. *Cement and Concrete Research*, 35(10), 1984-1992.
- Garcia-Lodeiro, I., Palomo, A., Fernández-Jiménez, A. & Macphee, D., 2011. Compatibility studies between NASH and CASH gels: Study in the ternary diagram $\text{Na}_2\text{O}-\text{CaO}-\text{Al}_2\text{O}_3-\text{SiO}_2-\text{H}_2\text{O}$. *Cement and Concrete Research*, 41(9), 923-931.
- Gilbert, R., 2002. Creep and shrinkage models for high strength concrete-proposals for inclusion in AS3600. *Australian Journal of Structural Engineering*, 4(2), 95-106.
- Glukhovskiy, V., 1967. *Soil Silicate Articles and Structures*. Kiev, Ukrain: Budivelnyk Publisher.
- Guo, X. & Shi, H., 2012. Self-solidification/stabilization of heavy metal wastes of class C fly ash-based geopolymers. *Journal of Materials in Civil Engineering*, 25(4), 491-496.
- Guo, X., Shi, H. & Dick, W., 2010. Compressive strength and microstructural characteristics of class C fly ash geopolymer. *Cement and Concrete Composites*, 32(2), 142-147.
- Halka, M. & Nordstrom, B., 2010. *Alkali and Alkaline Earth Metals*. NewYork: Infobase Publishing.

- Hanehara, S., Tomosawa, F., Kobayakawa, M. & Hwang, K., 2001. Effects of water/powder ratio, mixing ratio of fly ash, and curing temperature on pozzolanic reaction of fly ash in cement paste, *Cement and Concrete Research*, 31(1), 31-39.
- Hanjitsuwan, S., Hunpratub, S. Thongbai, P., Maensiri, S., Sata, V. & Chindaprasirt, P., 2014. Effects of NaOH concentrations on physical and electrical properties of high calcium fly ash geopolymer paste. *Cement and Concrete Composites*, 45, 9-14.
- Hansen, J., Kharecha, P., Sato, M., Masson-Delmotte, V., Ackerman, F., Beerling, D.J., Hearty, P.J., Hoegh-Guldberg, O., Hsu, S.L., Parmesan, C. & Rockstrom, J., 2013. Assessing “dangerous climate change”: required reduction of carbon emissions to protect young people, future generations and nature. *PloS One*, 8(12), e81648.
- Hardjito, D., Cheak, C. & Ing, C., 2008. Strength and setting times of low calcium fly ash-based geopolymer mortar. *Modern Applied Science*, 2(4), 3-11.
- Hardjito, D. & Fung, S., 2010. Fly ash-based geopolymer mortar incorporating bottom ash. *Modern Applied Science*, 4(1), 44-52.
- Hardjito, D., Wallah, S., Sumajouw, D. & Rangan, B., 2004. Factors influencing the compressive strength of fly ash-based geopolymer concrete. *Civil Engineering Dimension*, 6(2), 88-93.
- Hoeven, M.V.D., 2014. *Global Energy-Related Emissions of Carbon Dioxide Stalled in 2014*. [Online] Available at: <http://www.iea.org/newsroomandevents/news/2015/march/global-energy-related-emissions-of-carbon-dioxide-stalled-in-2014.html> [Accessed 6 February 2016].
- Hounsi, A., Lecomte-Nana, G., Djétéli, G. & Blanchart, P., 2013. Kaolin-based geopolymers: Effect of mechanical activation and curing process. *Construction and Building Materials*, 42, 105-113.
- Huntzinger, D. & Eatmon, T., 2009. A life-cycle assessment of Portland cement manufacturing: comparing the traditional process with alternative technologies. *Journal of Cleaner Production*, 17(7), 668-675.
- Hu, S., Wang, H., Zhang, G. & Ding, Q., 2008. Bonding and abrasion resistance of geopolymeric repair material made with steel slag. *Cement and Concrete Composites*, 30(3), 239-244.
- Iyer, R. & Scott, J., 2001. Power station fly ash-a review of value-added utilization outside of the construction industry. *Resources, Conservation and Recycling*, 31(3), 217-228.
- Jonathan, T., Ricketts, M., Loftin, K. & Frederick, S., 2003. *Standard Handbook for Civil Engineers*. 5th ed. NY, USA: The McGraw-Hill Companies.
- Kani, E., Allahverdi, A. & Provis, J., 2012. Efflorescence control in geopolymer binders based on natural pozzolan. *Cement and Concrete Composites*, 34(1), 25-33.

- Khale, D. & Chaudhary, R., 2007. Mechanism of geopolymerization and factors influencing its development: a review. *Journal of Materials Science*, 42(3), 729-746.
- Khater, H., 2011. Effect of calcium on geopolymerization of aluminosilicate wastes. *Journal of Materials in Civil Engineering*, 24(1), 92-101.
- Khater, H., 2012. Effect of cement kiln dust on geopolymer composition and its resistance to sulfate attack. *International Journal of Civil and Structural Engineering*, 2(3), 740.
- Kim, K., Jeon, S., Kim, J. & Yang, S., 2003. An experimental study on thermal conductivity of concrete. *Cement and Concrete Research*, 33(3), 363-371.
- Kobera, L., Slavík, R., Kolousek, D., Urbanová, M., Kotek, J. & Brus, J., 2011. Structural stability of aluminosilicate inorganic polymers: Influence of the preparation procedure. *Ceramics-Silikaty*, 55(4), 343-354.
- Koloušek, D., Brus, J., Urbanova, M., Andertova, J., Hulinsky, V. & Vorel, J., 2007. Preparation, structure and hydrothermal stability of alternative (sodium silicate-free) geopolymers. *Journal of Materials Science*, 42(22), 9267-9275.
- Komnitsas, K. & Zaharaki, D., 2007. Geopolymerisation: A review and prospects for the minerals industry. *Minerals Engineering*, 20(14), 1261-1277.
- Komnitsas, K., Zaharaki, D. & Perdikatsis, V., 2004. Geopolymerisation of low calcium ferronickel slags. *Journal of Materials Science*, 42(9), 3073-3082.
- Kong, D. & Sanjayan, J., 2010. Effect of elevated temperatures on geopolymer paste, mortar and concrete. *Cement and Concrete Research*, 40(2), 334-339.
- Kongkaew, B., 2007. *Sludge-Based Geopolymer*. Bangkok: Kasetsart University.
- Kumar, S. & Kumar, R., 2011. Mechanical activation of fly ash: Effect on reaction, structure and properties of resulting geopolymer. *Ceramics International*, 37(2), 533-541.
- Lam, L., Wong, Y. & Poon, C., 1998. Effect of fly ash and silica fume on compressive and fracture behaviors of concrete. *Cement and Concrete Research*, 28(2), 271-283.
- Lecomte, I., Henrist, C., Liegeois, M., Maseri, F., Rulmont, A. & Cloots, R., 2006. (Micro)-structural comparison between geopolymers, alkali-activated slag cement and Portland cement. *Journal of the European Ceramic Society*, 26(16), 3789-3797.
- Liew, Y., Kamarudin, H., Al Bakri, A.M., Luqman, M., Nizar, I.K., Ruzaidi, C.M. & Heah, C.Y., 2012. Processing and characterization of calcined kaolin cement powder. *Construction and Building Materials*, 30, 794-802.
- Lizcano, M., Gonzalez, A., Basu, S., Lozano, K. & Radovic, M., 2012. Effects of water content and chemical composition on structural properties of alkaline activated metakaolin-based geopolymers. *Journal of the American Ceramic Society*, 95(7), 2169-2177.
- MacGregor, J., 1997. *Reinforced Concrete Mechanics and Design*. 3rd ed. New Jersey: Prentice Hall.

- Maholtra, V., 2002. Introduction: sustainable development and concrete technology. *ACI Concrete International*, 24(7), 1-22.
- Mansur, M. & Islam, M., 2002. Interpretation of concrete strength for nonstandard specimens. *Journal of Materials in Civil Engineering*, 14(2), 151-155.
- Ma, Y., Hu, J. & Ye, G., 2012. The effect of activating solution on the mechanical strength, reaction rate, mineralogy, and microstructure of alkali-activated fly ash. *Journal of Materials Science*, 47(11), 4568-4578.
- McNaught, A., 2014. *IUPAC Compendium of Chemical Terminology: The Gold Book*. Version 2.3.3 ed. s.l.:International Union of Pure and Applied Chemistry.
- McNaught, A. & Wilkinson, A., 1997. *IUPAC. Compendium of Chemical Terminology*. Oxford: Blackwell Science.
- Mehta, P., 1986. *Concrete: Structure, Properties and Materials*. New Jersey: Prentice-Hall.
- Mehta, P., 2001. Reducing the environmental impact of concrete. *Concrete International*, 23(10), 61-66.
- Mehta, P. & Monteiro, P.J.M., 2006. *Concrete : Microstructure, Properties, and Materials*. 3rd ed. New York: McGraw-Hill.
- Memon, F., Nuruddin, M.F., Khan, S.H. & Shafiq, N.R., 2013. Effect of sodium hydroxide concentration on fresh properties and compressive strength of self-compacting geopolymer concrete. *Journal of Engineering Science and Technology*, 8(1), 44-56.
- Mishra, A., Choudhary, D., Jain, N., Kumar, M., Sharda, N. & Dutta, D., 2008. Effect of concentration of alkaline liquid and curing time on strength and water absorption of geopolymer concrete. *ARPN Journal of Engineering and Applied Sciences*, 3(1), 14-18.
- Moon, J., Bae, S., Celik, K., Yoon, S., Kim, K.H., Kim, K.S. & Monteiro, P.J., 2014. Characterization of natural pozzolan-based geopolymeric binders. *Cement and Concrete Composites*, 53, 97-104.
- Mostafa, N. & Brown, P., 2005. Heat of hydration of high reactive pozzolans in blended cements: Isothermal conduction calorimetry. *Thermochimica Acta*, 435(2), 162-167.
- Nath, P. & Sarker, P., 2012. Geopolymer concrete for ambient curing condition. *Australasian Structural Engineering Conference 2012: The past, present and future of Structural Engineering, 11 to 13 July 2012*. Perth, Western Australia, Engineers Australia.
- Nath, P. & Sarker, P., 2014. Effect of GGBFS on setting, workability and early strength properties of fly ash geopolymer concrete cured in ambient condition. *Construction and Building Materials*, 66, 163-171.

- Nath, P. & Sarker, P., 2015. Use of OPC to improve setting and early strength properties of low calcium fly ash geopolymer concrete cured at room temperature. *Cement and Concrete Composites*, 55, 205-214.
- Nath, S., Mukherjee, S., Maitra, S. & Kumar, S., 2014. Ambient and elevated temperature geopolymerization behaviour of class F fly ash. *Transactions of the Indian Ceramic Society*, 73(2), 126-132.
- Nazari, A., 2013. Compressive strength of geopolymers produced by ordinary Portland cement: Application of genetic programming for design. *Materials & Design*, 43, 356-366.
- Nuruddin, M., Kusbiantoro, A., Qazi, S. & Shafiq, N., 2011a. Compressive strength and interfacial transition zone characteristic of geopolymer concrete with different cast in-situ curing condition. *World Academy of Science, Engineering and Technology*, 14 to 16 November 2011. Paris, WASET, 25-28.
- Nuruddin, M., Qazi, S., Kusbiantoro, A. & Shafiq, N., 2011b. Utilisation of waste material in geopolymeric concrete. *Proceedings of the Institution of Civil Engineers-Construction Materials*, 164(6), 315-327.
- Oss, H. & Padovani, A., 2003. Cement manufacture and the environment part II: Environmental challenges and opportunities. *Journal of Industrial Ecology*, 7(1), 93-126.
- Pacheco-Torgal, F., Castro-Gomes, J. & Jalali, S., 2008a. Alkali-activated binders: A review. Part 1. Historical background, terminology, reaction mechanisms and hydration products. *Construction and Building Materials*, 22, 1305-1314.
- Pacheco-Torgal, F., Castro-Gomes, J. & Jalali, S., 2008b. Alkali-activated binders: A review. Part 2. About materials and binders manufacture. *Construction and Building Materials*, 22, 1315-1322.
- Pacheco-Torgal, F., Castro-Gomes, J. & Jalali, S., 2009. Tungsten mine waste geopolymeric binder: Preliminary hydration products investigations. *Construction and Building Materials*, 23(1), 200-209.
- Pacheco-Torgal, F., Castro-Gomes, J. & Jalali, S., 2007. Tungsten mine waste geopolymeric binder versus ordinary portland cement based concrete: abrasion and acid resistance. In: *International Conference Alkali Activated Materials-Research, Production and Utilization*. s.l.:Agentura Action M, 693-710.
- Pacheco-Torgal, F., Labrincha, J.A., Leonelli, C., Palamo, A. & Chindapasirt, P., 2014. Chapter 5: Setting, segregation and bleeding of alkali-activated cement, mortar and concrete binders. In: 1st, ed. *Handbook of Alkali-Activated Cements, Mortars and Concretes*. Abington Hall, Cambridge, UK: WoodHead Publishing Limited- Elsevier Science and Technology, 113-131.
- Palomo, A., Blanco-Varela, M.T., Granizo, M.L., Puertas, F., Vazquez, T. & Grutzeck, M.W., 1999. Chemical stability of cementitious materials based on metakaolin. *Cement and Concrete Research*, 29(7), 997-1004.

- Palomo, A., Fernández-Jiménez, A., Kovalchuk, G., Ordoñez, L.M. & Naranjo, M.C., 2007. OPC-fly ash cementitious systems: study of gel binders produced during alkaline hydration. *Journal of Materials Science*, 42(9), 2958-2966.
- Panagiotopoulou, C., Kontori, E., Perraki, T. & Kakali, G., 2007. Dissolution of aluminosilicate minerals and by-products in alkaline media. *Journal of Materials Science*, 42(9), 2967-2973.
- Pangdaeng, S., Phoo-ngernkham, T., Sata, V. & Chindaprasirt, P., 2014. Influence of curing conditions on properties of high calcium fly ash geopolymer containing Portland cement as additive. *Materials and Design*, 53, 269-274.
- Panias, D., Giannopoulou, I. & Perraki, T., 2007. Effect of synthesis parameters on the mechanical properties of fly ash-based geopolymers. *Colloids and Surfaces A: Physicochemical and Engineering Aspects*, 301(1), 246-254.
- Petermann, J., Saeed, A. & Hammons, M., 2010. *Alkali-Activated Geopolymers: A Literature Review*, Panama City, USA: Applied Research Associates, Inc.
- Phoo-ngernkham, T., Chindaprasirt, P., Sata, V., Hanjitsuwan, S. & Hatanaka, S., 2014. The effect of adding nano-SiO₂ and nano-Al₂O₃ on properties of high calcium fly ash geopolymer cured at ambient temperature. *Materials & Design*, 55, 58-65.
- Phoo-ngernkham, T., Chindaprasirt, P., Sata, V., Pangdaeng, S. & Sinsiri, T., 2013. Properties of high calcium fly ash geopolymer pastes with Portland cement as an additive. *International Journal of Minerals, Metallurgy, and Materials*, 20(2), 214-220.
- Phoo-ngernkham, T. & Sinsiri, T., 2011. Workability and compressive strength of geopolymer mortar from fly ash containing diatomite. *KKU Engineering Journal*, 38(1), 11-26.
- Puertas, F. & Torres-Carrasco, M., 2014. Use of glass waste as an activator in the preparation of alkali-activated slag: Mechanical strength and paste characterisation. *Cement and Concrete Research*, 57, 95-104.
- Raijiwala, D. & Patil, H., 2010. Geopolymer concrete: A green concrete. *2010 2nd International Conference on Chemical, Biological and Environmental Engineering (ICBEE 2010), 2 to 4 November 2010*. Cairo, Egypt, IEEE, 202-206.
- Rangan, B., Hardjito, D., Wallah, S. & Sumajouw, D., 2005. Studies on fly ash-based geopolymer concrete. *Proceedings of the World Congress Geopolymer, June 2005*. Saint Quentin, France, Geopolymer Institute, 133-137.
- Rashad, A. & Zeedan, S., 2011. The effect of activator concentration on the residual strength of alkali-activated fly ash pastes subjected to thermal load. *Construction and Building Materials*, 25(7), 3098-3107.
- Rattanasak, U. & Chindaprasirt, P., 2009. Influence of NaOH solution on the synthesis of fly ash geopolymer. *Minerals Engineering*, 22(12), 1073-1078.

- Rattanasak, U., Pankhet, K. & Chindaprasirt, P., 2011. Effect of chemical admixtures on properties of high-calcium fly ash geopolymer. *International Journal of Minerals, Metallurgy and Materials*, 18(3), 364-369.
- Reddy, D., Edouard, J. & Sobhan, K., 2012. Durability of fly ash-based geopolymer structural concrete in the marine environment. *Journal of Materials in Civil Engineering*, 25(6), 781-787.
- Rovnaník, P., 2010. Effect of curing temperature on the development of hard structure of metakaolin-based geopolymer. *Construction and Building Materials*, 24(7), 1176-1183.
- Roy, D., 1999. Roy, D.M., 1999. Alkali-activated cements opportunities and challenges. *Cement and Concrete Research*, 29(2), 249-254.
- Shi, C., Jiménez, A. & Palomo, A., 2011. New cements for the 21st century: The pursuit of an alternative to Portland cement. *Cement and Concrete Research*, 41(7), 750-763.
- Silo Transport, a., 2016. *Fly ash, How is fly ash produced?*. [Online] Available at: <http://www.silotransport.cz/en/fly-ash> [Accessed 6 February 2016].
- Škvára, F., Kopecký, L., Nemecek, J. & Bittnar, Z., 2006. Microstructure of geopolymer materials based on fly ash. *Ceramics-Silikáty*, 50(4), 208-215.
- Sofi, M., Van Deventer, J., Mendis, P. & Lukey, G., 2007. Engineering properties of inorganic polymer concretes (IPCs). *Cement and Concrete Research*, 37(2), 251-257.
- Somna, K., Jaturapitakkul, C., Kajitvichyanukul, P. & Chindaprasirt, P., 2011. NaOH-activated ground fly ash geopolymer cured at ambient temperature. *Fuel*, 90(6), 2118-2124.
- Songpiriyakij, S., Kubprasit, T., Jaturapitakkul, C. & Chindaprasirt, P., 2010. Compressive strength and degree of reaction of biomass-and fly ash-based geopolymer. *Construction and Building Materials*, 24(3), 236-240.
- Soroka, I., 1979. *Portland Cement Paste and Concrete*. Old Working, Surrey: Unwin Brothers Limited.
- Soroka, I., 1993. *Concrete in Hot Environments*. Oxfordshire: Spon Press.
- Sottisoplia, W. & Asavapisit, S., 2005. Immobilization of the plating sludge by activation of pulverized fuel ash with sodium silicate solution. *Thammasat Int. J. Sc. Tech*, 10(4), 7-15.
- Sujatha, T., Kannapiran, K. & Nagan, S., 2012. Strength assessment of heat cured geopolymer concrete slender column. *Asian Journal of Civil Engineering*, 13(5), 635-646.
- Sukmak, P., Horpibulsuk, S. & Shen, S., 2013. Strength development in clay-fly ash geopolymer. *Construction and Building Materials*, 40, 566-574.

- Sumajouw, D., Hardjito, D., Wallah, S. & Rangan, B., 2007. Fly ash-based geopolymer concrete: study of slender reinforced columns. *Journal of Materials Science*, 42(9), 3124-3130.
- Suwan, T. & Fan, M., 2014. Influence of OPC replacement and manufacturing procedures on the properties of self-cured geopolymer. *Construction and Building Materials*, 73, 551-561.
- Suwan, T., Fan, M. & Braimah, N., 2016. Internal heat liberation and strength development of self-cured geopolymers in ambient curing conditions. *Construction and Building Materials*, 114, 297-306.
- Taebuanhuad, S., Rattanasak, U. & Jenjirapanya, S., 2012. Strength behavior of fly ash geopolymer with microwave pre-radiation curing. *The Journal of Industrial Technology*, 8(2), 1-8.
- Tailby, J. & MacKenzie, K., 2010. Structure and mechanical properties of aluminosilicate geopolymer composites with Portland cement and its constituent minerals. *Cement and Concrete Research*, 40(5), 787-794.
- Tang, Z., Ma, S., Ding, J., Wang, Y., Zheng, S. & Zhai, G., 2013. Current status and prospect of fly ash utilization in China. *Proceedings of World of Coal Ash Conference (WOCA), 22 to 25 April 2013*. Lexington, Kentucky, WOCA, 1-7.
- Taylor, H., 1992. *Cement Chemistry*. Great Britain: St Edmundsbury Press Ltd.
- Tchakoute, H., Elimbi, A., Yanne, E. & Djangang, C., 2013. Utilization of volcanic ashes for the production of geopolymers cured at ambient temperature. *Cement and Concrete Composites*, 38, 75-81.
- Teixeira-Pinto, A. F. P. a. J. S., 2002. Geopolymer manufacture and application-Main problems when using concrete technology. *Geopolymers 2002 International Conference, October 2002*. Melbourne, Australia, Siloxo Pty Ltd.
- Temuujin, J. & Van Riessen, A., 2009. Effect of fly ash preliminary calcination on the properties of geopolymer. *Journal of Hazardous Materials*, 164(2), 634-639.
- Temuujin, J., Van Riessen, A. & Williams, R., 2009a. Influence of calcium compounds on the mechanical properties of fly ash geopolymer pastes. *Journal of Hazardous Materials*, 167(1), 82-88.
- Temuujin, J., Williams, R. & Van Riessen, A., 2009b. Effect of mechanical activation of fly ash on the properties of geopolymer cured at ambient temperature. *Journal of Materials Processing Technology*, 209(12), 5276-5280.
- Topçu, İ., Toprak, M. & Uygunoğlu, T., 2014. Durability and microstructure characteristics of alkali activated coal bottom ash geopolymer cement. *Journal of Cleaner Production*, 81, 211-217.

- Tran, D., Kroisová, D., Louda, P., Bortnovsky, O. & Bezucha, P., 2009. Effect of curing temperature on flexural properties of silica-based geopolymer-carbon reinforced composite. *Journal of Achievements in Materials and Manufacturing Engineering*, 37(2), 492-497.
- Turner, L. & Collins, F., 2013. Carbon dioxide equivalent (CO₂-e) emissions: A comparison between geopolymer and OPC cement concrete. *Construction and Building Materials*, 43, 125-130.
- Vaidya, S., Diaz, E. & Allouche, E., 2011. Experimental Evaluation of Self-Cure Geopolymer Concrete for Mass Pour Applications. *World of coal ash (woca) conference, May 2011*. Denver, Colorado, ACAA and CAER, 9-12.
- Van Jaarsveld, J., 2000. *The Physical and Chemical Characterization of Fly Ash-Based Geopolymer*. Melbourne: University of Melbourne.
- Van Jaarsveld, J. & Van Deventer, J., 1999. The effect of metal contaminants on the formation and properties of waste-based geopolymers. *Cement and Concrete Research*, 29(8), 1189-1200.
- Van Jaarsveld, J., Van Deventer, J. & Lukey, G., 2002. The effect of composition and temperature on the properties of fly ash-and kaolinite-based geopolymers. *Chemical Engineering Journal*, 89(1), 63-73.
- Wallah, S., 2009. Drying shrinkage of heat-cured fly ash-based geopolymer concrete. *Modern Applied Science*, 3(12), 14-21.
- Wang, H., Li, H. & Yan, F., 2005. Synthesis and mechanical properties of metakaolinite-based geopolymer. *Colloids and Surfaces A: Physicochemical and Engineering Aspects*, 268(1), 1-6.
- Weng, L. & Sagoe-Crentsil, K., 2007. Dissolution processes, hydrolysis and condensation reactions during geopolymer synthesis: Part I - Low Si/Al ratio systems. *Journal of Materials Science*, 42(9), 2997-3006.
- Winston, R., 2008. *Corrosion and Corrosion Control*. 4th ed. West Sussex: Wiley.
- Worrell, E., Price, L., Martin, N., Hendriks, C. & Meida, L.O., 2001. Carbon dioxide emissions from the global cement industry. *Annual Review of Energy and the Environment*, 26(1), 303-329.
- Xie, J., Yin, J., Chen, J. & Xu, J., 2009. Study on the geopolymer based on fly ash and slag. *Energy and Environment Technology*, 3, 578-581.
- Xu, H. & Van Deventer, J., 2000. The geopolymerisation of alumino-silicate minerals. *International Journal of Mineral Processing*, 59(3), 247-266.
- Xu, H. & Van Deventer, J., 2002. Geopolymerisation of multiple minerals. *Minerals Engineering*, 15(12), 1131-1139.

- Xu, H. & Van Deventer, J., 2003. The effect of alkali metals on the formation of geopolymeric gels from alkali-feldspars. *Colloids and Surfaces A: Physicochemical and Engineering Aspects*, 216(1), 27-44.
- Yang, K., Song, J., Ashour, A. & Lee, E., 2008. Properties of cementless mortars activated by sodium silicate. *Construction and Building Materials*, 22(9), 1981-1989.
- Yip, C., Lukey, G., Provis, J. & Van Deventer, J., 2008. Effect of calcium silicate sources on geopolymerisation. *Cement and Concrete Research*, 38(4), 554-564.
- Yip, C., Lukey, G. & Van Deventer, J., 2005. The coexistence of geopolymeric gel and calcium silicate hydrate at the early stage of alkaline activation. *Cement and Concrete Research*, 35(9), 1688-1697.
- Yip, C. & Van Deventer, J., 2003. Microanalysis of calcium silicate hydrate gel formed within a geopolymeric binder. *Journal of Materials Science*, 38(18), 3851-3860.
- Yi, S., Yang, E. & Choi, J., 2006. Effect of specimen sizes, specimen shapes, and placement directions on compressive strength of concrete. *Nuclear Engineering and Design*, 236, 115-127.
- Yu, Q., Sawayama, K., Sugita, S., Shoya, M. & Isojima, Y., 1999. The reaction between rice husk ash and $\text{Ca}(\text{OH})_2$ solution and the nature of its product. *Cement and Concrete Research*, 29(1), 37-43.
- Zhang, Z., Yao, X., Zhu, H. & Chen, Y., 2009. Role of water in the synthesis of calcined kaolin-based geopolymer. *Applied Clay Science*, 43(2), 218-223.
- Zheng, L., Wang, W. & Shi, Y., 2010. The effects of alkaline dosage and Si/Al ratio on the immobilization of heavy metals in municipal solid waste incineration fly ash-based geopolymer. *Chemosphere*, 79(6), 665-671.

APPENDIXES

**APPENDIX A:
ADDITIONAL DATA**

Table A.1 Compressive strength of geopolymer by prime materials

Type	Prime Materials (% wt)	Additives (% wt)	Si/Al Ratio ^a	Sample Type	Compression MPa /Aged ^b	Alkaline Materials	Curing		Sample size	References
							C°	Hrs		
controlled	Typical OPC	-	-	-	30.3 / 28	-	Ambient		150 mm Cubes	(Raijiwala & Patil, 2010)
controlled	Cement Repair	-	-	-	46.1 / 28	-	Ambient		40 mm Cubes	(Hu, et al., 2008)
IW	FA class F (90)	-	2.12	Paste	95.0 / 28	NaOH + Na ₂ SiO ₃	85	20	40×40×160 mm ³	(Fernández-Jiménez, et al., 2007)
IW	TMW (90)	CaOH ₂ (10)	3.20	Paste	75.0 / 56	NaOH + Na ₂ SiO ₃	Ambient		50 mm Cubes	(Pacheco-Torgal, et al., 2009)
IW	FA (80)	Water Sludge (20)	2.53	Paste	70.6 / 90	-	Ambient		38 mm Cubes	(Kongkaew, 2007)
IW	FA class F (90)	BA (10)	2.32	Paste	70.0 / 28	KOH + K ₂ SiO ₃	80	24	50 mm Cubes	(Hardjito & Fung, 2010)
IW	GBFS (100)	-	3.70	Paste	67.0 / 28	NaOH	38	90 ^d	25 mm Cubes	(Khater, 2012)
NM	MK (100)	-	1.40	Paste	65.0 / 28	NaOH + Na ₂ SiO ₃	65	10	Cy.dia. 13mm×26mm	(Wang, et al., 2005)
NM	Natural Pozzolan (100)	-	3.44	Paste	63.0 / 28	NaOH + Na ₂ SiO ₃	Ambient		20 mm Cubes	(Allahverdi, et al., 2008)
NM	MK (80)	Steel Slag (20)	1.71	Paste	44.5 / 28	NaOH + Na ₂ SiO ₃	Ambient		40 mm Cubes	(Hu, et al., 2008)
IW	FA (95) class F	Silicafume(5)	1.87	Mortar	35.0 / 28	NaOH + Na ₂ SiO ₃	85	48	50 mm Cubes	(Dutta, et al., 2010)
NM	Diatomite (100)	-	5.93	Paste	28.4 / 28	NaOH + Na ₂ SiO ₃	75	7 ^d	50 mm Cubes	(Phoo-ngernkham & Sinsiri, 2011)
NM	Kaolinite (100)	-	1.30	Paste	28.0 / 28	NaOH + Na ₂ SiO ₃	100	72	20 mm Cubes	(Hounsi, et al., 2013)
GW	Construction waste (70)	MK (20), CaOH ₂ (10)	38.00	Paste	26.1 / 7	NaOH + Na ₂ SiO ₃	80	24	25 mm Cubes	(Khater, 2011)
IW	GBFS (75)	CKD (25)	3.70	Paste	24.0 / 28	NaOH	38	90 ^d	25 mm Cubes	(Khater, 2012)

Note: Si/Al ratio of main prime material^a, days^b

Table A.1 Compressive strength of geopolymer by prime materials (Continued)

Type	Prime Materials (% wt)	Additives (% wt)	Si/Al Ratio ^a	Sample Type	Compression MPa / Aged ^b	Alkaline Materials	Curing		Sample size	References
							C°	Hrs		
GW	Waste Paper Sludge (100)	-	1.84	Concrete	17.5 / 28	NaOH + Na ₂ SiO ₃	Ambient		100 mm Cubes	(Anuar, et al., 2011)
IW	Ferronickel slug (100)	-	4.13	Paste	(15.8/28)	NaOH + Na ₂ SiO ₃	60	24	50 mm Cubes	(Komnitsas & Zaharaki, 2007)
IW	Copper mine tailing (100)	-	9.29	Paste	(15.0/7)	NaOH + Na ₂ SiO ₃	90	7d ^b	Cy. dia. 33.4mmx72.5mm	(Ahmari & Zhang, 2012)
NM	SiltyClay (75)	FA (25)	2.50	Paste	(14.0/28)	NaOH + Na ₂ SiO ₃	75	48	Cy. dia. 50mmx100mm	(Sukmak, et al., 2013)
NM	RHA (100)	-	8.28	Paste	(None/28)	NaOH + Na ₂ SiO ₃	60	24	Cy. dia. 30mmx60mm	(Songpiriyakij, et al., 2010)

Note: Si/Al ratio of main prime material^a, days^b

Table A.2 Strength of geopolymer synthesized in different manufacturing procedures

Mixture	w/s ^a	SiO ₂ /Al ₂ O ₃ ^b	Na ₂ O/PM ^c	Compressive strength (MPa)			
				3 days	7 days	14 days	28 days
GP (A)	0.191	3.58	9.64	-	4.75	7.24	13.59
GP (B)	0.191	3.58	9.64	-	2.93	6.91	13.24
GP (C)	0.191	3.58	9.64	-	2.35	6.04	11.29

^a Water-to-solid ratio, ^b Oxide molar ratio, ^c Na₂O-to-Prime material by mass.

Table A.3 Elemental compositions under various curing temperatures at the 28-day age

Mixtures	Si	Al	Ca	Na	K	O	Si/Al	Ca/Si
<i>OPC</i>								
10 °C	5.26	1.42	36.04	0.23	1.64	48.18	3.70	6.85
20 °C	4.95	1.37	37.89	0.02	1.01	47.52	3.61	7.65
40 °C	5.15	1.26	35.38	0.37	2.33	46.82	4.09	6.87
60 °C	5.20	1.36	41.65	-	0.92	49.21	3.82	8.01
70 °C	5.14	1.09	44.21	-	0.91	46.55	4.72	8.60
<i>Geopolymer Cement</i>								
10 °C	17.51	9.18	1.30	10.68	1.83	46.17	1.91	0.07
20 °C	21.36	11.30	2.30	11.98	-	45.23	1.89	0.11
40 °C	22.33	12.90	2.25	12.98	-	47.72	1.73	0.10
60 °C	23.36	13.05	2.60	12.44	-	48.55	1.79	0.11
70 °C	18.35	10.16	1.26	6.76	1.70	46.53	1.81	0.07
<i>GeoPC30</i>								
10 °C	13.36	8.19	15.17	3.73	1.65	43.12	1.63	1.14
20 °C	16.19	9.92	14.71	11.54	-	47.64	1.63	0.91
40 °C	12.60	6.88	15.82	5.38	1.86	43.39	1.83	1.26
60 °C	14.24	7.76	9.73	7.99	1.64	45.24	1.84	0.68
70 °C	14.50	7.60	12.10	8.00	1.80	46.20	1.91	0.83

APPENDIX B:
**CALCULATIONS OF WATER-TO-SOLID (w/s) RATIOS
AND OXIDE MOLAR RATIOS OF THE MIXTURES**

Table B.1 Calculation of Water-to-Solid (w/s) ratios of the mixtures

1. NaOH Sol = **15** Molar

- 1.1 NaOH solid (g.) in 1,000 cm³ of water = **600** g.
- 1.2 or weight (kg) per 1,000 cm³ of solution = **1.60** kg.
- 1.3 Water **1.00** kg contains NaOH solid (kg) = **0.60** kg.
- 1.4 % of NaOH solid by mass in the solution = **37.50** %

NaOH solution	% mass solid
NaOH 8 M	24.24
NaOH 10 M	28.57
NaOH 12 M	32.43
NaOH 14 M	35.90
NaOH 15 M	37.50
NaOH 16 M	39.02

2. Sodium silicate solution, chemical composition

- 2.1 SiO₂ = **32.10** %
- 2.2 Na₂O = **16.10** %
- 2.3 Water = **51.80** %
- 3. A/FA ratio = **0.40**
- 4. SS/SH ratio = **1.50**

3. Mixture proportion

No.	Mix No.	NaOH Molar	OPC w/c	OPC %mass	GP %mass	OPC (g)	OPC water (g)	Fly ash (g)	NaOH Sol (g)	SS Sol (g)	4% Added water (g)	% Added water	Mass OPC	Mass GP	Total of combination	w/s ratio
1	GP	15	-	-	100	-	-	500.00	80.00	120.00	-	0	-	700.00	700.00	0.191
2	OPC	-	0.253	100	-	500.00	126.50	-	-	-	-	0	626.50	-	626.50	0.253
3	GeoPC90	15	0.253	90	10	455.00	115.12	45.25	7.24	10.86	26.39	4	570.12	63.35	659.86	0.298
4	GeoPC80	15	0.253	80	20	409.00	103.48	91.51	14.64	21.96	26.69	4	512.48	128.12	667.29	0.292
5	GeoPC70	15	0.253	70	30	361.00	91.33	138.47	22.16	33.23	26.92	4	452.33	193.86	673.11	0.285
6	GeoPC50	15	0.253	50	50	264.00	66.79	236.28	37.80	56.71	27.57	4	330.79	330.79	689.15	0.272
7	GeoPC30	15	0.253	30	70	162.00	40.99	338.31	54.13	81.19	28.19	4	202.99	473.63	704.81	0.259
8	GeoPC20	15	0.253	20	80	109.00	27.58	390.22	62.44	93.65	-	0	136.58	546.31	682.89	0.203
9	GeoPC10	15	0.253	10	90	55.20	13.97	444.64	71.14	106.71	-	0	69.17	622.49	691.66	0.197

4. Calculation of water-to-solid (w/s) by mass

No.	Mix No.	NaOH Molar	OPC w/c	OPC %mass	GP %mass	OPC (g)	OPC water (g)	Fly ash (g)	NaOH Sol (g)		SS Sol (g)		Added water	Total		
									Solid (g)	Water (g)	Solid (g)	Water (g)		Water (g)	Solids (g)	w/s
1	GP	15	-	-	100	-	-	500.00	30.00	50.00	57.84	62.16	-	112.16	587.84	0.191
2	OPC	-	0.253	100	-	500.00	126.50	-	-	-	-	-	-	126.50	500.00	0.253
3	GeoPC90	15	0.253	90	10	455.00	115.12	45.25	2.71	4.52	5.23	5.63	26.39	151.66	508.20	0.298
4	GeoPC80	15	0.253	80	20	409.00	103.48	91.51	5.49	9.15	10.59	11.38	26.69	150.70	516.59	0.292
5	GeoPC70	15	0.253	70	30	361.00	91.33	138.47	8.31	13.85	16.02	17.21	26.92	149.32	523.80	0.285
6	GeoPC50	15	0.253	50	50	264.00	66.79	236.28	14.18	23.63	27.33	29.37	27.57	147.36	541.79	0.272
7	GeoPC30	15	0.253	30	70	162.00	40.99	338.31	20.30	33.83	39.14	42.06	28.19	145.07	559.74	0.259
8	GeoPC20	15	0.253	20	80	109.00	27.58	390.22	23.41	39.02	45.14	48.51	-	115.11	567.77	0.203
9	GeoPC10	15	0.253	10	90	55.20	13.97	444.64	26.68	44.46	51.44	55.28	-	113.71	577.95	0.197

Table B.2 Calculation of oxide molar ratios of the mixtures

1. Chemical compound of fly ash, batch I (%by mass)				2. Chemical compound of OPC (%by mass)				Oxide molecular weight								
SiO ₂	50.97	%		SiO ₂	12.22	%		Oxide	g							
Al ₂ O ₃	27.83	%		Al ₂ O ₃	3.85	%		SiO ₂	60.09							
Na ₂ O	1.13	%		Na ₂ O	0.00	%		Al ₂ O ₃	101.96							
CaO	2.62	%		CaO	73.82	%		Na ₂ O	61.98							
								H ₂ O	18.00							
								NaOH	39.99							
								CaO	56.08							
3. Sodium silicate composition (%by mass)				4. Sodium hydroxide composition (%by mass)												
SiO ₂	32.13	%		Molarity =	15 M	37.50	%									
Na ₂ O	16.07	%		Water		62.50	%									
Water	51.8	%														
SS concentration =				48.2%												
5. Calculation of molar ratio in geopolymer constituents												NaOH		Added water		
	Fly ash				OPC				Sodium silicate			Flakes			Water	
	CaO	SiO ₂	Al ₂ O ₃	Na ₂ O	CaO	SiO ₂	Al ₂ O ₃	Na ₂ O	SiO ₂	Na ₂ O	H ₂ O	Na ₂ O	H ₂ O		H ₂ O	H ₂ O
OPC	0.00	0.00	0.00	0.00	658.17	101.68	18.88	0.00	0.00	0.00	0.00	0.00	0.00	0.00	0.00	702.78
GeoPC90	2.11	38.38	12.35	0.82	598.93	92.53	17.18	0.00	5.81	2.82	31.25	3.39	3.39	25.14	786.17	
GeoPC80	4.28	77.62	24.98	1.67	538.38	83.17	15.44	0.00	11.74	5.69	63.20	6.86	6.86	50.83	723.17	
GeoPC70	6.47	117.45	37.80	2.52	475.20	73.41	13.63	0.00	17.77	8.62	95.63	10.39	10.39	76.94	657.00	
GeoPC50	11.04	200.42	64.49	4.31	347.51	53.69	9.97	0.00	30.32	14.70	163.20	17.72	17.72	131.25	524.22	
GeoPC30	15.81	286.96	92.34	6.17	213.25	32.94	6.12	0.00	43.41	21.05	233.65	25.38	25.38	187.95	384.33	
GeoPC20	18.23	331.00	106.51	7.11	143.48	22.17	4.12	0.00	50.07	24.28	269.50	29.28	29.28	216.81	153.22	
GeoPC10	20.77	377.16	121.36	8.11	72.66	11.23	2.08	0.00	57.06	27.67	307.09	33.36	33.36	247.01	77.61	
GP	23.36	424.11	136.48	9.12	0.00	0.00	0.00	0.00	64.16	31.11	345.33	37.51	37.51	277.78	0.00	

	Total moles					w/s	Na ₂ O / SM.	SiO ₂ / Al ₂ O ₃	CaO / SiO ₂
	CaO	SiO ₂	Al ₂ O ₃	Na ₂ O	H ₂ O				
OPC	658.17	101.68	18.88	-	702.78	0.25	-	-	-
GeoPC90	601.05	136.72	29.53	7.04	845.95	0.30	0.87	4.63	4.40
GeoPC80	542.66	172.54	40.42	14.23	844.06	0.29	1.76	4.27	3.15
GeoPC70	481.67	208.64	51.43	21.53	839.96	0.29	2.67	4.06	2.31
GeoPC50	358.55	284.43	74.46	36.73	836.39	0.27	4.55	3.82	1.26
GeoPC30	229.05	363.32	98.46	52.60	831.31	0.26	6.52	3.69	0.63
GeoPC20	161.71	403.24	110.63	60.67	668.81	0.20	7.53	3.65	0.40
GeoPC10	93.43	445.44	123.45	69.13	665.07	0.20	8.57	3.61	0.21
GP	23.36	488.28	136.48	77.74	660.62	0.19	9.64	3.58	0.05

SM. = Starting Material
w/s = water-to-solid ratio

Calculation reference:
D.Hardjito & B.V.Rangan (2005)

APPENDIX C:
PUBLICATIONS, CONFERENCES AND AWARDS

Journals:

- Suwan, T. and Fan, M. (2014) ‘Influence of OPC replacement and manufacturing procedures on the properties of Self-cured geopolymer’, *Construction and Building Materials*, 73, pp. 551-561. Elsevier.
- Suwan, T., Fan, M. and Braimah, N. (2016) ‘Internal heat liberation and strength development of self-cured geopolymers in ambient curing conditions’, *Construction and Building Materials*, 114, pp.297-306. Elsevier.
- Suwan, T. and Fan, M. ‘Effect of manufacturing process on mechanisms and mechanical properties of fly ash-based Geopolymer in ambient curing temperature’, *Materials and Manufacturing Processes*. Taylor & Francis (Accepted).
- Suwan, T., Fan, M. and Braimah, N. ‘Micro-mechanisms and compressive strength of geopolymer-Portland cementitious system under various curing temperature’, *Materials Chemistry and Physics*. Elsevier. (Accepted).

Papers under preparation:

- “The investigation on mechanisms and properties of Geopolymer-Portland (GeoPC) cementitious system”
- “Combination of pre-dry mixing process and Geopolymer-Portland (GeoPC) system: The production of Self-cured geopolymers”
- “Effect of Sample Size and Extra Internal Heat Accumulation on Strength of Self-Cured Geopolymers”

Conferences:

- International Conference on Software, Knowledge, Information Management and Applications (SKIMA2012), 9th-11th September 2012, Titled: Integration of Lifecycle Management and Prefabrication in Construction: Sustainable Concept for Residential Building Construction Sector in Thailand, Chengdu, China.
- International Conference on Software, Knowledge, Information Management and Applications (SKIMA2013), 18th -20th December 2013, Titled: Free cloud storage service: An online data-sharing solution for small-to-medium size construction companies in Thailand, ChiangMai, Thailand
- School of Engineer Research Conference 2014 (ResCon14) on 23rd-26th June 2014. Titled: Development of Self-cured geopolymer cement, Brunel University LONDON, UK.

- International conference of CONST ENG'14 Structure, Materials and Construction Engineering Conference on 20th-22nd November 2014, Titled: Development of Self-cured geopolymer cement: The performance in ambient curing conditions, DAKAM-Istanbul, Turkey.
- International conference of the 8th International Conference on Materials Science and Technology (MSAT-8), 15th-16nd December 2014, Titled: “The effects of additional OPC and Pre-dry mixing process on the mechanisms and properties of Self-cured geopolymer cement”, Bangkok, Thailand.
- Three Minute Thesis (3MT®) Competition, 25th February 2015, College Heats: College of Engineering, Design and Physical Sciences. Title: “Sustainable construction materials: Geopolymer cement”. Brunel University LONDON, UK.
- Presentation in *The Future emerging materials for green buildings work shop*, 30th October 2015, Title of “Self-cured Geopolymer cement: The performances in ambient curing conditions”, Brunel University LONDON, UK.

Posters presented:

- International conference of the 34th Annual Cement and Concrete Science Conference, 14th-16th September 2014. Titled: Development of Self-cured geopolymer cementitious system, University of Sheffield, UK.
- Brunel University Research Student Conference: Poster Presentation Conference, 11th-12th March 2014, Title: The development of Geopolymer-Portland cementitious systems, Brunel University LONDON, UK.
- Brunel University Research Student Conference: Poster Presentation Conference, 29th-30th April 2013. Title: Development of Self-curing geopolymer cement, Brunel University LONDON, UK.
- School of Engineer Research Conference 2013(ResCon13), 24th-26th June 2013, Title: Development of Self-curing geopolymer cement, Brunel University LONDON, UK.

Honours and Awards

- Vice-chancellor's Travel prize winner 2014. Brunel University LONDON, UK.
- 1st prize winner of extended abstract. School of Engineer Research Conference 2014 (ResCon14). Brunel University LONDON, UK. (23rd -26th June 2014).
- Vice-chancellor's Travel prize winner 2013. Brunel University LONDON, UK.

- Poster conference winner 2013 for early stage researcher. Brunel University Research Student Conference. Brunel University LONDON, UK. (29th -30th April 2013).

APPENDIX D:
PUBLISHED JOURNAL PAPERS



Influence of OPC replacement and manufacturing procedures on the properties of self-cured geopolymer



Teewara Suwan, Mizi Fan*

Department of Civil Engineering, School of Engineering and Design, Brunel University, Uxbridge, UB8 3PH London, United Kingdom

HIGHLIGHTS

- OPC replacement shortened setting time and increased early strength of GeoPC systems.
- Self-cured efficacy could be tailored with different manufacturing procedures.
- Pre dry-mixed process released intensive heat during synthesis.
- Geopolymer was cured in ambient conditions without external heat supply (18–22 °C).
- (#1) GeoPC and pre dry-mixed process can provide feasible production of self-cured GP.

ARTICLE INFO

Article history:

Received 15 July 2014

Received in revised form 18 September 2014

Accepted 25 September 2014

Keywords:

Ambient curing
Fly ash
Geopolymer
Manufacturing procedures
Raw material combination
Self-cured geopolymer

ABSTRACT

Geopolymer typically achieves its strength by heat curing, which is a limitation for in-field applications. This study develops self-cured technologies for fly ash-based geopolymer curing in ambient conditions without external heat supply. Two approaches, (i) the combination of OPC and Geopolymer (GeoPC), and (ii) different manufacturing procedures, were investigated. The results showed that the self-cured GeoPC could be developed with the setting time, early strength and microstructures of GeoPC enhancing when the amount of OPC replacement increased. The manufacturing procedure also directly influenced the solidifying behaviour and early strength development of geopolymer cement.

© 2014 Elsevier Ltd. All rights reserved.

1. Introduction

The Portland cement manufacturing is an energy intensive process and releases very large amount of greenhouse gas to atmosphere, and alternative cementitious systems have been studying to totally or partially replace the Ordinary Portland Cement (OPC) [1]. Alumina–silicate materials, especially fly ash and other pozzolanic industrial wastes, have been identified as starting materials to produce OPC-less cementitious material, called “Geopolymer Cement”. The production of alumina–silicate based geopolymer cement commonly use alkaline solutions, such as sodium silicate (Na_2SiO_3) and potassium or sodium hydroxide (KOH or NaOH), mixing with raw starting materials to form homogenous slurry. Heat above ambient temperature is applied approximately from 60 to 90 °C for 24 to 48 h for curing purpose.

Afterward, geopolymer will be continually cured or left in room temperature for further handlings [2] (Fig. 1).

The properties of geopolymer cement, tested in accordance with the testing standard of OPC, are in the same order as or even better than those made from OPC. Moreover, geopolymer are using waste materials and manufactured without the energy intensive process like that of OPC. Replacing OPC with alumina–silicate waste brings about the benefits not only for cost saving but also the reduction of environmental impact up to 9% less CO_2 emission when compared with OPC binder [3,4]. However, the requirement of heating for the curing process of the geopolymer has a significant implication for on-site operation of construction and energy consumption. The typical fly ash-based geopolymer paste cannot set within 24 h in ambient temperature [5], although adding some of calcium source can shorten the setting time of cement paste. Calcium content in geopolymer cement could be achieved by adding granulated blast furnace slag (GBFS), high calcium fly ash, steel slag, calcium hydroxide ($\text{Ca}(\text{OH})_2$) or even OPC [6–9]. This paper

* Corresponding author.

E-mail address: mizi.fan@brunel.ac.uk (M. Fan).

focuses on the curing processes and properties (i.e. setting time and early strength development) of Geopolymer-Portland cementitious materials (GeoPC) affected by calcium content (from OPC) in alkaline presence (from geopolymers) and different manufacturing processes. All of the approaches, five main different combinations and three different manufacturing processes, have been cured and investigated at the ambient temperature ($20 \pm 2^\circ\text{C}$).

2. Materials

The raw starting materials were coal-fired fly ash and Ordinary Portland Cement (OPC). The Pulverised Fly Ash (PFA) was delivered from Drax power station, North Yorkshire, UK under the brand name of CEMEX. Its properties comply with BS EN 450-1:2012 fineness category S and loss on ignition category B (Category S corresponds to the 12% 45 micro residue limit and loss on ignition category B covers the permissible range of 2–7% (in BS 3892 Pt.1). OPC purchased was CEM II/A-L. The main chemical compositions of the raw materials were examined by using Energy Dispersive X-ray Analysis (EDXA) technique and are given in Table 1.

Alkaline materials used in this study were sodium hydroxide (NaOH) and sodium silicate (Na_2SiO_3). The sodium hydroxide solution was prepared by dissolving sodium hydroxide pellets, from Fisher Scientific UK, in purified water with the desired concentration of 15 molar (M). Sodium silicate powder was also purchased from Fisher Scientific UK with an approximately SiO_2 to Na_2O ratio of 2.0. It was prepared to be a sodium silicate solution with a chemical composition of 48.20% solid and 51.80% purified water by mass.

3. Experimental procedures

The setting time test, with Vicat apparatus, of all fresh mixtures were performed immediately after the completion of mixing to define the initial and final setting time. The $40\text{ mm} \times 40\text{ mm} \times 160\text{ mm}$ prisms were used for both flexural and compressive strength test. All of samples were wrapped with plastic sheet after de-moulding and left in ambient temperature (18 to 22°C) until reach their testing age. The details of both mixing proportions and mixing processes are summarised as follows:

3.1. Combinations

3.1.1. Controlled OPC (OPC)

The controlled OPC paste was made of cement powder and the purified water with water to cement ratio (w/c) at its standard consistency of 0.25. In an ambient temperature, the synthesis started with mixing water and cement in accordance with the British Standard EN 196-3 for setting time test and EN 196-1 for compression test. After mixing, the fresh cement was placed in the prepared moulds.

3.1.2. Controlled geopolymer cement (GP)

The controlled geopolymer paste was composed of fly ash, sodium hydroxide and sodium silicate. The sodium hydroxide solution and sodium silicate solution were prepared and left over night before the mixing to ensure a full solution. The sodium silicate solution-to-sodium hydroxide solution (SS/SH) ratio by mass was 1.50. The alkaline solution-to-fly ash (A/FA) ratio used in the test was 0.40. Water-to-solids ratio was calculated by total mass of water in the mixture (the sum of the mass of water in the sodium silicate solution, sodium hydroxide solution and added water, if needed) to total mass of solid in mixture (the sum of the mass of fly ash, sodium hydroxide solids and silicate solids; mass of Na_2O and SiO_2 in sodium silicate solution). The mixing was done in an ambient condition with different designed manufacturing processes (described in Section 3.2). After mixing, the fresh geopolymer paste was placed in the prepared moulds.

3.1.3. Geopolymer-Portland cement (GeoPC)

The GeoPC was made from combination of geopolymer paste (GP) and OPC paste. The different combinations by mass of OPC-to-GP were prepared as details given in Table 2. The mixing was done in an ambient condition with process B. After that, the fresh combined paste was placed in the prepared moulds.

Table 1
Chemical composition of fly ash and OPC (% mass).

Materials	SiO_2	Al_2O_3	FeO	CaO	Na_2O	TiO_2	MgO	K_2O	SO_3
Fly ash	50.97	27.83	9.21	2.62	1.13	1.15	1.43	3.73	1.93
OPC	12.22	3.85	2.85	73.82	–	–	0.78	1.17	5.30

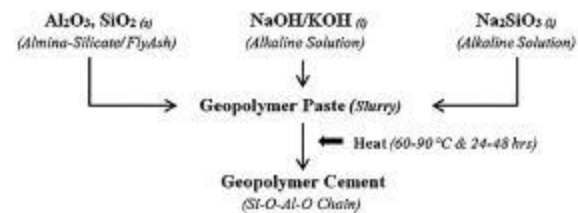


Fig. 1. Typical geopolymer manufacturing process.

3.2. Manufacturing processes

There were three different processes used in all controlled geopolymer paste synthesis, namely, the process A, B and C as follows: Process A: Fly ash was firstly mixed with sodium hydroxide solution in the standard mortar mixer for 90 s at low speed of $140 \pm 5\text{ rpm}$, then the mixer was stopped for 30 s to remove all the paste adhered to the wall and bottom part of the bowl and place it in the middle of the bowl. During this period, sodium silicate solution was added into the mixtures. After that, the mixer was restarted and run at low speed again for a further 90 s and, then placed the homogenous slurry in the moulds. Process B: Sodium hydroxide solution and sodium silicate solution were firstly prepared and left overnight before using in the experiment. Both of them were then mixed and stirred together for 60 s until becoming homogenous. This combined solution was then mixed with fly ash for 90 s in mixer at low speed. After 30 s stopping to remove all the paste adhered on the equipment, the mixer was restarted and run at low speed again for a further 90 s and then placed the homogenous slurry in the moulds.

Process C (Pre-dry-mixed process): Fly ash, sodium hydroxide and sodium silicate were firstly dry-mixed together. Then, the specific amount of water from the same concentration of alkaline solutions was calculated and used in the mixtures. The mixture was then mixed for 90 s at low speed and stopped for 30 s to remove all the paste adhered. The mixer was restarted and run at low speed again for a further 90 s before placing the homogenous slurry in the moulds. Testing diagram of synthesis processes is given in Fig. 2.

3.3. Analytical methods

To determine the setting time of each combination and manufacturing process, a Vicat apparatus was used in accordance with the British Standard BS EN 196-3:2005+A1:2008. In general, the quick setting directly relates to early strength development and load bearing capability of the cement paste. Compressive and flexural strength at early stage (3 day-age) were performed by using Instron Universal Testing Machine (UTM, 5989 Floor model) to measure the early strength development in accordance with the British Standard BS EN 196-1:2005, using $40 \times 40 \times 160\text{ mm}^3$ prisms. The testing results were simply reported in the unit of mega Pascal (MPa) for both flexural and compressive test. Scanning Electron Microscope (SEM), an ultra-high performance field emission scanning electron microscope Zeiss Supra 35VP, was used to observe the microstructures, particles and formations of specimens while the Energy Dispersive X-ray Analysis (EDXA) technique was used to define the chemical composition of raw materials. The X-ray diffraction (XRD) patterns were recorded on a Bruker D8 Advance diffractometer fitted with a Lynxeye XE high-resolution energy dispersive 1-D detector. The related research studies, however, were also used to analyse and explain the occurrences.

4. Results and Discussions

4.1. Curing process of GeoPC paste with different raw material combination

4.1.1. Setting times and setting behaviours

The testing series of setting time are the controlled OPC, controlled GP, GeoPC70, GeoPC50, GeoPC30, GeoPC10 and GeoPC5. It is interesting that high OPC content of GeoPCs have much lower setting time compared to whether OPC or GP. The initial setting time and final setting time of OPC were 138 and 196 min respectively, while controlled GP paste did not harden and could not be measured with Vicat needle in the first 24 h. It can be seen that the replacement by mass of OPC in geopolymer paste from 70%, 50% and 30% resulted in a fast setting of GeoPC, i.e. 11, 22, 13 min for initial setting times and 22, 32, 31 min for final setting time respectively. The longer setting times were required with less

Table 2
Details of OPC-to-GP mixtures and combinations.

Combinations	OPC:GP (% mass)	OPC (g)	Water (g)	FA (g)	Sodium silicate solution (g)	Sodium hydroxide solution 15 M (g)	Overall water-to-solid ratio
OPC	100:0	500.0	126.5	–	–	–	0.253
GP	0:100	–	–	500.0	120.0	80.0	0.191
GeoPC5	5:95	25.0	6.3	425.1	102.0	68.0	0.194
GeoPC10	10:90	50.0	12.6	402.7	96.7	64.4	0.197
GeoPC30	30:70	150.0	38.0	313.2	75.2	50.1	0.209
GeoPC50	50:50	250.0	63.2	223.8	53.7	35.8	0.221
GeoPC70	70:30	350.0	88.6	134.2	32.2	21.5	0.234

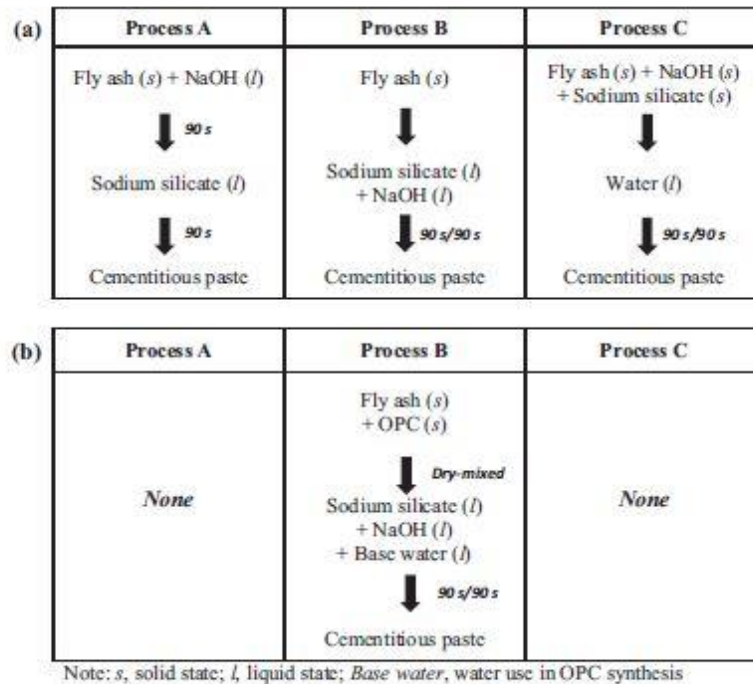


Fig. 2. Synthesis of (a) geopolymer and (b) geopolymer-Portland (GeoPC).

amount of OPC replacement of 10% and 5%, i.e. 87 and 255 min for initial setting times and 130 and 301 min for final setting time serially (Fig. 3).

(#6) For the study of setting behaviours of OPC and fly ash under alkalinity, OPC/fly ash (FA) was individually mixed with

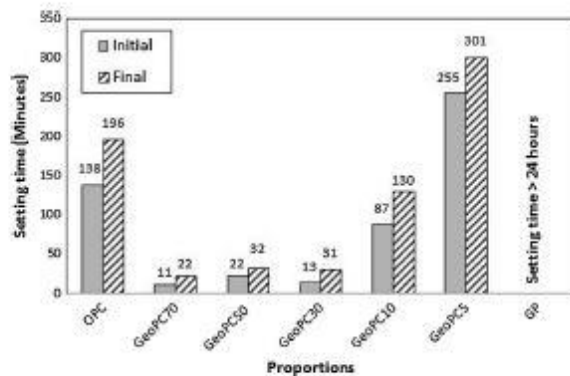


Fig. 3. Setting time of GeoPC paste.

sodium hydroxide solution (SH), sodium silicate solution (SS) and both of the solutions (SS + SH) to observe the reaction within alkaline environment. It was found that the OPC mode performs a rapid setting process, with ranking of the OPC with sodium silicate solution (OPC + SS, ~5 min) < OPC with sodium silicate and sodium hydroxide (OPC + SS + SH, ~5–10 min) < OPC with sodium hydroxide (OPC + SH, ~10 min), while the FA mode, FA with sodium silicate (FA + SS), FA with sodium hydroxide (FA + SH) and geopolymer (FA + SS + SH), could not set in the first 24 h (Fig. 4).

It can be seen that partial addition of OPC (Calcium source) directly affects the setting time of fly ash-based geopolymer paste. The contribution of calcium content in the system which obviously accelerates the setting of paste may be made from the calcium not only from OPC but also from GBFS, Ca(OH)₂, CaO or high calcium fly ash [8,10–12]. All Geopolymer-Portland cement systems (GeoPC) showed solidification much more significant than that occurring in pure geopolymer paste. It can be confirmed that the flash setting in OPC mode comes from a rapid chemical reaction between calcium mineral (in OPC) and alkaline activators, especially for sodium silicate (SS, Na₂SiO₃) rather than sodium hydroxide (SH, NaOH).

The exothermic reaction at early stage of the mixing may also provide the heat for the geopolymer mixture and hence further

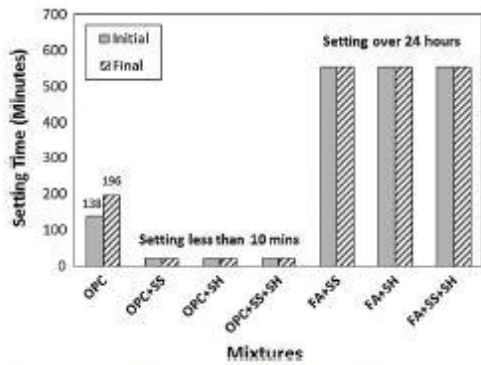


Fig. 4. Setting behaviours of OPC and FA in alkaline solutions.

accelerate the complex reactions within GeoPC system. Much shorter initial and final setting time of GeoPC70, GeoPC50 and GeoPC30 compared to those of GeoPC20 and GeoPC10 may reflect this effect, because the former may release sufficient heat for the requirement of active reaction of geopolymer. Nevertheless, it is evident that approximately 5–10 per cent of OPC replacement in geopolymers is able to provide similarly setting time as typical OPC.

4.1.2. Early strength

The compressive and flexural strength were conducted with three-day aged samples of process B for the controlled OPC, controlled GP, GeoPC70, GeoPC50 and GeoPC30. The early strength of GeoPC was closely related to the amount of OPC in the systems (Fig. 5). It is evident that although the addition of OPC to the Geopolymers is able to accelerate the curing process of GeoPC, the early strength of the GeoPC cannot reach to the level of that of OPC. The controlled OPC had the highest strength in both compression (48.77 MPa) and flexibility (5.30 MPa) in this study, while GP was not able to be tested in the first three days. The OPC replacement of 70%, 50% and 30% resulted in significant reductions of both mechanical strengths to 21.19, 14.07 and 13.80 MPa (Compression) respectively, and modulus of elasticity to 3.50, 2.54 and 1.07 MPa respectively.

Calcium mineral can affect an early strength development of fly ash-based geopolymers. In ambient conditions, the GeoPC system

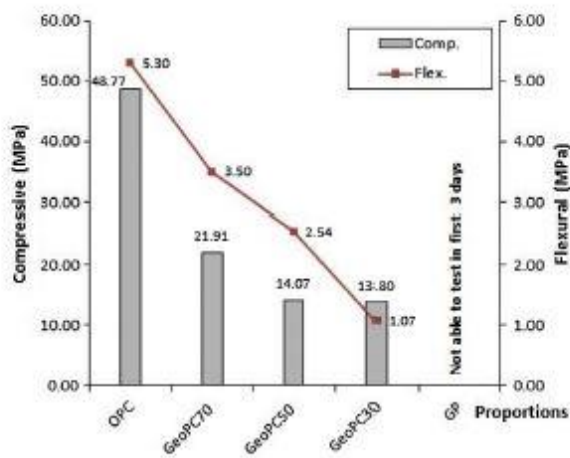


Fig. 5. Compressive and flexural strength with different proportions at 3-day aged.

may firstly form geopolymeric gel and followed by calcium silicate hydrate (CSH-main hydration product of Portland system) in the single binder of chemical reaction network. C–S–H gel in hydrated OPC generally achieves the strength after 5 h under alkaline condition or, alternatively, after formation of geopolymeric gel [13–15]. The combined formation was supported by Yip et al. (2008) which found that C–S–H formation tended to occur at low alkalinity in later stage. The network has less compact structure than OPC C–S–H phase, thus, lower strength was obtained [16,17]. Therefore, the early strength of GeoPC samples was developed due mainly to the quick reaction of calcium mineral and alkaline activators. In the GeoPC system, the strengthened structure was rapidly developed not only from chemical reaction inside the binder but also from an appropriate temperature of heat generated during mixing process [5,6] which gave rise to an increase of geopolymeric gel and such enhanced the mechanical strength in early stage [13,18]. This indicates that the heat release from the production may have accelerated the curing process of GeoPC.

(#3) In addition, the compressive strength was also carried out with the age of 7, 14 and 28 days. The results revealed a similar trend as occurred with the early strength, which increased when OPC replacement increased (Fig. 6).

4.1.3. Microstructure of GeoPC

Scanning Electron microscope (SEM) was used to analyze the microstructure of various GeoPCs made with the manufacturing process B and under the 28-day age. Some selected results of the microstructural observations of controlled OPC, GeoPC70, GeoPC30 and controlled GP are given in Fig. 7–10 respectively. It is apparent that GeoPC70 is less homogeneous than the controlled OPC, but its structure seemed to be denser and more compact than the controlled GP. For the GP cured in ambient conditions, both of the unreacted spherical ash particles and the geopolymeric matrix existed in the 28-days aged materials, which appeared as loose and amorphous structure. The presence of silica (Si), alumina (Al) and calcium (Ca) could also be observed and presented by typical EDX spectrum. Similarly as previous research of Dombrowski (2007), abundant unreacted fly ash particles still remained and surrounded by scattered geopolymeric gel, which results in lower mechanical strength than those cured under high temperature or even lower than the use of metakaolin as starting material [19]. Therefore, the early strength of the GeoPC70 was less than fully-hydrated OPC while would be much higher than both GeoPC30 and controlled GP.

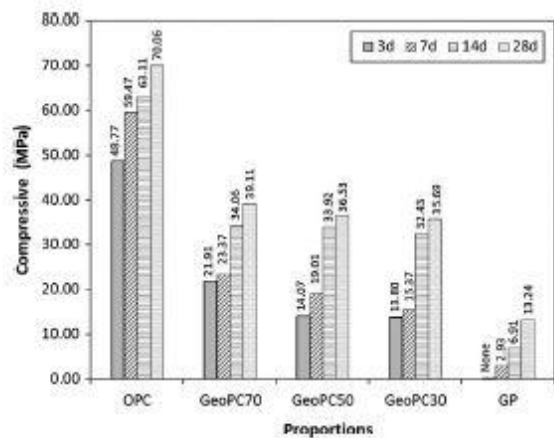


Fig. 6. Compressive strength of GeoPC systems at 3, 7, 14 and 28 days age.

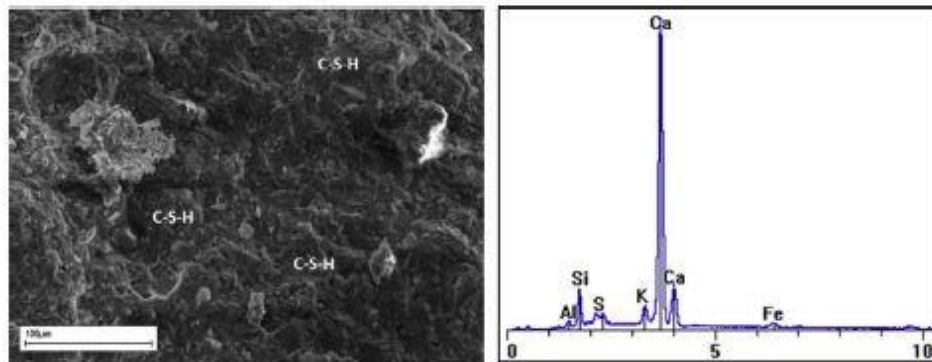


Fig. 7. SEM-EDX micrograph of controlled OPC (Si = 6.9%, Al = 1.0%, Ca = 83.1%).

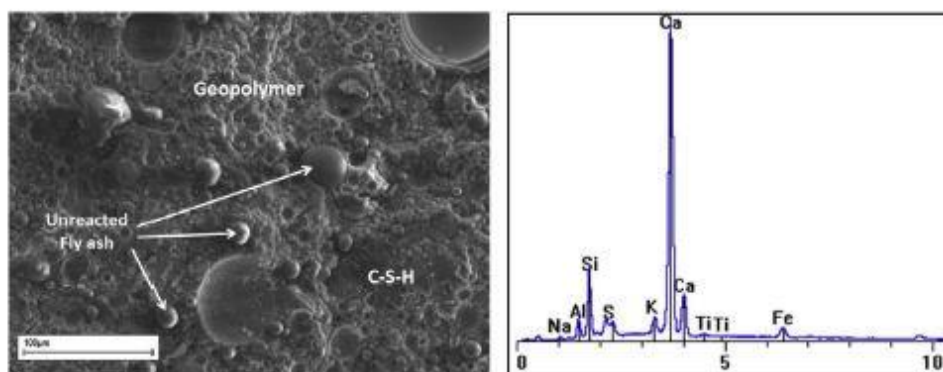


Fig. 8. SEM-EDX micrograph of GeoPC70 (Si = 10.4%, Al = 3.2%, Ca = 73.8%).

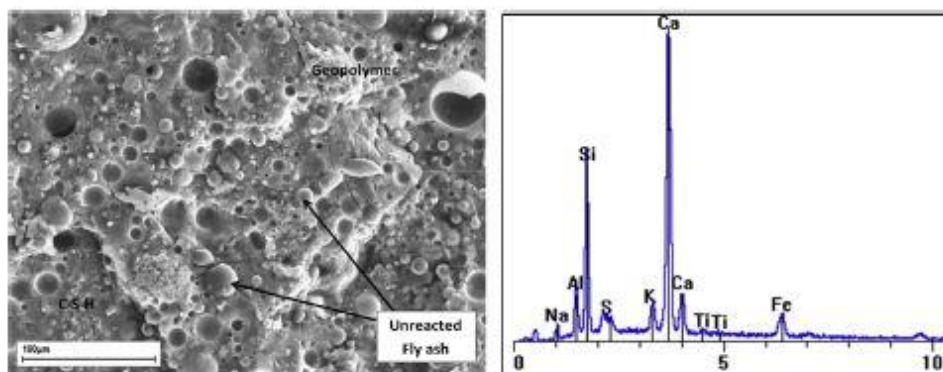


Fig. 9. SEM-EDX micrograph of GeoPC30 (Si = 21.2%, Al = 6.5%, Ca = 52.5%).

GeoPC30 micrograph shows more compact matrix and has less unreacted fly ash particles than controlled GP, although it has more porous structure than GeoPC70. This low calcium content could gain the majority formation of geopolymeric gel with partial CSH gel scattered in the entire network. The micrographs were found similar to the study of Skvara (2006) of using 60% fly ash with 40% ground slag (Slag is a calcium source). The fly ash-slag based geopolymers was also reported with the formation of both geopolymeric gel and C-SH, including unreacted slag particles by SEM [20].

In the system that main formation is geopolymeric gel, the lack of heat available results in weak bonding in early stage, therefore, low mechanical strength would be obtained. This negative charac-

teristic could be addressed to other small-to-none calcium content GeoPC in ambient curing conditions (GeoPC5 and GP). However, the strength of ambient-treatment geopolymers would develop over the time and undergo with both geopolymerization and hydration reaction [21].

As aforementioned, the coexistence of geopolymeric gel and C-S-H gel phase provided the fast setting behaviour due to the amount of calcium content, and the reaction of calcium content (from OPC) and alkaline has been considered for performing quick solidifying characteristics and resulting in the formation of two separate phases, geopolymers and C-S-H gel. This can further be confirmed from the C/S ratio tested in this study.

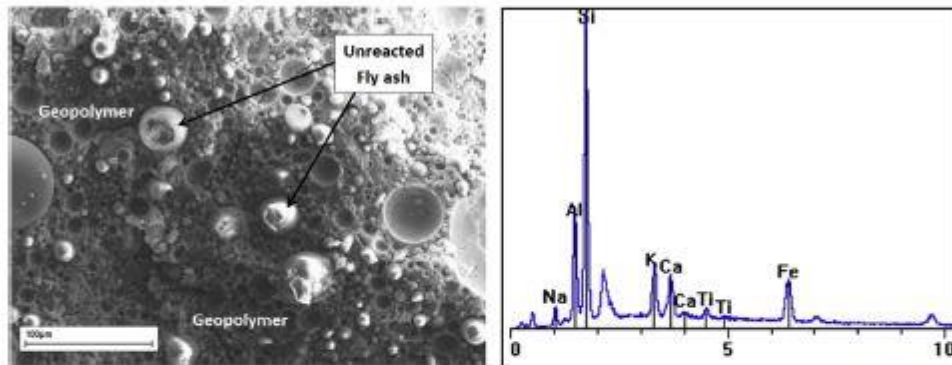


Fig. 10. SEM-EDX micrograph of controlled GP curing in ambient conditions (Si = 42.9%, Al = 15.1%, Ca = 7.8%).

Table 3
Oxide molar ratio of GeoPC combinations.

Combinations	Na ₂ O/ SiO ₂	Na ₂ O/ Al ₂ O ₃	SiO ₂ / Al ₂ O ₃	H ₂ O/ Na ₂ O	CaO/ SiO ₂
GP	0.16	0.57	3.58	8.50	0.05
GeoPC5	0.16	0.56	3.59	9.03	0.13
GeoPC10	0.16	0.56	3.61	9.62	0.21
GeoPC30	0.14	0.53	3.69	12.83	0.63
GeoPC50	0.13	0.49	3.82	18.59	1.26
GeoPC70	0.10	0.42	4.06	32.08	2.31

Table 3 shows the molar ratios between silicon, aluminium, sodium and calcium according to the combinations of OPC and geopolymer constituent added initially. From the EDX analysis, the CaO-to-SiO₂ (C/S) ratio increased with increase of OPC content in the mixes from C/S ratio of 0.13 in GeoPC5 up to 2.31 in GeoPC70, while C/S ratio of GP is 0.05. The C/S ratio had significant role in C-S-H formation which provides the fast setting behaviour and early strength to the cement. It can be seen from Fig. 11 that in ambient curing conditions, the shortened hardening period and good early strength development have improved with C/S ratio increased. The decrease in initial setting time and increase in early strength showed in power relation with a high degree of fits.

4.1.4. (#5) 4.1.4 XRD analysis of GeoPC

The XRD graphs of OPC, GeoPCs and GP are plotted in Fig. 12. The XRD pattern depicts the effect of OPC replacement in the GeoPC systems. It is well known that the hydrated OPC contains major crystalline phases of C-S-H gel phase, ettringite and portlandite while fly ash-based cement (GP) is a mixture of crystalline and amorphous phases [7,14,22]. The crystalline phases of quartz and mullite were detected as sharp peaks in geopolymer together with amorphous structure indicated by broad hump in the region of 20–35° 2θ. An increase of OPC replacement (from GeoPC30 to GeoPC70) led to a decrease in the intensity of quartz and mullite, while the evidence of C-S-H, C-A-S-H, N-A-S-H species (nepheline), hatrurite, calcite and portlandite appeared and consistently increased. The broad and amorphous hump were also found in the GeoPC systems, illustrating the coexistence of geopolymeric and hydrated OPC product in the single binder.

The appearance of N-A-S-H gel (nepheline) was found according to the high alkalinity of Na-containing solutions. The main composition of fly ash, silica and alumina, could form C-A-S-H phase with the available calcium mineral [7,14]. The findings can be drawn that the GeoPC system has a different reaction pathways depending on OH⁻ concentration and composition of starting materials, forming the coexistence of amorphous C-S-H/semi-crystalline phase (XRD

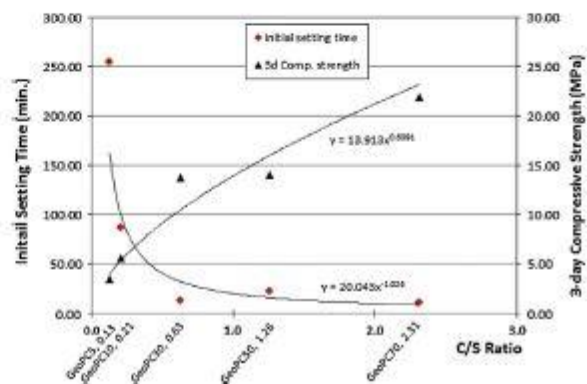


Fig. 11. The relationship among C/S ratios, Initial setting time and 3-day compressive strength.

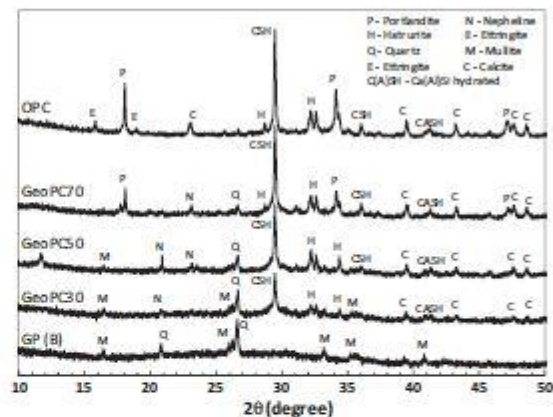


Fig. 12. XRD analysis of various GeoPC systems at the age of 28 days.

peak and hump) or N-A-S-H and C-A-S-H (main reaction product of fly ash activation) interfered in hydration product of GeoPC matrices [7,11].

It may be concluded that the self-cured GeoPC system had different formation from normal C-S-H gel in OPC or even geopolymeric gel in geopolymer cement. The quick forming of both amorphous C-S-H and semi-crystalline of geopolymeric network had initially structured when calcium mineral reacted with high

alkaline in the binder. The alkalinity of the pastes then decreased over the time, while the C–S–H gel increasingly formed in later state until the reaction completed. Eventually, for the final state of curing in ambient conditions, the GeoPC product will be a coexisted cross-linked network between geopolymeric and C–S–H structure in the single binder.

(#9) As aforementioned, the contribution of calcium content in the Fly ash-based geopolymer systems can be found by adding GBFS, $\text{Ca}(\text{OH})_2$, CaO, steel slag or even using high calcium fly ash. The mechanical properties, however, cannot reach the level of fully hydrated Portland cement or fully heat-cured geopolymer cement [6–12,23]. OPC, as a replacement material, has been chosen to be a calcium source in the systems due to the main reasons which are (i) OPC is widely and commercially available, (ii) OPC contains high potential energy compound (C_3A and C_2S), providing heat when hydrated and (iii) OPC is produced in accordance with any standard with dependable uniformity and quality. Although, OPC seems to exhibit negative manner against CO_2 reduction scheme, the maximum replacement in GeoPC systems would not be more than 30% to maintain setting behaviour and workability.

4.2. Curing process of GP with different manufacturing processes

Three different processes have been uniquely investigated in relation with specific combinations. Process A focused on the adding sequence of alkaline activators while the process B was on the process of raw material with the pre-mixed alkaline solubles. Another new route of geopolymer synthesis was also introduced in this research with pre dry-mixed of all solid materials, and then just added with water later as named the Process C. The manufacturing processes A and B have been used to prepare geopolymer due to the simply use of the dissolved alkaline solutions, including its disassociated into ion forms. However, for more convenient in practical work, process C (pre dry-mixed) seems to be more efficient in real-life operation than process A and B.

The heat generated from the dissolving solid alkaline may have an influence on the curing process of the geopolymer, such the heat liberation over the chemical reaction was investigated when dry materials react with water. Fig. 13 shows the results of heat evolution of those three alkaline preparations. It can be seen that in the first 5 min, NaOH 15 M, NaOH 10 M and sodium silicate reached

their maximum temperature at 93.0, 85.0 and 46.0 °C respectively. The temperature then steadily decreased to room temperature in approximately 4 h. The heat emitted from this hydration occurred due to the result of the chemical species being taken to lower energy state. It is apparent that NaOH dissolution produces more heat than sodium silicate and, in addition, the higher the concentration of NaOH, the higher temperature it generates. The results indicate that the processing procedures may result in an effect on the curing process of geopolymer as different procedures will give rise to different temperature/energy to the mixtures. The proposed process C, the dry-mixed method, may be able to produce sufficient heat during its hydration for a heat based- self cured geopolymer cement production.

4.2.1. Setting time of GP with different manufacturing processes

For the geopolymer paste (GP), it was found that all of manufacturing processes (A, B and C) were not able to produce geopolymer paste sufficiently for the setting time measurement in the first 24 h, while the process C clearly liberated much more heat and solidified faster than A and B. Fig. 14 shows the drying behaviour of process B (Fig. 14a) and process C (Fig. 14b) after leaving in the room temperature for 1 h. The plunged needle illustrated the wet, viscous and adhesive characteristics of process A and B, while the needle-hole was marked on the stiff cement of process C. (#7) In addition to specimens mass, heat loss and moisture loss, it can be clearly seen that the pre dry-mixed process (C) has a great potential of increasing the curing temperature itself during the synthesis, which would be at least one of main reasons for the self-curing process of geopolymer in the ambient conditions. Nevertheless, the influence of curing temperature was discussed in more details in the next Section 4.2.2.

4.2.2. Early strength of GP with different manufacturing processes

As aforementioned, all of GP pastes could not set in the first 3 days, therefore, the early strength testing was carried out at the 7th day. For the 7 day-aged geopolymer pastes, process A gained the highest compressive strength (4.75 MPa) and flexural strength (0.49 MPa), followed by process B of 2.93 MPa (compressive) and 0.41 MPa (Flexural). The lowest strength capability was from the process C with 2.35 MPa (compression) and 0.37 MPa (Flexibility) (Fig. 15).

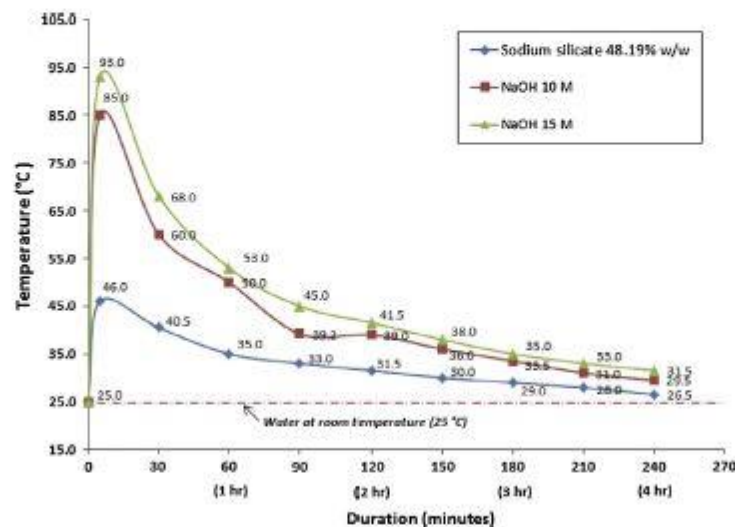


Fig. 13. Temperature of alkaline solution preparation.

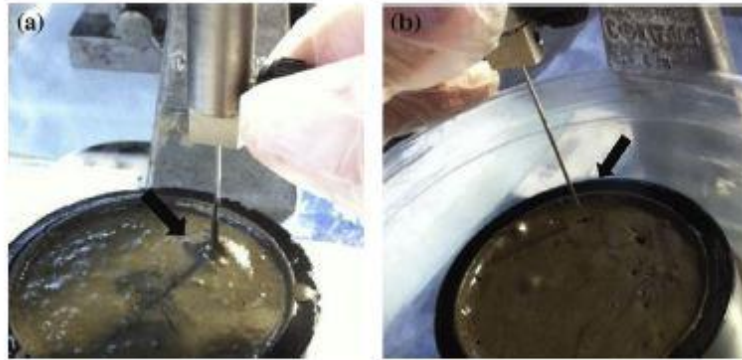


Fig. 14. Drying behaviour after 1 h of mixing process B (a) and process C (b).

It has been reported that the different manufacturing processes or mixing orders are able to produce different mechanical properties of the geopolymer cementitious products due to the unique characteristic and sequence of expedient formation [24,25]. The structural formation of GP was very slow in the ambient curing conditions, therefore, a prolonged period of time was required for the paste solidification (over 24 h). Uncompleted reaction of geopolymeric gelation obviously affected the early strength of geopolymer paste. In this study, although the process A had a very slow setting time, the GP paste gave the highest compressive strength due to more dissolution rate (from first mixed of hydroxide soluble) and more binder forming (from later added of silicate soluble). Process B obtained very similar setting time as process A, but the early compressive strength was lower. Although the combined alkaline solutions used in process B provided a better uniformity, the structural formation appeared to be inert and led to low mechanical properties [5,26]. During the fabrication, the process C seemed to be very hot and solidify much more intensively than that occurred in the process A or B. It might be due to the strong hydration among starting solids, alkaline materials and water in the system [14]. Moreover, the heat generated from the mixing of alkaline with water can lead to rapid loss of water content and fast set as happened in the mild-to-high temperature [11,20].

Without moisture loss protection, the formation of micro-cavities or porous structure has been left in the network after substantially and rapidly loss of water content [27]. Moreover, as alkaline activators used were in powder form, the dissolution might not as complete as use of alkaline solution. These causes led to a decrease

in mechanical strength, although the heat generated during preparation process provides a positive effect to the cement samples in term of curing [8,28]. This result was clearly supported by the analysis of Fourier Transform Infrared spectroscopy, FTIR and SEM in microstructure observation. Therefore, the early strength of process C was the lowest. (#4) The compressive strength at 14 and 28 days age was also carried out and given in Fig. 16. The strength developed with the time and the effects of the processes on the strength were similar to those on the early strength, with the highest compression being obtained by process A, followed by process B and C respectively.

(#8) With the general assumption of room temperature at around 20 ± 2 °C, numerous research papers have reported that the temperature around 40–60 °C can enhance the mechanical properties of fly ash-based or slag-based geopolymer cement, while the strength would be slightly enhanced at the curing temperature above room temperature (e.g. 25–30 °C) for a period of 24 h. However, very high heat curing (e.g. over 80 °C) can give negative effects to geopolymer properties due to a rapid loss of moisture content and micro-cavities in the structure [5,8,12,13,18,28–31]. Nevertheless, the appropriate or optimum curing temperature may be considered in a broad range, depending on the properties of starting materials. It has also been reported that applying mild temperature (around 30–40 °C) from external source, e.g. pre-heated alkaline solution [32], exposure to sunlight [33] and self-internal heat of massive amount-pouring [34] would also enhance the strength development of the geopolymers [11]. By this, the pre

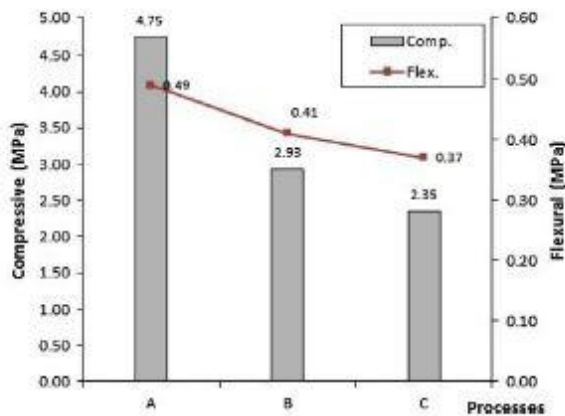


Fig. 15. Strength of geopolymer paste with different processes at 7-day aged.

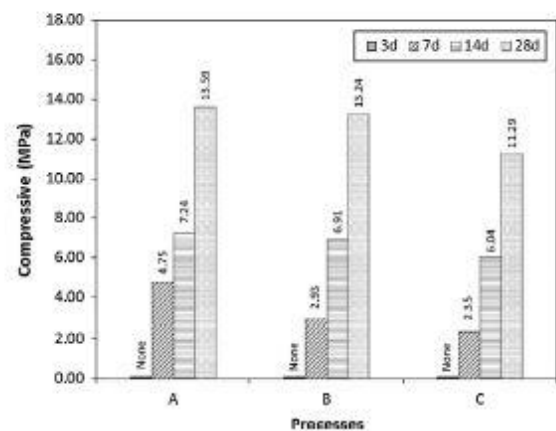


Fig. 16. Strength of geopolymer paste with different processes at 7, 14 and 28-day aged.

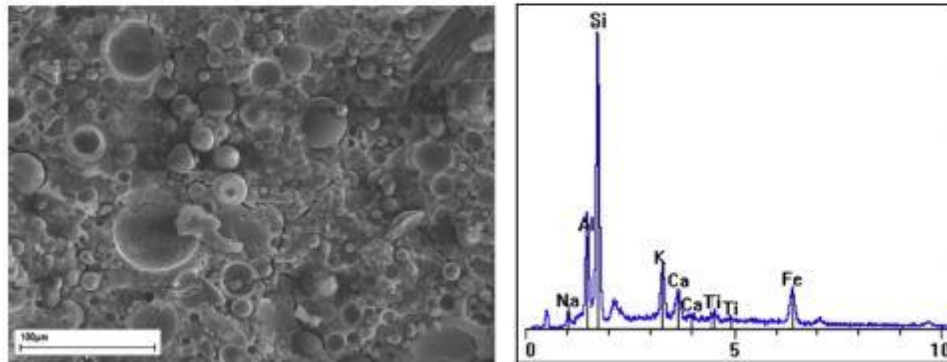


Fig. 17. SEM-EDX micrograph of GP process A curing in ambient conditions (Si = 45.8%, Al = 14.8%, Ca = 6.5%).

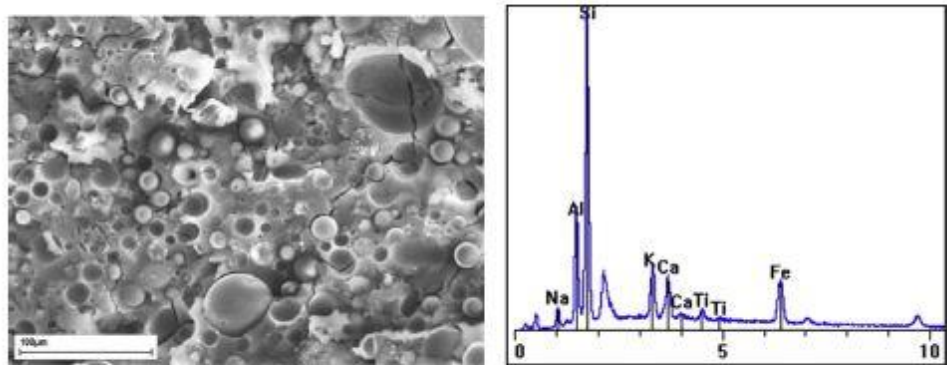


Fig. 18. SEM-EDX micrograph of GP process B curing in ambient conditions (Si = 42.9%, Al = 15.1%, Ca = 7.8%).

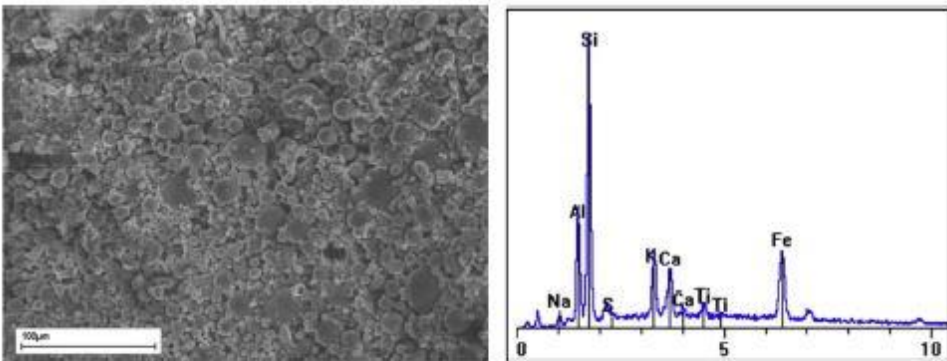


Fig. 19. SEM-EDX micrograph of GP process C curing in ambient conditions (Si = 34.0%, Al = 13.7%, Ca = 8.0%).

dry-mixed process (C) can be further developed or neatly combined with these mild curing approaches.

4.2.3. Microstructure of GP with different manufacturing procedures

The 28 day-aged GP produced with process A and B shows very similar appearance as porous and amorphous structure with some of unreacted fly ash particles surrounded by scattered geopolymeric gel, while the process C revealed loose structure with abundant of unreacted spherical ash particles. Therefore, higher mechanical strength was obtained by process A and B than process C, even though their mineral compositions (Si, Al, Ca) were quite similar as shown in Fig. 17–19.

4.2.4. XRD analysis of GP with different manufacturing procedure

The results of geopolymer manufactured with process A, B and C are given in Fig. 20. The major phase of all processes was amorphous as indicated by broad hump at the region of $20\text{--}35^\circ 2\theta$. The crystalline phases contained in all pastes were mullite, quartz and hematite. From the qualitative XRD, it is difficult to identify the amount of reaction products or to clearly define the effect of manufacturing process. However, with the obtained XRD patterns, there was little difference among process A, B and pre dry-mixed process (C). The manufacturing process provided very little effect on the primary phase identification of crystalline materials. Therefore, the effect of GP production processes may be more visible

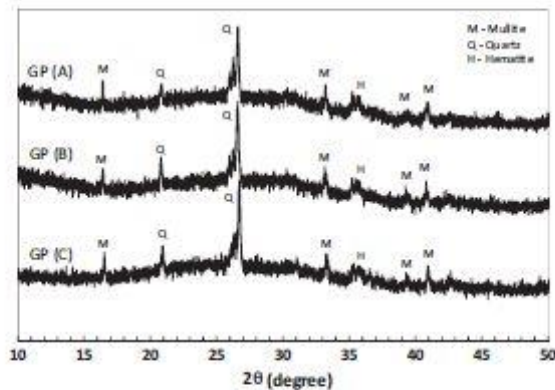


Fig. 20. XRD analysis of geopolymer process A, B and C at the age of 28 days.

from the results of the mechanical strength and micro-structural formation as aforementioned in SEM micrographs.

Consequently, it can be summarised that the manufacturing processes which could achieve the quickest setting characters was the process C, while the process A and B took longer time of setting. The highest early strength was obtained by the process A while the lowest early strength was obtained by the process C. The coexistence of geopolymeric gel and C–S–H gel phase in ambient conditions, which have also been proven by NMR spectroscopy, obviously influenced both setting time and mechanical strength of the binder [15]. Eventually, with manufacturing of pre dry-mixed process (C), another research direction has been proposed to develop “Just Adding Water” geopolymer as previous work on just adding water to calcined kaolin cement powder [35].

5. Conclusions

(1) In different proportions, it can be seen that the setting time of geopolymer is reduced when the amount of OPC increase from over 24 h to 4, 1.5 and 0.5 h by replacing OPC of 5%, 10% and 30% respectively. The early strength (3 day-aged) of specimens increase when amount of OPC increase from 0 to 14.07, 15.52 and 21.91 MPa of 100%GP, 30%OPC, 50%OPC and 70%OPC respectively. The results show that more forming of amorphous C–S–H gel (from calcium source of OPC) stimulates shorten setting behaviour and improve more early strength with denser matrices to the system, confirmed by SEM-EDX micrographs.

(2) In different manufacturing processes of 100% geopolymer paste with process A, B and C, it can be seen that all processes cannot set in the first 24 h. Only process C that seems to be more solidifying and stiffer after 1 h of mixing while, in the same time, release a lot of heat to environment. The mechanical strength test can be done at 7 day-aged with the highest strength of process A followed by Process B and C. It can be concluded that process A and B achieve more early strength due to more structure forming activities between starting materials and alkaline solutions, while process C showed many unreacted fly ash particles remaining with incomplete formation as alkaline powder was used. Loose structure and micro-cavities also appeared in matrices due to the rapid loss of moisture by its internal heat generation.

Overall, it can be proposed that the setting time and early strength of this cementing system can be controlled by adding some amount of calcium content (GeoPC systems) and, in addition, the mixing sequence and state of materials (different manufacturing process) can directly affect to properties of geopolymer cement. (#2) The main outcomes of this study are (i) to introduce a feasible production of GeoPC systems and (ii) to gain advantages of pre dry-

mixed process (C) in term of high potential heat liberation (beneficial effect on GP curing purpose) and concise the manufacturing process by just adding water to activate cementitious reaction. The further investigations could be addressed to the combination of these two approaches in ambient temperature, which is called “Self-cured geopolymer” and be addressed to on-site operation such as infrastructure works with in the minimum requirement for any standard.

References

- [1] Maholtra VM. Introduction: sustainable development and concrete Technology. *ACI Concr Int* 2002;24(7).
- [2] Dimas D, Giannopoulou IP, Panias D. Polymerization in sodium silicate solutions: a fundamental process in geopolymerization technology. *J Mater Sci* 2009;44:3719–30.
- [3] Rajiwala OB, Path HS. Geopolymer Concrete: a Green Concrete. In: 2nd international conference on chemical, biological and environmental engineering (ICBEE 2010); 2010, pp. 202–06.
- [4] Turner IK, Collins FG. Carbon dioxide equivalent (CO₂-e) emissions: a comparison between geopolymer and OPC cement concrete. *Constr Build Mater* 2013;43:125–30.
- [5] Hardjito D, Cheak CC, Ing CHL. Strength and setting times of low calcium fly ash-based geopolymer mortar. *Mod Appl Sci* 2008;2(4):3–11.
- [6] Nath P, Sarker PK. Geopolymer concrete for ambient curing condition. The Australasian Structural Engineering Conference 2012 (ASEC 2012), Perth, Western Australia; 2012.
- [7] Palomo A, Fernández-Jiménez A, Kovalchuk G, Ordoñez LM, Naranjo MC. Opfly ash cementitious systems: study of gel binders produced during alkaline hydration. *J Mater Sci* 2007;42:2958–66.
- [8] Chindaprasit P, Chareerat T, Hatanaka S, Cao T. High-strength geopolymer using fine high-calcium fly ash. *J Mater Civil Eng (ASCE)* 2011;264–70.
- [9] Hu S, Wang H, Zhang G, Ding Q. Bonding and abrasion resistance of geopolymeric repair material made with steel slag. *Cem Concr Compos* 2008;30:239–44.
- [10] Nath P, Sarker PK. Effect of GGBFS on setting, workability and early strength properties of fly ash geopolymer concrete cured in ambient condition. *Constr Build Mater* 2014;66:163–71.
- [11] Yip CK, Luky GC, Provis JL, Van Deventer JS. Effect of calcium silicate sources on geopolymerisation. *Cem Concr Res* 2008;38:554–64.
- [12] Chindaprasit P, Chareerat T, Sirivivatnanon V. Workability and strength of coarse high calcium fly ash geopolymer. *Cem Concr Compos* 2007;29:224–9.
- [13] Alonso S, Palomo A. Alkaline activation of metakaolin and calcium hydroxide mixtures: influence of temperature, activator concentration and solids ratio. *Mater Lett* 2001;47:55–62.
- [14] Tailly J, Mackenzie KJD. Structure and mechanical properties of aluminosilicate geopolymer composites with Portland cement and its constituent minerals. *Cem Concr Res* 2010;40:787–94.
- [15] Yip CK, Van Deventer JS. Microanalysis of calcium silicate hydrate gel formed within a geopolymeric binder. *J Mater Sci* 2003;38:3851–60.
- [16] Lecante I, Henrist C, Liegeois M, Maseri F, Rulmont A, Cloots R. (Micro-) structural comparison between geopolymers, alkali-activated slag cement and Portland cement. *J Euro Ceram Soc* 2006;26(16):3789–97.
- [17] Yip CK, Luky GC, Van Deventer JS. The coexistence of geopolymeric gel and calcium silicate hydrate at the early stage of alkaline activation. *Cem Concr Res* 2005;35:1688–97.
- [18] Rovnarik P. Effect of curing temperature on the development of hard structure of metakaolin-based geopolymer. *Constr Build Mater* 2010;24:1176–83.
- [19] Dombrowski K, Buchwald A, Weil M. The influence of calcium content on the structure and thermal performance of fly ash based geopolymers. *J Mater Sci* 2007;42:3033–43.
- [20] ŠKVRÁ F, KOPECKÝ L, NĚMČEK J, BITTŇAR Z. MICROSTRUCTURE OF GEOPOLYMER MATERIALS BASED ON FLY ASH. *Ceramics – Silikáty*, vol. 4; 2006, p. 208–15.
- [21] Divya K, Rubina C. Mechanism of geopolymerization and factors influencing its development: a review. *J Mater Sci* 2007;42:729–46.
- [22] Nath SK, Mukherjee S, Maitra S, Kumara S. Ambient and elevated temperature geopolymerization behaviour of class F fly ash. *Trans Indian Geol Soc* 2014;73(2):126–32.
- [23] Temuujin J, Van Riessen A, Williams R. Influence of calcium compounds on the mechanical properties of fly ash geopolymer pastes. *J Hazard Mater* 2009;167:82–8.
- [24] Torgal FP, Gomes JC, Jalali S. Alkali-activated binders: a review. Part 2. About materials and binders manufacture. *Constr Build Mater* 2008;22:1315–22.
- [25] Kobera L, Slavík R, Koloušek D, Urbanová M, Kotek J, Brus J. Structural stability of aluminosilicate inorganic polymers: influence of the preparation procedure. *Ceramics – Silikáty* 2011;55(4):343–54.
- [26] Palomo A, Blanco-Varela MT, Granizo ML, Puertasa F, Vazquez T, Grutzeck MW. Chemical stability of cementitious materials based on metakaolin. *Cem Concr Res* 1999;29:987–1004.
- [27] Songpiriyakij S, Kulprasit T, Jaturapitakul C, Chindaprasit P. Compressive strength and degree of reaction of biomass- and fly ash-based geopolymer. *Constr Build Mater* 2010;24:236–40.

- [28] Van Jaarsveld JGS, Van Deventer JSJ, Lukey GC. The effect of composition and temperature on the properties of fly ash- and kaolinite-based geopolymers. *Chem Eng J* 2002;89:63–73.
- [29] Reddy DV, Edouard JB, Sobhan K. Durability of Fly ash-based geopolymer structural concrete in the marine environment. *J Mater Civil Eng* 2012;25(6):781–7.
- [30] Hounsi AD, Lecomte-Nana GL, Djétéli G, Blanchart P. Kaolin-based geopolymers: effect of mechanical activation and curing process. *Constr Build Mater* 2013;42:105–13.
- [31] Hardjito D, Wallah SE, Sumajouw DMJ, Rangan BV. Factors influencing the compressive strength of fly ash-based geopolymer concrete. *Civil Eng Dimension* 2004;6(2):88–93.
- [32] Dutta D, Chakrabarty S, Bose C, Ghos S. Evaluation of geopolymer properties with temperature imposed on activator prior mixing with fly ash. *Int J Civil Struct Eng* 2012;3:205–13.
- [33] Nuruddin MF, Kusriantoro A, Qaz SA, Shafiq N. Utilisation of waste material in geopolymeric concrete. *Constr Mater* 2011;164(CM6):315–27.
- [34] Vaidya S, Diaz B, Allouche EN. Experimental evaluation of self-cure geopolymer concrete for mass pour application. *World of Coal Ash (WOCA) Conference – May 9–12, 2011 Denver, CO, USA*; 2011.
- [35] Liew YM, Kamarudin H, Mustafa A1, Bakri AM, Luqman M, Nizar IK, Ruzaidi CM. Processing and characterization of calcined kaolin cement powder. *Constr Build Mater* 2012;30:794–802.



Internal heat liberation and strength development of self-cured geopolymers in ambient curing conditions



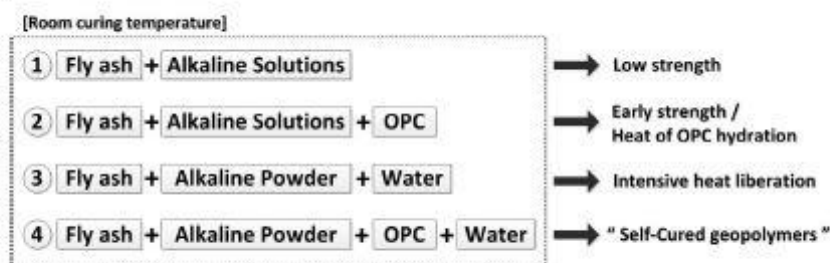
Teewara Suwan, Mizi Fan*, Nuhu Braimah

College of Engineering, Design and Physical Sciences, Brunel University, Uxbridge, UB8 3PH London, United Kingdom

HIGHLIGHTS

- Inclusion of OPC increased early strength and shortened setting time of GeoPC system.
- Heat liberation in GeoPC system was mainly influenced by (inclusion) OPC hydration.
- Pre dry-mixing process released intensive heat when reacted with water.
- Pre dry-mixing process provided ability for practical work and in-field applications.
- GeoPC system and Pre dry-mixing could achieve the Self-cured GP production.

GRAPHICAL ABSTRACT



ARTICLE INFO

Article history:

Received 1 November 2015

Received in revised form 24 March 2016

Accepted 29 March 2016

Keywords:

Ambient curing

Heat liberation

Manufacturing procedure

Microstructure

Self-cured geopolymers

ABSTRACT

Curing geopolymers with a temperature around 40–90 °C can significantly improve the mechanical properties and mechanisms of reaction. There is a challenge to develop GP with its abilities of curing in ambient temperature (22 ± 2 °C) without external source of heat supply for on-site practices. This study is extended from the previous research work on the influence of OPC inclusion and manufacturing process. The main aim is to study and evaluate the effects of additional OPC (GeoPC system) and manufacturing procedures on accumulated-internal heat liberation and strength development of low calcium fly ash-based geopolymer paste. The results showed that the GeoPC compounds and manufacturing procedures were closely related to the curing process, internal heat, microstructure development and hence properties of the end products. Both optimum GeoPC mixtures and new-introduced mixing method (pre dry-mixing) have been generated, providing clear potential and basis of the development of self-cured geopolymers to achieve the mechanical strength and for on-site construction under ambient conditions.

© 2016 Published by Elsevier Ltd.

1. Introduction

Ordinary Portland cement (OPC) is an energy consuming product with high carbon dioxide (CO₂) emission along its production process. To reduce the amount of greenhouse gas, alternatives have been studying to partially or totally replace the consumption of

OPC [1]. Many research studies have revealed that fly ash, blast furnace slag and other aluminosilicate materials can be used as prime materials to produce a cementitious binder by activating with alkaline solutions, which is known as alkaline-activated cement or geopolymer cement [2–5]. Due to the complexity of various factors affecting its reaction, the definite mechanism of the alkaline-activated cement is not yet fully understood. However, many researchers agree that its mechanism consists of three-stage model which are dissolution, gelation and polymerization/hardening

* Corresponding author.

E-mail address: mizi.fan@brunel.ac.uk (M. Fan).

[6,7]. Apart from that, the term “Geopolymers” (by Davidovits J., 1979) is also used and receives much more attention as an alternative binder for construction material [8,9]. The final reaction products of those systems can be C-S-H (Ca + Si), zeolite/polymers (Si + Al) or C,N-A-S-H (Ca,Na + Al + Si) which mainly depend on the characteristics of raw starting materials and alkaline activators [6,10–17].

In construction sector, Geopolymers (GP) is developed and theoretically produced by utilising industrial by-products or wastes such as fly ash, silica fume or even agro-waste ashes. Fly ash, a by-product from coal-fired power station, seems to be the most widely used prime material for the production of geopolymers because of its richness in alumina-silica composition and the considerable un-utilised quantity [18]. The most commonly used alkaline materials are a combination of sodium hydroxide or potassium hydroxide (NaOH, KOH) with sodium silicate or potassium silicate (Na_2SiO_3 , K_2SiO_3) [8,19]. Curing condition is one of the major factors affecting the mechanical properties and micro-structures of geopolymers. At ambient temperature around 20–25 °C, fly ash-based geopolymers does not completely harden and could not be tested on compressive strength in the first day after synthesis [20,21]. Somehow, it has been found to achieve very high strength in both early and later stages when cured in high temperature e.g. 40–90 °C [2,3,22–24]. Furthermore, some of its properties have also been reported to be similar as or even better than those of OPC [4,18].

A numerous researchers have studied on the improvement of setting and strength properties of fly ash-based geopolymers without high temperature curing. The considered challenge is to step over the limitation of heat curing process: precast components, and to be more convenient in practical works or in field applications. Some additives such as ground granulated blast furnace slag, gypsum, Portland cement or even high calcium fly ash are studied in order to enhance the reasonable strength development in ambient curing conditions [14,18,25–28]. The use of OPC as an additive in geopolymers is widespread due to its uniformity complied with any standard and its global availability as a commercial construction material. This hybrid cementitious system is generally classified as an alkali-activated Portland blended cements or alkali-activated Portland fly ash cement [29] or, sometimes, called Geopolymer-Portland cement (GeoPC) [21]. Incorporating Portland cement to the system leads to significant effects on the setting behaviour and early strength development. The extra heat liberated by exothermic reaction of OPC and water could also provide a positive effect enhancing its mechanical properties and microstructures [10].

Another latent factor influencing the properties of geopolymers is mixing order. It is confirmed that the optimum/proper mixing order leads to better results, especially for any alkaline-activated binder [19,30]. For general mixing, alkaline solutions (e.g. NaOH and Na_2SiO_3) are firstly prepared and left over-night to confirm a complete dissolution. Prime materials and those alkaline solutions are incorporated and mixed together at the same time [31–34]. Apart from that, the separate mixing is also studied. Hydroxide soluble (e.g. NaOH) is initially mixed with prime materials, and subsequently added by silicate soluble (e.g. Na_2SiO_3) [17,25,34,35]. Those two aforementioned procedures, general mixing and separate mixing, provided a satisfactory result as fully dissolved alkaline activators are used. However, the separate mixing process seemed to get slightly higher strength than that of normal mixing. As the initial mixing with NaOH solution led to a high rate of leaching, more silica, alumina and other ions from prime materials are therefore obtained, leading to more degree of geopolymerization [31,34,36,37]. In addition, pre-dry mixed process (working with solid activators instead of alkaline solutions) was proposed to be developed by just mix with water [29]. The attempts to simplify

geopolymers mixing process, by crushing fully-activated final product into powder, and adding water to re-activate the reaction again as called “one-part geopolymers” or “just adding water geopolymers”, were also studied [38–40]. With the pre dry-mixed process, extra water in the system might be required in order to sufficiently activate all solid materials, therefore, low mechanical strength may be obtained by the increase of water-to-solid (w/s) ratio. However, the main aims of the development of this dry-mixed process should be primarily focused on its advantages in term of practical work in field applications, and properties.

The previous work, from our intensive study on self-curing geopolymers, concluded that the self-cured geopolymers could be developed with the setting time and early strength being affected by the OPC replacement and the manufacturing procedures [21]. The main aim of this paper is to study and evaluate the effects of additional OPC (GeoPC system) and potential manufacturing procedures (pre dry-mixing process) on accumulated-internal heat liberation and strength development of low calcium fly ash geopolymer paste as “Self-cured geopolymers”.

2. Materials

Coal-fired fly ash was supplied by the Drax power station, North Yorkshire, UK. Its properties comply with BS EN 450-1:2012, fineness category S and loss on ignition category B (similar to low calcium fly ash class F specified by ASTM: C618). OPC was commercial CEM II/A-L under the brand name of Cemex. The chemical compositions of fly ash and OPC were examined by using the Energy dispersive X-ray Analysis (EDXA) technique and are summarised in Table 1. Alkaline materials used in this study were sodium hydroxide (NaOH) and sodium silicate (Na_2SiO_3). The sodium hydroxide pearl was purchased from the Fisher Scientific, UK and prepared as a solution with the concentration of 15 M (M). Sodium silicate powder was also purchased from the Fisher Scientific, UK with a SiO_2 to Na_2O ratio (M, Modulus) of 2.0. The sodium silicate solution with 48.20% w/w was used in the experimental work. To prepare sodium silicate solution, solid powder was weighted in the container and filled with the designated amount of purified water (e.g. 48.20 g of sodium silicate powder and 51.80 g of purified water).

3. Experimental details

3.1. Mixture designation of OPC, geopolymers and GeoPC pastes

OPC paste was made of cement powder and the purified water with the water-to-cement ratio (w/c) at its standard consistency of 0.25. Geopolymer paste was manufactured with general mixing process (process B, see Section 3.2) and composed of fly ash, sodium hydroxide and sodium silicate. The sodium hydroxide and sodium silicate solutions were prepared and left overnight before uses to ensure a thorough solution achieved. The sodium silicate solution-to-sodium hydroxide solution (SS/SH) ratio by mass was 1.50 and the constant alkaline liquid-to-fly ash (A/FA) ratio by mass was 0.40. A series of Geopolymer-Portland cement paste (GeoPC) was made from the designation mass of GP and OPC paste in general mixing process (process B, see Section 3.2). The mass of each material used, including alkaline solution and water, was calculated individually from the designed GP and OPC pastes (e.g. GeoPC30 is composed of 70% GP-paste and 30% OPC-paste). The mass of each material used in GeoPC system, including alkaline solution and water, was calculated individually from the designed GP and OPC pastes). A standard mortar mixer with speed of 140 ± 5 rpm was used to synthesize each mixture in a ambient temperature of 18–22 °C. It is noted that the GeoPC mixtures which have OPC replacement from GeoPC30 to GeoPC90 were synthesized with 4% added-water in order to obtain the workability in practical work.

Table 1
Chemical composition of fly ash and commercial OPC.

Materials	SiO ₂	Al ₂ O ₃	FeO	CaO	Na ₂ O	TiO ₂	MgO	K ₂ O	SO ₃
Fly ash	50.97	27.83	9.21	2.62	1.13	1.15	1.43	3.73	1.93
OPC	12.22	3.85	2.85	73.82	–	–	0.78	1.17	5.30

3.2. Manufacturing process of geopolymer paste

3.2.1. Separate mixing process (A): fly ash + NaOH solution, then Na₂SiO₃ solution

Fly ash was firstly mixed with sodium hydroxide solution for 90 s to form slurry. The mixer was then stopped for 30 s to remove all the paste adhered to the wall and the bottom to the middle part of the bowl. During this period, sodium silicate solution was added into the mixer and mixed together for another 90 s. After well-mixing, the homogenous slurry was placed in the prepared moulds.

3.2.2. General mixing process (B): prime material(s) + mixed NaOH and Na₂SiO₃ solutions

Sodium hydroxide and sodium silicate solutions were firstly prepared and mixed together until becoming homogenous before uses. To mix GeoPC, the designated amount of OPC powder and fly ash were initially dry-mixed together for 90 s in the mixer. Then, the combined solution (plus OPC-water for GeoPC mixture) was then mixed with prime material(s) for 90 s. The mixer was then stopped for 30 s to remove all the paste adhered to the wall and the bottom to the middle part of the bowl. Then, the mixer was restarted again and run for further 90 s. After well-mixing, the homogenous slurry was placed in the prepared moulds.

3.2.3. Pre dry-mixing process (C): fly ash + alkaline solids, then add with water

Fly ash, sodium hydroxide pearl and sodium silicate powder were firstly dry-mixed together. The specific amount of water based on the same ratio of water-to-solid as those used in the process A and B was then added in the mixture and mixed together for 90 s. The mixer was then stopped for 30 s to remove all the paste adhered to the wall and the bottom to the middle part of the bowl. Then, the mixer was restarted again and run for further 90 s. After well-mixing, the homogenous slurry was placed in the prepared moulds. Details of mixture designation and its overall water-to-solid (w/s) ratio are as given in Table 2.

3.3. Analytical techniques

The results of setting time were extendedly studied from previous research by using Vicat apparatus (EN 196-3) [41]. Compressive strength of prismatic samples (40 × 40 × 160 mm³) of all pastes was determined by using the Instron universal testing

machine (UTM) in accordance with the British Standard EN 196-1 [42]. All samples for compression test were kept in plastic bags and cured in the temperature controlled chamber at 20 ± 2 °C until reach the testing age of 7, 14 and 28 days for GP and 3, 7, 14 and 28 days for GeoPC mixtures. The X-Ray diffraction (XRD) patterns were recorded on a Bruker D8 Advance diffractometer fitted with a Lynxeye XE high-resolution energy dispersive 1-D detector. The samples were determined by using DIFFRAC.SUITE software. The scanning range between 5 and 100° 2θ was covered in a 35-min period. Scanning Electron microscope (SEM) was used to observe the microstructures, and the Energy dispersive X-ray Analysis (SEM-EDXA) technique was used to identify the chemical compositions of the resulted products.

Measurement of internal heat accumulated inside the samples was carried out by recording temperature using thermocouples embedded in three different positions in specimens. Type K thermocouples were placed inside the cylindrical samples (100 mm dia. and 200 mm height; Volume = 1570 cm³) along with the centre of its vertical axis. The probes were aligned vertically with 5 cm spacing from base plate to the top. The heat liberation at the position of bottom (ai0), middle (ai1) and top (ai2) was recorded, together with the temperature inside (ai3) and outside (ai4) the insulated container. An average temperature of ai0 to ai2 was used to represent the heat liberated from each specimen. The thermocouples were connected to a National Instrument 16-Channel thermocouple input module (NI 9213), which was run concurrently with Labview Signal Express programme. A high performance insulator, 10 mm aerogel, was attached to the bottom, side and top cover of the container in order to protect the heat loss during the experiment. The physical properties of that aerogel are 0.15 g/cm³ of density, 0.014 W/m K of thermal conductivity and 1 kJ/kg K of specific heat capacity. The designation of delay time (the period of time from the mixing to recording the data) was 15 min to allow placing paste into the mould and setting up the measurement equipment. The data was recorded every 60 s for a period of 24 h to observe the heat generated inside specimens (Fig. 1). It is, however, noted that the measurement is intended to report in degree Celsius (°C) rather than the rate of energy evolution (J/g) because it can be practically compared with that of typical geopolymers curing at the temperature of 40–90 °C in the oven. In addition, the temperature in SI unit (Kelvin; K) is also presented along with that degree Celsius for all measurement of the samples in this test.

Table 2
Details of mixture designation and the overall water-to-solid ratios.

Mixture	Fly ash (g)	OPC (g)	Na ₂ SiO ₃ sol ^a (g)	NaOH sol ^a (g)	Na ₂ SiO ₃ solid (g)	NaOH solid (g)	Purified water (g)	Overall w/s ratios
GeoPC system								
OPC	–	500.0	–	–	–	–	126.5	0.253
GeoPC90 (B) ^a	45.2	455.0	10.9	7.2	–	–	141.5	0.298
GeoPC70 (B) ^a	138.5	361.0	33.2	22.2	–	–	118.3	0.285
GeoPC50 (B) ^a	236.3	264.0	56.7	37.8	–	–	94.4	0.272
GeoPC30 (B) ^a	338.3	162.0	81.2	54.1	–	–	69.2	0.259
GeoPC10 (B)	444.6	55.2	106.7	71.1	–	–	14.0	0.197
GP (B)	500.0	–	120.0	80.0	–	–	–	0.191
Manufacturing process of geopolymers								
GP (A)	500.0	–	120.0	80.0	–	–	–	0.191
GP (B)	500.0	–	120.0	80.0	–	–	–	0.191
GP (C)	500.0	–	–	–	57.8	30.0	112.2	0.191

^a 4% added water.

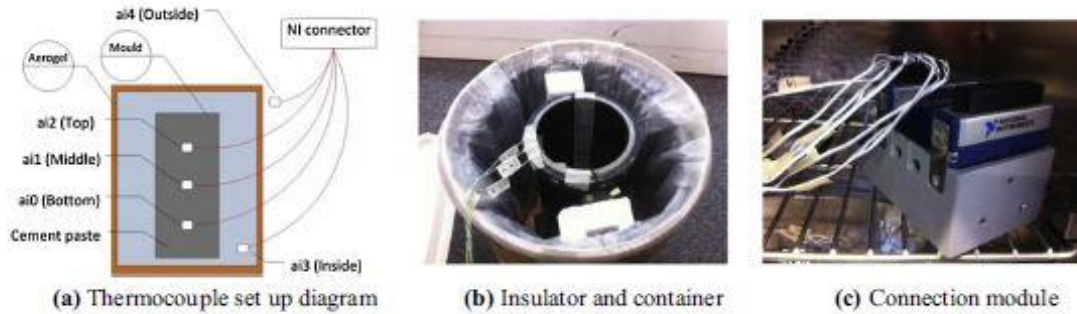


Fig. 1. Set up of the curing measurement in insulated container.

4. Results and discussion

4.1. Setting time of GeoPC system and GP in different manufacturing processes

The results of setting time, which was extensively studied from previous work [21], are presented in Fig. 2. Rapid solidifying process was observed in all GeoPC pastes when compared to fly ash-based GP. An increase in solidification rate and rapid setting were influenced by the main contribution of extra precipitation of (C,N)-A-S-H from calcium mineral (in OPC) with alkaline activators [10]. Moreover, the significant increase in compressive strength was also obtained when the amount of OPC replacement increase. The formation of mixed amorphous geopolymeric gel and (C,N)-A-S-H phases were also proved by the XRD analysis (Fig. 7). It is, alternatively, can be summarised that the amount of OPC inclusion could control the setting behaviour of GeoPC system. In addition, for GP in different manufacturing processes, it was found that the setting time of the mixtures with all those manufacturing processes were not able to be measured in the first 24 h. However, the process C clearly liberated much more heat and solidified faster than the processes A and B.

4.2. Measurement of internal heat accumulated inside the samples

4.2.1. Internal heat of GeoPC systems

The internal heat accumulated inside the samples from three embedded thermocouples of each combination was recorded for a period of 24 h. It should be noted that the temperature measured

from these three thermocouples were slightly different: the top position (ai2) had the highest temperature followed by the middle (ai1) and the bottom (ai0) position, e.g. a set of ai2 = 30.2 °C, ai1 = 29.8 °C and ai0 = 29.5 °C. The reason is that the nature of heat moves upward, resulting in higher temperature in the upper section of specimens than that in the lower section.

It can be seen that the OPC had the highest heat accumulation of 73 °C, while the maximum temperature of GeoPC90, GeoPC70, GeoPC50 and GeoPC30 were 42 °C, 39 °C, 35 °C and 29 °C respectively. GeoPC10 had low internal heat measured with the maximum temperature of 26 °C, similar as the controlled GP that liberated heat at the peak of 27 °C (Fig. 3). The internal heat accumulated inside the samples of GeoPC mixtures may be induced by the hydration reaction of OPC, which consisted of high potential energy compound, C₃A (Tricalcium aluminate, 866 J/g) and C₃S (Tricalcium silicate, 460 J/g) [43]. The main heat evolution of the GeoPC mixtures may thus be obtained from the contained OPC, together with minor heat being promoted by the reaction of OPC and alkaline solution.

It is interesting that increasing OPC not only increased the temperature of the mixtures but also relatively shifted the peak of temperature toward the 10th h (peak of controlled OPC). The peak of temperature measurement of GeoPC10, GeoPC30, GeoPC50 and GeoPC70 were at the 3rd, 5th, 5th and 9th hour respectively, while GP was in the first 20 min of mixing (Fig. 4). The time of peak temperature was mainly shortened (less than 10th h of the controlled OPC) by the appropriate proportion with forceful reaction between calcium mineral (Ca) in OPC and alkaline soluble in GP which led to a rapid formation of the mixed C-S-H and N-A-S-H [11–17]. For the

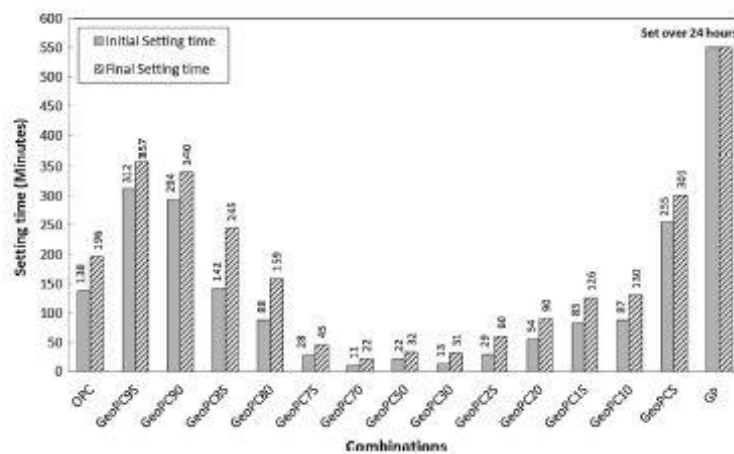


Fig. 2. Setting time of OPC, GP and GeoPC paste.

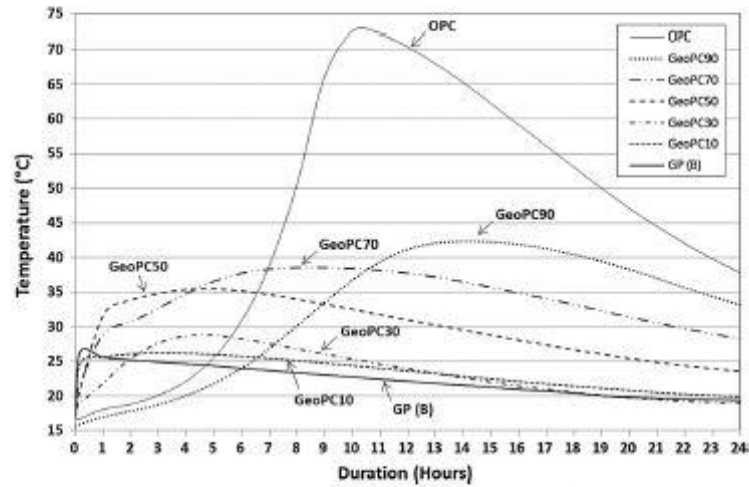


Fig. 3. Heat evolution during a 24 h-period of GeoPC.

mixtures with low OPC content (or higher alkaline soluble from GP), e.g. GeoPC10, most of Ca may react with abundant alkaline in the mixtures and very little amount of Ca may be left for OPC-hydration reaction. Less internal heat and low peak time, therefore, were recorded. It can be concluded that higher GP content (i.e. higher alkaline soluble) in GeoPC system requires shorter time for the mixtures to reach their peak temperature.

On the other hand, although GeoPC90 achieved higher temperature than other GeoPC combinations (GeoPC70, 50, 30 and 10), the peak of temperature were at the 14th h or 4 h longer than OPC. It seems that the reaction was retarded with this low-alkalinity combination. This behaviour conforms to the results of setting time (Fig. 2) that GeoPC90, including GeoPC85 and GeoPC5, exhibited longer setting time than OPC. It is apparent that the peak temperature of GeoPC systems which have OPC content less than approximately 85% (GeoPC85) would occur earlier than that of OPC (10 h), while the rest of mixtures studied took longer time to reach the peak. Therefore, the maximum temperature and time to reach the peak were noticeably influenced by the rate of reaction between prime constituents, and alkaline activators in the systems.

However, the internal heat accumulated inside the controlled OPC in this test had similar characteristic as that of the general rate of heat evolution of pure OPC paste when measured with isothermal calorimeter (mW/g s or J/g) [44].

4.2.2. Internal heat of geopolymers in different manufacturing processes

The heat liberation of alkaline activators, sodium hydroxide and sodium silicate, during aqueous alkaline preparation (of 500 g. solution) was previously measured in order to calculate its effect in the process C. It can be seen that the temperature abruptly increased after adding water to alkaline solids and then steadily decreased to room temperature in a approximately 4 h. It is apparent that the sodium hydroxide (NaOH) dissolution produced more heat than sodium silicate and, in addition, a higher concentration of NaOH generated higher temperature (Fig. 5). The reasons is that the chemical species of alkaline materials were brought to a lower energy state when dissolved with water (H₂O) to be Na⁺ and OH⁻ for sodium hydroxide and 2Na⁺ + SiO₂(OH)₂²⁻ for sodium silicate [45]. In general, the cross-linked SiO₄ and AlO₄ tetrahedral

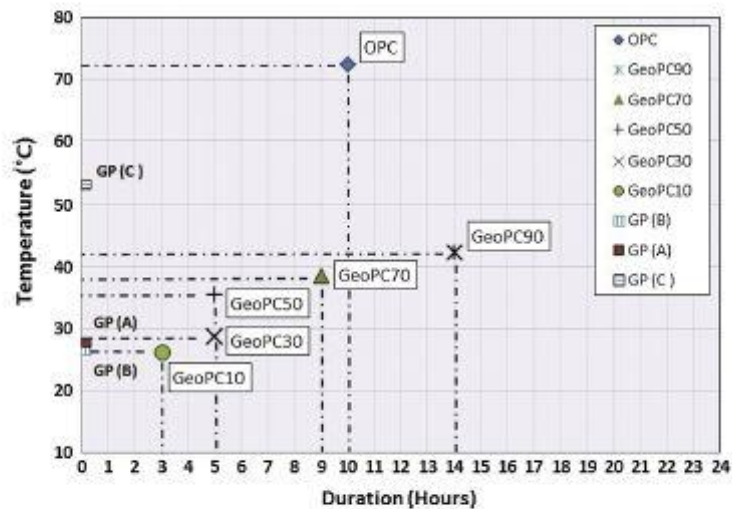


Fig. 4. The maximum temperature against the time of each combination.

of GP are formed when the negative charge on Al^{3+} is balanced with positive charge of alkaline ion (Na^+), forming N-A-S-H [11]. The presence of Ca^{2+} (from OPC) in alkaline solution could lead to the formation of natural hydration-CSH or C-A-SH or N-A-S-H. The final reaction products of those systems can be C-S-H ($Ca + Si$), zeolite/polymers ($Si + Al$) or C,N-A-S-H ($Ca, Na + Al + Si$) which mainly depend on the characteristics of raw starting materials and alkaline activators. In addition, the presence of C-S-H and C,N-A-S-H can be observed in XRD analysis (Fig. 7) [12–17].

As seen in Fig. 6, the measurement of internal heat accumulated inside the samples were examined as the rise of temperature of GP mixtures with three different processes A, B and C. It is apparent that the processes A and B release very limited heat above room temperature at the peak of approximately 28 °C and 27 °C in the first 20 min of mixing. After that, the temperature reduced steadily to room temperature at 21 °C and 19 °C within 24th h. On the other hand, the process C had much higher temperature than A and B after mixing with water. Its highest temperature reached around 54 °C in the first 20 min and maintained above 40 °C for over 8 hours. Then, it cooled down slowly to around 24 °C at the 24th h. The limited heat liberated in the processes A and B was generated by the chemical reactions among various alkaline ions and fly ash inside the paste (hydration and geopolymerization). The dissolution of fly ash, in initial stage, underwent with a slight exothermic reaction which led to less heat emission. On the contrary, the heat emitted from the process C was almost two times higher than those of the processes A and B. This means that the dry-mixed method (process C) could be able to produce heat during the hydration of alkaline solid, which could realise the development of a heat based- self cured geopolymer cement. For general case, the temperature could be kept inside the mixture for longer than 8 hours if this process (C) is used to produce geopolymer mortar (paste and sand) or concrete (paste and aggregates) due to the heat accumulated by those aggregates. As far as geopolymers was produced with the huge volume (massive amount) together with good protection in heat and moisture loss, it could also maintain internal heat and provide positive curing conditions itself.

4.3. Compressive strength of GeoPC system and GP in different manufacturing processes

The compressive strength of GeoPC system was examined with samples at 3, 7, 14 and 28 days (Table 3). It can be seen that the

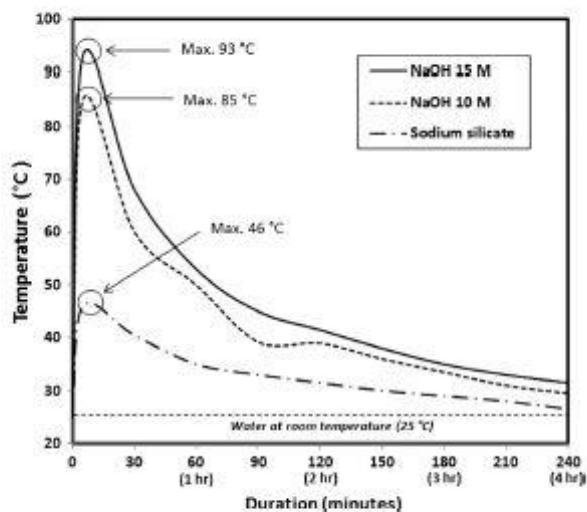


Fig. 5. Heat evolution of alkaline solution preparation.

strength development of GeoPC systems follow that of OPC, i.e. gradually strengthening with the increase of time from the first three day to 28 day-aged. The strength increased when the amount of OPC increased, corresponding to the internal heat liberation, although the strength of the GeoPC cannot reach to the level of that OPC. For example, at the 28 day-aged, GeoPC30, GeoPC70 and GeoPC90 achieved the strength of 35.69, 39.11 and 51.32 MPa respectively, while the controlled OPC achieved that of 70.06 MPa.

In GeoPC systems, soluble hydroxide strongly dissolves the minerals from source of materials, indicated by the forming character of the mixtures, while soluble silicate, which is normally used as another source of silica, improves the binding activity or geopolymerization of geopolymers [31,36,37]. The strength of GeoPC in ambient temperature resulted from participation and formation of calcium silicate hydrate, C-S-H (main hydration product of Portland cement) and C-S-H co-existed with N-A-S-H gel, which is responsible for the fast setting and early strength development [11–17,28,32]. Moreover, the internal heat which was generated inside the specimens would further enhance the formation of geopolymeric gel, improving its mechanical strength [46]. Nevertheless, overall lower strength of GeoPC mixtures was obtained in an ambient-curing temperature because those mixtures may still have less crystallinity as well as poor reactivity than that of normal OPC C-S-H phases as indicated by XRD analysis (Fig. 7) [47–49].

All of GP pastes could not set in the first 3 days, therefore, the first compression test was carried out at 7 day-age, followed by 14 and 28 day-aged (Table 3). The structural formation of GP was very slow in the ambient curing condition, therefore, a prolonged period of time was required for the paste solidification (over 3–5 days). Uncompleted reaction of geopolymeric gelation also affected the early strength of geopolymer paste.

Process A resulted in the highest mechanical strength due to more dissolution rate (from initial mix of hydroxide solution) and more binding activity (from later added of silicate solution) [25,35]. Process B, the most widely used method, provided a better uniformity but the structural formation appeared to be inert and led to slightly lower compressive strength than process A [12,19,30]. Process C solidified much more intensively than those occurred in the process A or B by the strong hydration among starting materials, alkaline solids and water in the system. Without moisture protection, the heat generated from process C can lead to a rapid loss of moisture. Micro cavities, which were left in the structure, could give rise to an adverse effect in mechanical strength. Although the obtained heat provided good curing conditions as similar as happened in mild-to-medium temperature curing [50,51], incomplete dissolution could lead to low reaction rate. The compressive strength of process C was, thus, lower than that of process A and B. In contrast, it can be summarised that the process C could achieve the quickest setting characters with intensive heat liberation, while the processes A and B took longer time to set. Process A gained the highest compressive strength followed by process B and C in all testing ages. Overall, the extra heat obtained from OPC hydration (GeoPC system) and strong exothermic reaction from alkaline dissolution (Dry-mixing process) could provide a positive effect for curing purpose of that geopolymers which give rise in its mechanical strength.

4.4. Morphology analysis and microstructures of GeoPC systems

The XRD patterns GeoPC mixtures are as presented in Fig. 7. At the testing age of 28 days, GP consists mainly of semi-crystalline and amorphous phases which are indicated by the sharp peak (quartz and mullite) and a broad hump in the region of 20–35° 2 θ respectively. The peaks which corresponding to C-S-H, calcite and nepheline increased when additional OPC increase from 10%

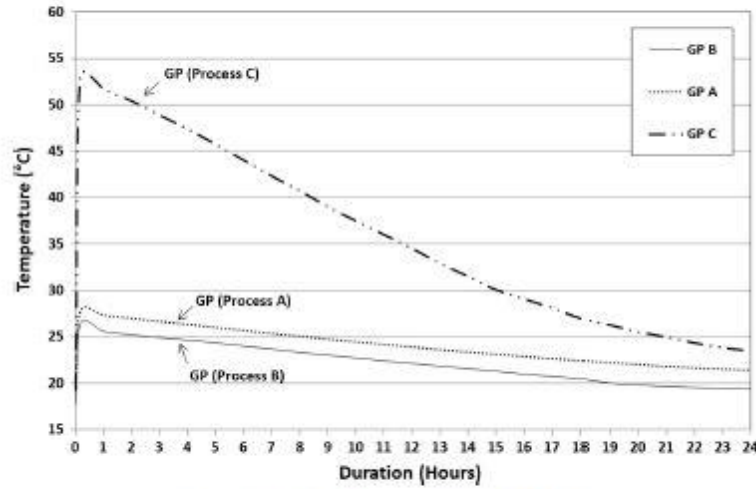


Fig. 6. Heat evolution during a 24 h-period of pure GP.

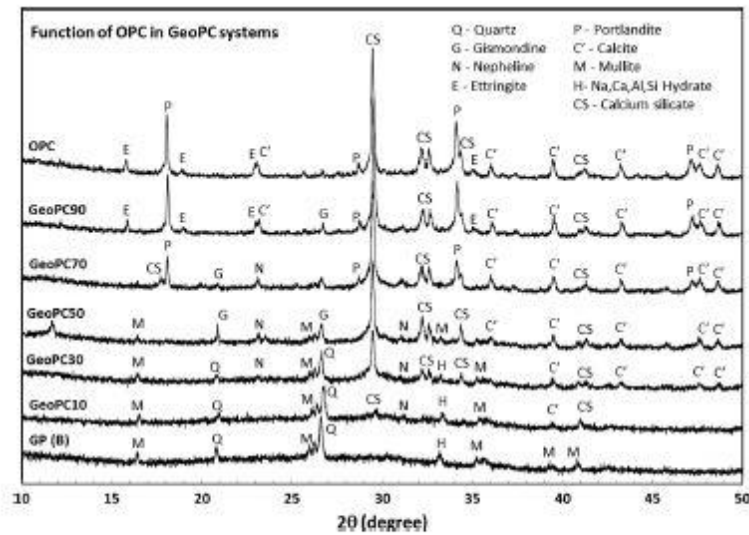


Fig. 7. X-ray diffraction patterns of GeoPC system at 28 days age.

Table 3
Compressive strength of GeoPC system and GP in different manufacturing processes.

Mixture	CaO/SiO ₂ ^a	SiO ₂ /Al ₂ O ₃ ^a	Compressive strength (MPa)			
			3 days	7 days	14 days	28 days
GeoPC system						
OPC	-	-	48.8	59.5	63.1	70.1
GeoPC90	4.40	4.63	30.2	36.2	44.6	51.3
GeoPC80	3.14	4.27	18.2	24.6	33.8	39.2
GeoPC70	2.31	4.06	21.9	23.4	34.1	39.1
GeoPC50	1.26	3.82	14.1	19.0	33.9	36.5
GeoPC30	0.63	3.69	13.8	15.4	32.4	35.7
GeoPC20	0.40	3.64	11.1	14.8	29.4	35.7
GeoPC10	0.21	3.61	5.7	5.8	18.2	23.5
GP (B)	0.05	3.58	-	2.9	6.9	13.2
Manufacturing process of geopolimer						
GP (A)	0.05	3.58	-	4.8	7.2	13.6
GP (B)	0.05	3.58	-	2.9	6.9	13.2
GP (C)	0.05	3.58	-	2.4	6.0	11.3

^a Oxide molar ratio.

(GeoPC10) to 90% (GeoPC90) while the intensity of quartz and mullite continuously decreased. More crystalline phases of portlandite, ettringite and calcite are clearly appeared and increased with high percentage of OPC from the GeoPC70 to the fully hydrated OPC.

The XRD analysis of 3 days age was also studied in order to compare its changes in later stage. It, however, exhibited very similar characteristic as 28 days which could lead to good early strength of the final products. The appearance of N-A-S-H compound was found according to the high alkalinity of Na-containing solutions. The main composition of fly ash (silica and alumina) could form C-A-S-H phase with the available calcium mineral. The findings can be drawn that the GeoPC system has a different reaction pathways depending on Na⁺ and OH⁻ concentration and the composition of prime materials, forming the coexistence of amorphous C-S-H/semi-crystalline phases (XRD peak and hump) or (C,N)-A-S-H (main reaction product of fly ash activation; 0.8CaO·0.2Na₂O·Al₂O₃·3.0SiO₂·6H₂O) interfered in hydration product of GeoPC matrices [11]. The coexistence formations of

Table 4
Some of selected SEM images of GeoPC system at 28 days age.

Mixture	SEM images	SEM-EDX spectrums
(a) OPC		
(b) GeoPC90		
(c) GeoPC50		
(d) GeoPC10		
(e) GP		

both crystalline and amorphous were found in the GeoPC mixtures, illustrating the mix of geopolymeric gel and hydrated OPC product in the single binder.

Table 4 reveals some SEM images and EDX spectrums of GeoPC mixtures varied from GeoPC90 to GeoPC10 at the age of 28 days. It is apparent that a micrograph of GeoPC90 is very similar to those of controlled OPC. High OPC content resulted in compact and firm structure, leading to an increase in mechanical strength.

Microstructures of GeoPC50 and GeoPC10 were less homogeneous than that of GeoPC90. Nevertheless, their structures looked denser and more compact than that of the GP. Gel pores of spherical particles, loose matrices and some of remaining unreacted fly ash particles could be one of major factors of poor mechanical performances for low-OPC content mixtures (GeoPC10 or even GP) curing in ambient conditions. It can be seen in EDX spectrums that high percentage of OPC inclusion (e.g. GeoPC90) had a considerable intensity in Ca with a majority of C-(A)-S-H gel, while low percentage of OPC inclusion (e.g. GeoPC10) had a substantial amount of Si and Al of (C,N)-A-S-H or geopolymeric gel.

4.5. Effect of oxide molar ratio on setting time and compressive strength of GeoPC system

CaO-to-SiO₂ (C/S) and SiO₂-to-Al₂O₃ (Si/Al) ratio were plotted against setting time and 28-day compressive strength (Fig. 8). The higher C/S ratio generally provides more C-S-H and C,N-A-S-H formation, while higher Si/Al ratio offers more available silica and alumina which resulted in an increase in the strength of GeoPC.

The similar results of good strength from C-S-H forming were also reported with the metakaolin-based geopolymers and GBFS-as a source of calcium additive-geopolymers [12,52,53]. The setting time had similar characteristic as open-up parabolic curve in both C/S and Si/Al plotting. As aforementioned, the Ca from OPC together with available Si and Al mainly provided an extra participation in the systems [10], thus, a proper setting time could be achieved with an appropriate combination of those GeoPC mixtures. The self-cured optimum combinations in ambient temperature may be able to achieve the compressive strength with the C/S ratio of 0.21–0.40 and Si/Al ratio of 3.61–3.64 (GeoPC10-GeoPC20), providing the strength approximately 23–35 MPa at 28 days age. The benefits are not only in term of mechanical properties but also in both economic and environmental aspects from replacing OPC with industrial waste, fly ash.

5. Conclusions

The internal heat liberation and the strength development of the developed self-curing geopolymers have been studied with the addition of OPC and their processing procedures in ambient curing temperature. Some specific conclusions are summarised as follows;

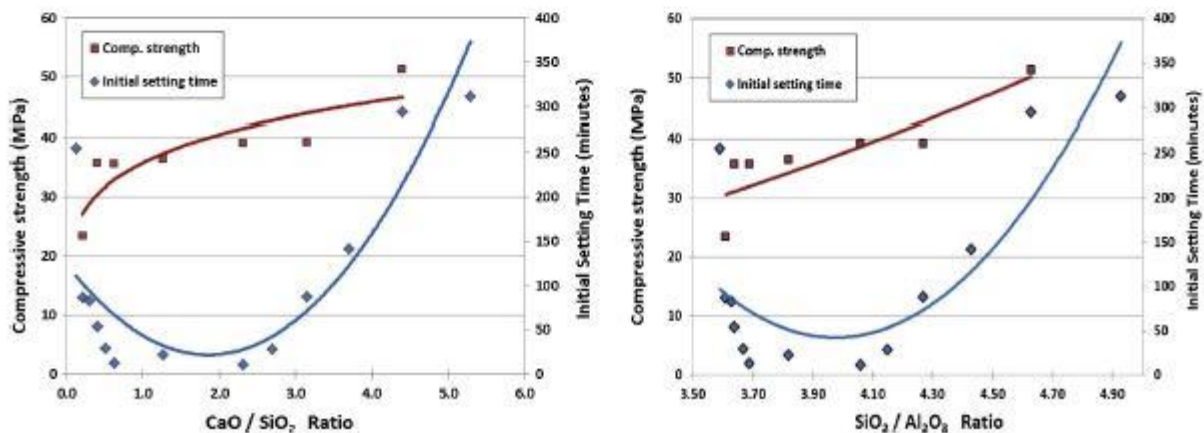


Fig. 8. CaO/SiO₂ ratio (Left) and SiO₂/Al₂O₃ ratio (Right) vs. 28d-strength and setting time.

- (1) The internal heat accumulated inside the GeoPC samples was mainly induced by the OPC hydration which could promote more appropriate curing condition. The optimum combination, which could achieve in term of mechanical properties, economic and environmental aspects, is in the range of GeoPC10 to GeoPC20. Whilst, pre dry-mixing process (C), it clearly generated much more heat and solidification characteristic which could provide a positive curing condition to the fly ash-based geopolymers.
- (2) The addition of OPC in the GP systems (GeoPC) hence directly enhanced the setting time and early strength development. An extra participation of C-S-H and C₂N-A-S-H from available Ca (from OPC) in the systems resulted in the microstructure improvement, indicating by dense and compact matrix.
- (3) The formation of geopolymers in all manufacturing processes underwent with very slow rate in ambient curing temperature in their early age. Separate mixing process (A) achieved higher mechanical strength than process B due to more dissolution rate and more binding activity of subsequent mixing order of alkaline solutions. As dry-mixing process (C) required extra water in the system, lack of reasonable dissolution of solid materials could lead to poor microstructure, resulting in the lowest strength.
- (4) Overall, the enhancement in mechanical properties of suitable GeoPC mixtures, together with alternative heat supplies from GeoPC combinations and dry-mixed process (C) could provide sufficient internal heat for the curing regime of GP. The experiment of this self-cured geopolymers has been established forwarding the potential development for onsite engineering applications.

References

- [1] V.M. Maholtra, Introduction: sustainable development and concrete technology, *ACI Concr. Int.* 24 (7) (2002).
- [2] D. Dimas, I.P. Giannopoulou, D. Papias, Polymerization in sodium silicate solutions: a fundamental process in geopolymerization technology, *J. Mater. Sci.* 44 (2009) 3719–3730.
- [3] K. Vijai, R. Kumutha, B.G. Vishnuram, Effect of types of curing on strength of geopolymer concrete, *Int. J. Phys. Sci.* 5 (9) (2010) 1419–1423.
- [4] O.B. Rajiwal, H.S. Path, Geopolymer concrete: a green concrete, in: 2nd International Conference on Chemical, Biological and Environmental Engineering (ICBEE 2010), 2010, pp. 202–206.
- [5] S. Andini, R. Goffi, F. Colangelo, T. Grieco, F. Montagnaro, L. Santoro, Coal fly ash as raw material for the manufacture of geopolymer-based products, *Waste Manage.* 28 (2008) 416–423.
- [6] F. Pacheco-Torgal, J. Castro-Gomes, S. Jalali, Alkali-activated binders: a review Part 1. Historical background, terminology, reaction mechanisms and hydration products, *Constr. Build. Mater.* 22 (2008) 1305–1314.
- [7] V.D. Glukhovskiy, *Soil Silicate Articles and Structures*, Budivelnik Publisher, Kiev, Ukraine, 1967.
- [8] J. Davidovits (Ed.), *Geopolymer Chemistry and Applications*, 3rd ed., Institut Geopolymère, France, 2011.
- [9] C. Li, H. Sun, L. Li, A review: the comparison between alkali-activated slag (Si + Ca) and metakaolin (Si + Al) cements, *Cem. Concr. Res.* 40 (2010) 1341–1349.
- [10] S. Pangdaeng, T. Phoo-ngernkham, V. Sata, P. Chindaprasit, Influence of curing conditions on properties of high calcium fly ash geopolymer containing Portland cement as additive, *Mater. Des.* 53 (2014) 269–274.
- [11] A. Palomo, A. Fernández-Jiménez, G. Kovalchuk, L.M. Ordon- ez, M.C. Naranjo, Opo-fly ash cementitious systems: study of gel binders produced during alkaline hydration, *J. Mater. Sci.* 42 (2007) 2958–2966.
- [12] C.K. Yip, G.C. Lukey, J.S.J. Van Deventer, The coexistence of geopolymeric gel and calcium silicate hydrate at the early stage of alkaline activation, *Cem. Concr. Res.* 35 (2005) 1688–1697.
- [13] J. Temuujin, A. Van Riessen, R. Williams, Influence of calcium compounds on the mechanical properties of fly ash geopolymer pastes, *J. Hazard. Mater.* 167 (2009) 82–88.
- [14] J. Tailby, K.J.D. Mackenzie, Structure and mechanical properties of aluminosilicate geopolymer composites with Portland cement and its constituent minerals, *Cem. Concr. Res.* 40 (2010) 787–794.
- [15] C.K. Yip, J.S.J. Van Deventer, Microanalysis of calcium silicate hydrate gel formed within a geopolymeric binder, *J. Mater. Sci.* 38 (2003) 3851–3860.
- [16] I. Lecomte, C. Henrist, M. Ligeois, F. Maseri, A. Rulmont, R. Cloots, (Micro-) structural comparison between geopolymers, alkali-activated slag cement and Portland cement, *J. Eur. Ceram. Soc.* 26 (16) (2006) 3789–3797.
- [17] S. Hanjitsuwan, S. Hunpratum, P. Thongbai, S. Maensiri, V. Sata, P. Chindaprasit, Effects of NaOH concentrations on physical and electrical properties of high calcium fly ash geopolymer paste, *Cem. Concr. Compos.* 45 (45) (2014) 9–14.
- [18] P. Nath, P.K. Sarker, Use of OPC to improve setting and early strength properties of low calcium fly ash geopolymer concrete cured at room temperature, *Cem. Concr. Compos.* 55 (2015) 205–214.
- [19] F. Pacheco-Torgal, J. Castro-Gomes, S. Jalali, Alkali-activated binders: a review Part 2. About materials and binders manufacture, *Constr. Build. Mater.* 22 (2008) 1315–1322.
- [20] H.M. Khater, Effect of calcium on geopolymerization of aluminosilicate wastes, *J. Mater. Civ. Eng.* 24 (1) (2012) 92–101.
- [21] T. Suwan, M. Fan, Influence of OPC replacement and manufacturing procedures on the properties of self-cured geopolymer, *Constr. Build. Mater.* 73 (2014) 551–561.
- [22] T. Bakharev, Thermal behaviour of geopolymers prepared using class F fly ash and elevated temperature curing, *Cem. Concr. Res.* 36 (2006) 1134–1147.
- [23] T. Bakharev, Geopolymeric materials prepared using Class F fly ash and elevated temperature curing, *Cem. Concr. Res.* 35 (2005) 1224–1232.
- [24] S.K. Nath, S. Mukherjee, S. Maitra, S. Kumara, Ambient and elevated temperature geopolymerization behaviour of Class F fly ash, *Trans. Indian Ceram. Soc.* 73 (2) (2014) 126–132.
- [25] P. Chindaprasit, T. Chareerat, S. Hatanaka, T. Cao, High-strength geopolymer using fine high-calcium fly ash, *J. Mater. Civ. Eng.* 23 (3) (2011) 264–270.
- [26] P. Nath, P.K. Sarker, Effect of GGBFS on setting, workability and early strength properties of fly ash geopolymer concrete cured in ambient condition, *Constr. Build. Mater.* 66 (2014) 163–171.
- [27] A. Nazari, Compressive strength of geopolymers produced by ordinary Portland cement: application of genetic programming for design, *Mater. Des.* 43 (2013) 356–366.
- [28] T. Phoo-ngernkham, P. Chindaprasit, V. Sata, S. Pangdaeng, Properties of high calcium fly ash geopolymer pastes with Portland cement as an additive, *Int. J. Miner. Metall. Mater.* 20 (2) (2013) 214.
- [29] C. Shi, A.F. Jiménez, A. Palomo, New cements for the 21st century: the pursuit of an alternative to Portland cement, *Cem. Concr. Res.* 41 (2011) 750–763.
- [30] A. Pinto, P. Fernandes, J. Said, Geopolymer manufacture and applications – main problems when using concrete technology, in: *Proceedings of 2002 Geopolymer Conference*, 2002, Melbourne, Australia.
- [31] B. Chatveera, N. Makul, Properties of geopolymer mortar produced from fly ash and rice husk ash: influences of fly ash-rice husk ash ratio and Na₂SiO₃-NaOH ratio under curing by microwave energy, *J. Res. Dev. TU 3 (35) (2012) 299–309*.
- [32] S. Ahmari, L. Zhang, Utilization of cement kiln dust (CKD) to enhance mine tailings-based geopolymer bricks, *Constr. Build. Mater.* 40 (2013) 1002–1011.
- [33] M.F. Nuruddin, A. Kusiantoro, S.A. Qaz, N. Shafiq, Utilisation of waste material in geopolymeric concrete, *Constr. Mater.* 164 (CM6) (2011) 315–327.
- [34] U. Ratanasak, P. Chindaprasit, Influence of NaOH solution on the synthesis of fly ash geopolymer, *Miner. Eng.* 22 (2009) 1073–1078.
- [35] P. Chindaprasit, T. Chareerat, V. Sirivivatnanon, Workability and strength of coarse high calcium fly ash geopolymer, *Cem. Concr. Compos.* 29 (2007) 224–229.
- [36] P. Paisitrisawat, Utilization of Fly Ash From Fluidized-Bed Combustion as Raw Material for Geopolymer, Burapha University, 2009. Unpublished Chemistry.
- [37] P. Sukmak, S. Horpibulsuk, S.L. Shen, Strength development in clay-fly ash geopolymer, *Constr. Build. Mater.* 40 (2013) 566–574.
- [38] P. Duxson, J.L. Provis, Designing precursors for geopolymer cements, *J. Am. Ceram. Soc.* 91 (12) (2008) 3864–3869.
- [39] D. Feng, J.L. Provis, J.S.J. Van Deventer, Thermal activation of albite for the synthesis of one-part mix geopolymers, *J. Am. Ceram. Soc.* 95 (2) (2012) 565–572.
- [40] Y.M. Liew, H. Kamarudin, A.M. Mustafa Al Bakri, M. Luqman, I.K. Nizar, C.M. Ruzaidi, Processing and characterization of calcined kaolin cement powder, *Constr. Build. Mater.* 30 (2012) 794–802.
- [41] BS EN 196-3:2005+A1:2008, *Methods of Testing Cement-Part 3: Determination of Setting Times and Soundness*, British standard, 2008.
- [42] BS EN 196-1:2005, *Methods of Testing Cement-Part 1: Determination of Strength*, British standard, 2005.
- [43] G.C. Bye, *PORTLAND CEMENT Composition, Production and Properties*, Pergamon Press, UK, 1983.
- [44] N.Y. Mostafa, P.W. Brown, Heat of hydration of high reactive pozzolans in blended cements: isothermal conduction calorimetry, *Thermochim. Acta* 435 (2005) 162–167.
- [45] W. Sottisopha, S. Asavapit, Immobilization of the plating sludge by activation of pulverized fuel ash with sodium silicate solution, *Thammasat Int. J. Sci. Technol.* 10 (4) (2005) 7–15.
- [46] J. Moon, S. Bae, K. Celik, S. Yoon, K. Kim, K.S. Kim, P.J.M. Monteiro, Characterization of natural pozzolan-based geopolymeric binders, *Cem. Concr. Compos.* 53 (2014) 97–104.
- [47] K. Sonna, C. Jaturapitakkul, P. Kajitvichyanukul, P. Chindaprasit, NaOH-activated ground fly ash geopolymer cured at ambient temperature, *Fuel* 90 (2011) 2118–2124.
- [48] E. Altan, S.T. Erdogan, Alkali activation of a slag at ambient and elevated temperatures, *Cem. Concr. Compos.* 34 (2012) 131–139.

- [49] J. Temuujin, R. Williams, A. Van Riessen, Effect of mechanical activation of fly ash on the properties of geopolymer cured at ambient temperature, *J. Mater. Process. Technol.* 209 (2009) 5276–5280.
- [50] C.K. Yip, G.C. Lukey, J.L. Provis, J.S.J. Van Deventer, Effect of calcium silicate sources on geopolymerisation, *Cem. Concr. Res.* 38 (2008) 554–564.
- [51] F. Škvára, L. Kopecký, J. Nimeček, Z. Bittnar, Microstructure of geopolymer materials based on fly ash, *Ceram. – Silikáty* 4 (2006) 208–215.
- [52] L. Zuda, Z. Pavlik, P. Rovnanikova, P. Bayer, R. Cerny, Properties of alkali activated aluminosilicate material after thermal load, *Int. J. Thermophys.* 27 (4) (2006) 1250–1263.
- [53] B.V. Rangan, Fly ash-based geopolymer concrete, in: *Proceedings of the International Workshop on Geopolymer Cement and Concrete*, 2010.